

World Journal of *Gastroenterology*

World J Gastroenterol 2021 August 28; 27(32): 5297-5459



OPINION REVIEW

- 5297 Management of Flood syndrome: What can we do better?
Strainiene S, Peciulyte M, Strainys T, Stundiene I, Savlan I, Liakina V, Valantinas J

REVIEW

- 5306 Radiomics and machine learning applications in rectal cancer: Current update and future perspectives
Stanzione A, Verde F, Romeo V, Boccadifuoco F, Mainenti PP, Maurea S
- 5322 Could the burden of pancreatic cancer originate in childhood?
Diaconescu S, Gilcă-Blanariu GE, Poamaneagra S, Marginean O, Paduraru G, Stefanescu G

MINIREVIEWS

- 5341 Application of artificial intelligence in preoperative imaging of hepatocellular carcinoma: Current status and future perspectives
Feng B, Ma XH, Wang S, Cai W, Liu XB, Zhao XM
- 5351 Artificial intelligence application in diagnostic gastrointestinal endoscopy - Deus ex machina?
Correia FP, Lourenço LC
- 5362 Faecal microbiota transplantation enhances efficacy of immune checkpoint inhibitors therapy against cancer
Kang YB, Cai Y
- 5376 Immune checkpoint inhibitor-related hepatotoxicity: A review
Remash D, Prince DS, McKenzie C, Strasser SI, Kao S, Liu K

ORIGINAL ARTICLE**Basic Study**

- 5392 Therapeutic effect of *Cistanche deserticola* on defecation in senile constipation rat model through stem cell factor/C-kit signaling pathway
Zhang X, Zheng FJ, Zhang Z
- 5404 Recombinant angiopoietin-like protein 4 attenuates intestinal barrier structure and function injury after ischemia/reperfusion
Wang ZY, Lin JY, Feng YR, Liu DS, Zhao XZ, Li T, Li SY, Sun JC, Li SF, Jia WY, Jing HR

Retrospective Study

- 5424 Prolonged survival in patients with hand-foot skin reaction secondary to cooperative sorafenib treatment
Ochi M, Kamoshida T, Araki M, Ikegami T

- 5438** Contrast-enhanced ultrasound imaging for intestinal lymphoma
Cui NY, Gong XT, Tian YT, Wang Y, Zhang R, Liu MJ, Han J, Wang B, Yang D

Observational Study

- 5448** Intestinal ischemic manifestations of SARS-CoV-2: Results from the ABDOCOVID multicentre study
Norsa L, Bonaffini PA, Caldato M, Bonifacio C, Sonzogni A, Indriolo A, Valle C, Furfaro F, Bonanomi A, Franco PN, Gori M, Smania V, Scaramella L, Forzenigo L, Vecchi M, Solbiati M, Costantino G, Danese S, D'Antiga L, Sironi S, Elli L

ABOUT COVER

Editorial Board Member of *World Journal of Gastroenterology*, Luca Mastracci, MD, Associate Professor, Anatomic Pathology, Department of Surgical Sciences and Integrated Diagnostics (DISC), University of Genova, Ospedale Policlinico San Martino, Largo Rosanna Benzi 10, Genova 16132, Italy. luca.mastracci@unige.it

AIMS AND SCOPE

The primary aim of *World Journal of Gastroenterology* (WJG, *World J Gastroenterol*) is to provide scholars and readers from various fields of gastroenterology and hepatology with a platform to publish high-quality basic and clinical research articles and communicate their research findings online. WJG mainly publishes articles reporting research results and findings obtained in the field of gastroenterology and hepatology and covering a wide range of topics including gastroenterology, hepatology, gastrointestinal endoscopy, gastrointestinal surgery, gastrointestinal oncology, and pediatric gastroenterology.

INDEXING/ABSTRACTING

The WJG is now indexed in Current Contents®/Clinical Medicine, Science Citation Index Expanded (also known as SciSearch®), Journal Citation Reports®, Index Medicus, MEDLINE, PubMed, PubMed Central, and Scopus. The 2021 edition of Journal Citation Report® cites the 2020 impact factor (IF) for WJG as 5.742; Journal Citation Indicator: 0.79; IF without journal self cites: 5.590; 5-year IF: 5.044; Ranking: 28 among 92 journals in gastroenterology and hepatology; and Quartile category: Q2. The WJG's CiteScore for 2020 is 6.9 and Scopus CiteScore rank 2020: Gastroenterology is 19/136.

RESPONSIBLE EDITORS FOR THIS ISSUE

Production Editor: Jia-Hui Li; Production Department Director: Yu-Jie Ma; Editorial Office Director: Ze-Mao Gong.

NAME OF JOURNAL

World Journal of Gastroenterology

ISSN

ISSN 1007-9327 (print) ISSN 2219-2840 (online)

LAUNCH DATE

October 1, 1995

FREQUENCY

Weekly

EDITORS-IN-CHIEF

Andrzej S Tarnawski, Subrata Ghosh

EDITORIAL BOARD MEMBERS

<http://www.wjgnet.com/1007-9327/editorialboard.htm>

PUBLICATION DATE

August 28, 2021

COPYRIGHT

© 2021 Baishideng Publishing Group Inc

INSTRUCTIONS TO AUTHORS

<https://www.wjgnet.com/bpg/gerinfo/204>

GUIDELINES FOR ETHICS DOCUMENTS

<https://www.wjgnet.com/bpg/GerInfo/287>

GUIDELINES FOR NON-NATIVE SPEAKERS OF ENGLISH

<https://www.wjgnet.com/bpg/gerinfo/240>

PUBLICATION ETHICS

<https://www.wjgnet.com/bpg/GerInfo/288>

PUBLICATION MISCONDUCT

<https://www.wjgnet.com/bpg/gerinfo/208>

ARTICLE PROCESSING CHARGE

<https://www.wjgnet.com/bpg/gerinfo/242>

STEPS FOR SUBMITTING MANUSCRIPTS

<https://www.wjgnet.com/bpg/GerInfo/239>

ONLINE SUBMISSION

<https://www.f6publishing.com>

Management of Flood syndrome: What can we do better?

Sandra Strainiene, Milda Peciulyte, Tomas Strainys, Ieva Stundiene, Ilona Savlan, Valentina Liakina, Jonas Valantinas

ORCID number: Sandra Strainiene 0000-0003-1884-1353; Milda Peciulyte 0000-0001-5369-0170; Tomas Strainys 0000-0001-9080-3998; Ieva Stundiene 0000-0002-2569-3638; Ilona Savlan 0000-0002-3689-5040; Valentina Liakina 0000-0001-8685-1292; Jonas Valantinas 0000-0003-4534-2293.

Author contributions: Strainiene S and Peciulyte M wrote the original manuscript and reviewed the literature; Liakina V, Stundiene I, Strainys T, and Savlan I reviewed and edited the manuscript; Savlan I, Liakina V, Stundiene I, and Valantinas J were responsible for revising the manuscript for important intellectual content; All authors issued final approval for this version to be submitted and agree to be accountable for all aspects of this work.

Conflict-of-interest statement: The authors declare that they have no conflicts of interest.

Open-Access: This article is an open-access article that was selected by an in-house editor and fully peer-reviewed by external reviewers. It is distributed in accordance with the Creative Commons Attribution NonCommercial (CC BY-NC 4.0) license, which permits others to distribute, remix, adapt, build upon this work non-commercially, and license their derivative works

Sandra Strainiene, Milda Peciulyte, Ieva Stundiene, Ilona Savlan, Valentina Liakina, Jonas Valantinas, Clinic of Gastroenterology, Nephrourology and Surgery, Centre of Hepatology, Gastroenterology and Dietetics, Institute of Clinical Medicine, Vilnius University, Vilnius 03104, Lithuania

Tomas Strainys, Clinic of Anesthesiology and Reanimatology, Centre of Anesthesiology, Intensive Care and Pain Management, Institute of Clinical Medicine, Vilnius University, Vilnius 03104, Lithuania

Valentina Liakina, Department of Chemistry and Bioengineering, Faculty of Fundamental Science, Vilnius Gediminas Technical University, Vilnius 10223, Lithuania

Corresponding author: Valentina Liakina, PhD, Senior Researcher, Clinic of Gastroenterology, Nephrourology and Surgery, Centre of Hepatology, Gastroenterology and Dietetics, Institute of Clinical Medicine, Vilnius University, 21 M.K. Ciurlionio Street, Vilnius 03104, Lithuania. valentina.liakina@santa.lt

Abstract

Approximately 20% of cirrhotic patients with ascites develop umbilical herniation. These patients usually suffer from multisystemic complications of cirrhosis, have a significantly higher risk of infection, and require accurate surveillance—especially in the context of the coronavirus disease 2019 pandemic. The rupture of an umbilical hernia, is an uncommon, life-threatening complication of large-volume ascites and end-stage liver disease resulting in spontaneous paracentesis, also known as Flood syndrome. Flood syndrome remains a challenging condition for clinicians, as recommendations for its management are lacking, and the available evidence for the best treatment approach remains controversial. In this paper, four key questions are addressed regarding the management and prevention of Flood syndrome: (1) Which is the best treatment approach—conservative treatment or urgent surgery? (2) How can we establish the individual risk for herniation and possible hernia rupture in cirrhotic patients? (3) How can we prevent umbilical hernia ruptures? And (4) How can we manage these patients in the conditions created by the coronavirus disease 2019 pandemic?

Key Words: Umbilical hernia rupture; Ascites; Cirrhosis; Flood syndrome; COVID-19; Literature review

©The Author(s) 2021. Published by Baishideng Publishing Group Inc. All rights reserved.

on different terms, provided the original work is properly cited and the use is non-commercial. See: <http://creativecommons.org/licenses/by-nc/4.0/>

Manuscript source: Invited manuscript

Specialty type: Gastroenterology and hepatology

Country/Territory of origin: Lithuania

Peer-review report's scientific quality classification

Grade A (Excellent): 0
Grade B (Very good): B
Grade C (Good): 0
Grade D (Fair): 0
Grade E (Poor): 0

Received: February 18, 2021

Peer-review started: February 18, 2021

First decision: May 1, 2021

Revised: May 3, 2021

Accepted: August 3, 2021

Article in press: August 3, 2021

Published online: August 28, 2021

P-Reviewer: Gallo P

S-Editor: Fan JR

L-Editor: Filipodia

P-Editor: Li JH



Core Tip: Flood syndrome is a rare, life-threatening complication of large-volume ascites and end-stage liver disease resulting in a sudden umbilical hernia rupture and spontaneous paracentesis. It remains a challenge for clinicians, as recommendations for the management of this syndrome are lacking. The establishment of the individual risk for herniation and possible hernia rupture, timely prevention, and elective surgical treatment might reduce the risk of complications and the need for urgent surgery.

Citation: Strainiene S, Peculyte M, Strainys T, Stundiene I, Savlan I, Liakina V, Valantinas J. Management of Flood syndrome: What can we do better? *World J Gastroenterol* 2021; 27(32): 5297-5305

URL: <https://www.wjgnet.com/1007-9327/full/v27/i32/5297.htm>

DOI: <https://dx.doi.org/10.3748/wjg.v27.i32.5297>

INTRODUCTION

Ascites is one of the most common complications of liver cirrhosis, manifesting to a variable extent in over 50% of cases. It is also one of the signs of decompensated cirrhosis that is associated with a poor prognosis[1,2]. The occurrence of ascites impairs patients' working and social lives, leads to more frequent hospitalization, requires chronic treatment, and is a direct cause of further complications—such as spontaneous bacterial peritonitis, restrictive ventilatory dysfunction, and abdominal hernias[2]. The incidence of an umbilical hernia (UH) in cirrhotic patients with ascites is approximately 20%, which is 10 times higher than in the general population, and may be up to 40% in cases of large-volume ascites[3-6].

In rare cases, patients with large-volume ascites develop the severe complication of a ruptured UH, resulting in the leakage of ascitic fluid through a skin lesion (Figure 1). This is also known as Flood syndrome, and it was first described by Frank B. Flood in 1961[5,7,8]. This is a life-threatening complication with a significant morbidity and mortality rate of 30%. The rupture of the UH is contributed to by local trauma or a sudden rise in intraabdominal pressure caused by coughing, vomiting, straining, increasing ascites, or heavy lifting[9,10].

Possible complications of the ruptured UH are the evisceration of the small intestine, the incarceration of the bowel, cellulitis, peritonitis, sepsis, and hypotension caused by massive paracentesis[11,12]. The management of Flood syndrome is the subject of much debate due to the lack of high-quality prospective studies and the absence of clear recommendations.

WHICH IS THE BEST TREATMENT APPROACH—CONSERVATIVE TREATMENT OR URGENT SURGERY?

Mortality rates after urgent surgical repair of the hernia vary between 6%–20%, compared to 60%–80% after only supportive care[5,13-15]. The stabilization of the patient's condition, local wound care, optimal control of ascites, correction of the electrolyte imbalance, coagulopathy and thrombocytopenia, and antimicrobial prophylaxis are the critical points for managing a ruptured UH[5,13,16]. The timing of the surgery is also contested, as there is no reliable data on the optimal duration of conservative treatment. The surgical procedure is often delayed due to the high incidence of postoperative complications, such as wound dehiscence and evisceration caused by the re-accumulation of the ascites, bleeding due to coagulopathy, and the inadequate synthesis of clotting factors[5]. The key points of the management of Flood syndrome are summarized in Figure 2.

Pre-operative and surgical management

Evaluation: Patients with liver disease are at a higher risk of surgical and anesthesia-related complications. This risk depends upon the type of liver disease and its severity, the surgical procedure, and the type of anesthesia[17]. Both the model for end-stage liver disease (MELD) score and the Child-Turcotte-Pugh (CTP) classification, combined with the American Society of Anesthesiologists Classification, have been



Figure 1 Flood syndrome. Infected ulceration of the ruptured umbilical hernia in a patient with ascites and liver cirrhosis (personal archives).

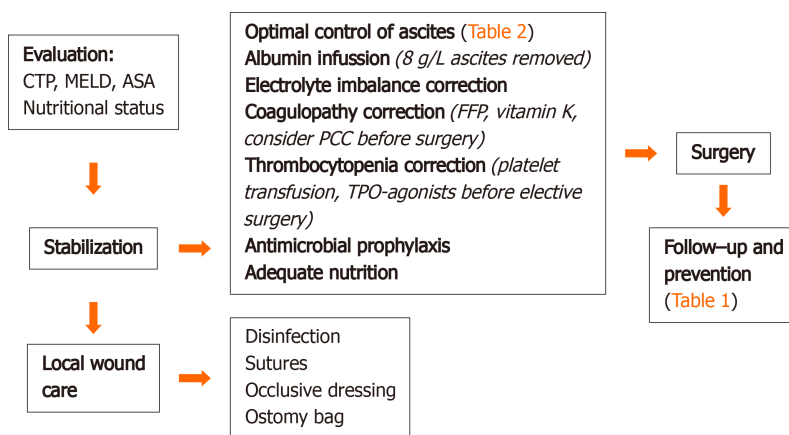


Figure 2 Management of Flood syndrome. ASA: American Society of Anesthesiologists; CTP: Child-Turcotte-Pugh; FFP: Fresh frozen plasma; MELD: Model for end-stage liver disease; PCC: Prothrombin complex concentrate; TPO: Thrombopoietin.

suggested for the stratification of the risks of hernia surgery, but neither appear to be ubiquitously applicable[17]. The main predictor of operative risk in patients with cirrhosis is the CTP classification, but more recent studies suggest that the MELD score might be superior in this regard[18]. Patients with a CTP score > 10 or a MELD score > 20 pose a high risk of postoperative decompensation, including liver failure, worsening encephalopathy, bleeding, wound infection, renal failure, hypoxia, intractable ascites, UH recurrence, and prolonged ileus[5,17,19]. Therefore, it is important to stabilize the patient's condition and to initiate conservative treatment prior to surgery.

Local wound care: Local wound care is one of the first steps in the management of Flood syndrome. Proper disinfection of the area around the skin lesion and control of the peritoneal fluid leakage are crucial in preventing infection and excessive ascites loss. Massive spontaneous paracentesis may lead to severe electrolyte disbalance and paracentesis-induced circulatory dysfunction. Macerations at the UH site might be addressed with two Z sutures and covered with an occlusive dressing. An ostomy bag is used to collect the remaining ascitic fluid.

Stabilization: The optimal control of ascites is one of the main goals in managing a ruptured UH and preventing herniation. Inadequately controlled ascites increase the risk of wound infection and the relapse of the hernia by 75%[5,14]. The main strategies of controlling ascites according to the European Association for the Study of the Liver guidelines are presented in Table 1.

Plasma volume expansion therapy with albumin infusion (8 g/L ascites removed) is recommended to prevent paracentesis-induced circulatory dysfunction in cases with a high volume (5 L of ascites) of spontaneous paracentesis[2]. There is also some promising data regarding cheaper alternative preventive measures, such as colloids,

Table 1 Risk for herniation and possible hernia rupture establishment and prevention of umbilical hernia rupture/reoccurrence

| Risk establishment | Prevention |
|--|---|
| <p>Questions to ask</p> <p>(1) Ascites control: (a) Changes in the abdomen volume; (b) Fluid balance; (c) Weight; (d) Use of prescribed treatment; (2) Nutrition (any signs of malnutrition?); (3) Alcohol intake; (4) Surgeries in the abdomen; (5) Pre-existing hernias; (6) Employment (heavy lifting activities); (7) Comorbidities; (8) Constipation; (9) Medicaments used; and (10) Changes in the abdomen, umbilical area visual appearance</p> | <p>(1) Education; (2) Risk establishment; and (3) Risk management: (a) Lifestyle modification; (b) Management of the underlying liver disease; (c) Management of ascites; (d) Doctor-patient communication; and (e) Communication between medical specialists</p> <p>Patients with UH</p> <p>(1) All the above; (2) Avoid heavy lifting, rapid movement; (3) Abdominal surgeon consult; and (4) Elective surgery in stable patients</p> |

UH: Umbilical hernia.

vasoconstrictors (midodrine, terlipressin), and lowering the standard doses of the albumin, but these approaches are not yet recommended by international guidelines [20-23].

It is also essential to evaluate the patient's nutritional status, as these patients are often cachectic and malnourished. A protein-rich diet (2000 kcal/d, with 40-50 g of protein) is recommended to address the patient's nutritional needs. The patient's dietary needs might be covered orally with additional protein supplementation or *via* enteral feeding. Vitamin B group supplementation is also mandatory, especially in patients with alcohol-related cirrhosis [24].

Patients with liver disease undergoing surgery might be at risk of both thrombosis and bleeding, due to dysregulated coagulation and a diminished hemostatic reserve [25-27]. Therefore, cirrhotic patients need to be carefully assessed for the risk of bleeding before surgery. Prothrombin time, international normalized ratio (INR), and platelet count have been formally recommended for the purpose of determining coagulation status in clinical practice. However, the relationship between prothrombin time/INR and the risk of bleeding in cirrhosis is disputable. Isolated evaluations of bleeding or clotting time are also of little prognostic value in patients with liver diseases during pre-operative screening [28].

Fresh frozen plasma and vitamin K therapy (phytomenadione 10 mg/mL) are currently used to address coagulopathy as a standard of care to manage active bleeding or prophylaxis before invasive procedures [29,30]. In cases of urgent surgery, prothrombin complex concentrate (PCC) might be used to prevent bleeding in selected patients with severe coagulopathy. Drebes *et al* [26] recently reviewed PCC's clinical use in patients with acute/chronic liver disease in a retrospective single-center study [26]. In their study, 20-25 IU/kg of PCC was administered to patients with INR 4, and 30 IU/kg for patients with INR 4. PCC therapy effectively improved the results of the coagulation test, with no evidence of an increased risk of thromboembolism. These findings highlighted the need to assess further PCC's potential role as a form of hemostatic therapy in liver disease patients. The use of PCC before urgent surgery should therefore be considered.

Thrombocytopenia is another issue associated with liver cirrhosis. Prophylactical or periprocedural platelet transfusion, splenic artery embolization, transjugular intrahepatic portosystemic shunts, and a splenectomy are well documented methods of treating thrombocytopenia. Recently, thrombopoietin receptor agonists (avatrombopag and lusutrombopag) were approved by the United States Food and Drug Administration for the non-invasive treatment of thrombocytopenia in patients with chronic liver disease undergoing a surgical procedure. These new drugs are considered safe and effective alternatives to platelet transfusions [31,32].

Surgical approach: The importance of the surgical treatment of the UH rupture in patients with ascites was first described by Kirkpatrick and Schubert, who calculated that the mortality rate was 60% in conservatively treated patients, compared to 14% in those who underwent herniorrhaphy [15]. However, there is a much higher risk of complications and a higher morbidity rate after the urgent surgical repair of an UH [33, 34].

In terms of the surgical method, most authors suggest that the best option seems to be a primary closure with non-absorbable sutures [5,9,14]. Synthetic meshes may not be an appropriate technique in patients with ascites due to a higher risk of infection and a

possible ingrowth of the mesh[5,35]. However, a single randomized study of 80 patients demonstrated that the use of a synthetic mesh in cirrhotic patients with complicated UHs was related to a lower rate of hernia reoccurrence[16]. UHs reoccurred in 14.2% of patients who underwent suture repair, compared to 2.7% in the mesh repair group ($P < 0.05$). The incidence of infection at the surgical site was not significant in either group: 8.5% in the conventional fascial repair group and 16.2% in the mesh repair group ($P > 0.05$). However, the mean duration of hospital stay was significantly longer in the mesh repair group ($P < 0.05$)[16].

Finally, it is essential to treat these patients in a tertiary center with specialized surgical and intensive care units due to the increased risk of infection, bleeding, and postoperative decompensation of cirrhosis[36]. Smaller hospitals cannot provide appropriate care because of their lack of experience[7,37]. In such cases, several alternative methods are described, including the successful placement of a pig-tail drain with no recurrence of ascitic fluid leakage and the injection of fibrin glue into the defect to stem drainage[38-40]. These approaches allow natural wound healing, though they remain temporary solutions. Ulceration or necrosis over a UH should be considered a dangerous sign; a warning of an impending rupture, and such patients should be referred to urgent surgical treatment[11].

HOW CAN WE ESTABLISH THE INDIVIDUAL RISK FOR HERNIATION AND POSSIBLE HERNIA RUPTURE IN CIRRHOTIC PATIENTS?

The main etiological factors for the development of UHs are ascites, weakened abdominal wall muscles, malnutrition, and the recanalization of pre-existing openings promoted by increased abdominal pressure[5,6,37].

A UH rupture is usually the result of multiple risk factors. Alcohol consumption is one of the major causes of decompensated cirrhosis with ascites. Cirrhosis alone causes malnutrition and sarcopenia, resulting in weakened abdominal wall muscles. Harmful alcohol consumption is also associated with nutritional deficiencies, including protein-calorie malnutrition and cachexia[24,41]. It is also necessary to consider comorbidities that can put limitations on the patient's physical activity and nutrition, such as epilepsy, depression, and related medication (antiepileptics, antidepressants). Previous abdominal surgeries and pre-existing hernias are also severe risk factors for UHs due to the presence of a weakened abdominal wall. Therefore, careful anamnesis is essential (Table 1).

HOW CAN WE PREVENT UH RUPTURES? HOW CAN WE AVOID UH REOCCURRENCE?

General measures for UH prevention consist of the continuous education of the patient and their family members, lifestyle modification, and the avoidance of alcohol, tobacco, constipation, and heavy lifting. Hernia trusses are controversial as they may worsen the hernia, and they should only be used temporarily, if at all[42].

The main methods of preventing UH occurrence and rupture specifically for cirrhotic patients are the optimal control of ascites using medical therapies or regular paracentesis as *per* general guidelines (Table 2)[2,5,17].

The management of underlying liver disease improves the outlook for the reversible components of hepatic decompensation. In most patients with alcoholic cirrhosis, abstinence may reduce or even normalize portal pressure, resulting in the increased ease of treatment of ascites or their disappearance altogether[1]. Alcohol-induced liver cirrhosis is a double pathology, hence the management of both liver cirrhosis and dependence is essential. The main treatment methods are total abstinence, correction of malnutrition, vitamins, and microelements, and the primary and secondary prophylaxis of the complications of cirrhosis. Specific treatment with S-adenosyl-L-methionine, propyluracil, colchicine, and anabolic steroids is debated [41].

It is also essential to monitor carefully the patient with ascites and to consider elective UH repair as soon as herniation appears. This can help to prevent UH rupture and minimize the number of postoperative complications. The watch-and-wait policy was previously applied to patients with ascites and UHs, and surgery was performed only after the occurrence of complications[6]. However, in recent decades, some changes have occurred as novel studies have demonstrated that elective UH repair in

Table 2 Summary of the guidelines on the management of ascites

| | Treatment |
|--|--|
| Main measures | Moderate restriction of sodium intake, 80–120 mmol/d (4.6–6.9 g of salt/d) Adequate nutrition: Protein-rich diet (2000 kcal/d, protein–40–50 g/d), vitamin therapy Correction of electrolyte imbalance Adequate fluid intake: No restriction needed in patients with normal serum sodium concentration; in hyponatremic patients (< 130 mmol/L), restrict fluid intake to 1.0–1.5 L/d Daily track of weight (or measure fluid intake and diuresis) The maximum recommended weight loss during diuretic therapy: (1) 0.5 kg/d in patients without edema; and (2) 1 kg/d in patients with edema |
| Mild and moderate ascites (grade I–II ^a) | Aldosterone antagonists: Spironolactone 50–100 mg/d (maximum of 400 mg/d) ± loop diuretics: Furosemide 20–40 mg/d (maximum of 160 mg/d) Torsemide (10–40 mg/d) if no response to furosemide Distal diuretics: Amiloride 5–20 mg/d; triamterene 100 mg 2 k./d. (if aldosterone antagonists are not tolerated) Combined dosage of diuretics: Spironolactone 50–100–200–300–400 mg/d (in 100 mg steps) + furosemide 20–40–80–120–160 mg/d (in 40 mg steps) (or adequate doses of other diuretics) |
| Large ascites (grade III ^a) | LVP Albumin infusion (8 g/L of ascitic fluid removed) Minimal effective dose of diuretics to prevent the re-accumulation of ascites after LVP |
| Refractory ascites | Repeated partial or large volume paracentesis + albumin infusion Withdrawn diuretics Transjugular intrahepatic portosystemic shunt Alternative drugs: (1) α1 adrenergic agonists–midodrine 7.5 mg 3 times/d; (2) Vasopressin analog–terlipressin 1–2 mg/d intravenous; and (3) α2 adrenergic agonists–clonidine Alfapump system Liver transplantation |

LVP: Large volume paracentesis.

patients with liver cirrhosis and ascites can be performed with less morbidity. Conservative management leads to a higher incidence of incarceration, with subsequent hernia repair in the emergency setting[34,43,44]. Marsman *et al*[43] compared the outcome of operative and conservative treatment in patients with liver cirrhosis and ascites complicated by UHs. Elective hernia repair was successful without complications or recurrence in around 70.5% of patients, while complications such as wound-related problems (superficial wound infection, necrosis, hematoma) were noted in 17.6% of cases. Initial conservative management was effective in only 23% of patients [41]. A single-center prospective study on patients listed for liver transplantation showed that elective UH repair is preferable to urgent repair in patients with cirrhosis and ascites[44].

Therefore, elective herniorrhaphy is now recommended in patients with cirrhosis and ascites after the patient is stabilized using optimal medical management, to prevent an emergent presentation of incarceration or UH rupture[17,33]. There are several contraindications for elective surgery in patients with liver disease, such as acute liver failure, acute renal failure, acute viral hepatitis, alcoholic hepatitis, cardiomyopathy, hypoxemia, severe coagulopathy, and thrombocytopenia (despite treatment)[17].

Efforts should be taken to avoid recurrent ascites in the postoperative period, as they lead to impaired wound healing and possible risks of dehiscence[17]. Measures for preventing the reoccurrence of the UH after surgery are the same as preventive methods against UH rupture (Table 1).

According to the literature, just 33% of patients with ascites receive only treatments that are supported by guidelines and high-quality evidence[43]. Furthermore, over one-third of patients hospitalized due to cirrhosis complications are readmitted within 1 mo of discharge[45,46]. Many patients do not seek proper care until decompensation,

and some do not follow or cannot afford treatment. Clearly, the current management of cirrhosis leaves room for improvement, especially during the conditions of the coronavirus disease 2019 (COVID-19) pandemic.

HOW CAN WE MANAGE PATIENTS IN THE CONDITIONS CREATED BY THE COVID-19 PANDEMIC?

Clinicians must be aware that the COVID-19 pandemic has negatively impacted the care of patients with chronic liver disease[47]. This might result in a higher incidence of decompensated cirrhosis when patients do not receive treatment correction on time. There is also an increased risk of a growing incidence of alcohol-induced and non-alcoholic fatty liver disease-related cirrhosis. Patient care is challenging; along with telemedicine and the near-impossibility of physical examination, clinicians must be more accurate and foresee potential future issues. Moreover, not every patient can or indeed wants to use telemedicine, as many patients represent vulnerable cohorts. However, there are some steps that can be taken to address these challenges.

First, we must make more effort than ever before to encourage and educate patients and their relatives. Visual methods can be used, such as written instructions for the patient (in a patient-friendly form), educational video seminars, and other materials. We must ask key questions (during teleconsultation) to establish the patient's risks (Table 1), and we must cooperate. Cooperation between patient and doctor and communication between different medical specialists is essential in managing patients with liver cirrhosis and ascites. All clinicians must be aware of the possible complications of ascites and refer the patient to a specialist consultation in a timely manner.

CONCLUSION

The rupture of the UH and spontaneous paracentesis in patients with decompensated cirrhosis is a rare and dangerous complication that remains a challenge for gastroenterologists, surgeons, and anesthesiologists. The stabilization of the patient's overall condition, adequate control of ascites, and local wound care are the main goals of therapy before the primary repair of the hernia. Gastroenterologists and general practitioners should establish the risk to the individual patient regarding herniation and possible hernia rupture *via* careful follow-up. Timely prevention of UH and elective surgical treatment can reduce the risk of complications and the need for urgent surgery, decrease overall hospitalization time, and improve the patient's quality of life.

ACKNOWLEDGEMENTS

We would like to thank Vilnius University Hospital's Santaros Clinic for their close collaboration.

REFERENCES

- 1 **Biecker E.** Diagnosis and therapy of ascites in liver cirrhosis. *World J Gastroenterol* 2011; **17**: 1237-1248 [PMID: 21455322 DOI: 10.3748/wjg.v17.i10.1237]
- 2 **European Association for the Study of the Liver.** European Association for the Study of the Liver. EASL Clinical Practice Guidelines for the management of patients with decompensated cirrhosis. *J Hepatol* 2018; **69**: 406-460 [PMID: 29653741 DOI: 10.1016/j.jhep.2018.03.024]
- 3 **Coelho JC, Claus CM, Campos AC, Costa MA, Blum C.** Umbilical hernia in patients with liver cirrhosis: A surgical challenge. *World J Gastrointest Surg* 2016; **8**: 476-482 [PMID: 27462389 DOI: 10.4240/wjgs.v8.i7.476]
- 4 **Dumas M, Breton JC, Pestre Alexandre M, Girard PL, Giordano C.** [Current status of the therapy of human African trypanosomiasis]. *Presse Med* 1985; **14**: 253-256 [PMID: 3157106 DOI: 10.1007/s10029-019-02056-x]
- 5 **Chatzizacharias NA, Bradley JA, Harper S, Butler A, Jah A, Huguet E, Praseedom RK, Allison M, Gibbs P.** Successful surgical management of ruptured umbilical hernias in cirrhotic patients. *World J Gastroenterol* 2015; **21**: 3109-3113 [PMID: 25780312 DOI: 10.3748/wjg.v21.i10.3109]
- 6 **Salamone G, Licari L, Guercio G, Campanella S, Falco N, Scerrino G, Bonventre S, Geraci G,**

- Cocorullo G, Gulotta G. The abdominal wall hernia in cirrhotic patients: a historical challenge. *World J Emerg Surg* 2018; **13**: 35 [PMID: 30065783 DOI: 10.1186/s13017-018-0196-z]
- 7 **Malespin M**, Moore CM, Fialho A, de Melo SW Jr, Benyashvili T, Kothari AN, di Sabato D, Kallwitz ER, Cotler SJ, Lu AD. Case Series of 10 Patients with Cirrhosis Undergoing Emergent Repair of Ruptured Umbilical Hernias: Natural History and Predictors of Outcomes. *Exp Clin Transplant* 2019; **17**: 210-213 [PMID: 28697716 DOI: 10.6002/ect.2017.0086]
 - 8 **FLOOD FB**. Spontaneous perforation of the umbilicus in Laennec's cirrhosis with massive ascites. *N Engl J Med* 1961; **264**: 72-74 [PMID: 13700320 DOI: 10.1056/NEJM196101122640204]
 - 9 **Good DW**, Royds JE, Smith MJ, Neary PC, Eguare E. Umbilical hernia rupture with evisceration of omentum from massive ascites: a case report. *J Med Case Rep* 2011; **5**: 170 [PMID: 21539740 DOI: 10.1186/1752-1947-5-170]
 - 10 **Cobb WS**, Burns JM, Kercher KW, Matthews BD, James Norton H, Todd Heniford B. Normal intraabdominal pressure in healthy adults. *J Surg Res* 2005; **129**: 231-235 [PMID: 16140336 DOI: 10.1016/j.jss.2005.06.015]
 - 11 **Choo EK**, McElroy S. Spontaneous bowel evisceration in a patient with alcoholic cirrhosis and an umbilical hernia. *J Emerg Med* 2008; **34**: 41-43 [PMID: 17976794 DOI: 10.1016/j.jemermed.2007.03.035]
 - 12 **DeLuca IJ**, Grossman ME. Flood syndrome. *JAAD Case Rep* 2015; **1**: 5-6 [PMID: 27075124 DOI: 10.1016/j.jidcr.2014.09.003]
 - 13 **Fagan SP**, Awad SS, Berger DH. Management of complicated umbilical hernias in patients with end-stage liver disease and refractory ascites. *Surgery* 2004; **135**: 679-682 [PMID: 15179375 DOI: 10.1016/j.surg.2003.12.010]
 - 14 **Telem DA**, Schiano T, Divino CM. Complicated hernia presentation in patients with advanced cirrhosis and refractory ascites: management and outcome. *Surgery* 2010; **148**: 538-543 [PMID: 20346479 DOI: 10.1016/j.surg.2010.01.002]
 - 15 **Kirkpatrick S**, Schubert T. Umbilical hernia rupture in cirrhotics with ascites. *Dig Dis Sci* 1988; **33**: 762-765 [PMID: 3286159 DOI: 10.1007/BF01540442]
 - 16 **Ammar SA**. Management of complicated umbilical hernias in cirrhotic patients using permanent mesh: randomized clinical trial. *Hernia* 2010; **14**: 35-38 [PMID: 19727551 DOI: 10.1007/s10029-009-0556-4]
 - 17 **Northup PG**, Friedman LS, Kamath PS. AGA Clinical Practice Update on Surgical Risk Assessment and Perioperative Management in Cirrhosis: Expert Review. *Clin Gastroenterol Hepatol* 2019; **17**: 595-606 [PMID: 30273751 DOI: 10.1016/j.cgh.2018.09.043]
 - 18 **O'Leary JG**, Friedman LS. Predicting surgical risk in patients with cirrhosis: from art to science. *Gastroenterology* 2007; **132**: 1609-1611 [PMID: 17428482 DOI: 10.1053/j.gastro.2007.03.016]
 - 19 **Friedman LS**. Surgery in the patient with liver disease. *Trans Am Clin Climatol Assoc* 2010; **121**: 192-204; discussion 205 [PMID: 20697561]
 - 20 **Moreau R**, Asselah T, Condat B, de Kerguenec C, Pessione F, Bernard B, Poynard T, Binn M, Grangé JD, Valla D, Lebre C. Comparison of the effect of terlipressin and albumin on arterial blood volume in patients with cirrhosis and tense ascites treated by paracentesis: a randomised pilot study. *Gut* 2002; **50**: 90-94 [PMID: 11772973 DOI: 10.1136/gut.50.1.90]
 - 21 **Singh V**, Kumar R, Nain CK, Singh B, Sharma AK. Terlipressin vs albumin in paracentesis-induced circulatory dysfunction in cirrhosis: a randomized study. *J Gastroenterol Hepatol* 2006; **21**: 303-307 [PMID: 16460491 DOI: 10.1111/j.1440-1746.2006.04182.x]
 - 22 **Tandon P**, Tsuyuki RT, Mitchell L, Hoskinson M, Ma MM, Wong WW, Mason AL, Gutfreund K, Bain VG. The effect of 1 mo of therapy with midodrine, octreotide-LAR and albumin in refractory ascites: a pilot study. *Liver Int* 2009; **29**: 169-174 [PMID: 18492024 DOI: 10.1111/j.1478-3231.2008.01778.x]
 - 23 **Alsebaey A**, Rewisha E, Waked I. Paracentesis-induced circulatory dysfunction: are there albumin alternatives? *Egypt Liver J* 2020; **10**: 39 [DOI: 10.1186/s43066-020-00047-7]
 - 24 **Plauth M**, Cabré E, Riggio O, Assis-Camilo M, Pirlich M, Kondrup J, DGEM (German Society for Nutritional Medicine), Ferenci P, Holm E, Vom Dahl S, Müller MJ, Nolte W; ESPEN (European Society for Parenteral and Enteral Nutrition). ESPEN Guidelines on Enteral Nutrition: Liver disease. *Clin Nutr* 2006; **25**: 285-294 [PMID: 16707194 DOI: 10.1016/j.clnu.2006.01.018]
 - 25 **Monroe DM**, Hoffman M. The coagulation cascade in cirrhosis. *Clin Liver Dis* 2009; **13**: 1-9 [PMID: 19150304 DOI: 10.1016/j.cld.2008.09.014]
 - 26 **Drebes A**, de Vos M, Gill S, Fosbury E, Mallett S, Burroughs A, Agarwal B, Patch D, Chowdary P. Prothrombin Complex Concentrates for Coagulopathy in Liver Disease: Single-Center, Clinical Experience in 105 Patients. *Hepatol Commun* 2019; **3**: 513-524 [PMID: 30976742 DOI: 10.1002/hep4.1293]
 - 27 **Agarwal B**, Wright G, Gatt A, Riddell A, Vemala V, Mallett S, Chowdary P, Davenport A, Jalan R, Burroughs A. Evaluation of coagulation abnormalities in acute liver failure. *J Hepatol* 2012; **57**: 780-786 [PMID: 22735303 DOI: 10.1016/j.jhep.2012.06.020]
 - 28 **Harrison MF**. The Misunderstood Coagulopathy of Liver Disease: A Review for the Acute Setting. *West J Emerg Med* 2018; **19**: 863-871 [PMID: 30202500 DOI: 10.5811/westjem.2018.7.37893]
 - 29 **Shah NL**, Intagliata NM, Northup PG, Argo CK, Caldwell SH. Procoagulant therapeutics in liver disease: a critique and clinical rationale. *Nat Rev Gastroenterol Hepatol* 2014; **11**: 675-682 [PMID: 25023035 DOI: 10.1038/nrgastro.2014.121]
 - 30 **Lee WM**, Stravitz RT, Larson AM. Introduction to the revised American Association for the Study of

- Liver Diseases Position Paper on acute liver failure 2011. *Hepatology* 2012; **55**: 965-967 [PMID: 22213561 DOI: 10.1002/hep.25551]
- 31 **Saab S**, Brown RS Jr. Management of Thrombocytopenia in Patients with Chronic Liver Disease. *Dig Dis Sci* 2019; **64**: 2757-2768 [PMID: 31011942 DOI: 10.1007/s10620-019-05615-5]
 - 32 **Khemichian S**, Terrault NA. Thrombopoietin Receptor Agonists in Patients with Chronic Liver Disease. *Semin Thromb Hemost* 2020; **46**: 682-692 [PMID: 32820479 DOI: 10.1055/s-0040-1715451]
 - 33 **Odom SR**, Gupta A, Talmor D, Novack V, Sagy I, Evenson AR. Emergency hernia repair in cirrhotic patients with ascites. *J Trauma Acute Care Surg* 2013; **75**: 404-409 [PMID: 24089110 DOI: 10.1097/TA.0b013e31829e2313]
 - 34 **Gray SH**, Vick CC, Graham LA, Finan KR, Neumayer LA, Hawn MT. Umbilical herniorrhaphy in cirrhosis: improved outcomes with elective repair. *J Gastrointest Surg* 2008; **12**: 675-681 [PMID: 18270782 DOI: 10.1007/s11605-008-0496-9]
 - 35 **Smith R**. Hernia Repair in Patients with Cirrhosis. In: Lim R, editor. *Multidisciplinary Approaches to Common Surgical Problems*. Springer, 2019: 267-281 [DOI: 10.1007/978-3-030-12823-4]
 - 36 **Bhangui P**, Laurent A, Amathieu R, Azoulay D. Assessment of risk for non-hepatic surgery in cirrhotic patients. *J Hepatol* 2012; **57**: 874-884 [PMID: 22634123 DOI: 10.1016/j.jhep.2012.03.037]
 - 37 **Andraus W**, Pinheiro RS, Lai Q, Haddad LBP, Nacif LS, D'Albuquerque LAC, Lerut J. Abdominal wall hernia in cirrhotic patients: emergency surgery results in higher morbidity and mortality. *BMC Surg* 2015; **15**: 65 [PMID: 25990110 DOI: 10.1186/s12893-015-0052-y]
 - 38 **Sadik KW**, Bonatti H, Schmitt T. Injection of fibrin glue for temporary treatment of an ascites leak from a ruptured umbilical hernia in a patient with liver cirrhosis. *Surgery* 2008; **143**: 574 [PMID: 18374059 DOI: 10.1016/j.surg.2007.12.005]
 - 39 **Melcher ML**, Lobato RL, Wren SM. A novel technique to treat ruptured umbilical hernias in patients with liver cirrhosis and severe ascites. *J Laparoendosc Adv Surg Tech A* 2003; **13**: 331-332 [PMID: 14617394 DOI: 10.1089/109264203769681745]
 - 40 **Nguyen ET**, Tuddud-Hans LA. Flood Syndrome: Spontaneous Umbilical Hernia Rupture Leaking Ascitic Fluid-A Case Report. *Perm J* 2017; **21**: 16-152 [PMID: 28678688 DOI: 10.7812/TPP/16-152]
 - 41 **Singal AK**, Bataller R, Ahn J, Kamath PS, Shah VH. ACG Clinical Guideline: Alcoholic Liver Disease. *Am J Gastroenterol* 2018; **113**: 175-194 [PMID: 29336434 DOI: 10.1038/ajg.2017.469]
 - 42 **Kingsnorth A**, LeBlanc K. Hernias: inguinal and incisional. *Lancet* 2003; **362**: 1561-1571 [PMID: 14615114 DOI: 10.1016/S0140-6736(03)14746-0]
 - 43 **Marsman HA**, Heisterkamp J, Halm JA, Tilanus HW, Metselaar HJ, Kazemier G. Management in patients with liver cirrhosis and an umbilical hernia. *Surgery* 2007; **142**: 372-375 [PMID: 17723889 DOI: 10.1016/j.surg.2007.05.006]
 - 44 **Eker HH**, van Ramshorst GH, de Goede B, Tilanus HW, Metselaar HJ, de Man RA, Lange JF, Kazemier G. A prospective study on elective umbilical hernia repair in patients with liver cirrhosis and ascites. *Surgery* 2011; **150**: 542-546 [PMID: 21621237 DOI: 10.1016/j.surg.2011.02.026]
 - 45 **Kanwal F**, Kramer JR, Buchanan P, Asch SM, Assioun Y, Bacon BR, Li J, El-Serag HB. The quality of care provided to patients with cirrhosis and ascites in the Department of Veterans Affairs. *Gastroenterology* 2012; **143**: 70-77 [PMID: 22465432 DOI: 10.1053/j.gastro.2012.03.038]
 - 46 **Volk ML**, Tocco RS, Bazick J, Rakoski MO, Lok AS. Hospital readmissions among patients with decompensated cirrhosis. *Am J Gastroenterol* 2012; **107**: 247-252 [PMID: 21931378 DOI: 10.1038/ajg.2011.314]
 - 47 **Boettler T**, Newsome PN, Mondelli MU, Maticic M, Cordero E, Cornberg M, Berg T. Care of patients with liver disease during the COVID-19 pandemic: EASL-ESCMID position paper. *JHEP Rep* 2020; **2**: 100113 [PMID: 32289115 DOI: 10.1016/j.jhepr.2020.100113]

Radiomics and machine learning applications in rectal cancer: Current update and future perspectives

Arnaldo Stanzione, Francesco Verde, Valeria Romeo, Francesca Boccadifuoco, Pier Paolo Mainenti, Simone Maurea

ORCID number: Arnaldo Stanzione 0000-0002-7905-5789; Francesco Verde 0000-0002-9823-4678; Valeria Romeo 0000-0002-1603-6396; Francesca Boccadifuoco 0000-0001-6003-362X; Pier Paolo Mainenti 0000-0003-3592-808X; Simone Maurea 0000-0002-8269-3765.

Author contributions: Stanzione A, Verde F, Romeo V, Boccadifuoco F, Mainenti PP, and Maurea S equally contributed to this paper with conception and design of the study, literature review and analysis, drafting and critical revision and editing, and final approval of the final version.

Conflict-of-interest statement: The authors declare that they have no conflicting interests.

Open-Access: This article is an open-access article that was selected by an in-house editor and fully peer-reviewed by external reviewers. It is distributed in accordance with the Creative Commons Attribution NonCommercial (CC BY-NC 4.0) license, which permits others to distribute, remix, adapt, build upon this work non-commercially, and license their derivative works on different terms, provided the original work is properly cited and the use is non-commercial. See: <http://creativecommons.org/License>

Arnaldo Stanzione, Francesco Verde, Valeria Romeo, Francesca Boccadifuoco, Simone Maurea, Department of Advanced Biomedical Sciences, University of Naples "Federico II", Naples 80131, Italy

Pier Paolo Mainenti, Institute of Biostructures and Bioimaging, National Council of Research, Napoli 80131, Italy

Corresponding author: Valeria Romeo, MD, Academic Research, Doctor, Research Fellow, Department of Advanced Biomedical Sciences, University of Naples "Federico II", Via Sergio Pansini 5, Naples 80131, Italy. valeria.romeo@unina.it

Abstract

The high incidence of rectal cancer in both sexes makes it one of the most common tumors, with significant morbidity and mortality rates. To define the best treatment option and optimize patient outcome, several rectal cancer biological variables must be evaluated. Currently, medical imaging plays a crucial role in the characterization of this disease, and it often requires a multimodal approach. Magnetic resonance imaging is the first-choice imaging modality for local staging and restaging and can be used to detect high-risk prognostic factors. Computed tomography is widely adopted for the detection of distant metastases. However, conventional imaging has recognized limitations, and many rectal cancer characteristics remain assessable only after surgery and histopathology evaluation. There is a growing interest in artificial intelligence applications in medicine, and imaging is by no means an exception. The introduction of radiomics, which allows the extraction of quantitative features that reflect tumor heterogeneity, allows the mining of data in medical images and paved the way for the identification of potential new imaging biomarkers. To manage such a huge amount of data, the use of machine learning algorithms has been proposed. Indeed, without prior explicit programming, they can be employed to build prediction models to support clinical decision making. In this review, current applications and future perspectives of artificial intelligence in medical imaging of rectal cancer are presented, with an imaging modality-based approach and a keen eye on unsolved issues. The results are promising, but the road ahead for translation in clinical practice is rather long.

Key Words: Rectal cancer; Radiomics; Radiogenomics; Artificial intelligence; Machine

[s/by-nc/4.0/](#)**Manuscript source:** Invited manuscript**Specialty type:** Radiology, nuclear medicine and medical imaging**Country/Territory of origin:** Italy**Peer-review report's scientific quality classification**

Grade A (Excellent): A, A

Grade B (Very good): B

Grade C (Good): 0

Grade D (Fair): 0

Grade E (Poor): 0

Received: January 27, 2021**Peer-review started:** January 27, 2021**First decision:** March 7, 2021**Revised:** March 13, 2021**Accepted:** July 22, 2021**Article in press:** July 22, 2021**Published online:** August 28, 2021**P-Reviewer:** Alves A, De Ridder M**S-Editor:** Liu M**L-Editor:** Filipodia**P-Editor:** Liu JH

learning; Deep learning

©The Author(s) 2021. Published by Baishideng Publishing Group Inc. All rights reserved.

Core Tip: Rectal cancer is a common malignancy requiring a multidisciplinary approach to ensure the best clinical management. Diagnostic imaging has contributed to increased survival rates and provided crucial information on the course of rectal cancer patients. Artificial intelligence, and in particular radiomics and machine learning, are promising techniques that could further enhance the value of medical imaging, allowing the building of decision support tools based on quantitative data. We herein present and discuss the potential role of artificial intelligence in rectal cancer applied to different medical imaging modalities.

Citation: Stanzione A, Verde F, Romeo V, Boccadifuoco F, Mainenti PP, Maurea S. Radiomics and machine learning applications in rectal cancer: Current update and future perspectives. *World J Gastroenterol* 2021; 27(32): 5306-5321

URL: <https://www.wjgnet.com/1007-9327/full/v27/i32/5306.htm>

DOI: <https://dx.doi.org/10.3748/wjg.v27.i32.5306>

INTRODUCTION

In 2020, more than 40,000 cases of rectal cancer (RC) were expected in the United States alone, with a higher incidence in men than in women and a median age at diagnosis of 63 years[1]. However, over the past years there has been an improvement in RC management associated with a reduction of mortality and higher survival rates, mainly related to earlier diagnosis and more effective treatment[2]. While endoscopy represents the gold standard for RC diagnosis, there are several factors to be considered that influence prognosis and therapeutic strategy, including local tumor extent (T), lymph nodes status (N) and presence of distant metastases (M)[3]. Indeed, radical surgery with curative intent (*i.e.* total mesorectal excision, TME) is recommended as a first-line strategy in patients with locally confined disease after neoadjuvant chemoradiotherapy (nCRT) for locally advanced RC (LARC). Metastatic patients, on the other hand, usually undergo systemic therapies such as chemotherapy, targeted therapy, or immunotherapy[4,5]. Diagnostic imaging plays a crucial role for pretreatment disease staging, with a multimodal approach commonly being necessary [6]. Magnetic resonance imaging (MRI) is regarded as the most valuable imaging modality for primary loco-regional staging of RC and restaging after nCRT[7,8]. Computed tomography (CT) scans are routinely performed to detect distant metastases, with the most common metastatic sites being the liver and lungs[2]. Currently, hybrid imaging by positron emission tomography/CT (PET/CT) could provide useful prognostic data for RC, even if its role still remains to be defined[6,9]. Likewise, the potential of simultaneously acquired PET and MRI still has to be explored[10]. However, conventional image assessment has recognized limitations that are driving the research towards the identification and validation of novel strategies to further increase the value of diagnostic imaging[11-13]. In this setting, a post processing quantitative technique known as radiomics appears particularly promising, with encouraging evidence collected in recent years[14,15]. Radiomics has been frequently and successfully coupled with artificial intelligence (AI), and in particular machine learning (ML) approaches in the field of oncologic imaging[16-19]. This review aims to introduce readers to the concepts of radiomics and ML and to present the state-of-the-art of RC radiomics-ML applications, with an imaging modality-based approach, highlighting their strengths and drawbacks.

RADIOMICS AND ML: WHAT, WHY, AND HOW

Trying to quantify what is visually assessed in medical imaging is a rather difficult task, and radiologists have traditionally provided qualitative information and semi-quantitative data in their reports[20]. However, this leads to a large amount of unused

data remaining hidden in medical images[21]. Furthermore, semantic descriptors of cancer imaging phenotype (*e.g.*, “central necrosis”, “irregular margin”, and “diffusely heterogeneous”) are prone to poor intra- and interobserver reliability, experience dependent, and might not significantly reflect actual tumor biology[22]. Indeed, tumors are not considered to be homogeneous entities but instead composed of various cell clones with biologically relevant differences[23]. Radiomics allows the conversion of images into mineable data with the high-throughput extraction of quantitative parameters (*i.e.* radiomics features) that capture the heterogeneities and provide important information on cancer phenotype[24]. Radiomics is a multistep process beginning with image acquisition and followed by image segmentation, which is the two- or three-dimensional delineation of the region of interest (ROI), usually represented by the primary tumor. Image segmentation can be manual, performed by a human operator; semiautomatic, performed by AI and manually adjusted; or automatic, exclusively performed by AI[25]. Subsequently, hundreds of radiomics features can be extracted from the ROI using specifically designed formulae conveying different information, including shape, first-order (based on the distribution of pixel intensities), second and higher-order features (accounting for pixel intensities spatial distribution)[26]. Correlating radiomics features to the outcomes of interest is the endpoint of radiomics, and many believe it could open the gateway to precision medicine[27,28]. However, such a huge amount of data can be more easily handled by AI rather than traditional statistical methods[21]. Indeed, ML is a branch of AI focused on algorithms that can be trained for a task they were not specifically programmed to perform[29]. The algorithms are essentially used for classification problems, with the main oncologic imaging application being decision support in various settings that include detection, characterization, and monitoring[30-32]. To properly train an ML algorithm, “the curse of dimensionality,” which is a set of issues arising when working with a number of features much higher than the patient population must be avoided. Feature reduction can be achieved in several ways that may also be combined to achieve better results[33,34]. Indeed, an excessive number of features increases the chances of finding nongeneralizable correlations (*i.e.* overfitting). On the other hand, complex relationships might need more features to build a proper prediction model [35]. Finally, trained ML classifiers need to be tested to verify generalizability on external data not used in the training process and possibly provided by different institutions[36]. A kind of ML algorithm called deep learning (DL), based on neural networks (NN), does not necessarily require image segmentation and learns autonomously the best features for performing data classification[37]. A brief description of the most commonly applied ML algorithms in RC radiomics can be found in [Table 1](#).

RADIOMICS AND ML APPLICATIONS IN RC: MRI

Thanks to its superb contrast resolution, MRI plays a pivotal role in the diagnostic pathway of RC patients, particularly for primary local staging and restaging after treatment[38]. Indeed, in addition to T and N staging, MRI provides valuable information such as the circumferential resection margin, defined as the minimum distance between the tumor and the mesorectal fascia, as well as extramural venous invasion (EMVI), an independent negative prognostic factor for RC[39,40]. In the following paragraphs, radiomics and ML approaches proposed to further increase the value of MRI in the assessment of RC are described.

Staging

Currently, MRI represents the first-choice imaging modality for determining RC local extent. However, the assessment of T stage is a challenging task, and staging failures often occur in the differentiation between T2 in which the tumor involves the muscularis propria and T3, in which the tumor involves perirectal tissue beyond the muscularis propria[41]. Decision support tools based on MRI radiomics and ML might be able to aid radiologists in this endeavor[42-44]. Using multilayer perceptron, a DL model powered by T2-weighted (T2w) radiomics features from pretreatment MRI, Ma *et al*[42] were able to discriminate between patients with T1 or T2 and those with T3 or T4 RC with 76% sensitivity and 74% specificity. Similar results were found using diffusion-weighted imaging (DWI) to extract radiomics features in a recent investigation on 115 patients. A logistic regression (LR) algorithm reached a sensitivity of 79% and a specificity of 74% for the same classification problem[43]. Finally, an LR model built with T2w images, both with and without fa-suppression, radiomics

Table 1 Overview of the most widely adopted machine learning algorithms in rectal cancer imaging

| Algorithm name | Description |
|---------------------------------|---|
| Random forest | An ensemble method that combines multiple decision trees (a class of predictive learning models used in supervised ML) to obtain more accurate results for classification and regression tasks |
| Support vector machine | A linear approach used mainly for classification problems with the aim to find the best hyper plane which most accurately separate input data into two classes |
| Logistic regression | A classifier used to obtain the best fitting model for the relationship between multiple predictor variables and a dichotomous outcome |
| LASSO | A regularized regression method that performs both variable selection and regularization in order to optimally fit the resulting generalized statistical model |
| Naive Bayes | A classifier relying on the Bayes Theorem to model the probability of an outcome based on the strong (naive) independence assumptions between the features data |
| Quadratic discriminant analysis | A subtype of Dimensionality Reduction Algorithms that turn high-dimensional data into low-dimensional data retaining the most significant features of original data for the prediction of the class label |
| ANN | A subgroup of ML composed of neuronal-like multi-layered networks allowing to automatically extract features without prior labelling and perform complex operations |
| CNN | As subset of ANN containing multiple computational hidden layers that filter and compute high-dimensional data to enhance the learning of high-level tasks (deep learning) |

ANN: Artificial neural network; CNN: Convolutional neural network; LASSO: Least absolute shrinkage and selection operator; ML: Machine learning.

features achieved a sensitivity of 88% and specificity of 61% for classifying T1-2 vs T3-4 in a group of 174 patients[44].

MRI is also considered the imaging gold standard for the assessment of lymph node involvement in RC, but it suffers from a relatively low specificity, with potential negative implications on patient outcome[45]. Indeed, the management of patients with different nodal status is a highly debated and complex topic[46]. Radiomics has been proposed as a feasible solution to enhance the accuracy of MRI for N staging in RC patients[47]. In a recent retrospective single-center study in 152 patients, T2w radiomics were coupled to a random forest (RF) algorithm to create an ML classifier that was able to discriminate N0 from N1-2 patients with a sensitivity of 79% and a specificity of 72% [42]. Once again, similar results (81% sensitivity and 68% specificity) were found with LR and a different ML model derived from DWI radiomics features [43]. In both studies, pretreatment MRI scans were used, and the primary tumor was segmented. With a different approach, Zhu *et al*[48] extracted collective radiomics features from all noticeable lymph nodes on T2w images acquired before and after nCRT in patients with LARC; the LR model was trained to predict pathological node status after nCRT with a group of 143 patients, and had a sensitivity of 95% and a specificity of 60% in the validation cohort of 72 patients. The sensitivity was slightly lower and the specificity slightly higher than those reached by radiologist in the same patient cohorts (100% and 43%). Notwithstanding the specificity insufficient for clinical needs, such models might be useful tools for radiologists in the assessment of N stage in RC.

Finally, the identification of distant metastases in RC patients usually relies on imaging modalities other than MRI. Nevertheless, it should be mentioned that radiomics of the primary tumor was able to provide valuable information for the prediction of synchronous (already present at the time of diagnosis) or metachronous (developed after treatment) liver metastases[49-51] as well as synchronous metastases to other sites[52]. With specific regard to metachronous liver metastases, radiomics of T2w and post-contrast T1-weighted dynamic contrast enhanced (DCE) images were combined to build two ML predictive models, a support vector machine (SVM) and LR, with cross-validation in 108 patients[50]. The LR algorithm had the best performance, but not significantly better than SVM, with 83% sensitivity and 76% specificity, confirming the potential of radiomics and ML for the identification of RC patients who will develop liver metastases after treatment.

Predicting response to nCRT in patients with LARC

While TME should follow nCRT in patients with LARC, the role of surgery in patients with a complete response to nCRT is currently debated, and a “watch and wait” strategy has been proposed[53]. Indeed, patients who achieve a pathological complete response (pCR) after nCRT have better long-term outcomes compared with non-pCR

patients, and could therefore be managed differently[54]. Unfortunately, pCR cannot be accurately predicted before surgery by conventional evaluation of MR images[55]. Recently, several radiomics features extracted from T2w, DWI, and DCE sequences have been investigated as possible imaging biomarkers for pCR prediction, with promising results[56-58]. The main studies that aimed to build classification models using ML algorithms for preoperative prediction of pCR after nCRT are shown in Table 2. Overall, the performance of the different models is encouraging. While a trend can be observed, with lower values found in those studies that validated the model in an external dataset and thus with the better chances of high generalizability, it is difficult to draw a final conclusion from the available evidence[59,60]. Most studies focused on MRI scans acquired before nCRT had started, extracting radiomics features from highly available sequences (*i.e.* T2w). The ideal approach exploits an advantage of radiomics that allows developing predictive models using medical images as they are acquired in the clinical routine[61]. On the other hand, each of the retrospective studies presented its own model, with a certain degree of heterogeneity that does not facilitate translation into clinical practice. An overview of the main studies proposing MRI radiomics and ML algorithms for the prediction of nCRT outcomes other than pCR is reported in Table 3. In those studies, the ML models were generally designed to classify patients into two groups (*i.e.* good and poor responders to nCRT), with one study prospectively designed but lacking external validation[62].

Additionally, recent studies explored the feasibility of radiomics nomograms, based on the combination of a radiomics signature and either a pretreatment MRI T stage[63] or a post treatment tumor length[64], to predict pCR to nCRT. In particular, Liu *et al* [64] built and validated a radiomics signature in LARC patients using T2w in 152 and DWI images in 70 the T2w and DWI images were acquired both before and after nCRT. An SVM ML algorithm incorporating signatures and post treatment tumor length in a nomogram was able to reach a final diagnostic accuracy of 94% in the prediction of pCR. Finally, Wang *et al*[65] developed a radiomics signature to classify good responders and poor responders to nCRT with an LR ML algorithm and radiomics features from T2w, DWI, and DCE sequences. When combined in a nomogram with MRI T stage and circumferential resection margin as well as apparent diffusion coefficient values, they were able to predict a good response with a sensitivity of 71% and a specificity of 88%.

Genotyping

Radiogenomics aims to correlate imaging features of a disease with its genotypic characteristics and represents the next step in a radiology-pathology correlation[66]. Radiomics and radiogenomics are not equivalent, and both qualitative and quantitative imaging features can be used for radiogenomic analysis, with quantitative data having promising associations with genetic mutations in RC[67]. Among the negative genetic prognostic factors in RC, KRAS mutations are associated with poor response to epidermal growth factor receptor-targeted antibodies[68] and an increased risk of developing distant metastases[69]. In a recent multicenter study by Cui *et al* [70], three classifiers (decision tree, SVM and LR) powered by T2w-based radiomics features were trained to predict KRAS mutations in data from 213 patients and validated in both an internal cohort of 91 patients and external cohort of 86. The SVM obtained the greatest area under the receiver operating characteristic curve (AUC) in the training dataset (0.72), which was substantially confirmed in the internal (AUC = 0.68) as well as external (AUC = 0.71) validation cohorts. The finding supports the potential generalizability of such models. Interestingly, in the same study, no associations were found between KRAS status and baseline clinical and histopathological data. More optimistic results were recently published using a decision tree classifier (AUC = 0.88) by a different study group[71], but the sample size was substantially smaller (60 patients) and the model was not externally validated. Finally, T2w-based radiomics have been also paired with DL, with an artificial NN discriminating between patients with or without KRAS mutations and a classification error of 13% [72].

Assessing high-risk histopathological variables

Several histopathological characteristics, EMVI, differentiation degree, and perineural invasion (PNI) for example, are associated with poor clinical outcome and need to be considered in the risk stratification of patients with RC. It is fair to assume that a reliable pretreatment evaluation of these high-risk variables would ease the transition toward precision medicine[5]. ML classifiers applied to MRI radiomics features have been recently explored in this setting[73-75]. As previously highlighted, MRI can be used to identify EMVI; however, its sensitivity is not as high as desirable[76]. To

Table 2 Key characteristics of the main studies using radiomics and machine learning algorithms on magnetic resonance images to predict pathologic complete response after neoadjuvant chemoradiotherapy in patients with locally advanced rectal cancer

| Ref. | Study design (n of sites) | Number of patients | Definition of pCR | MRI field strength (n of scanners) | MRI timing | MRI sequence | ML algorithm | Data powering algorithm | Validation | Performance (AUC) |
|---|---------------------------------|--------------------|---------------------------------|--------------------------------------|--------------------------------|--------------------------------------|--------------|---|---|-------------------|
| Antunes <i>et al</i> [59], 2020 | Retrospective (3) | 104 | TRG 0 according to AJCC | 1.5 and 3 T (> 10) | Pre-nCRT | T2w | RF | Radiomics features | External validation | 0.71 |
| Ferrari <i>et al</i> [106], 2019 | Retrospective (1) | 55 | TRG 4 according to Dowrak-Rodel | 3 T (1) | Pre-, mid- and post-nCRT | T2w | RF | Radiomics features | Internal validation (train/ test split) | 0.86 |
| Horvat <i>et al</i> [107], 2018 | Retrospective (1 ¹) | 114 | ypT0N0 | 1,5 and 3 T (4) | Post-nCRT | T2w | RF | Radiomics features | Internal validation (cross-validation) | 0.93 |
| Nie <i>et al</i> [108], 2016 | Retrospective (1) | 48 | ypT0N0 | 3 T (1) | Pre-nCRT | T2w, DWI, pre and post-contrast T1w | ANN | Radiomics features | Internal validation (cross-validation) | 0.84 |
| Petkovska <i>et al</i> [109], 2020 | Retrospective (1 ¹) | 102 ² | ypT0N0 | 1,5 and 3 T (4) | Pre-nCRT | T2w | SVM | Radiomics and semantic features | Internal validation (train/ test split) | 0.75 |
| Shaish <i>et al</i> [110], 2020 | Retrospective (2) | 132 | ypT0N0 | 1,5 and 3 T (multiple ³) | Pre-nCRT | T2w | LR | Radiomics features | Internal validation (train/ test split) | 0.80 |
| Shi <i>et al</i> [111], 2019 | Retrospective (1) | 51 | TRG 0 according to Ryan | 3 T (1) | Pre- and mid-Ncrt ⁴ | T2w, DWI, pre- and post-contrast T1w | CNN | Radiomics features | Internal validation (cross-validation) | 0.83 |
| van Griethuysen <i>et al</i> [60], 2019 | Retrospective (2) | 133 | ypT0/TRG1 according to Mandard | 1,5 T (3) | Pre-nCRT | T2w and DWI | LR | Radiomics features | External validation | 0.77 |
| Yi <i>et al</i> [112], 2019 | Retrospective (1) | 134 | ypT0N0 | 1,5 and 3 T (2) | Pre-nCRT | T2w | SVM | Radiomics, clinical and semantic features | Internal validation (train/ test split) | 0.88 |

¹< 10% of scans from other institutions.

²All previously included in Horvat *et al* [107], 2018.

³Inclusion of patients with MRI performed elsewhere but treated at study sites.

⁴Both MRI scans were not available for all patients. In all studies, three-dimensional manual segmentation of the primary tumor was performed to extract radiomic features, except for Shaish *et al* [110], mesorectal compartment) and van Griethuysen *et al* [60] (semiautomatic segmentation). ANN: Artificial neural network; CNN: Convolutional neural network; AUC: Area under the receiver operating characteristic curve; DWI: Diffusion-weighted imaging; LR: Logistic regression; ML: Machine learning; MRI: Magnetic resonance imaging; nCRT: Neoadjuvant chemoradiotherapy; RF: Random forest; SVM: Support vector machine; T1w: T1-weighted; T2w: T2-weighted; TRG: Tumor regression grade.

overcome current MRI limitations, Yu *et al* [73] built a nomogram based on both a DCE MRI radiomics signature and clinical data, finding that it outperformed conventional quantitative perfusion parameters such as Ktrans in the prediction of EMVI, with a sensitivity of 88.9% and a specificity of 78.3% in the validation cohort.

Well-differentiated tumors are associated with better outcomes of RC patients [77]. In a large cohort of 345 patients retrospectively enrolled at a single institution, Meng *et al* [74] explored the performance of three ML classifiers, RF, SVM, and least absolute shrinkage, and selection operator (LASSO) to identify well-differentiated RC. Radiomics features were extracted from multiple MRI sequences, including T2w, DWI, and DCE. The LASSO algorithm had the best performance, with an AUC of 0.72 in the validation dataset. Finally, PNI, the tumor spreading along the nerve sheath, is a histopathological factor known to be associated with poor prognosis [78]. Using T2w

Table 3 Key characteristics of the main studies using radiomics and machine learning algorithms on magnetic resonance images to predict outcome other than pathologic complete response after neoadjuvant chemoradiotherapy in patients with locally advanced rectal cancer

| Ref. | Study design (n of sites) | Number of patients | Prediction task | CT phase (n of CT scanner) | Segmentation method | ML algorithm | Data powering algorithm | Validation | Performance |
|---------------------------------|---------------------------|--------------------|------------------------|----------------------------|-------------------------------|--------------|---------------------------------|---|----------------|
| Bibault <i>et al</i> [85], 2018 | Retrospective (3) | 99 | pCR after nCRT | Unenhanced (3) | Manual - 3D | DNN | Radiomics and clinical features | Internal validation (cross-validation) | AUC: 0.72 |
| Hamerla <i>et al</i> [86], 2019 | Retrospective (1) | 169 | pCR after nCRT | Unenhanced (1) | Manual - 3D | RF | Radiomics features | Internal validation (cross-validation) | Accuracy: 0.87 |
| Yuan <i>et al</i> [87], 2020 | Retrospective (1) | 91 | pCR after nCRT | Unenhanced (1) | Manual - 3D | RF | Radiomics features | Internal validation (train/validation split) | Accuracy: 0.84 |
| Wu <i>et al</i> [90], 2019 | Retrospective (1) | 102 | MSI status | Venous phase - DECT (2) | Manual - 3 2D ROIs for lesion | LR | Radiomics features | Internal validation (train/validation / test split) | AUC: 0.87 |
| Fan <i>et al</i> [91], 2019 | Retrospective (1) | 100 | MSI status | Portal venous phase (2) | Semiautomatic - 3D | NB | Radiomics features | Internal validation (cross-validation) | AUC: 0.75 |
| Wu <i>et al</i> [92], 2020 | Retrospective (1) | 173 | KRAS mutation | Portal venous phase (3) | Manual + DL - single 2D ROI | LR | Radiomics features | Internal validation (train/test split) | C-index: 0.83 |
| Wang <i>et al</i> [94], 2019 | Retrospective (1) | 411 | Prediction of survival | Unenhanced (1) | Manual - 3D | 10-F CV | Radiomics and clinical features | Internal validation (cross-validation) | C-index: 0.73 |

In all studies, three-dimensional manual segmentation of the primary tumor was performed to extract radiomic features, with the exceptions of Alvarez-Jimenez *et al*[113] (rectal wall), van Griethuysen *et al*[60] (semiautomatic segmentation) and Yang *et al*[115] (two-dimensional manual segmentation). ANN: Artificial neural network; AUC: Area under the receiver operating characteristic curve; CNN: Convolutional neural network; DWI: Diffusion-weighted imaging; EMLM: Ensemble machine learning model; GR: Good responders; LASSO: Least absolute shrinkage and selection operator; RF: Random forest; LR: Logistic regression; ML: Machine learning; MRI: Magnetic resonance imaging; QDA: Quadratic discriminant analysis; SVM: Support vector machine; T1w: T1-weighted; T2w: T2-weighted; TRG: Tumor regression grade.

10F-CV: 10-fold cross-validation; CT: Computed tomography; DECT: Dual-energy computed tomography; DNN: Deep neural network; LR: Logistic regression; ML: Machine learning; MSI: Microsatellite instability; NB: Naive Bayes; nCRT: Neoadjuvant chemoradiotherapy; pCR: Pathologic complete response; RF: Random forest.

radiomics and AI, Chen *et al*[79] developed a nomogram to predict the presence of PNI in RC patients (AUC = 0.85). A decision curve analysis confirmed the clinical utility of their nomogram, but the sample size of only seven PNI-positive patients in the test dataset requires validation of this preliminary findings in larger datasets.

RADIOMICS AND ML APPLICATIONS IN RC: CT

In the management of RC, CT is commonly used as the initial staging modality, allowing accurate nodal and metastases staging and target volume delineation before radiation therapy in patients with LARC[6]. Conversely, the role of CT in RC pretreatment local staging as well as restaging after nCRT is limited because of its intrinsically lower contrast resolution compared with MRI[80,81]. Nevertheless, much effort has been directed toward the use of CT data beyond clinical indications, with the aim of developing CT-based radiomics signatures reflecting tumor heterogeneity[82]. CT images contain robust volumetric data that are highly reproducible across patients and are an ideal source of data to feed AI systems[83,84]. In that perspective, ML models that can find correlations of RC CT radiomics features that can be used to predict outcomes such as complete response to nCRT in LARC patients, genetic profiles, overall survival, and segmentation (Table 4).

Table 4 Key characteristics of the main studies using radiomics and machine learning algorithms on computed tomography for v prediction tasks

| Ref. | Study design (n of sites) | Number of patients | Prediction task | CT phase (n of CT scanner) | Segmentation method | ML algorithm | Data powering algorithm | Validation | Performance |
|---------------------------------|---------------------------|--------------------|------------------------|----------------------------|-------------------------------|--------------|---------------------------------|---|----------------|
| Bibault <i>et al</i> [85], 2018 | Retrospective (3) | 99 | pCR after nCRT | Unenhanced (3) | Manual - 3D | DNN | Radiomics and clinical features | Internal validation (cross-validation) | AUC: 0.72 |
| Hamerla <i>et al</i> [86], 2019 | Retrospective (1) | 169 | pCR after nCRT | Unenhanced (1) | Manual - 3D | RF | Radiomics features | Internal validation (cross-validation) | Accuracy: 0.87 |
| Yuan <i>et al</i> [87], 2020 | Retrospective (1) | 91 | pCR after nCRT | Unenhanced (1) | Manual - 3D | RF | Radiomics features | Internal validation (train/validation split) | Accuracy: 0.84 |
| Wu <i>et al</i> [90], 2019 | Retrospective (1) | 102 | MSI status | Venous phase - DECT (2) | Manual - 3 2D ROIs for lesion | LR | Radiomics features | Internal validation (train/validation / test split) | AUC: 0.87 |
| Fan <i>et al</i> [91], 2019 | Retrospective (1) | 100 | MSI status | Portal venous phase (2) | Semiautomatic - 3D | NB | Radiomics features | Internal validation (cross-validation) | AUC: 0.75 |
| Wu <i>et al</i> [92], 2020 | Retrospective (1) | 173 | KRAS mutation | Portal venous phase (3) | Manual + DL - single 2D ROI | LR | Radiomics features | Internal validation (train/test split) | C-index: 0.83 |
| Wang <i>et al</i> [94], 2019 | Retrospective (1) | 411 | Prediction of survival | Unenhanced (1) | Manual - 3D | 10-F CV | Radiomics and clinical features | Internal validation (cross-validation) | C-index: 0.73 |

10F-CV: 10-fold cross-validation; CT: Computed tomography; DECT: Dual-energy computed tomography; DNN: Deep neural network; LR: Logistic regression; ML: Machine learning; MSI: Microsatellite instability; NB: Naive Bayes; nCRT: Neoadjuvant chemoradiotherapy; pCR: Pathologic complete response; RF: Random forest.

Predicting response to nCRT in patients with LARC

Bibault *et al*[85] explored the reliability of deep NN (DNN) integrating clinical features (T stage) and robust radiomics CT-based features in assessing the pCR to nCRT in a multicenter cohort of patients with LARC. The DNN model predicted pCR with an accuracy of 80% compared with 69.5% achieved with an LR model using only the TNM stage and an SVM model with the same parameters as the DNN that had an accuracy of 71.58%. Similarly, Hamerla *et al*[86] reported an accuracy of 87% for prediction of pCR after nCRT using an ML algorithm and CT radiomics data, but they noted that the model was not generalizable because of bias introduced by an imbalanced distribution of the minority class (pCR: 13% and non-pCR = 87%) in the study population. In another study, Yuan *et al*[87] tested and compared different ML algorithms using robust CT-based radiomics features significantly correlated with pCR. The best performing model was an RF with an accuracy of 83.9% in the test population. Interestingly, these studies used radiomics features extracted from unenhanced CT scans used for radiotherapy planning. The process highlights the potential value of nonroutine CT data for pretreatment risk stratification.

Genotyping

Recent studies have shown encouraging results with regard to the high predictive ability of AI-radiomics CT-based models of the biologic behavior of RC, in terms of microsatellite instability (MSI) status and KRAS gene mutations, which are considered significant molecular markers of improved prognosis and adjuvant therapy[11,88,89]. Wu *et al*[90] developed a pretreatment predictive model of MSI status in RC using ML radiomics features extracted from venous phase images of iodine-based material decomposition with dual-energy CT (DECT). Performance of the model was tested on images acquired with a different DECT scanner, and achieving a diagnostic accuracy of 79%. The result suggests a possible link between iodine DECT images and augmented tumor vascularization. In a preliminary retrospective study, Fan *et al*[91] found that an ML model combining clinical and CT radiomics features had a better classification performance for MSI status (AUC = 0.75) in stage II RC patients than models using only clinical features (AUC = 0.60) or only radiomics features (AUC = 0.70).

Another research group[92] investigated the performance of a model that used handcrafted radiomics signatures combined with those in a DL algorithm. The combined model was able to discriminate patients with mutant or the wild-type KRAS with a sensitivity of 80% and a specificity of 72% in the validation cohort, thus showing a good predictive performance.

Prognosis

An active field of AI oncology-related research is the discovery of new clinical and imaging tumor biomarkers that are correlated with prognosis, with the goal of developing accurate predictive models of treatment response based on personalized tumor profiles[93]. Wang *et al*[94] explored the use of CT-based ML models powered by clinical and radiomics features to assess the prognostic outcomes of LARC patients treated with nCRT. Radiomics features were extracted from nonenhanced CT images used for planning the treatment of 411 LARC patients. Images analyzed by unsupervised ML did not find a relationship between the clinical and radiomics features. A supervised ML model with embedded radiomics and clinical parameters had an improved overall survival prediction in the testing set and a c-index of 0.73 which was significantly better ($P = 0.044$) than the performance of the model using only clinical factors (c-index = 0.67).

RADIOMICS AND ML APPLICATIONS IN RC: MULTIMODAL AND HYBRID IMAGING

The advantage of multimodality and hybrid imaging in oncology is mainly related to the combined evaluation of anatomical and functional tumor characteristics. Radiomics and ML could further increase the potential value of the techniques[95]. However, the number of studies evaluating RC is still limited, and the role of multimodal radiomics and ML models has mainly been investigated for the prediction of response to nCRT in patients with LARC[96,97]. In a single-center study in 169 patients, Shen *et al*[96] developed an RF model based on baseline PET/CT images that accurately predicted pCR to nCRT in LARC patients, with a sensitivity of 81.8% and a specificity of 97.3%. Another study confirmed the feasibility of combining pretreatment MRI data from T2w sequences and PET radiomics features to build a prediction model able to identify responders or nonresponders. ML algorithms were used for semiautomatic segmentation of the primary tumor in both sets of images[97]. The final LR model had a sensitivity of 86% and specificity of 83%. Beyond nuclear medicine, Li *et al*[98] described a multimodal radiomics-based nomogram with features extracted from baseline MRI and CT images, which better performed better than individual imaging techniques in the prediction of response to nCRT. Although multimodal radiomics for RC is in its infancy, the encouraging preliminary reports support the idea that it could allow an even more comprehensive assessment of tumor characteristics compared with individual images.

CURRENT LIMITATIONS AND FUTURE PERSPECTIVES

The available evidence confirms that AI is a feasible tool to broaden the spectrum of information that medical imaging can provide for the management of RC patients. Nevertheless, there is a risk that negative results are not published because of publication bias[99]. Furthermore, what could theoretically be done is not ready for clinical practice at present. Indeed, there are many exploratory studies and very few confirmatory ones to support the use of one radiomics-ML model over another. A possible solution to the problems of verifying generalizability and comparing the performance of different models proposed for the same prediction task might be the use of open-source data[100]. Indeed, a publicly available large dataset from multiple institutions could serve as a common benchmark to verify whether the available models can reproduce previous results while we wait for well-designed prospective clinical trials that will overcome the limitations of retrospective studies. Currently, there is a great interest in public imaging datasets, but their quality might be heterogeneous[101]. It should also be considered that significant variations in radiomics and ML pipelines make it difficult to compare studies. Adherence to shared guidelines for AI study design is this highly advisable[102]. Another issue of concern that could prevent widespread adoption of radiomics-ML prediction models is manual

segmentation. It is often necessary, but is a time-consuming procedure that requires automatization. However, AI could also solve that problem. Recent studies have described the use of DL for fully automated segmentation of RC on both CT and MR images, with encouraging accuracy and computational time results[103,104]. Several of the radiomics-ML models described in this review had promising accuracy, but it should be noted that the potential clinical utility of such models depends on multiple factors, such as their added value in comparison with current gold standards, the cost-effectiveness of their implementation, and their actual impact on clinical practice. Decision curve analysis might be helpful in the analysis[34]. Finally, a recent study found that the overall quality of radiomics studies in oncology is below the desired standards, suggesting that most of the problems identified in the field of RC radiomics are shared among the studies involving different types of cancer[105].

CONCLUSION

Medical images contain mineable data with great potential. AI appears to be a convenient tool to harness their value for RC management. AI in imaging can support physicians in the transition toward precision medicine for RC patients, but there is still a long road ahead and it is time to start moving to the next step. Robust prospective multicenter studies and clinical trials are needed to confirm the clinical implications of this new methodology.

REFERENCES

- 1 Siegel RL, Miller KD, Jemal A. Cancer statistics, 2020. *CA Cancer J Clin* 2020; **70**: 7-30 [PMID: 31912902 DOI: 10.3322/caac.21590]
- 2 Dekker E, Tanis PJ, Vleugels JLA, Kasi PM, Wallace MB. Colorectal cancer. *Lancet* 2019; **394**: 1467-1480 [PMID: 31631858 DOI: 10.1016/S0140-6736(19)32319-0]
- 3 Keller DS, Berho M, Perez RO, Wexner SD, Chand M. The multidisciplinary management of rectal cancer. *Nat Rev Gastroenterol Hepatol* 2020; **17**: 414-429 [PMID: 32203400 DOI: 10.1038/s41575-020-0275-y]
- 4 Benson AB, Venook AP, Al-Hawary MM, Arain MA, Chen YJ, Ciombor KK, Cohen S, Cooper HS, Deming D, Garrido-Laguna I, Grem JL, Gunn A, HOFFE S, Hubbard J, Hunt S, Kirilcuk N, Krishnamurthi S, Messersmith WA, Meyerhardt J, Miller ED, Mulcahy MF, Nurkin S, Overman MJ, Parikh A, Patel H, Pedersen K, Saltz L, Schneider C, Shibata D, Skibber JM, Sofocleous CT, Stoffel EM, Stotsky-Himelfarb E, Willett CG, Johnson-Chilla A, Gurski LA. NCCN Guidelines Insights: Rectal Cancer, Version 6.2020. *J Natl Compr Canc Netw* 2020; **18**: 806-815 [PMID: 32634771 DOI: 10.6004/jnccn.2020.0032]
- 5 Glynn-Jones R, Wyrwicz L, Tiret E, Brown G, Rödel C, Cervantes A, Arnold D; ESMO Guidelines Committee. Rectal cancer: ESMO Clinical Practice Guidelines for diagnosis, treatment and follow-up. *Ann Oncol* 2017; **28**: iv22-iv40 [PMID: 28881920 DOI: 10.1093/annonc/mdx224]
- 6 Heo SH, Kim JW, Shin SS, Jeong YY, Kang HK. Multimodal imaging evaluation in staging of rectal cancer. *World J Gastroenterol* 2014; **20**: 4244-4255 [PMID: 24764662 DOI: 10.3748/wjg.v20.i15.4244]
- 7 Horvat N, Carlos Tavares Rocha C, Clemente Oliveira B, Petkovska I, Gollub MJ. MRI of Rectal Cancer: Tumor Staging, Imaging Techniques, and Management. *Radiographics* 2019; **39**: 367-387 [PMID: 30768361 DOI: 10.1148/rg.2019180114]
- 8 Beets-Tan RGH, Lambregts DMJ, Maas M, Bipat S, Barbaro B, Curvo-Semedo L, Fenlon HM, Gollub MJ, Gourtsoyianni S, Halligan S, Hoeffel C, Kim SH, Laghi A, Maier A, Rafaelsen SR, Stoker J, Taylor SA, Torkzad MR, Blomqvist L. Magnetic resonance imaging for clinical management of rectal cancer: Updated recommendations from the 2016 European Society of Gastrointestinal and Abdominal Radiology (ESGAR) consensus meeting. *Eur Radiol* 2018; **28**: 1465-1475 [PMID: 29043428 DOI: 10.1007/s00330-017-5026-2]
- 9 Maffione AM, Montesi G, Caroli P, Colletti PM, Rubello D, Matteucci F. Is It Time to Introduce PET/CT in Rectal Cancer Guidelines? *Clin Nucl Med* 2020; **45**: 611-617 [PMID: 32558716 DOI: 10.1097/RLU.00000000000003132]
- 10 Catalano OA, Lee SI, Parente C, Cauley C, Furtado FS, Striar R, Soricelli A, Salvatore M, Li Y, Umutlu L, Cañamaque LG, Groshar D, Mahmood U, Blaszkowsky LS, Ryan DP, Clark JW, Wo J, Hong TS, Kunitake H, Bordeianou L, Berger D, Ricciardi R, Rosen B. Improving staging of rectal cancer in the pelvis: the role of PET/MRI. *Eur J Nucl Med Mol Imaging* 2021; **48**: 1235-1245 [PMID: 33034673 DOI: 10.1007/s00259-020-05036-x]
- 11 Mainenti PP, Stanzione A, Guarino S, Romeo V, Ugga L, Romano F, Storto G, Maurea S, Brunetti A. Colorectal cancer: Parametric evaluation of morphological, functional and molecular tomographic imaging. *World J Gastroenterol* 2019; **25**: 5233-5256 [PMID: 31558870 DOI: 10.3748/wjg.v25.i35.5233]

- 12 **Mainenti PP**, Pizzuti LM, Segreto S, Comerci M, Fronzo S, Romano F, Crisci V, Smaldone M, Laccetti E, Storto G, Alfano B, Maurea S, Salvatore M, Pace L. Diffusion volume (DV) measurement in endometrial and cervical cancer: A new MRI parameter in the evaluation of the tumor grading and the risk classification. *Eur J Radiol* 2016; **85**: 113-124 [PMID: [26724655](#) DOI: [10.1016/j.ejrad.2015.10.014](#)]
- 13 **Romeo V**, Cuocolo R, Ricciardi C, Ugga L, Cocozza S, Verde F, Stanzione A, Napolitano V, Russo D, Improta G, Elefante A, Staibano S, Brunetti A. Prediction of Tumor Grade and Nodal Status in Oropharyngeal and Oral Cavity Squamous-cell Carcinoma Using a Radiomic Approach. *Anticancer Res* 2020; **40**: 271-280 [PMID: [31892576](#) DOI: [10.21873/anticancer.13949](#)]
- 14 **Gillies RJ**, Kinahan PE, Hricak H. Radiomics: Images Are More than Pictures, They Are Data. *Radiology* 2016; **278**: 563-577 [PMID: [26579733](#) DOI: [10.1148/radiol.2015151169](#)]
- 15 **Horvat N**, Bates DDB, Petkovska I. Novel imaging techniques of rectal cancer: what do radiomics and radiogenomics have to offer? *Abdom Radiol (NY)* 2019; **44**: 3764-3774 [PMID: [31055615](#) DOI: [10.1007/s00261-019-02042-y](#)]
- 16 **Cuocolo R**, Cipullo MB, Stanzione A, Romeo V, Green R, Cantoni V, Ponsiglione A, Ugga L, Imbriaco M. Machine learning for the identification of clinically significant prostate cancer on MRI: a meta-analysis. *Eur Radiol* 2020; **30**: 6877-6887 [PMID: [32607629](#) DOI: [10.1007/s00330-020-07027-w](#)]
- 17 **Comelli A**, Bignardi S, Stefano A, Russo G, Sabini MG, Ippolito M, Yezzi A. Development of a new fully three-dimensional methodology for tumours delineation in functional images. *Comput Biol Med* 2020; **120**: 103701 [PMID: [32217282](#) DOI: [10.1016/j.compbiomed.2020.103701](#)]
- 18 **Stanzione A**, Cuocolo R, Del Grosso R, Nardiello A, Romeo V, Travaglino A, Raffone A, Bifulco G, Zullo F, Insabato L, Maurea S, Mainenti PP. Deep Myometrial Infiltration of Endometrial Cancer on MRI: A Radiomics-Powered Machine Learning Pilot Study. *Acad Radiol* 2021; **28**: 737-744 [PMID: [32229081](#) DOI: [10.1016/j.acra.2020.02.028](#)]
- 19 **Stanzione A**, Ricciardi C, Cuocolo R, Romeo V, Petrone J, Sarnataro M, Mainenti PP, Improta G, De Rosa F, Insabato L, Brunetti A, Maurea S. MRI Radiomics for the Prediction of Fuhrman Grade in Clear Cell Renal Cell Carcinoma: a Machine Learning Exploratory Study. *J Digit Imaging* 2020; **33**: 879-887 [PMID: [32314070](#) DOI: [10.1007/s10278-020-00336-y](#)]
- 20 **Bi WL**, Hosny A, Schabath MB, Giger ML, Birkbak NJ, Mehrta A, Allison T, Arnaout O, Abbosh C, Dunn IF, Mak RH, Tamimi RM, Tempny CM, Swanton C, Hoffmann U, Schwartz LH, Gillies RJ, Huang RY, Aerts HJWL. Artificial intelligence in cancer imaging: Clinical challenges and applications. *CA Cancer J Clin* 2019; **69**: 127-157 [PMID: [30720861](#) DOI: [10.3322/caac.21552](#)]
- 21 **Koçak B**, Durmaz EŞ, Ateş E, Kılıçkesmez Ö. Radiomics with artificial intelligence: a practical guide for beginners. *Diagn Interv Radiol* 2019; **25**: 485-495 [PMID: [31650960](#) DOI: [10.5152/dir.2019.19321](#)]
- 22 **Yip SS**, Aerts HJ. Applications and limitations of radiomics. *Phys Med Biol* 2016; **61**: R150-R166 [PMID: [27269645](#) DOI: [10.1088/0031-9155/61/13/R150](#)]
- 23 **Aerts HJ**, Velazquez ER, Leijenaar RT, Parmar C, Grossmann P, Carvalho S, Bussink J, Monshouwer R, Haibe-Kains B, Rietveld D, Hoebers F, Rietbergen MM, Leemans CR, Dekker A, Quackenbush J, Gillies RJ, Lambin P. Decoding tumour phenotype by noninvasive imaging using a quantitative radiomics approach. *Nat Commun* 2014; **5**: 4006 [PMID: [24892406](#) DOI: [10.1038/ncomms5006](#)]
- 24 **Nougaret S**, Tibermacine H, Tardieu M, Sala E. Radiomics: an Introductory Guide to What It May Foretell. *Curr Oncol Rep* 2019; **21**: 70 [PMID: [31240403](#) DOI: [10.1007/s11912-019-0815-1](#)]
- 25 **Avanzo M**, Stancanello J, El Naqa I. Beyond imaging: The promise of radiomics. *Phys Med* 2017; **38**: 122-139 [PMID: [28595812](#) DOI: [10.1016/j.ejmp.2017.05.071](#)]
- 26 **Rogers W**, Thulasi Seetha S, Refaee TAG, Lieverse RIY, Granzier RWY, Ibrahim A, Keek SA, Sanduleanu S, Primakov SP, Beuque MPL, Marcus D, van der Wiel AMA, Zerka F, Oberije CJG, van Timmeren JE, Woodruff HC, Lambin P. Radiomics: from qualitative to quantitative imaging. *Br J Radiol* 2020; **93**: 20190948 [PMID: [32101448](#) DOI: [10.1259/bjr.20190948](#)]
- 27 **Aerts HJ**. The Potential of Radiomic-Based Phenotyping in Precision Medicine: A Review. *JAMA Oncol* 2016; **2**: 1636-1642 [PMID: [27541161](#) DOI: [10.1001/jamaoncol.2016.2631](#)]
- 28 **Ibrahim A**, Primakov S, Beuque M, Woodruff HC, Halilaj I, Wu G, Refaee T, Granzier R, Widaatalla Y, Hustinx R, Mottaghy FM, Lambin P. Radiomics for precision medicine: Current challenges, future prospects, and the proposal of a new framework. *Methods* 2021; **188**: 20-29 [PMID: [32504782](#) DOI: [10.1016/j.ymeth.2020.05.022](#)]
- 29 **Cuocolo R**, Caruso M, Perillo T, Ugga L, Petretta M. Machine Learning in oncology: A clinical appraisal. *Cancer Lett* 2020; **481**: 55-62 [PMID: [32251707](#) DOI: [10.1016/j.canlet.2020.03.032](#)]
- 30 **Giger ML**. Machine Learning in Medical Imaging. *J Am Coll Radiol* 2018; **15**: 512-520 [PMID: [29398494](#) DOI: [10.1016/j.jacr.2017.12.028](#)]
- 31 **Choy G**, Khalilzadeh O, Michalski M, Do S, Samir AE, Panykh OS, Geis JR, Pandharipande PV, Brink JA, Dreyer KJ. Current Applications and Future Impact of Machine Learning in Radiology. *Radiology* 2018; **288**: 318-328 [PMID: [29944078](#) DOI: [10.1148/radiol.2018171820](#)]
- 32 **Hosny A**, Parmar C, Quackenbush J, Schwartz LH, Aerts HJWL. Artificial intelligence in radiology. *Nat Rev Cancer* 2018; **18**: 500-510 [PMID: [29777175](#) DOI: [10.1038/s41568-018-0016-5](#)]
- 33 **Tseng HH**, Wei L, Cui S, Luo Y, Ten Haken RK, El Naqa I. Machine Learning and Imaging Informatics in Oncology. *Oncology* 2020; **98**: 344-362 [PMID: [30472716](#) DOI: [10.1159/000493575](#)]
- 34 **Lambin P**, Leijenaar RTH, Deist TM, Peerlings J, de Jong EEC, van Timmeren J, Sanduleanu S,

- Larue RTHM, Even AJG, Jochems A, van Wijk Y, Woodruff H, van Soest J, Lustberg T, Roelofs E, van Elmpt W, Dekker A, Mottaghy FM, Wildberger JE, Walsh S. Radiomics: the bridge between medical imaging and personalized medicine. *Nat Rev Clin Oncol* 2017; **14**: 749-762 [PMID: 28975929 DOI: 10.1038/nrclinonc.2017.141]
- 35 **Erickson BJ**, Korfiatis P, Akkus Z, Kline TL. Machine Learning for Medical Imaging. *Radiographics* 2017; **37**: 505-515 [PMID: 28212054 DOI: 10.1148/rg.2017160130]
- 36 **Mayerhoefer ME**, Materka A, Langs G, Häggström I, Szczypiński P, Gibbs P, Cook G. Introduction to Radiomics. *J Nucl Med* 2020; **61**: 488-495 [PMID: 32060219 DOI: 10.2967/jnumed.118.222893]
- 37 **Chartrand G**, Cheng PM, Vorontsov E, Drozdal M, Turcotte S, Pal CJ, Kadoury S, Tang A. Deep Learning: A Primer for Radiologists. *Radiographics* 2017; **37**: 2113-2131 [PMID: 29131760 DOI: 10.1148/rg.2017170077]
- 38 **Kalisz KR**, Enzerra MD, Paspulati RM. MRI Evaluation of the Response of Rectal Cancer to Neoadjuvant Chemoradiation Therapy. *Radiographics* 2019; **39**: 538-556 [PMID: 30844347 DOI: 10.1148/rg.2019180075]
- 39 **Gaertner WB**, Kwaan MR, Madoff RD, Melton GB. Rectal cancer: An evidence-based update for primary care providers. *World J Gastroenterol* 2015; **21**: 7659-7671 [PMID: 26167068 DOI: 10.3748/wjg.v21.i25.7659]
- 40 **Ale Ali H**, Kirsch R, Razaz S, Jhaveri A, Thippavong S, Kennedy ED, Jhaveri KS. Extramural venous invasion in rectal cancer: overview of imaging, histopathology, and clinical implications. *Abdom Radiol (NY)* 2019; **44**: 1-10 [PMID: 29967984 DOI: 10.1007/s00261-018-1673-2]
- 41 **Curvo-Semedo L**. Rectal Cancer: Staging. *Magn Reson Imaging Clin N Am* 2020; **28**: 105-115 [PMID: 31753230 DOI: 10.1016/j.mric.2019.09.003]
- 42 **Ma X**, Shen F, Jia Y, Xia Y, Li Q, Lu J. MRI-based radiomics of rectal cancer: preoperative assessment of the pathological features. *BMC Med Imaging* 2019; **19**: 86 [PMID: 31747902 DOI: 10.1186/s12880-019-0392-7]
- 43 **Yin JD**, Song LR, Lu HC, Zheng X. Prediction of different stages of rectal cancer: Texture analysis based on diffusion-weighted images and apparent diffusion coefficient maps. *World J Gastroenterol* 2020; **26**: 2082-2096 [PMID: 32536776 DOI: 10.3748/wjg.v26.i17.2082]
- 44 **Lu HC**, Wang F, Yin JD. Texture Analysis Based on Sagittal Fat-Suppression and Transverse T2-Weighted Magnetic Resonance Imaging for Determining Local Invasion of Rectal Cancer. *Front Oncol* 2020; **10**: 1476 [PMID: 33014786 DOI: 10.3389/fonc.2020.01476]
- 45 **Nougaret S**, Jhaveri K, Kassam Z, Lall C, Kim DH. Rectal cancer MR staging: pearls and pitfalls at baseline examination. *Abdom Radiol (NY)* 2019; **44**: 3536-3548 [PMID: 31115601 DOI: 10.1007/s00261-019-02024-0]
- 46 **Christou N**, Meyer J, Toso C, Ris F, Buchs NC. Lateral lymph node dissection for low rectal cancer: Is it necessary? *World J Gastroenterol* 2019; **25**: 4294-4299 [PMID: 31496614 DOI: 10.3748/wjg.v25.i31.4294]
- 47 **Yang L**, Liu D, Fang X, Wang Z, Xing Y, Ma L, Wu B. Rectal cancer: can T2WI histogram of the primary tumor help predict the existence of lymph node metastasis? *Eur Radiol* 2019; **29**: 6469-6476 [PMID: 31278581 DOI: 10.1007/s00330-019-06328-z]
- 48 **Zhu H**, Zhang X, Li X, Shi Y, Zhu H, Sun Y. Prediction of pathological nodal stage of locally advanced rectal cancer by collective features of multiple lymph nodes in magnetic resonance images before and after neoadjuvant chemoradiotherapy. *Chin J Cancer Res* 2019; **31**: 984-992 [PMID: 31949400 DOI: 10.21147/j.issn.1000-9604.2019.06.14]
- 49 **Shu Z**, Fang S, Ding Z, Mao D, Cai R, Chen Y, Pang P, Gong X. MRI-based Radiomics nomogram to detect primary rectal cancer with synchronous liver metastases. *Sci Rep* 2019; **9**: 3374 [PMID: 30833648 DOI: 10.1038/s41598-019-39651-y]
- 50 **Liang M**, Cai Z, Zhang H, Huang C, Meng Y, Zhao L, Li D, Ma X, Zhao X. Machine Learning-based Analysis of Rectal Cancer MRI Radiomics for Prediction of Metachronous Liver Metastasis. *Acad Radiol* 2019; **26**: 1495-1504 [PMID: 30711405 DOI: 10.1016/j.acra.2018.12.019]
- 51 **Liu M**, Ma X, Shen F, Xia Y, Jia Y, Lu J. MRI-based radiomics nomogram to predict synchronous liver metastasis in primary rectal cancer patients. *Cancer Med* 2020; **9**: 5155-5163 [PMID: 32476295 DOI: 10.1002/cam4.3185]
- 52 **Liu H**, Zhang C, Wang L, Luo R, Li J, Zheng H, Yin Q, Zhang Z, Duan S, Li X, Wang D. MRI radiomics analysis for predicting preoperative synchronous distant metastasis in patients with rectal cancer. *Eur Radiol* 2019; **29**: 4418-4426 [PMID: 30413955 DOI: 10.1007/s00330-018-5802-7]
- 53 **López-Campos F**, Martín-Martín M, Fornell-Pérez R, García-Pérez JC, Die-Trill J, Fuentes-Mateos R, López-Durán S, Domínguez-Rullán J, Ferreiro R, Riquelme-Oliveira A, Hervás-Morón A, Couñago F. Watch and wait approach in rectal cancer: Current controversies and future directions. *World J Gastroenterol* 2020; **26**: 4218-4239 [PMID: 32848330 DOI: 10.3748/wjg.v26.i29.4218]
- 54 **Maas M**, Nelemans PJ, Valentini V, Das P, Rödel C, Kuo LJ, Calvo FA, García-Aguilar J, Glynne-Jones R, Haustermans K, Mohiuddin M, Pucciarelli S, Small W Jr, Suárez J, Theodoropoulos G, Biondo S, Beets-Tan RG, Beets GL. Long-term outcome in patients with a pathological complete response after chemoradiation for rectal cancer: a pooled analysis of individual patient data. *Lancet Oncol* 2010; **11**: 835-844 [PMID: 20692872 DOI: 10.1016/S1470-2045(10)70172-8]
- 55 **Sclafani F**, Brown G, Cunningham D, Wotherspoon A, Mendes LST, Balyasnikova S, Evans J, Peckitt C, Begum R, Tait D, Tabernero J, Glimelius B, Roselló S, Thomas J, Oates J, Chau I. Comparison between MRI and pathology in the assessment of tumour regression grade in rectal

- cancer. *Br J Cancer* 2017; **117**: 1478-1485 [PMID: [28934761](#) DOI: [10.1038/bjc.2017.320](#)]
- 56 **Aker M**, Ganeshan B, Afaq A, Wan S, Groves AM, Arulampalam T. Magnetic Resonance Texture Analysis in Identifying Complete Pathological Response to Neoadjuvant Treatment in Locally Advanced Rectal Cancer. *Dis Colon Rectum* 2019; **62**: 163-170 [PMID: [30451764](#) DOI: [10.1097/DCR.0000000000001224](#)]
- 57 **Yang L**, Qiu M, Xia C, Li Z, Wang Z, Zhou X, Wu B. Value of High-Resolution DWI in Combination With Texture Analysis for the Evaluation of Tumor Response After Preoperative Chemoradiotherapy for Locally Advanced Rectal Cancer. *AJR Am J Roentgenol* 2019; **1-8** [PMID: [30860889](#) DOI: [10.2214/AJR.18.20689](#)]
- 58 **Zou HH**, Yu J, Wei Y, Wu JF, Xu Q. Response to neoadjuvant chemoradiotherapy for locally advanced rectum cancer: Texture analysis of dynamic contrast-enhanced MRI. *J Magn Reson Imaging* 2019; **49**: 885-893 [PMID: [30079601](#) DOI: [10.1002/jmri.26254](#)]
- 59 **Antunes JT**, Ofshteyn A, Bera K, Wang EY, Brady JT, Willis JE, Friedman KA, Marderstein EL, Kalady MF, Stein SL, Puryrsko AS, Paspulati R, Gollamudi J, Madabhushi A, Viswanath SE. Radiomic Features of Primary Rectal Cancers on Baseline T₂-Weighted MRI Are Associated With Pathologic Complete Response to Neoadjuvant Chemoradiation: A Multisite Study. *J Magn Reson Imaging* 2020; **52**: 1531-1541 [PMID: [32216127](#) DOI: [10.1002/jmri.27140](#)]
- 60 **van Griethuysen JJM**, Lambregts DMJ, Trebeschi S, Lahaye MJ, Bakkers FCH, Vliegen RFA, Beets GL, Aerts HJWL, Beets-Tan RGH. Radiomics performs comparable to morphologic assessment by expert radiologists for prediction of response to neoadjuvant chemoradiotherapy on baseline staging MRI in rectal cancer. *Abdom Radiol (NY)* 2020; **45**: 632-643 [PMID: [31734709](#) DOI: [10.1007/s00261-019-02321-8](#)]
- 61 **Tiwari P**, Verma R. The Pursuit of Generalizability to Enable Clinical Translation of Radiomics. *Radiol Artif Intell* 2021; **3**: e200227 [PMID: [33847697](#) DOI: [10.1148/ryai.2020200227](#)]
- 62 **Shayesteh SP**, Alikhassani A, Fard Esfahani A, Miraei M, Geramifar P, Bitarafan-Rajabi A, Haddad P. Neo-adjuvant chemoradiotherapy response prediction using MRI based ensemble learning method in rectal cancer patients. *Phys Med* 2019; **62**: 111-119 [PMID: [31153390](#) DOI: [10.1016/j.ejmp.2019.03.013](#)]
- 63 **Cui Y**, Yang X, Shi Z, Yang Z, Du X, Zhao Z, Cheng X. Radiomics analysis of multiparametric MRI for prediction of pathological complete response to neoadjuvant chemoradiotherapy in locally advanced rectal cancer. *Eur Radiol* 2019; **29**: 1211-1220 [PMID: [30128616](#) DOI: [10.1007/s00330-018-5683-9](#)]
- 64 **Liu Z**, Zhang XY, Shi YJ, Wang L, Zhu HT, Tang Z, Wang S, Li XT, Tian J, Sun YS. Radiomics Analysis for Evaluation of Pathological Complete Response to Neoadjuvant Chemoradiotherapy in Locally Advanced Rectal Cancer. *Clin Cancer Res* 2017; **23**: 7253-7262 [PMID: [28939744](#) DOI: [10.1158/1078-0432.CCR-17-1038](#)]
- 65 **Wang J**, Liu X, Hu B, Gao Y, Chen J, Li J. Development and validation of an MRI-based radiomic nomogram to distinguish between good and poor responders in patients with locally advanced rectal cancer undergoing neoadjuvant chemoradiotherapy. *Abdom Radiol (NY)* 2021; **46**: 1805-1815 [PMID: [33151359](#) DOI: [10.1007/s00261-020-02846-3](#)]
- 66 **Pinker K**, Shitano F, Sala E, Do RK, Young RJ, Wibmer AG, Hricak H, Sutton EJ, Morris EA. Background, current role, and potential applications of radiogenomics. *J Magn Reson Imaging* 2018; **47**: 604-620 [PMID: [29095543](#) DOI: [10.1002/jmri.25870](#)]
- 67 **Horvat N**, Veeraraghavan H, Pelossof RA, Fernandes MC, Arora A, Khan M, Marco M, Cheng CT, Gonen M, Golia Pernicka JS, Gollub MJ, Garcia-Aguillar J, Petkovska I. Radiogenomics of rectal adenocarcinoma in the era of precision medicine: A pilot study of associations between qualitative and quantitative MRI imaging features and genetic mutations. *Eur J Radiol* 2019; **113**: 174-181 [PMID: [30927944](#) DOI: [10.1016/j.ejrad.2019.02.022](#)]
- 68 **Sorich MJ**, Wiese MD, Rowland A, Kichenadasse G, McKinnon RA, Karapetis CS. Extended RAS mutations and anti-EGFR monoclonal antibody survival benefit in metastatic colorectal cancer: a meta-analysis of randomized, controlled trials. *Ann Oncol* 2015; **26**: 13-21 [PMID: [25115304](#) DOI: [10.1093/annonc/mdu378](#)]
- 69 **Zhu K**, Yan H, Wang R, Zhu H, Meng X, Xu X, Dou X, Chen D. Mutations of KRAS and PIK3CA as independent predictors of distant metastases in colorectal cancer. *Med Oncol* 2014; **31**: 16 [PMID: [24861917](#) DOI: [10.1007/s12032-014-0016-6](#)]
- 70 **Cui Y**, Liu H, Ren J, Du X, Xin L, Li D, Yang X, Wang D. Development and validation of a MRI-based radiomics signature for prediction of KRAS mutation in rectal cancer. *Eur Radiol* 2020; **30**: 1948-1958 [PMID: [31942672](#) DOI: [10.1007/s00330-019-06572-3](#)]
- 71 **Oh JE**, Kim MJ, Lee J, Hur BY, Kim B, Kim DY, Baek JY, Chang HJ, Park SC, Oh JH, Cho SA, Sohn DK. Magnetic Resonance-Based Texture Analysis Differentiating KRAS Mutation Status in Rectal Cancer. *Cancer Res Treat* 2020; **52**: 51-59 [PMID: [31096736](#) DOI: [10.4143/crt.2019.050](#)]
- 72 **Xu Y**, Xu Q, Ma Y, Duan J, Zhang H, Liu T, Li L, Sun H, Shi K, Xie S, Wang W. Characterizing MRI features of rectal cancers with different KRAS status. *BMC Cancer* 2019; **19**: 1111 [PMID: [31727020](#) DOI: [10.1186/s12885-019-6341-6](#)]
- 73 **Yu X**, Song W, Guo D, Liu H, Zhang H, He X, Song J, Zhou J, Liu X. Preoperative Prediction of Extramural Venous Invasion in Rectal Cancer: Comparison of the Diagnostic Efficacy of Radiomics Models and Quantitative Dynamic Contrast-Enhanced Magnetic Resonance Imaging. *Front Oncol* 2020; **10**: 459 [PMID: [32328461](#) DOI: [10.3389/fonc.2020.00459](#)]
- 74 **Meng X**, Xia W, Xie P, Zhang R, Li W, Wang M, Xiong F, Liu Y, Fan X, Xie Y, Wan X, Zhu K,

- Shan H, Wang L, Gao X. Preoperative radiomic signature based on multiparametric magnetic resonance imaging for noninvasive evaluation of biological characteristics in rectal cancer. *Eur Radiol* 2019; **29**: 3200-3209 [PMID: 30413959 DOI: 10.1007/s00330-018-5763-x]
- 75 **He B**, Ji T, Zhang H, Zhu Y, Shu R, Zhao W, Wang K. MRI-based radiomics signature for tumor grading of rectal carcinoma using random forest model. *J Cell Physiol* 2019; **234**: 20501-20509 [PMID: 31074022 DOI: 10.1002/jcp.28650]
- 76 **Kim TH**, Woo S, Han S, Suh CH, Vargas HA. The Diagnostic Performance of MRI for Detection of Extramural Venous Invasion in Colorectal Cancer: A Systematic Review and Meta-Analysis of the Literature. *AJR Am J Roentgenol* 2019; **213**: 575-585 [PMID: 31063424 DOI: 10.2214/AJR.19.21112]
- 77 **Xiao H**, Yoon YS, Hong SM, Roh SA, Cho DH, Yu CS, Kim JC. Poorly differentiated colorectal cancers: correlation of microsatellite instability with clinicopathologic features and survival. *Am J Clin Pathol* 2013; **140**: 341-347 [PMID: 23955452 DOI: 10.1309/AJCP8P2DYNKGRBVI]
- 78 **Dhadda AS**, Bessell EM, Scholefield J, Dickinson P, Zaitoun AM. Mandard tumour regression grade, perineural invasion, circumferential resection margin and post-chemoradiation nodal status strongly predict outcome in locally advanced rectal cancer treated with preoperative chemoradiotherapy. *Clin Oncol (R Coll Radiol)* 2014; **26**: 197-202 [PMID: 24485884 DOI: 10.1016/j.clon.2014.01.001]
- 79 **Chen J**, Chen Y, Zheng D, Pang P, Zhang H, Zheng X, Liao J. Pretreatment MR-based radiomics nomogram as potential imaging biomarker for individualized assessment of perineural invasion status in rectal cancer. *Abdom Radiol (NY)* 2021; **46**: 847-857 [PMID: 32870349 DOI: 10.1007/s00261-020-02710-4]
- 80 **García-Figueiras R**, Baleato-González S, Padhani AR, Luna-Alcalá A, Marhuenda A, Vilanova JC, Osorio-Vázquez I, Martínez-de-Alegria A, Gómez-Caamaño A. Advanced Imaging Techniques in Evaluation of Colorectal Cancer. *Radiographics* 2018; **38**: 740-765 [PMID: 29676964 DOI: 10.1148/rg.2018170044]
- 81 **Delli Pizzi A**, Basilico R, Cianci R, Seccia B, Timpani M, Tavoletta A, Caposiena D, Faricelli B, Gabrielli D, Caulo M. Rectal cancer MRI: protocols, signs and future perspectives radiologists should consider in everyday clinical practice. *Insights Imaging* 2018; **9**: 405-412 [PMID: 29675627 DOI: 10.1007/s13244-018-0606-5]
- 82 **Eloyan A**, Yue MS, Khachatryan D. Tumor heterogeneity estimation for radiomics in cancer. *Stat Med* 2020; **39**: 4704-4723 [PMID: 32964647 DOI: 10.1002/sim.8749]
- 83 **Park BW**, Kim JK, Heo C, Park KJ. Reliability of CT radiomic features reflecting tumour heterogeneity according to image quality and image processing parameters. *Sci Rep* 2020; **10**: 3852 [PMID: 32123281 DOI: 10.1038/s41598-020-60868-9]
- 84 **Haibe-Kains B**, Adam GA, Hosny A, Khodakarami F, Massive Analysis Quality Control (MAQC) Society Board of Directors, Waldron L, Wang B, McIntosh C, Goldenberg A, Kundaje A, Greene CS, Broderick T, Hoffman MM, Leek JT, Korthauer K, Huber W, Brazma A, Pineau J, Tibshirani R, Hastie T, Ioannidis JPA, Quackenbush J, Aerts HJWL. Transparency and reproducibility in artificial intelligence. *Nature* 2020; **586**: E14-E16 [PMID: 33057217 DOI: 10.1038/s41586-020-2766-y]
- 85 **Bibault JE**, Giraud P, Housset M, Durdux C, Taieb J, Berger A, Coriat R, Chaussade S, Dousset B, Nordlinger B, Burgun A. Deep Learning and Radiomics predict complete response after neo-adjuvant chemoradiation for locally advanced rectal cancer. *Sci Rep* 2018; **8**: 12611 [PMID: 30135549 DOI: 10.1038/s41598-018-30657-6]
- 86 **Hamerla G**, Meyer HJ, Hamsch P, Wolf U, Kuhnt T, Hoffmann KT, Surov A. Radiomics Model Based on Non-Contrast CT Shows No Predictive Power for Complete Pathological Response in Locally Advanced Rectal Cancer. *Cancers (Basel)* 2019; **11**: 1680 [PMID: 31671766 DOI: 10.3390/cancers11111680]
- 87 **Yuan Z**, Frazer M, Zhang GG, Latifi K, Moros EG, Feygelman V, Felder S, Sanchez J, Dessureault S, Imanirad I, Kim RD, Harrison LB, Hoffe SE, Frakes JM. CT-based radiomic features to predict pathological response in rectal cancer: A retrospective cohort study. *J Med Imaging Radiat Oncol* 2020; **64**: 444-449 [PMID: 32386109 DOI: 10.1111/1754-9485.13044]
- 88 **Li K**, Luo H, Huang L, Zhu X. Microsatellite instability: a review of what the oncologist should know. *Cancer Cell Int* 2020; **20**: 16 [PMID: 31956294 DOI: 10.1186/s12935-019-1091-8]
- 89 **Li W**, Li H, Liu R, Yang X, Gao Y, Niu Y, Geng J, Xue Y, Jin X, You Q, Meng H. Comprehensive Analysis of the Relationship Between RAS and RAF Mutations and MSI Status of Colorectal Cancer in Northeastern China. *Cell Physiol Biochem* 2018; **50**: 1496-1509 [PMID: 30359964 DOI: 10.1159/000494649]
- 90 **Wu J**, Zhang Q, Zhao Y, Liu Y, Chen A, Li X, Wu T, Li J, Guo Y, Liu A. Radiomics Analysis of Iodine-Based Material Decomposition Images With Dual-Energy Computed Tomography Imaging for Preoperatively Predicting Microsatellite Instability Status in Colorectal Cancer. *Front Oncol* 2019; **9**: 1250 [PMID: 31824843 DOI: 10.3389/fonc.2019.01250]
- 91 **Fan S**, Li X, Cui X, Zheng L, Ren X, Ma W, Ye Z. Computed Tomography-Based Radiomic Features Could Potentially Predict Microsatellite Instability Status in Stage II Colorectal Cancer: A Preliminary Study. *Acad Radiol* 2019; **26**: 1633-1640 [PMID: 30929999 DOI: 10.1016/j.acra.2019.02.009]
- 92 **Wu X**, Li Y, Chen X, Huang Y, He L, Zhao K, Huang X, Zhang W, Dong M, Huang J, Xia T, Liang C, Liu Z. Deep Learning Features Improve the Performance of a Radiomics Signature for Predicting KRAS Status in Patients with Colorectal Cancer. *Acad Radiol* 2020; **27**: e254-e262 [PMID:

- 31982342 DOI: [10.1016/j.acra.2019.12.007](https://doi.org/10.1016/j.acra.2019.12.007)]
- 93 **Verde F**, Romeo V, Stanzione A, Maurea S. Current trends of artificial intelligence in cancer imaging. *Artif Intell Med Imaging* 2020; **1**: 87-93 [DOI: [10.35711/aimi.v1.i3.87](https://doi.org/10.35711/aimi.v1.i3.87)]
 - 94 **Wang J**, Shen L, Zhong H, Zhou Z, Hu P, Gan J, Luo R, Hu W, Zhang Z. Radiomics features on radiotherapy treatment planning CT can predict patient survival in locally advanced rectal cancer patients. *Sci Rep* 2019; **9**: 15346 [PMID: [31653909](https://pubmed.ncbi.nlm.nih.gov/31653909/) DOI: [10.1038/s41598-019-51629-4](https://doi.org/10.1038/s41598-019-51629-4)]
 - 95 **Wei L**, Osman S, Hatt M, El Naqa I. Machine learning for radiomics-based multimodality and multiparametric modeling. *Q J Nucl Med Mol Imaging* 2019; **63**: 323-338 [PMID: [31527580](https://pubmed.ncbi.nlm.nih.gov/31527580/) DOI: [10.23736/S1824-4785.19.03213-8](https://doi.org/10.23736/S1824-4785.19.03213-8)]
 - 96 **Shen WC**, Chen SW, Wu KC, Lee PY, Feng CL, Hsieh TC, Yen KY, Kao CH. Predicting pathological complete response in rectal cancer after chemoradiotherapy with a random forest using ¹⁸F-fluorodeoxyglucose positron emission tomography and computed tomography radiomics. *Ann Transl Med* 2020; **8**: 207 [PMID: [32309354](https://pubmed.ncbi.nlm.nih.gov/32309354/) DOI: [10.21037/atm.2020.01.107](https://doi.org/10.21037/atm.2020.01.107)]
 - 97 **Giannini V**, Mazzetti S, Bertotto I, Chiarenza C, Cauda S, Delmastro E, Bracco C, Di Dia A, Leone F, Medico E, Pisacane A, Ribero D, Stasi M, Regge D. Predicting locally advanced rectal cancer response to neoadjuvant therapy with ¹⁸F-FDG PET and MRI radiomics features. *Eur J Nucl Med Mol Imaging* 2019; **46**: 878-888 [PMID: [30637502](https://pubmed.ncbi.nlm.nih.gov/30637502/) DOI: [10.1007/s00259-018-4250-6](https://doi.org/10.1007/s00259-018-4250-6)]
 - 98 **Li ZY**, Wang XD, Li M, Liu XJ, Ye Z, Song B, Yuan F, Yuan Y, Xia CC, Zhang X, Li Q. Multimodal radiomics model to predict treatment response to neoadjuvant chemotherapy for locally advanced rectal cancer. *World J Gastroenterol* 2020; **26**: 2388-2402 [PMID: [32476800](https://pubmed.ncbi.nlm.nih.gov/32476800/) DOI: [10.3748/wjg.v26.i19.2388](https://doi.org/10.3748/wjg.v26.i19.2388)]
 - 99 **Buvat I**, Orlhac F. The Dark Side of Radiomics: On the Paramount Importance of Publishing Negative Results. *J Nucl Med* 2019; **60**: 1543-1544 [PMID: [31541033](https://pubmed.ncbi.nlm.nih.gov/31541033/) DOI: [10.2967/jnumed.119.235325](https://doi.org/10.2967/jnumed.119.235325)]
 - 100 **van Timmeren JE**, Cester D, Tanadini-Lang S, Alkadhi H, Baessler B. Radiomics in medical imaging-"how-to" guide and critical reflection. *Insights Imaging* 2020; **11**: 91 [PMID: [32785796](https://pubmed.ncbi.nlm.nih.gov/32785796/) DOI: [10.1186/s13244-020-00887-2](https://doi.org/10.1186/s13244-020-00887-2)]
 - 101 **Oakden-Rayner L**. Exploring Large-scale Public Medical Image Datasets. *Acad Radiol* 2020; **27**: 106-112 [PMID: [31706792](https://pubmed.ncbi.nlm.nih.gov/31706792/) DOI: [10.1016/j.acra.2019.10.006](https://doi.org/10.1016/j.acra.2019.10.006)]
 - 102 **Mongan J**, Moy L, Kahn CE Jr. Checklist for Artificial Intelligence in Medical Imaging (CLAIM): A Guide for Authors and Reviewers. *Radiol Artif Intell* 2020; **2**: e200029 [PMID: [33937821](https://pubmed.ncbi.nlm.nih.gov/33937821/) DOI: [10.1148/ryai.2020200029](https://doi.org/10.1148/ryai.2020200029)]
 - 103 **Men K**, Boimel P, Janopaul-Naylor J, Zhong H, Huang M, Geng H, Cheng C, Fan Y, Plastaras JP, Ben-Josef E, Xiao Y. Cascaded atrous convolution and spatial pyramid pooling for more accurate tumor target segmentation for rectal cancer radiotherapy. *Phys Med Biol* 2018; **63**: 185016 [PMID: [30109986](https://pubmed.ncbi.nlm.nih.gov/30109986/) DOI: [10.1088/1361-6560/aada6c](https://doi.org/10.1088/1361-6560/aada6c)]
 - 104 **Trebeschi S**, van Griethuysen JJM, Lambregts DMJ, Lahaye MJ, Parmar C, Bakers FCH, Peters NHGM, Beets-Tan RGH, Aerts HJWL. Deep Learning for Fully-Automated Localization and Segmentation of Rectal Cancer on Multiparametric MR. *Sci Rep* 2017; **7**: 5301 [PMID: [28706185](https://pubmed.ncbi.nlm.nih.gov/28706185/) DOI: [10.1038/s41598-017-05728-9](https://doi.org/10.1038/s41598-017-05728-9)]
 - 105 **Park JE**, Kim D, Kim HS, Park SY, Kim JY, Cho SJ, Shin JH, Kim JH. Quality of science and reporting of radiomics in oncologic studies: room for improvement according to radiomics quality score and TRIPOD statement. *Eur Radiol* 2020; **30**: 523-536 [PMID: [31350588](https://pubmed.ncbi.nlm.nih.gov/31350588/) DOI: [10.1007/s00330-019-06360-z](https://doi.org/10.1007/s00330-019-06360-z)]
 - 106 **Ferrari R**, Mancini-Terracciano C, Voena C, Rengo M, Zerunian M, Ciardiello A, Grasso S, Mare' V, Paramatti R, Russomando A, Santacesaria R, Satta A, Solfaro Camillocci E, Faccini R, Laghi A. MR-based artificial intelligence model to assess response to therapy in locally advanced rectal cancer. *Eur J Radiol* 2019; **118**: 1-9 [PMID: [31439226](https://pubmed.ncbi.nlm.nih.gov/31439226/) DOI: [10.1016/j.ejrad.2019.06.013](https://doi.org/10.1016/j.ejrad.2019.06.013)]
 - 107 **Horvat N**, Veeraraghavan H, Khan M, Blazic I, Zheng J, Capanu M, Sala E, Garcia-Aguilar J, Gollub MJ, Petkovska I. MR Imaging of Rectal Cancer: Radiomics Analysis to Assess Treatment Response after Neoadjuvant Therapy. *Radiology* 2018; **287**: 833-843 [PMID: [29514017](https://pubmed.ncbi.nlm.nih.gov/29514017/) DOI: [10.1148/radiol.2018172300](https://doi.org/10.1148/radiol.2018172300)]
 - 108 **Nie K**, Shi L, Chen Q, Hu X, Jabbour SK, Yue N, Niu T, Sun X. Rectal Cancer: Assessment of Neoadjuvant Chemoradiation Outcome based on Radiomics of Multiparametric MRI. *Clin Cancer Res* 2016; **22**: 5256-5264 [PMID: [27185368](https://pubmed.ncbi.nlm.nih.gov/27185368/) DOI: [10.1158/1078-0432.CCR-15-2997](https://doi.org/10.1158/1078-0432.CCR-15-2997)]
 - 109 **Petkovska I**, Tixier F, Ortiz EJ, Golia Pernicka JS, Paroder V, Bates DD, Horvat N, Fuqua J, Schilsky J, Gollub MJ, Garcia-Aguilar J, Veeraraghavan H. Clinical utility of radiomics at baseline rectal MRI to predict complete response of rectal cancer after chemoradiation therapy. *Abdom Radiol (NY)* 2020; **45**: 3608-3617 [PMID: [32296896](https://pubmed.ncbi.nlm.nih.gov/32296896/) DOI: [10.1007/s00261-020-02502-w](https://doi.org/10.1007/s00261-020-02502-w)]
 - 110 **Shaish H**, Aukerman A, Vanguri R, Spinelli A, Armenta P, Jambawalikar S, Makkar J, Bentley-Hibbert S, Del Portillo A, Kiran R, Monti L, Bonifacio C, Kirienko M, Gardner KL, Schwartz L, Keller D. Radiomics of MRI for pretreatment prediction of pathologic complete response, tumor regression grade, and neoadjuvant rectal score in patients with locally advanced rectal cancer undergoing neoadjuvant chemoradiation: an international multicenter study. *Eur Radiol* 2020; **30**: 6263-6273 [PMID: [32500192](https://pubmed.ncbi.nlm.nih.gov/32500192/) DOI: [10.1007/s00330-020-06968-6](https://doi.org/10.1007/s00330-020-06968-6)]
 - 111 **Shi L**, Zhang Y, Nie K, Sun X, Niu T, Yue N, Kwong T, Chang P, Chow D, Chen JH, Su MY. Machine learning for prediction of chemoradiation therapy response in rectal cancer using pre-treatment and mid-radiation multi-parametric MRI. *Magn Reson Imaging* 2019; **61**: 33-40 [PMID: [31059768](https://pubmed.ncbi.nlm.nih.gov/31059768/) DOI: [10.1016/j.mri.2019.05.003](https://doi.org/10.1016/j.mri.2019.05.003)]

- 112 **Yi X**, Pei Q, Zhang Y, Zhu H, Wang Z, Chen C, Li Q, Long X, Tan F, Zhou Z, Liu W, Li C, Zhou Y, Song X, Li Y, Liao W, Li X, Sun L, Pei H, Zee C, Chen BT. MRI-Based Radiomics Predicts Tumor Response to Neoadjuvant Chemoradiotherapy in Locally Advanced Rectal Cancer. *Front Oncol* 2019; **9**: 552 [PMID: [31293979](#) DOI: [10.3389/fonc.2019.00552](#)]
- 113 **Alvarez-Jimenez C**, Antunes JT, Talasila N, Bera K, Brady JT, Gollamudi J, Marderstein E, Kalady MF, Purysko A, Willis JE, Stein S, Friedman K, Paspulati R, Delaney CP, Romero E, Madabhushi A, Viswanath SE. Radiomic Texture and Shape Descriptors of the Rectal Environment on Post-Chemoradiation T2-Weighted MRI are Associated with Pathologic Tumor Stage Regression in Rectal Cancers: A Retrospective, Multi-Institution Study. *Cancers (Basel)* 2020; **12**: 2027 [PMID: [32722082](#) DOI: [10.3390/cancers12082027](#)]
- 114 **Bulens P**, Couwenberg A, Intven M, Debucquoy A, Vandecaveye V, Van Cutsem E, D'Hoore A, Wolthuis A, Mukherjee P, Gevaert O, Haustermans K. Predicting the tumor response to chemoradiotherapy for rectal cancer: Model development and external validation using MRI radiomics. *Radiother Oncol* 2020; **142**: 246-252 [PMID: [31431368](#) DOI: [10.1016/j.radonc.2019.07.033](#)]
- 115 **Yang C**, Jiang ZK, Liu LH, Zeng MS. Pre-treatment ADC image-based random forest classifier for identifying resistant rectal adenocarcinoma to neoadjuvant chemoradiotherapy. *Int J Colorectal Dis* 2020; **35**: 101-107 [PMID: [31786652](#) DOI: [10.1007/s00384-019-03455-3](#)]
- 116 **Zhu HT**, Zhang XY, Shi YJ, Li XT, Sun YS. A Deep Learning Model to Predict the Response to Neoadjuvant Chemoradiotherapy by the Pretreatment Apparent Diffusion Coefficient Images of Locally Advanced Rectal Cancer. *Front Oncol* 2020; **10**: 574337 [PMID: [33194680](#) DOI: [10.3389/fonc.2020.574337](#)]

Could the burden of pancreatic cancer originate in childhood?

Smaranda Diaconescu, Georgiana Emmanuela Gîlcă-Blanariu, Silvia Poamaneagra, Otilia Marginean, Gabriela Paduraru, Gabriela Stefanescu

ORCID number: Smaranda

Diaconescu [0000-0001-8018-7191](https://orcid.org/0000-0001-8018-7191);
Georgiana Emmanuela Gîlcă-Blanariu
[0000-0002-5590-6462](https://orcid.org/0000-0002-5590-6462); Silvia
Poamaneagra [0000-0001-7312-5937](https://orcid.org/0000-0001-7312-5937);
Otilia Marginean [0000-0003-2313-7643](https://orcid.org/0000-0003-2313-7643);
Gabriela Paduraru [0000-0002-6765-6018](https://orcid.org/0000-0002-6765-6018);
Gabriela Stefanescu [0000-0002-1394-8648](https://orcid.org/0000-0002-1394-8648).

Author contributions: All authors contributed equally to the conception, design, preparation and writing of this review.

Conflict-of-interest statement: The authors have no conflicts of interest to declare for this article.

Open-Access: This article is an open-access article that was selected by an in-house editor and fully peer-reviewed by external reviewers. It is distributed in accordance with the Creative Commons Attribution NonCommercial (CC BY-NC 4.0) license, which permits others to distribute, remix, adapt, build upon this work non-commercially, and license their derivative works on different terms, provided the original work is properly cited and the use is non-commercial. See: <http://creativecommons.org/licenses/by-nc/4.0/>

Manuscript source: Invited manuscript

Specialty type: Gastroenterology

Smaranda Diaconescu, Gabriela Paduraru, Department of Pediatrics, “Grigore T. Popa” University of Medicine and Pharmacy, Iasi 700115, Romania

Smaranda Diaconescu, Silvia Poamaneagra, Gabriela Paduraru, Department of Pediatric Gastroenterology, St Mary Emergency Children's Hospital, Iasi 700309, Romania

Georgiana Emmanuela Gîlcă-Blanariu, Gabriela Stefanescu, Department of Gastroenterology and Hepatology, “Grigore T. Popa” University of Medicine and Pharmacy, Iasi 700115, Romania

Georgiana Emmanuela Gîlcă-Blanariu, Gabriela Stefanescu, Department of Gastroenterology and Hepatology, “St. Spiridon” Emergency Hospital, Iasi 700111, Romania

Silvia Poamaneagra, Doctoral School, George Emil Palade University of Medicine, Pharmacy, Science and Technology, Targu Mures 540142, Romania

Otilia Marginean, Department of Pediatrics, Research Center of Disturbance of Growth and Development on Children-Belive, University of Medicine and Pharmacy “Victor Babes” Timisoara, Timisoara 300041, Romania

Otilia Marginean, First Clinic of Pediatrics, “Louis Turcanu” Emergency Children's Hospital, Timisoara 300011, Romania

Corresponding author: Smaranda Diaconescu, MD, PhD, Professor, Department of Pediatrics, “Grigore T. Popa” University of Medicine and Pharmacy, 16 Universității str, Iasi 700115, Romania. turti23@yahoo.com

Abstract

The presence of pancreatic cancer during childhood is extremely rare, and physicians may be tempted to overlook this diagnosis based on age criteria. However, there are primary malignant pancreatic tumors encountered in pediatric patients, such as pancreatoblastoma, and tumors considered benign in general but may present a malignant potential, such as the solid pseudo-papillary tumor, insulinoma, gastrinoma, and vasoactive intestinal peptide secreting tumor. Their early diagnosis and management are of paramount importance since the survival rates tend to differ for various types of these conditions. Many pediatric cancers may present pancreatic metastases, such as renal cell carcinoma, which may evolve with pancreatic metastatic disease even after two or more decades. Several childhood diseases may create a predisposition for the development of pancreatic cancer during adulthood; hence, there is a need for extensive screening strategies and complex programs to facilitate the transition from pediatric to adult

and hepatology

Country/Territory of origin:

Romania

Peer-review report's scientific quality classification

Grade A (Excellent): 0

Grade B (Very good): B, B

Grade C (Good): C, C, C

Grade D (Fair): 0

Grade E (Poor): 0

Received: January 28, 2021

Peer-review started: January 28, 2021

First decision: May 13, 2021

Revised: June 8, 2021

Accepted: July 30, 2021

Article in press: July 30, 2021

Published online: August 28, 2021

P-Reviewer: Huang CY, Liu B,

Morelli L, Zhao CF

S-Editor: Zhang H

L-Editor: Filipodia

P-Editor: Liu JH



healthcare. Nevertheless, genetic studies highlight the fact the specific gene mutations and family aggregations may be correlated with a special predisposition towards pancreatic cancer. This review aims to report the main pancreatic cancers diagnosed during childhood, the most important childhood diseases predisposing to the development of pancreatic malignancies, and the gene mutations associates with pancreatic malignant tumors.

Key Words: Pancreatic cancer; Pancreatic metastasis; Childhood; Adult; Screening; Transition

©The Author(s) 2021. Published by Baishideng Publishing Group Inc. All rights reserved.

Core Tip: Pancreatic malignant tumors are rarely found during childhood, their prognosis being linked to the type of tumor and its capacity to evolve towards metastasis. Also, there are types of cancer diagnosed in pediatric patients which may present with pancreatic metastasis later, during adulthood. Various conditions, when diagnosed during childhood, may be associated with the later onset of pancreatic cancer. Also, several genetic mutations have been linked to the development of pancreatic malignancies. We discuss here the above-mentioned topics in the context of a comprehensive literature review.

Citation: Diaconescu S, Gilcă-Blanariu GE, Poamaneagra S, Marginean O, Paduraru G, Stefanescu G. Could the burden of pancreatic cancer originate in childhood? *World J Gastroenterol* 2021; 27(32): 5322-5340

URL: <https://www.wjgnet.com/1007-9327/full/v27/i32/5322.htm>

DOI: <https://dx.doi.org/10.3748/wjg.v27.i32.5322>

INTRODUCTION

In spite of technological, economic and healthcare progress, pancreatic cancer remains correlated with high mortality rates, its diagnosis at an early stage being of paramount importance for a favorable outcome, but this objective has proven exceedingly difficult to achieve. Researchers in the field have attempted to correlate the appearance of malignant pancreatic tumors with various local or systemic diseases and/or genetic mutations. The preventive management in cases of high risk for pancreatic cancer begins during childhood, by assessing and, whenever possible, treating the predisposing factors[1].

Pancreatic tumors are rarely found among the pediatric population; therefore, their study is limited to isolated case reports or case series. From a histological point of view, pancreatic tumors differ during childhood and adulthood, with a tendency for a better prognosis and clinical outcome at younger ages[2].

This review aims at reporting the primary pancreatic malignant tumors encountered during childhood, the pediatric cancers with the capacity to evolve towards pancreatic metastatic disease, the conditions diagnosable at a pediatric age that may predispose to pancreatic cancer during adulthood, and the most important gene mutations correlated with a predisposition towards pancreatic cancer (Table 1).

PANCREATIC MALIGNANT TUMORS IN CHILDREN

In general, pancreatic tumors are divided into epithelial (exocrine, of acinar, ductal, or undetermined cell origin; or endocrine) and non-epithelial types. The most frequent pancreatic tumor among children is of acinar cell origin, pancreatoblastoma. Solid pseudo-papillary tumors present a low malignant potential and are mostly encountered in young female patients. Rare types of pancreatic cancer may be found in children, such as acinar cell carcinoma and the extremely rare ductal adenocarcinomas. In rare cases, neonatal hypoglycemia can be caused by a focal or diffuse neuroendocrine adenoma of the gland[3].

Table 1 Pediatric pancreatic cancers**Pediatric pancreatic malignant tumors**

Pancreatoblastoma
 Solid pseudo-papillary tumors
 Insulinoma
 Gastrinoma
 VIPoma
 Acinar cell carcinoma
 Ductal adenocarcinoma
 Mucinous cystic neoplasm
 Lymphoma: Hodgkin lymphoma, large cell lymphoma, Burkitt's lymphoma
 Germ cell tumors
 Primitive neuroectoderm tumors: extraosseous Ewing's sarcoma
 Mesenchymal tumors: rhabdomyosarcoma, leiomyosarcoma, schwannoma

Pediatric cancers evolving with pancreatic metastatic disease

Renal cell carcinoma
 Sarcomas
 Colorectal carcinoma
 Neuroblastoma

Diseases (diagnosable) in pediatric patients predisposing to pancreatic cancer at adult age

Obesity
 Diabetes mellitus, glucose metabolism disturbances and insulin resistance
 Chronic and hereditary pancreatitis
 Cystic fibrosis
 McCune Albright syndrome
 Multiple endocrine neoplasia type I
 Von Hippel Lindau disease
 Li Fraumeni syndrome

The pancreas may be also involved into neoplastic processes arising from the adjacent structures, such as lymphomas, teratomas, rhabdomyosarcomas and primitive neuroectodermal tumors. Secondary involvement may be seen during metastatic disease originating from neuroblastomas[4].

The study based on the data provided by the United States' National Cancer Institute for the Surveillance, Epidemiology and End Result (SEER) Database confirmed the scarcity of malignant pancreatic tumors in the pediatric population; data collected from a 30-year period of time identified only 58 patients aged under 20 years suffering from malignant pancreatic tumors[4].

Pancreatoblastoma

Pancreatoblastoma was described for the first time in a 15-mo-old male patient in 1957, and was originally termed "infantile adenocarcinoma of the pancreas"[5]. Later, histological similarities were found between the newly discovered type of tumor and the undifferentiated or incompletely differentiated fetal acini at 7-8 wk of gestation in the embryo, and the term "pancreatoblastoma" was imposed[6].

Most cases of pancreatoblastomas are sporadic but there have been cases of congenital nature associated with Beckwith-Wiedemann syndrome (macrosomia, macroglossia, visceromegaly, omphalocele and an increased risk for embryonal tumors, such as nephroblastoma, hepatoblastoma, rhabdomyosarcoma and mostly cystic pancreatoblastoma)[7].

Mostly encountered in pediatric patients aged 0 to 9-years-old, pancreatoblastomas are exceptionally rare in adults.

Pancreatoblastoma usually appears as a large well-defined solitary mass, with lobulated margins ranging between 1.5 cm and 20 cm, and with half of the cases arising from the cephalo-pancreatic region. It may present as a cystic mass accompanied by necrosis, especially when associated with Beckwith-Wiedemann syndrome[3].

Although it has been mostly cited in the male population, Rasalkar *et al*[8] reported two cases of pancreatoblastoma in 2 girls, aged 9-years-old and 11-years-old. The symptomatology included pain and discomfort in the epigastric region, accompanied by a local lump and food intolerance. In both cases, the mass had disordered the local anatomy by displacing the splenic vessels, right kidney, the renal veins and the inferior vena cava. The tumor was located on the head of the pancreas in the first case and on the distal body and pancreatic tail in the second case.

Other symptoms associated with pancreatoblastomas include weight loss, anorexia, fatigue, lethargy, and jaundice in rare cases. Local invasion has been cited, mostly involving the adjacent pancreas, biliary tree, and the local vessels, including the portal and the mesenteric veins. The most common sites of metastases are the liver and abdominal lymph nodes, but there have been case reports of rarely located metastasis, such as to the lungs, brain, omentum, colon, spleen and adrenal glands[9].

Solid pseudo-papillary tumors

Pseudo-papillary tumors of the pancreas are rarely encountered tumors of exocrine origin, having a strong female predilection and being diagnosed during childhood in half of the cases[3]. The literature suggests that they present no preference regarding location on the pancreas, a low-grade malignant potential and a favorable long-term prognosis after surgical treatment[10].

The histological origin of these tumors is not yet clear but it has been linked to ductal cells, endocrine or multipotent stem cells. One important issue is the possibility of recurrence and, hence, the mandatory imaging follow-up. Authors have reported cases of metastasis in the liver, regional lymph nodes, omentum, mesentery and peritoneum[11].

In a 15-year retrospective study, the authors found 11 patients with pseudo-papillary tumors presenting with abdominal pain or palpable abdominal mass, digestive intolerance, and 1 case of traumatic tumor rupture leading to hemoperitoneum; two cases were diagnosed incidentally during medical examinations for other diseases. In this lot, preoperative serum tumor markers were assessed as follows: α -fetoprotein, carcinoembryonic antigen, carbohydrate antigen (CA) 125 were within normal ranges, whereas elevated levels of CA 19-9 were found in 3 of 10 patients[10].

Insulinoma

Insulinomas are particularly rare in children, either the sporadic form or when associated with multiple endocrine neoplasia type 1 (MEN1). Although more than 90% of insulinomas are benign, there have been cases of malignant insulinomas, characterized by the World Health Organization (WHO) according to their metastatic potential and risk of recurrence and mortality. A tumor size larger than 2 cm as well as the presence of cytokeratin 19 and tumor staging and grading with Ki 67 > 2% are reported predictors for the metastatic disease. The most common sites of metastasis are the regional lymph nodes, the liver and bone[12].

The clinical manifestations include symptoms associated with neuroglycopenia, such as loss of consciousness, confusion, dizziness and lethargy, or with adrenergic stimulation, such as hunger, weight gain, tachycardia, palpitations and arterial hypertension; hypoglycemia may be difficult to recognize in neonates and small children up to 2 years of age because of the poor adrenergic symptoms. In these cases, the symptomatology associates with seizures, apnea and lethargy[13].

In a 20-year retrospective study, the fact that metastatic liver disease may appear years after the initial diagnosis and presumed curative surgical treatment of insulinomas was highlighted. In these cases, the metastatic liver disease manifested as recurrent, severe hypoglycemic episodes leading to coma[14].

Gastrinoma

Pancreatic gastrinomas are, in frequency, the second mostly encountered pancreatic neuroendocrine tumors (pNETs) after insulinomas. In children, this is an uncommon tumor, its diagnosis being based on complex biological and imagistic investigations. Because of its rarity, many cases of pediatric gastrinomas remain undiagnosed for

years; evidence of digestive ulcers associated with elevated levels of fasting gastrin is usually diagnostic for a gastrinoma associated with Zollinger-Ellison syndrome, but these findings have to be correlated with advanced imaging investigations in order to assess tumor localization and invasion. In the pediatric population, the malignancy rate is close to 30%, poor prognosis being associated with tumor size (> 3 cm), metastatic disease (especially hepatic, lymph nodes and bone metastasis), female gender, inadequate gastric hypersecretion control as well as the histopathological features[15].

According to the WHO classification, gastrinomas present with different potential of malignization corresponding to the degree of differentiation, as follows: Well differentiated gastrinomas with benign/uncertain behavior; well-differentiated gastrinomas with low-grade malignant behavior; and, poorly differentiated gastrinomas with high-grade malignant potential[16].

Massaro *et al*[17] reported a case of a gastrinoma with hepatic metastasis in a child investigated for Zollinger-Ellison syndrome who eventually underwent orthoptic liver transplant.

The symptomatology of sporadic pancreatic gastrinomas includes epigastric pain due to severe peptic ulcer disease, heartburn, chronic diarrhea, gastrointestinal (GI) bleeding, nausea and vomiting. There are pancreatic gastrinomas associated with *MEN1* mutation, which may manifest clinically at younger ages, before hyperparathyroidism; hence, complex management including assessment of ionized calcium and serum parathormone levels is important[16].

Vasoactive intestinal peptide secreting tumors

The vasoactive intestinal peptide secreting tumors (VIPomas) gather together a group of neuroendocrine tumors characterized by the secretion of the vasoactive intestinal peptide, resulting in the “WDHA” syndrome (featuring achlorhydria, hypokalemia and watery diarrhea). The literature suggests that 60%-80% of VIPomas have malignant potential and present with metastasis at first diagnosis. During childhood, VIPomas are usually diagnosed between 2-4 years of age, but there have been cases at younger age (Reindl *et al*[18] start their series with a 2-mo-old patient).

Metastasis are mostly located in the liver, but rare case of lymph node, lung and kidney metastasis have been described[19].

Acinar cell carcinoma

Carcinoma originating from the acinar cells represents a rare type of pancreatic cancer, although it is more frequently encountered during childhood compared to ductal cell adenocarcinoma. Even though the acinar cells represent the most commonly found cells in the pancreas, their malignant transformation accounts for only 1% of pancreatic exocrine tumors[20].

The histological differentiation between acinar cell carcinoma and pancreatoblastoma may be difficult in children, as their macroscopic and microscopic features tend to be similar. Other distinct characteristics include the presence of calcifications in one-third of the cases and the tendency for intratumoral hemorrhage[21].

Illyés *et al*[22] report the particular case of a 10-year-old male who presented with clinical and biological manifestations associated with Cushing’s syndrome and was later diagnosed with pancreatic acinar cell carcinoma invading the retroperitoneum which evolved with multiple metastasis.

Ductal adenocarcinoma

Ductal adenocarcinomas are exceptionally rare entities in childhood. In spite of some case reports before 1993 and considering the current advancements in medicine and immunohistochemistry, these cases are no longer considered ductal adenocarcinomas [23].

The literature suggests that ductal adenocarcinomas appearing at a young age may present with a tendency for poor differentiation and a high degree of metastasis. The 5-year survival rate is similar to that in adults (2%-4%), although there have been authors who supported a lower survival rate due to delayed diagnosis in children and young adults[3].

Mucinous cystic neoplasms

Pancreatic cystic lesions usually present with a good prognosis in children, but rare cases of malignant (high grade dysplasia) or premalignant (low or intermediate grade dysplasia) course have been described. Recent studies suggest that mucinous cystic neoplasm is asymptomatic and discovered incidentally, and the malignant potential has to be considered, especially in tumors larger than 4 cm[24].

Lymphoma

Lymphomas may originate from the pancreatic tissue itself or may involve the pancreas with the true origin lying in the peripancreatic lymph nodes. During childhood, the most common type of lymphoma involving the pancreas is non-Hodgkin lymphoma; pancreatic and peripancreatic invasion can be seen in cases of large cell lymphoma and Burkitt's lymphoma. The pancreas involvement may be suggested by the presence of the mass itself or by a diffuse infiltration of the gland accompanied by local edema due to a process of acute pancreatitis or tumor lysis syndrome. There have been case reports of primary pancreatic lymphomas at a pediatric age manifested with obstructive jaundice, misleading the diagnosis towards a false acute cholestatic hepatitis[25,26].

Intrinsic pancreatic lymphomas usually affect female patients and manifest with nonspecific symptoms associated with the mass effect (abdominal pain, digestive intolerance). Imaging studies do not offer specific information and in order to make a definitive differential diagnosis from other pancreatic masses, a histological exam remains mandatory[27].

The literature reports less than 10 cases of pancreatic lymphoma manifesting as acute pancreatitis at debut. Athmani *et al*[28] report the case of a 6-year-old female with a rapidly progressive jaundice; in that case, abdominal imaging showed an important increase in the pancreatic size, homogeneous hepatomegaly and intra- and extrahepatic biliary ducts' dilatation. Ultimately, the histopathological examination set the diagnosis of Burkitt's lymphoma.

Standard diagnostic criteria for primary pancreatic lymphoma include absence of superficial lymphadenopathy, no enlargement of mediastinal lymph nodes visible on chest radiography, normal leukocyte count, the main mass located in the pancreas with peripancreatic lymph nodes involvement, and the absence of hepatic or splenic involvement[29].

Germ cell tumors

Extragenital germ cell tumors represent 1%-3% of all childhood tumors. Even though their occurrence, originating from an upper abdominal organ, is exceedingly uncommon, they have been described on the head of the pancreas and causing biliary dilatation and mass-effect related symptoms. Based on the morphological characteristics and on the degree of differentiation, the WHO classifies teratomas as mature and immature[30].

Even though the malignant potential of pancreatic teratomas is yet to be established, 7%-10% of retroperitoneal teratomas with other localization are malignant[31]. For example, in other teratomas, the presence of yolk sac tumor microfoci may promote a malignant relapse after an incomplete surgical resection[32].

Primitive neuroectodermal tumors

Primitive neuroectodermal tumors usually originate in the bone and soft tissue, and there have been cases where they originated from solid organs containing neuroendocrine cells, like the pancreas, which accounts for 0.3% of primary pancreatic neoplasms at all ages[33].

In a literature review of extraosseous Ewing's sarcoma of the pancreas, Bose *et al*[34] pointed out the fact that the symptomatology usually associates with abdominal pain and jaundice; there were 2 particular cases in females of pediatric age where the tumor manifested with precocious puberty and 2 cases of GI bleeding and secondary iron deficiency anemia.

Primitive neuroectodermal tumors present an aggressive behavior, mostly due to the metastatic power; the most usual sites for metastasis are lungs, liver, bone and bone marrow.

Mesenchymal tumors

In children, the most common malignant mesenchymal tumor involving the pancreas is rhabdomyosarcoma. A percentage (specifically 15%) of rhabdomyosarcomas diagnosed during childhood originate from a site other than the head, neck, genitourinary tract and extremities. When situated in the abdomen, rhabdomyosarcomas can have originated from any part of the GI tract, including the extrahepatic biliary tract, pancreas and omentum; malignant ascites is an uncommon feature. An appreciable amount (specifically 14%) of these children present with metastatic disease at the initial diagnosis; the most common sites for metastasis are the lungs (36%), bone marrow (22%) and bones (7%)[35].

In rare cases, leiomyosarcomas may arise from the pancreatic duct and blood vessel walls within the pancreas; although rarely encountered, there have been cases of pancreatic leiomyosarcomas in children aged 14 and older[36].

Pancreatic schwannomas are rarely described in the literature, and more than 90% of them are benign tumors. However, there have been cases, mostly associated with von Recklinghausen disease, where the authors have described large schwannomas with malignant characteristics. Usually found on the pancreatic head and body, they usually manifest as nonspecific abdominal pain, weight loss, jaundice or GI bleeding [37].

Complete surgical resection is the treatment of choice in cases of pancreatic schwannomas, especially due to the fact that the character of malignancy cannot be established pre/during surgery and the fact that they do not respond to radiotherapy or chemotherapy[38].

Sheng *et al*[39] reported the first case of a low-grade malignancy pancreatic solitary fibrous tumor in a pediatric patient, a 14-mo-old male toddler.

PEDIATRIC CANCERS EVOLVING WITH PANCREATIC METASTATIC DISEASE

Metastatic pancreatic disease accounts for less than 2% of the entire pancreatic malignancies[40].

Pancreatic metastasis are rare entities that usually appear years after the diagnosis of the primary tumor. Following a topical literature review, authors reported that 62.6% of pancreatic metastasis appeared secondary to renal cell carcinoma, 7.2% secondary to sarcomas and 6.2% secondary to colorectal carcinoma[41]. Renal cell carcinoma is extremely rare in children, representing 1.8% to 6.3% of all types of renal cancers. Metastases originating from renal cell carcinomas usually present themselves as solitary or multiple masses inside the pancreas, which may occur even 20 years after the primary tumor manifestation. It is mandatory that the differential diagnosis of a pancreatic mass in patients with a history of renal cell carcinoma include secondary pancreatic metastasis[42].

Kim *et al*[43] reported the case of a 4-year-old male with stage 4 neuroblastoma, who presented with pancreatic metastasis manifesting as acute pancreatitis and rapidly progressive severe cholestasis. Farah *et al*[44] reported the case of a 15-year-old female who developed pancreatic metastasis due to an alveolar rhabdomyosarcoma located into the paranasal sinuses.

Pediatric pancreatic malignant tumors present with different degrees of aggressiveness and different potential for metastatic disease or local recurrences. The overall survival rates of pancreatic cancer diagnosed during childhood is not well established, but the 5-year survival rate for particular tumors ranges from more than 95% for some to as low as 2%-4% for ductal adenocarcinomas. For example, Bien *et al*[45] highlighted the fact that the 5-year survival rate of patients with pancreatoblastomas ranges between 30%-50%, despite surgical treatment and chemotherapy.

The 5-year survival rate for solid pseudo-papillary tumors has been reported between 95%-98% after complete surgical resection[46]. Primitive neuroectodermal tumors are highly aggressive and present with very poor prognosis; the 5-year survival rate is reported to be 50%[47].

Brecht *et al*[4] analyzed 5-year overall survival in a group of 228 patients under the age of 30 diagnosed with malignant pancreatic tumors (100 carcinomas, 85 endocrine tumors, 8 solid pseudopapillary neoplasms, 11 pancreatoblastomas). The data were extracted from the United States National Cancer Institute's SEER Public-use Database from 1973 to 2004. According to this study, 5-year overall survival (OAS) varied widely as follows: According to stage, it was 87%, 68%, 21 % for local ($n = 54$), regional ($n = 42$), distant metastatic disease ($n = 108$), respectively. According to histological types, OAS of patients with carcinoma was 33%, endocrine tumors 58%, solid pseudo-papillary tumor of the pancreas 88%, pancreatoblastomas 66%. Following multivariate analysis, tumor stage, histology and age group are important and independent predictors for outcome.

Similar results were recently reported by Picado *et al*[48] analyzing the Data from the National Cancer Database (2004-2014) which included 109 children with pancreatic tumors. The 5-year overall survival by tumor histology was 95% for pseudopapillary tumors, 75% for neuroblastomas, 70% for pancreatoblastomas, 51% for endocrine tumors, 43% for sarcomas, and 34% for adenocarcinomas. On multivariable analysis, the strongest predictor of survival was the surgical resection[48].

Another recently published study, performed on 65 patients under the age of 21 diagnosed with pancreatic neoplasms, who followed the outcome after pancreaticoduodenectomy, reported that the 5-year overall survival by tumor histology was 95% for pseudopapillary neoplasm, 75% for neuroblastomas, 70% for pancreatoblastomas, 51% for endocrine tumors, 43% for sarcomas, and 34% for adenocarcinomas. In this study, the outcome was primarily associated with histology[49].

The burden of a diagnosis such as pancreatic cancer is often associated with adulthood, and pediatricians are tempted to overlook this possibility, especially in a toddler or young child. Diagnostic delays/mistakes are not uncommon at this age and they lead to worse outcome due to the aggressiveness of the local mass and the metastatic character.

DISEASES (DIAGNOSABLE) IN PEDIATRIC PATIENTS PREDISPOSING TO PANCREATIC CANCER AT ADULT AGE

Obesity

Various studies have highlighted a connection between increased body mass index (BMI) and the risk for pancreatic cancer[50-52].

It has been observed that a BMI of at least 30 kg/m² was associated with a significantly increased risk of pancreatic cancer compared with a BMI of less than 23 kg/m² [relative risk (RR): 1.72, 95%CI: 1.19-2.48], while an inverse relationship was also highlighted for moderate physical activity when comparing the highest to the lowest categories (RR: 0.45, 95%CI: 0.29-0.70), particularly among those with a BMI of at least 25 kg/m²[53].

Moreover, it has been suggested that obese individuals develop pancreatic cancer earlier in life compared to patients with a normal weight, while also having lower survival rates following the diagnosis of pancreatic cancer[51,54].

Recent studies have also shown that overweight status and obesity in late adolescence and early adulthood are associated with an increased risk of this type of cancer[55,56].

Taking these aspects into consideration, researchers also questioned whether increased body weight during childhood would also be associated with adult pancreatic cancer. A prospective Danish cohort study including over 293000 individuals for whom data on height and BMI between the ages of 7 and 13 years were available, linked this information with data from Danish Cancer Registry. This study highlighted that increased BMI at every age from 7-13 years was significantly and positively associated with pancreatic cancer in adulthood, diagnosed up until age 70 [57].

Furthermore, the American National Institutes of Health-AARP (formerly known as the American Association of Retired Persons) Diet and Health Study Cohort and several pooled analyses of cohort studies also revealed that adolescent or early adulthood body size would be positively associated with pancreatic cancer[51,58].

BMI in children aged 7-13 was identified as being associated with the development of pancreatic cancer in adulthood[57].

These positive associations were not dependent of the evolution of BMI later in life, indicating that the risk was established to a certain extent in earlier life. Consequently, in the context of increased prevalence of childhood obesity, improved strategies for prevention and early management of childhood obesity should be considered to diminish the risk for developing pancreatic cancer in adulthood, but also for other various diseases including cardiovascular diseases and other types of neoplasia[59-61].

Diabetes mellitus, glucose metabolism, and insulin resistance

The relationship between diabetes and pancreatic cancer has been investigated extensively, since numerous epidemiologic studies have described an association between these two entities; a meta-analysis including 88 cohort and case-control studies identified an around 2-fold risk (RR: 2.08, 95%CI: 1.87-2.32) of pancreatic malignancy in diabetic patients compared to patients without diabetes[62-64].

However, the exact direction of this association is under debate, with some data suggesting that diabetes may be a consequence rather than a cause of pancreatic cancer, while others support the bidirectional relationship between the two entities, taking into account some pathophysiological background, such as the fact that insulin resistance, as well as obesity may be mediated by reduced levels of plasma adiponectin, a fat-derived hormone that has insulin-sensitizing and anti-inflammatory properties[65-67].

All these data have come from studies including adult populations and mainly focused on type 2 diabetes mellitus, with less data on type 1 diabetes mellitus. A systematic review of studies that assessed risk of pancreatic cancer in people with diabetes, specifically mentioning whether it was type 1 or type 2 diabetes, or a surrogate for type 1 diabetes, such as young age at onset, suggested that the risk of pancreatic cancer is comparably increased both for type 1 and type 2 diabetes. The results of this systematic review also underlined some causality within this relationship. With regard to type 2 diabetes, a bidirectional relationship can be called upon, meaning that insulin resistance and diabetes may be induced by undiagnosed cancer or precancerous conditions of the pancreas, but considering the increased risk of pancreatic cancer reported as 1.5- to 2-fold higher in type 2 diabetes even when impaired glucose tolerance is detected more than 10 years before onset of cancer, suggesting that reverse causality does not individually and exclusively explain the association[68,69].

With regard to type 1 diabetes, it is likely, considering the early age at its onset, that it precedes pancreatic cancer rather than the other way round; therefore, type 1 diabetes should be considered a risk factor for pancreatic cancer[70].

Large cohort studies indicated that cancer risk in type 1 diabetes is rather low, but other authors reported that this risk is comparable between type 1 and type 2 diabetes. As older studies report, type 1 diabetes associates an overall modestly increased cancer risk[71].

Both epidemiological and genetic studies have tried to prove the association between type 2 diabetes and pancreatic cancer. Pierce *et al*[72] analyzed the 37 risk alleles attributed to type 2 diabetes and found a significant positive association between 2 of these alleles and pancreatic cancer.

However, the currently available data is limited and further studies including large type 1 and 2 diabetes and nondiabetic cohorts are needed.

Chronic pancreatitis

Chronic pancreatitis is a risk factor for pancreatic adenocarcinoma, independent of etiology[73,74].

Although the exact pathophysiology is not yet clear, several signaling pathways have been identified as activated during pancreatic inflammation, in the context of repeated DNA damage, error-prone repair mechanisms, and the progressive accumulation of genetic mutations, ultimately stimulating the development of pancreatic cancer[75]. Pancreas precancerous histologic changes are associated with a sequential accumulation of genetic defects, namely pancreatic intraepithelial neoplasms, which are present in sporadic pancreatic adenocarcinomas and also in patients with a history of chronic pancreatitis. Mutations found in the early stages involve the *kRas* gene, followed by *p16/CDKN2A*, *TP53* and *SMAD4/DPC4* genes[76]. Mutations in all four genes have been recognized as driver mutations that trigger neoplastic transformation and tumor progression[77].

Non-hereditary chronic pancreatitis is also an important risk factor for pancreatic cancer[73,74]. Reports from the International Pancreatitis Study Group identified a cumulative risk of 1.8% at 10 years and 4% at 20 years for pancreatic cancer, independent of the etiology of chronic pancreatitis[78]. More recent data included in a meta-analysis has suggested that the risk of pancreatic cancer was elevated 16-fold in patients with more than 2 years since their diagnosis of chronic pancreatitis, and even though this risk declines over time, it persists even after long-term follow-up. After at least 9 years of follow-up from the time of diagnosis of chronic pancreatitis, this patient category still had an over 3-fold increased risk of pancreatic cancer compared to patients without chronic pancreatitis[79].

Although these data were obtained from an adult population, they raise concern regarding the pediatric population, especially when considering patients with hereditary pancreatitis. Pancreatitis is rare in the pediatric population and frequently reported as idiopathic pancreatitis, showing gaps in the identification of the etiology. Recently, it was shown that genetic factors play a far more important role in the development of chronic pancreatitis in infancy and childhood than previously thought [80].

Hereditary pancreatitis is defined as two first-degree relatives or at least three second-degree relatives in two or more generations with chronic pancreatitis for which there is no other etiology. Several mutations have been associated with hereditary pancreatitis, from the initial description of the mutation in the cationic trypsinogen gene (*PRSS1*) by Whitcomb *et al*[81] to mutations in the *SPINK1*, *CPA1* and *CFTR* genes[82-85].

Due to a lack of specific signs and even to a sometimes quiet presentation, hereditary pancreatitis is frequently diagnosed at an advanced stage[86].

In some sporadic cases, mutations compatible with hereditary pancreatitis can be found without a corresponding family history, which could be explained by inheritance from unaffected carrier parents or even spontaneous *de novo* mutations[75, 87].

Although progress has been made in diagnosing hereditary pancreatitis, the therapeutic pathway for this entity in children is still under debate[80]. Furthermore, counseling in patients with hereditary pancreatitis and their families should cover several aspects, from highly penetrant childhood-onset disease to a predisposition for pancreatic cancer in adulthood[88].

Studies are suggesting that *PRSS1* and *CFTR* gene mutations may not be directly linked with the development of pancreatic cancer. The onset of hereditary pancreatitis during childhood or early adulthood favors the perpetual exposure to chronic inflammation. The link between inflammation and cancer may not be limited to a subset of tumors but may be present within different types of cancer including lung, bladder, digestive, skin, and vulvar cancer. Hence, even though mutations in the *PRSS1* and *CFTR* genes are not directly associated with pancreatic cancer, chronic inflammation may favor tumor formation[89].

Beyond hereditary pancreatitis, other genetically determined conditions, including exocrine pancreatic insufficiency could evolve towards chronic pancreatitis and therefore potentially associate an increased risk for pancreatic cancer. Among these, Shwachman-Diamond syndrome is included. This a rare multi-organ recessive disease, mainly characterized by bone marrow failure leading to increased risk of transformation to myelodysplastic syndrome, skeletal defects, short stature, and pancreatic insufficiency contributing to the failure to thrive[90].

Cystic fibrosis

The cystic fibrosis phenotype results from mutations in the gene encoding the cystic fibrosis transmembrane conductance regulator protein encoded by the *CFTR* gene and is among the most common autosomal recessive disease in White people having an increased risk of pancreatic cancer[91].

A meta-analysis investigating the risk for various cancers in cystic fibrosis patients identified a standardized incidence ratio of 6.18 (95%CI: 1.31-29.27), which is 2-fold to 5-fold higher in patients who had undergone lung transplantation in this setting[92]. Since there is an excess risk of early-onset pancreatic cancer in patients with cystic fibrosis, interventions for avoiding this setting should be identified. These could range from tackling environmental factors to gene therapy targeting mucin genes. Considering that nutritional deficiencies represent another possible risk factor for cancer, appropriate nutritional interventions to avoid or correct deficits should also be considered[93].

Mccune-Albright syndrome

McCune-Albright syndrome (MAS) represents a rare disorder, characterized by variable phenotypic expressions, including fibrous dysplasia of bone, hyperfunctioning endocrinopathies, and café-au-lait macules, in the context of a somatic gain-of-function mutation in the *GNAS* gene, which encodes the cAMP-regulating protein $G\alpha_s$, taking place early in embryonic development[94]. These types of *GNAS* mutations were previously identified in various types of neoplasias (pituitary, thyroid, appendiceal, and gonadal tumors, and breast cancer)[95-99].

Since there is such a wide range of pathology associated with MAS, it is essential to define them all and to establish an optimal screening strategy and clinical management. The activating *GNAS* mutations have been identified as somatic driver mutations in sporadic intraductal papillary mucinous neoplasms (IPMNs) and various GI lesions, also suggesting a potential role in pancreatic and GI tumorigenesis[100].

In a cohort of patients with MAS, about 46% developed IPMNs, which have risk for malignant degeneration[100,101]. This can lead to IPMN-associated adenocarcinoma but also to developing concurrent or distinct ductal adenocarcinoma, a pattern which has been described in a 2%-9% of patients who are being followed for IPMN[102,103].

Consequently, GI manifestations in MAS are common and include precursory pancreatic lesions for pancreatic cancer; therefore, patients with MAS may benefit from evaluation for GI pathology. Even though the optimal care for pancreatic lesions in MAS is not clearly shaped, a thorough GI history-taking at every visit and consideration of imaging with abdominal magnetic resonance imaging/magnetic resonance cholangiopancreatography would be useful[100].

A small observational study describes the link between MAS and pancreatic cancer, liver adenoma and choledochal cysts *via* the cAMP pathway. Taking into consideration this association, the authors suggest that all patients suffering from MAS should benefit from routine screening by magnetic resonance imaging (MRI) and if no lesion is observed, surveillance MRI may be performed every 5 years[104].

MEN1

MEN1 mutations cause a rare hereditary tumor syndrome, with an autosomal dominant transmission and high degree of penetrance. *MEN1* tumors are caused by inactivating mutations of the tumor suppressor gene *MEN1*, and is characterized by a predisposition to a multitude of endocrine and nonendocrine tumors[105]. The classical phenotype includes hyperplasia and/or tumors of parathyroid, enteropancreatic, and/or anterior pituitary origin, with 30%–70% of patients developing enteropancreatic tumors, either functional or non-functional pancreatic endocrine pancreatic tumors upon reaching middle age[106]. Germline *MEN1* mutations have also been noted in families with only a parathyroid disorder, namely familial isolated primary hyperparathyroidism, but this type of mutation has also been reported in some cases of “sporadic” pNETs[107-109].

Considering the pattern of transmission and variety of manifestations, the Endocrine Society’s clinical practice guidelines for *MEN1* recommend a complex surveillance scheme commencing at early pediatric age, aiming to detect early and manage optimally *MEN1*-associated manifestations and tumors[110]. Recommended screening for pancreatic tumors in this setting begins early, at age 5 for insulinoma, with recommendation for yearly evaluation of fasting glucose and insulin level; for other pNETs, screening is recommended beginning at age 10, with evaluation of chromogranin A, pancreatic polypeptide, glucagon, vasoactive intestinal peptide levels and annual imaging, comprising magnetic resonance imaging, computed tomography or endoscopic ultrasound, considering that large pancreatic tumors may develop between 10 and 20 years of age[105].

Von Hippel-Lindau disease

Von Hippel–Lindau (vHL) disease is an autosomal dominant syndrome which occurs secondary to germline mutations in the *VHL* tumor suppressor gene, with patients being at risk of developing visceral cysts and tumors throughout the body[111]. Most commonly, the pancreas and kidneys are involved, with development of cystic lesions, but there is also an increased risk of developing neoplasms, often with clear cell features, including cerebellar and retinal hemangioblastomas, adrenal pheochromocytomas, clear cell renal cell carcinomas, pancreatic neuroendocrine tumors and pancreatic serous cystadenomas.

Although the most frequent pancreatic lesions include pancreatic cysts, which are found in 75% of vHL patients, one-fifth of the vHL patients will present pNETs, arising earlier than in non-syndromic patients, mostly in the fourth decade of life[112, 113].

Considering the increased potential for metastatic disease of pNETs in vHL patients and also the risk for metastasis generally associated with pNETs, regardless of the histologic grade, surgical resection is typically recommended for all pNETs greater than 2 cm[114]. However, taking into account the possibility of recurrent pNETs in vHL patients, in the context of the particular genetic background, the therapeutic decision must be well considered[115]. Although these lesions most commonly present during adulthood, screening and surveillance should begin in the pediatric years for patients with vHL disease.

Li Fraumeni syndrome

Li Fraumeni syndrome (LFS) is inherited in an autosomal dominant manner, which implies an increased risk for multiple primary cancers in affected individuals[116]. The most frequently implied cancers include bone and soft tissue sarcomas, leukemia, breast cancer, and brain tumors; subsequent evidence highlighted a broader spectrum of neoplasia, including cancers of the lung, digestive tract, prostate, ovary and pancreas, as well as lymphoma and melanoma[117,118].

Germline mutations in the tumor suppressor gene *TP53* are mainly incriminated for this syndrome; however, the absence of detectable germline *TP53* mutations in some LFS families suggests other genes are potentially involved in this syndrome[119].

There are various diagnostic criteria for the syndrome, such as the one included in the classical definition, which was afterwards extended for Li Fraumeni-like syndrome (an entity which shares some features of LFS but does not meet the strict LFS diagnostic criteria), in order to establish the criteria for *TP53* genetic testing[120]. Since

there is such a diversity of types of neoplasia which could arise in the context of LFS, we currently lack appropriate clinical surveillance strategies in this setting. Moreover, in the absence of a thorough knowledge on potential clinical benefits, psychosocial and economic impact of a comprehensive clinical surveillance protocol on early cancer detection, including pancreatic cancer screening, in asymptomatic *TP53* mutation carriers remains unknown.

OTHER GENE MUTATIONS ASSOCIATED WITH A PREDISPOSITION FOR PANCREATIC CANCER

Genetic risk factors play a major role in the development of pancreatic cancer, even if we are considering hereditary pancreatic cancer, familial pancreatic cancer or cases of pancreatic cancer associated with a familial cancer syndrome. The genetic predisposition for developing a particular malignancy has been of interest over the last decades, and several gene variants have been linked to an increased risk for pancreatic cancer, such as *BRCA1* and *BRCA2*, *STK11*, *PRSS1*, *PALB2*, *ATM*, *CDKN2A*, *APC*, *MLH1*, *MSH6*, *MSH2*, and *PMS2*[121].

However, this area of genetic research is still providing new information with the expectation to develop tests in order to assess the individual risk factors for pancreatic cancer, especially inside families with pancreatic cancer patients.

The definition of familial pancreatic cancer implies the existence of at least one pair of first-degree relatives suffering from pancreatic cancer, in the absence of a particular syndrome inside the family[122].

BRCA1 and *BRCA2* mutations are highly associated with inherited breast and ovarian cancer, but in carriers other types of cancer occur at higher rates than in the general population, including of pancreatic cancer. Brose *et al*[123] emphasize the fact that the general population risk of 1.3% transforms into a 2.8 RR for pancreatic cancer in people who carry the *BRCA1* mutation.

Familial atypical multiple mole melanoma syndrome is disease related to a cell cycle regulator gene for the p16 protein product, *CDKN2A*. Screening should begin early in childhood, in order to capture the early debut of both malignant melanoma and pancreatic cancer[124].

APC gene mutations are associated with the onset of familial adenomatous polyposis, a condition which, classically, increases the risk for colorectal cancer. Nowadays, evidence strongly suggests a correlation between inherited mutation of this gene and duodenal, thyroid, hepatic and pancreatic cancers[125].

The hereditary non-polyposis colorectal cancer known as Lynch syndrome also accounts for an increased risk for pancreatic cancer (1.3%-4%)[126]. Geary *et al*[127] pointed out the 30-fold increased risk for pancreatic cancer in patients with particular germline mutations in genes associated with the appearance of Lynch syndrome, such as *MLH1*, *MSH2*, *MSH6* and *PMS2*.

Complete family medical history is of paramount importance in assessing the particular risk for pancreatic cancer. In risk stratification, early molecular studies and germline mutation testing are mandatory.

CONCLUSION

Pancreatic cancer is generally considered an adulthood condition. In spite of this fact, its origins may lay in diseases or predisposing conditions which may be diagnosed at an early age, hence the need for rigorous screening strategies in patients with hereditary diseases connected with pancreatic cancer or familial aggregation of such conditions. Clinicians should be aware of rare conditions diagnosed during childhood, which may associate an increased risk for adult-onset pancreatic cancer. Also, the rare diagnosis of pancreatic cancer should be taken into consideration even at a pediatric age, especially when facing previously considered idiopathic acute pancreatitis or cholestatic hepatitis. The clinical features associated with pancreatic or peripancreatic masses may mimic other diseases and their management should include extensive imaging and histopathological examinations.

Malignant pancreatic tumors remain extremely rare in children and young adults and limited data on incidence and outcomes are available. Entities change over the age groups towards a predominantly increased number of carcinomas with worse outcome in older patients. The overall survival of pediatric patients with pancreatic

tumors is grim, and the survival rates tend to vary between different tumors. Given the rarity and aggressivity of many histological types of pancreatic tumors in children, in many instances it is difficult to assess whether there is any link between pancreatic cancer in childhood and adulthood.

International collaboration is needed to learn more about pediatric pancreatic tumors and to study the link between pancreatic tumors in childhood and adulthood.

Prophylaxis strategies should include weight control during childhood, screening for diabetes mellitus at younger ages, early routine imagistic investigations in cases with a predisposition towards pancreatic cancer or pancreatic metastasis. MRI and endoscopic ultrasonography are the recommended screening methods for pancreatic lesions. Also, screening strategies should include parents, siblings and children of patients with pancreatic cancer, especially in cases where there are more than 2 pancreatic cancer patients within the same biological family.

The implementation of transition programs from pediatric to adult healthcare services remains mandatory for these patients, namely childhood pancreatic cancer survivors or children with predisposing conditions for pancreatic malignancies.

REFERENCES

- 1 **Yu DC**, Kozakewich HP, Perez-Atayde AR, Shamberger RC, Weldon CB. Childhood pancreatic tumors: a single institution experience. *J Pediatr Surg* 2009; **44**: 2267-2272 [PMID: 20006007 DOI: 10.1016/j.jpedsurg.2009.07.078]
- 2 **van den Akker M**, Angelini P, Taylor G, Chami R, Gerstle JT, Gupta A. Malignant pancreatic tumors in children: a single-institution series. *J Pediatr Surg* 2012; **47**: 681-687 [PMID: 22498381 DOI: 10.1016/j.jpedsurg.2011.11.046]
- 3 **Chung EM**, Travis MD, Conran RM. Pancreatic tumors in children: radiologic-pathologic correlation. *Radiographics* 2006; **26**: 1211-1238 [PMID: 16844942 DOI: 10.1148/rg.264065012]
- 4 **Brecht IB**, Schneider DT, Klöppel G, von Schweinitz D, Barthlen W, Hamre MR. Malignant pancreatic tumors in children and young adults: evaluation of 228 patients identified through the Surveillance, Epidemiology, and End Result (SEER) database. *Klin Padiatr* 2011; **223**: 341-345 [PMID: 22012608 DOI: 10.1055/s-0031-1287836]
- 5 **BECKER WF**. Pancreatoduodenectomy for carcinoma of the pancreas in an infant; report of a case. *Ann Surg* 1957; **145**: 864-70; discussions, 870 [PMID: 13425296 DOI: 10.1097/0000658-195706000-00008]
- 6 **Horie A**, Yano Y, Kotoo Y, Miwa A. Morphogenesis of pancreatoblastoma, infantile carcinoma of the pancreas: report of two cases. *Cancer* 1977; **39**: 247-254 [PMID: 188539 DOI: 10.1002/1097-0142(197701)39:1<247::aid-cnrcr2820390138>3.0.co;2-f]
- 7 **Cheng H**, Yang S, Ren Q, Yang W, Han W, Chang X, Zhu Z, Qin H, Wang H. Pancreatectomies for pediatric pancreatic tumors: A single institute experience from 2007 to 2018. *J Pediatr Surg* 2020; **55**: 1722-1726 [PMID: 31575410 DOI: 10.1016/j.jpedsurg.2019.08.051]
- 8 **Rasalkar DD**, Paunipagar BK, Chu WC. Two Children with Pancreatoblastomas. *J Hong Kong Col Radiol* 2010; **13**: 133-136
- 9 **Montemarano H**, Lonergan GJ, Bulas DI, Selby DM. Pancreatoblastoma: imaging findings in 10 patients and review of the literature. *Radiology* 2000; **214**: 476-482 [PMID: 10671596 DOI: 10.1148/radiology.214.2.r00fe36476]
- 10 **Park JY**, Kim SG, Park J. Solid pseudopapillary tumor of the pancreas in children: 15-year experience at a single institution with assays using an immunohistochemical panel. *Ann Surg Treat Res* 2014; **86**: 130-135 [PMID: 24761421 DOI: 10.4174/ast.2014.86.3.130]
- 11 **Guo N**, Zhou QB, Chen RF, Zou SQ, Li ZH, Lin Q, Wang J, Chen JS. Diagnosis and surgical treatment of solid pseudopapillary neoplasm of the pancreas: analysis of 24 cases. *Can J Surg* 2011; **54**: 368-374 [PMID: 21939604 DOI: 10.1503/cjs.011810]
- 12 **Nagtegaal ID**, Odze RD, Klimstra D, Paradis V, Rugge M, Schirmacher P, Washington KM, Carneiro F, Cree IA; WHO Classification of Tumours Editorial Board. The 2019 WHO classification of tumours of the digestive system. *Histopathology* 2020; **76**: 182-188 [PMID: 31433515 DOI: 10.1111/his.13975]
- 13 **Miron I**, Diaconescu S, Aprodu G, Ioniuc I, Diaconescu MR, Miron L. Diagnostic Difficulties in a Pediatric Insulinoma: A Case Report. *Medicine (Baltimore)* 2016; **95**: e3045 [PMID: 26986124 DOI: 10.1097/MD.0000000000003045]
- 14 **Hirshberg B**, Cochran C, Skarulis MC, Libutti SK, Alexander HR, Wood BJ, Chang R, Kleiner DE, Gorden P. Malignant insulinoma: spectrum of unusual clinical features. *Cancer* 2005; **104**: 264-272 [PMID: 15937909 DOI: 10.1002/cncr.21179]
- 15 **Nath AL**, Saxena NA, Kulkarni BK, Borwankar SS, Lahoti HN, Oak SN. Zollinger-Ellison Syndrome in a 12-year-old Child. *J Indian Assoc Pediatr Surg* 2017; **22**: 168-169 [PMID: 28694576 DOI: 10.4103/0971-9261.207623]
- 16 **Jensen RT**, Niederle B, Mitry E, Ramage JK, Steinmuller T, Lewington V, Scarpa A, Sundin A, Perren A, Gross D, O'Connor JM, Pauwels S, Kloppel G; Frascati Consensus Conference;

- European Neuroendocrine Tumor Society. Gastrinoma (duodenal and pancreatic). *Neuroendocrinology* 2006; **84**: 173-182 [PMID: 17312377 DOI: 10.1159/000098009]
- 17 **Massaro SA**, Emre SH. Metastatic gastrinoma in a pediatric patient with Zollinger-Ellison syndrome. *J Pediatr Hematol Oncol* 2014; **36**: e13-e15 [PMID: 23426004 DOI: 10.1097/MPH.0b013e318282dadf]
 - 18 **Reindl T**, Degenhardt P, Luck W, Riebel T, Sarioglu N, Henze G, Driever PH. [The VIP-secreting tumor as a differential diagnosis of protracted diarrhea in pediatrics]. *Klin Padiatr* 2004; **216**: 264-269 [PMID: 15455292 DOI: 10.1055/s-2004-44901]
 - 19 **Yeh PJ**, Chen SH, Lai JY, Lai MW, Chiu CH, Chao HC, Wu RC, Wang CJ, Chen CC. Rare Cases of Pediatric Vasoactive Intestinal Peptide Secreting Tumor With Literature Review: A Challenging Etiology of Chronic Diarrhea. *Front Pediatr* 2020; **8**: 430 [PMID: 32850544 DOI: 10.3389/fped.2020.00430]
 - 20 **Al-Hader A**, Al-Rohil RN, Han H, Von Hoff D. Pancreatic acinar cell carcinoma: A review on molecular profiling of patient tumors. *World J Gastroenterol* 2017; **23**: 7945-7951 [PMID: 29259370 DOI: 10.3748/wjg.v23.i45.7945]
 - 21 **Park M**, Koh KN, Kim BE, Im HJ, Kim DY, Seo JJ. Pancreatic neoplasms in childhood and adolescence. *J Pediatr Hematol Oncol* 2011; **33**: 295-300 [PMID: 21464765 DOI: 10.1097/MPH.0b013e318206990a]
 - 22 **Illyés G**, Luczay A, Benyó G, Kálmán A, Borka K, Köves K, Rác K, Tulassay T, Schaff Z. Cushing's syndrome in a child with pancreatic acinar cell carcinoma. *Endocr Pathol* 2007; **18**: 95-102 [PMID: 17917000 DOI: 10.1007/s12022-007-0018-4]
 - 23 **Lüttges J**, Stigge C, Pacena M, Klöppel G. Rare ductal adenocarcinoma of the pancreas in patients younger than age 40 years. *Cancer* 2004; **100**: 173-182 [PMID: 14692038 DOI: 10.1002/cncr.11860]
 - 24 **Luo JJ**, Baksh FK, Pfeifer JD, Eastman JT, Beyer FC 3rd, Dehner LP. Abdominal mucinous cystic neoplasm in a male child. *Pediatr Dev Pathol* 2008; **11**: 46-49 [PMID: 18237233 DOI: 10.2350/07-01-0220.1]
 - 25 **Sood V**, Agrawal N, Alam S, Rawat D, Khanna R, Bansal K, Bihari C. Primary Pancreatic Lymphoma Simulating Acute Cholestatic Hepatitis in a 7-Year-Old Child. *ACG Case Rep J* 2015; **2**: 190-192 [PMID: 26157960 DOI: 10.14309/crj.2015.51]
 - 26 **Shet NS**, Cole BL, Iyer RS. Imaging of pediatric pancreatic neoplasms with radiologic-histopathologic correlation. *AJR Am J Roentgenol* 2014; **202**: 1337-1348 [PMID: 24848833 DOI: 10.2214/AJR.13.11513]
 - 27 **Arenas García BR**. [Primary pancreatic lymphoma in pediatric patients]. *Radiologia* 2007; **49**: 125-127 [PMID: 17403343 DOI: 10.1016/s0033-8338(07)73733-5]
 - 28 **Athmani I**, Le Rouzic MA, Valduga J, Mansuy L, Contet A, Galloy MA, Fouyssac F, Chastagner P. Pediatric pancreatic Burkitt lymphoma with obstructive jaundice: case report of a six-year-old child. *Arch Clin Cases* 2017; **4** [DOI: 10.22551/2017.17.0404.10114]
 - 29 **Amodio J**, Brodsky JE. Pediatric Burkitt lymphoma presenting as acute pancreatitis: MRI characteristics. *Pediatr Radiol* 2010; **40**: 770-772 [PMID: 20135116 DOI: 10.1007/s00247-009-1475-3]
 - 30 **Wang J**, Yin Y, Cai Z, Shen C, Yin X, Chen X, Zhao Z, Zhang B. Pediatric pancreatic teratoma: A case report and literature review. *Medicine (Baltimore)* 2019; **98**: e18001 [PMID: 31725669 DOI: 10.1097/MD.0000000000018001]
 - 31 **Zhou XH**, Ma JK, Valluru B, Sharma K, Liu L, Hu JB. Diagnosis and differentiation of mature cystic teratoma of pancreas from its mimics: A case report. *Medicine (Baltimore)* 2020; **99**: e23267 [PMID: 33217853 DOI: 10.1097/MD.0000000000023267]
 - 32 **Harms D**, Zahn S, Göbel U, Schneider DT. Pathology and molecular biology of teratomas in childhood and adolescence. *Klin Padiatr* 2006; **218**: 296-302 [PMID: 17080330 DOI: 10.1055/s-2006-942271]
 - 33 **Teixeira U**, Goldoni M, Unterleider M, Diedrich J, Balbinot D, Rodrigues P, Monteiro R, Gomes D, Sampaio J, Fontes P, Waechter F. Primitive Neuroectodermal Tumor of the Pancreas: A Case Report and Review of the Literature. *Case Rep Surg* 2015; **2015**: 276869 [PMID: 26101685 DOI: 10.1155/2015/276869]
 - 34 **Bose P**, Murugan P, Gillies E, Holter JL. Extrasosseous Ewing's sarcoma of the pancreas. *Int J Clin Oncol* 2012; **17**: 399-406 [PMID: 21892669 DOI: 10.1007/s10147-011-0311-6]
 - 35 **McCarville MB**, Spunt SL, Pappo AS. Rhabdomyosarcoma in pediatric patients: the good, the bad, and the unusual. *AJR Am J Roentgenol* 2001; **176**: 1563-1569 [PMID: 11373233 DOI: 10.2214/ajr.176.6.1761563]
 - 36 **Riddle ND**, Quigley BC, Browarsky I, Bui MM. Leiomyosarcoma arising in the pancreatic duct: a case report and review of the current literature. *Case Rep Med* 2010; **2010**: 252364 [PMID: 20589089 DOI: 10.1155/2010/252364]
 - 37 **Aggarwal G**, Satsangi B, Shukla S, Lahoti BK, Mathur RK, Maheshwari A. Rare asymptomatic presentations of schwannomas in early adolescence: three cases with review of literature. *Int J Surg* 2010; **8**: 203-206 [PMID: 20167297 DOI: 10.1016/j.ijssu.2010.01.012]
 - 38 **Cayirli H**, Tanriverdi HI, Ozguven AA, Gunsar C, Ersoy B, Kandiloglu AR. Schwannoma Localized Retroperitoneally in a 14-Year-Old Boy. *Case Rep Pediatr* 2016; **2016**: 1210874 [PMID: 28078159 DOI: 10.1155/2016/1210874]
 - 39 **Sheng Q**, Xu W, Liu J, Shen B, Deng X, Wu Y, Wu W, Yu S, Wang X, Lv Z. Pancreatic solitary

- fibrous tumor in a toddler managed by pancreaticoduodenectomy: a case report and review of the literature. *Onco Targets Ther* 2017; **10**: 1853-1858 [PMID: 28392706 DOI: 10.2147/OTT.S133650]
- 40 **Lee M**, Song JS, Hong SM, Jang SJ, Kim J, Song KB, Lee JH, Cho KJ. Sarcoma metastasis to the pancreas: experience at a single institution. *J Pathol Transl Med* 2020; **54**: 220-227 [PMID: 32311873 DOI: 10.4132/jptm.2020.03.04]
- 41 **Adler H**, Redmond CE, Heneghan HM, Swan N, Maguire D, Traynor O, Hoti E, Geoghegan JG, Conlon KC. Pancreatectomy for metastatic disease: a systematic review. *Eur J Surg Oncol* 2014; **40**: 379-386 [PMID: 24462547 DOI: 10.1016/j.ejso.2013.12.022]
- 42 **Abdellah A**, Selma K, Elamin M, Asmae T, Lamia R, Abderrahmane M, Sanaa el M, Hanan E, Tayeb K, Noureddine B. Renal cell carcinoma in children: case report and literature review. *Pan Afr Med J* 2015; **20**: 84 [PMID: 26090042 DOI: 10.11604/pamj.2015.20.84.5791]
- 43 **Kim EY**, Yoo SY, Kim JH, Sung KW. Pancreatic metastasis in a child suffering with treated stage 4 neuroblastoma. *Korean J Radiol* 2008; **9**: 84-86 [PMID: 18253081 DOI: 10.3348/kjr.2008.9.1.84]
- 44 **Farah RA**, Kamen BA. Parameningeal alveolar rhabdomyosarcoma with an isolated pancreatic metastasis. *Pediatr Hematol Oncol* 1999; **16**: 463-467 [PMID: 10505324 DOI: 10.1080/088800199277038]
- 45 **Bien E**, Godzinski J, Dall'igna P, Defachelles AS, Stachowicz-Stencel T, Orbach D, Bisogno G, Cecchetto G, Warmann S, Ellerkamp V, Brennan B, Balcerska A, Rapala M, Brecht I, Schneider D, Ferrari A. Pancreatoblastoma: a report from the European cooperative study group for paediatric rare tumours (EXPeRT). *Eur J Cancer* 2011; **47**: 2347-2352 [PMID: 21696948 DOI: 10.1016/j.ejca.2011.05.022]
- 46 **You L**, Yang F, Fu DL. Prediction of malignancy and adverse outcome of solid pseudopapillary tumor of the pancreas. *World J Gastrointest Oncol* 2018; **10**: 184-193 [PMID: 30079144 DOI: 10.4251/wjgo.v10.i7.184]
- 47 **Hsieh L**, Burjonrappa S. Pediatric pancreatic tumors: a review of current concepts. *J Pancreas* 2016; **17**: 257-262
- 48 **Picado O**, Ferrantella A, Zabalo C, Rao K, Thorson CM, Sola JE, Perez EA. Treatment patterns and outcomes for pancreatic tumors in children: an analysis of the National Cancer Database. *Pediatr Surg Int* 2020; **36**: 357-363 [PMID: 31989243 DOI: 10.1007/s00383-020-04617-z]
- 49 **Vasudevan SA**, Ha TN, Zhu H, Heaton TE, LaQuaglia MP, Murphy JT, Barry WE, Goodhue C, Kim ES, Aldrink JH, Polites SF, Leraas HJ, Rice HE, Tracy ET, Lautz TB, Superina RA, Davidoff AM, Langham MR Jr, Murphy AJ, Bütter A, Davidson J, Glick RD, Grijalva J, Gow KW, Ehrlich PF, Newman EA, Lal DR, Malek MM, Le-Nguyen A, Piché N, Rothstein DH, Short SS, Meyers R, Dasgupta R. Pancreaticoduodenectomy for the treatment of pancreatic neoplasms in children: A Pediatric Surgical Oncology Research Collaborative study. *Pediatr Blood Cancer* 2020; **67**: e28425 [PMID: 32658372 DOI: 10.1002/pbc.28425]
- 50 **Carreras-Torres R**, Johansson M, Gaborieau V, Haycock PC, Wade KH, Relton CL, Martin RM, Davey Smith G, Brennan P. The Role of Obesity, Type 2 Diabetes, and Metabolic Factors in Pancreatic Cancer: A Mendelian Randomization Study. *J Natl Cancer Inst* 2017; **109** [PMID: 28954281 DOI: 10.1093/jnci/djx012]
- 51 **Li D**, Morris JS, Liu J, Hassan MM, Day RS, Bondy ML, Abbruzzese JL. Body mass index and risk, age of onset, and survival in patients with pancreatic cancer. *JAMA* 2009; **301**: 2553-2562 [PMID: 19549972 DOI: 10.1001/jama.2009.886]
- 52 **Aune D**, Greenwood DC, Chan DS, Vieira R, Vieira AR, Navarro Rosenblatt DA, Cade JE, Burley VJ, Norat T. Body mass index, abdominal fatness and pancreatic cancer risk: a systematic review and non-linear dose-response meta-analysis of prospective studies. *Ann Oncol* 2012; **23**: 843-852 [PMID: 21890910 DOI: 10.1093/annonc/mdr398]
- 53 **Michaud DS**, Giovannucci E, Willett WC, Colditz GA, Stampfer MJ, Fuchs CS. Physical activity, obesity, height, and the risk of pancreatic cancer. *JAMA* 2001; **286**: 921-929 [PMID: 11509056 DOI: 10.1001/jama.286.8.921]
- 54 **Yuan C**, Bao Y, Wu C, Kraft P, Ogino S, Ng K, Qian ZR, Rubinson DA, Stampfer MJ, Giovannucci EL, Wolpin BM. Prediagnostic body mass index and pancreatic cancer survival. *J Clin Oncol* 2013; **31**: 4229-4234 [PMID: 24145341 DOI: 10.1200/JCO.2013.51.7532]
- 55 **Genkinger JM**, Kitahara CM, Bernstein L, Berrington de Gonzalez A, Brotzman M, Elena JW, Giles GG, Hartge P, Singh PN, Stolzenberg-Solomon RZ, Weiderpass E, Adami HO, Anderson KE, Beane-Freeman LE, Buring JE, Fraser GE, Fuchs CS, Gapstur SM, Gaziano JM, Helzlsouer KJ, Lacey JV Jr, Linet MS, Liu JJ, Park Y, Peters U, Purdue MP, Robien K, Schairer C, Sesso HD, Visvanathan K, White E, Wolk A, Wolpin BM, Zeleniuch-Jacquotte A, Jacobs EJ. Central adiposity, obesity during early adulthood, and pancreatic cancer mortality in a pooled analysis of cohort studies. *Ann Oncol* 2015; **26**: 2257-2266 [PMID: 26347100 DOI: 10.1093/annonc/mdv355]
- 56 **Stolzenberg-Solomon RZ**, Schairer C, Moore S, Hollenbeck A, Silverman DT. Lifetime adiposity and risk of pancreatic cancer in the NIH-AARP Diet and Health Study cohort. *Am J Clin Nutr* 2013; **98**: 1057-1065 [PMID: 23985810 DOI: 10.3945/ajcn.113.058123]
- 57 **Nogueira L**, Stolzenberg-Solomon R, Gamborg M, Sørensen TIA, Baker JL. Childhood body mass index and risk of adult pancreatic cancer. *Curr Dev Nutr* 2017; **1** [PMID: 29388617 DOI: 10.3945/cdn.117.001362]
- 58 **Genkinger JM**, Spiegelman D, Anderson KE, Bernstein L, van den Brandt PA, Calle EE, English DR, Folsom AR, Freudenheim JL, Fuchs CS, Giles GG, Giovannucci E, Horn-Ross PL, Larsson SC, Leitzmann M, Männistö S, Marshall JR, Miller AB, Patel AV, Rohan TE, Stolzenberg-Solomon RZ,

- Verhage BA, Virtamo J, Willcox BJ, Wolk A, Ziegler RG, Smith-Warner SA. A pooled analysis of 14 cohort studies of anthropometric factors and pancreatic cancer risk. *Int J Cancer* 2011; **129**: 1708-1717 [PMID: 21105029 DOI: 10.1002/ijc.25794]
- 59 **Wang Y**, Lim H. The global childhood obesity epidemic and the association between socio-economic status and childhood obesity. *Int Rev Psychiatry* 2012; **24**: 176-188 [PMID: 22724639 DOI: 10.3109/09540261.2012.688195]
- 60 **Park MH**, Falconer C, Viner RM, Kinra S. The impact of childhood obesity on morbidity and mortality in adulthood: a systematic review. *Obes Rev* 2012; **13**: 985-1000 [PMID: 22731928 DOI: 10.1111/j.1467-789X.2012.01015.x]
- 61 **Kitahara CM**, Gamborg M, Berrington de González A, Sørensen TI, Baker JL. Childhood height and body mass index were associated with risk of adult thyroid cancer in a large cohort study. *Cancer Res* 2014; **74**: 235-242 [PMID: 24247722 DOI: 10.1158/0008-5472.CAN-13-2228]
- 62 **Aggarwal G**, Kamada P, Chari ST. Prevalence of diabetes mellitus in pancreatic cancer compared to common cancers. *Pancreas* 2013; **42**: 198-201 [PMID: 23000893 DOI: 10.1097/MPA.0b013e3182592c96]
- 63 **Bosetti C**, Rosato V, Li D, Silverman D, Petersen GM, Bracci PM, Neale RE, Muscat J, Anderson K, Gallinger S, Olson SH, Miller AB, Bas Bueno-de-Mesquita H, Scelo G, Janout V, Holcatova I, Lagiou P, Serraino D, Lucenteforte E, Fabianova E, Baghurst PA, Zatonski W, Foretova L, Fontham E, Bamlet WR, Holly EA, Negri E, Hassan M, Prizment A, Cotterchio M, Cleary S, Kurtz RC, Maisonneuve P, Trichopoulos D, Polesel J, Duell EJ, Boffetta P, La Vecchia C, Gadirian P. Diabetes, antidiabetic medications, and pancreatic cancer risk: an analysis from the International Pancreatic Cancer Case-Control Consortium. *Ann Oncol* 2014; **25**: 2065-2072 [PMID: 25057164 DOI: 10.1093/annonc/mdu276]
- 64 **Batabyal P**, Vander Hoorn S, Christophi C, Nikfarjam M. Association of diabetes mellitus and pancreatic adenocarcinoma: a meta-analysis of 88 studies. *Ann Surg Oncol* 2014; **21**: 2453-2462 [PMID: 24609291 DOI: 10.1245/s10434-014-3625-6]
- 65 **Chari ST**, Leibson CL, Rabe KG, Timmons LJ, Ransom J, de Andrade M, Petersen GM. Pancreatic cancer-associated diabetes mellitus: prevalence and temporal association with diagnosis of cancer. *Gastroenterology* 2008; **134**: 95-101 [PMID: 18061176 DOI: 10.1053/j.gastro.2007.10.040]
- 66 **Salvatore T**, Marfella R, Rizzo MR, Sasso FC. Pancreatic cancer and diabetes: A two-way relationship in the perspective of diabetologist. *Int J Surg* 2015; **21** Suppl 1: S72-S77 [PMID: 26123386 DOI: 10.1016/j.ijssu.2015.06.063]
- 67 **Bao Y**, Giovannucci EL, Kraft P, Stampfer MJ, Ogino S, Ma J, Buring JE, Sesso HD, Lee IM, Gaziano JM, Rifai N, Pollak MN, Cochrane BB, Kaklamani V, Lin JH, Manson JE, Fuchs CS, Wolpin BM. A prospective study of plasma adiponectin and pancreatic cancer risk in five US cohorts. *J Natl Cancer Inst* 2013; **105**: 95-103 [PMID: 23243202 DOI: 10.1093/jnci/djs474]
- 68 **Gullo L**, Pezzilli R, Morselli-Labate AM; Italian Pancreatic Cancer Study Group. Diabetes and the risk of pancreatic cancer. *N Engl J Med* 1994; **331**: 81-84 [PMID: 8208269 DOI: 10.1056/NEJM199407143310203]
- 69 **Huxley R**, Ansary-Moghaddam A, Berrington de González A, Barzi F, Woodward M. Type-II diabetes and pancreatic cancer: a meta-analysis of 36 studies. *Br J Cancer* 2005; **92**: 2076-2083 [PMID: 15886696 DOI: 10.1038/sj.bjc.6602619]
- 70 **Stevens RJ**, Roddam AW, Beral V. Pancreatic cancer in type 1 and young-onset diabetes: systematic review and meta-analysis. *Br J Cancer* 2007; **96**: 507-509 [PMID: 17224924 DOI: 10.1038/sj.bjc.6603571]
- 71 **Zendehdel K**, Nyrén O, Ostenson CG, Adami HO, Ekblom A, Ye W. Cancer incidence in patients with type 1 diabetes mellitus: a population-based cohort study in Sweden. *J Natl Cancer Inst* 2003; **95**: 1797-1800 [PMID: 14652242 DOI: 10.1093/jnci/djg105]
- 72 **Pierce BL**, Austin MA, Ahsan H. Association study of type 2 diabetes genetic susceptibility variants and risk of pancreatic cancer: an analysis of PanScan-I data. *Cancer Causes Control* 2011; **22**: 877-883 [PMID: 21445555 DOI: 10.1007/s10552-011-9760-5]
- 73 **Bang UC**, Benfield T, Hyldstrup L, Bendtsen F, Beck Jensen JE. Mortality, cancer, and comorbidities associated with chronic pancreatitis: a Danish nationwide matched-cohort study. *Gastroenterology* 2014; **146**: 989-994 [PMID: 24389306 DOI: 10.1053/j.gastro.2013.12.033]
- 74 **Duell EJ**, Lucenteforte E, Olson SH, Bracci PM, Li D, Risch HA, Silverman DT, Ji BT, Gallinger S, Holly EA, Fontham EH, Maisonneuve P, Bueno-de-Mesquita HB, Gadirian P, Kurtz RC, Ludwig E, Yu H, Lowenfels AB, Seminara D, Petersen GM, La Vecchia C, Boffetta P. Pancreatitis and pancreatic cancer risk: a pooled analysis in the International Pancreatic Cancer Case-Control Consortium (PanC4). *Ann Oncol* 2012; **23**: 2964-2970 [PMID: 22767586 DOI: 10.1093/annonc/mds140]
- 75 **Weiss FU**. Pancreatic cancer risk in hereditary pancreatitis. *Front Physiol* 2014; **5**: 70 [PMID: 24600409 DOI: 10.3389/fphys.2014.00070]
- 76 **Hruban RH**, Takaori K, Klimstra DS, Adsay NV, Albores-Saavedra J, Biankin AV, Biankin SA, Compton C, Fukushima N, Furukawa T, Goggins M, Kato Y, Klöppel G, Longnecker DS, Lüttges J, Maitra A, Offerhaus GJ, Shimizu M, Yonezawa S. An illustrated consensus on the classification of pancreatic intraepithelial neoplasia and intraductal papillary mucinous neoplasms. *Am J Surg Pathol* 2004; **28**: 977-987 [PMID: 15252303 DOI: 10.1097/01.pas.0000126675.59108.80]
- 77 **Korc M**. Driver mutations: a roadmap for getting close and personal in pancreatic cancer. *Cancer Biol Ther* 2010; **10**: 588-591 [PMID: 20716952 DOI: 10.4161/cbt.10.6.13128]

- 78 **Lowenfels AB**, Maisonneuve P, Cavallini G, Ammann RW, Lankisch PG, Andersen JR, Dimagno EP, Andrén-Sandberg A, Domellöf L. Pancreatitis and the risk of pancreatic cancer. International Pancreatitis Study Group. *N Engl J Med* 1993; **328**: 1433-1437 [PMID: [8479461](#) DOI: [10.1056/NEJM199305203282001](#)]
- 79 **Kirkegård J**, Mortensen FV, Cronin-Fenton D. Chronic Pancreatitis and Pancreatic Cancer Risk: A Systematic Review and Meta-analysis. *Am J Gastroenterol* 2017; **112**: 1366-1372 [PMID: [28762376](#) DOI: [10.1038/ajg.2017.218](#)]
- 80 **Kargl S**, Kienbauer M, Duba HC, Schöfl R, Pumberger W. Therapeutic step-up strategy for management of hereditary pancreatitis in children. *J Pediatr Surg* 2015; **50**: 511-514 [PMID: [25840052](#) DOI: [10.1016/j.jpedsurg.2014.05.016](#)]
- 81 **Whitcomb DC**, Gorry MC, Preston RA, Furey W, Sossenheimer MJ, Ulrich CD, Martin SP, Gates LK Jr, Amann ST, Toskes PP, Liddle R, McGrath K, Uomo G, Post JC, Ehrlich GD. Hereditary pancreatitis is caused by a mutation in the cationic trypsinogen gene. *Nat Genet* 1996; **14**: 141-145 [PMID: [8841182](#) DOI: [10.1038/ng1096-141](#)]
- 82 **Witt H**, Luck W, Hennies HC, Classen M, Kage A, Lass U, Landt O, Becker M. Mutations in the gene encoding the serine protease inhibitor, Kazal type 1 are associated with chronic pancreatitis. *Nat Genet* 2000; **25**: 213-216 [PMID: [10835640](#) DOI: [10.1038/76088](#)]
- 83 **Witt H**, Beer S, Rosendahl J, Chen JM, Chandak GR, Masamune A, Bence M, Szmola R, Oracz G, Macek M Jr, Bhatia E, Steigenberger S, Lasher D, Bühler F, Delaporte C, Tebbing J, Ludwig M, Pilsak C, Saum K, Bugert P, Masson E, Paliwal S, Bhaskar S, Sobczynska-Tomaszewska A, Bak D, Balacak I, Choudhuri G, Nageshwar Reddy D, Rao GV, Thomas V, Kume K, Nakano E, Kakuta Y, Shimosegawa T, Durko L, Szabó A, Schnür A, Hegyi P, Rakonczay Z Jr, Pfützner R, Schneider A, Groneberg DA, Braun M, Schmidt H, Witt U, Friess H, Algül H, Landt O, Schuelke M, Krüger R, Wiedenmann B, Schmidt F, Zimmer KP, Kovacs P, Stumvoll M, Blüher M, Müller T, Janecke A, Teich N, Grützmann R, Schulz HU, Mössner J, Keim V, Löhr M, Férec C, Sahin-Tóth M. Variants in CPA1 are strongly associated with early onset chronic pancreatitis. *Nat Genet* 2013; **45**: 1216-1220 [PMID: [23955596](#) DOI: [10.1038/ng.2730](#)]
- 84 **Sharer N**, Schwarz M, Malone G, Howarth A, Painter J, Super M, Braganza J. Mutations of the cystic fibrosis gene in patients with chronic pancreatitis. *N Engl J Med* 1998; **339**: 645-652 [PMID: [9725921](#) DOI: [10.1056/NEJM199809033391001](#)]
- 85 **Sobczyńska-Tomaszewska A**, Bak D, Oralewska B, Oracz G, Norek A, Czerska K, Mazurczak T, Teisseyre M, Socha J, Zagulski M, Bal J. Analysis of CFTR, SPINK1, PRSS1 and AAT mutations in children with acute or chronic pancreatitis. *J Pediatr Gastroenterol Nutr* 2006; **43**: 299-306 [PMID: [16954950](#) DOI: [10.1097/01.mpg.0000232570.48773.df](#)]
- 86 **Mastoraki A**, Tzortzopoulou A, Tsela S, Danias N, Sakorafas G, Smyrniotis V, Arkadopoulos N. Hereditary pancreatitis: dilemmas in differential diagnosis and therapeutic approach. *J Gastrointest Cancer* 2014; **45**: 22-26 [PMID: [24242859](#) DOI: [10.1007/s12029-013-9559-6](#)]
- 87 **Simon P**, Weiss FU, Zimmer KP, Rand S, Brinkmann B, Domschke W, Lerch MM. Spontaneous and sporadic trypsinogen mutations in idiopathic pancreatitis. *JAMA* 2002; **288**: 2122 [PMID: [12413370](#) DOI: [10.1001/jama.288.17.2122](#)]
- 88 **Shelton CA**, Grubs RE, Umopathy C, Yadav D, Whitcomb DC. Impact of hereditary pancreatitis on patients and their families. *J Genet Couns* 2020; **29**: 971-982 [PMID: [32026589](#) DOI: [10.1002/jgc4.1221](#)]
- 89 **Kong X**, Sun T, Kong F, Du Y, Li Z. Chronic Pancreatitis and Pancreatic Cancer. *Gastrointest Tumors* 2014; **1**: 123-134 [PMID: [26674754](#) DOI: [10.1159/000365306](#)]
- 90 **Warren AJ**. Molecular basis of the human ribosomopathy Shwachman-Diamond syndrome. *Adv Biol Regul* 2018; **67**: 109-127 [PMID: [28942353](#) DOI: [10.1016/j.jbior.2017.09.002](#)]
- 91 **Slae M**, Wilschanski M. Cystic fibrosis: a gastrointestinal cancer syndrome. *Lancet Oncol* 2018; **19**: 719-720 [PMID: [29706381](#) DOI: [10.1016/S1470-2045\(18\)30250-X](#)]
- 92 **Yamada A**, Komaki Y, Komaki F, Micic D, Zullow S, Sakuraba A. Risk of gastrointestinal cancers in patients with cystic fibrosis: a systematic review and meta-analysis. *Lancet Oncol* 2018; **19**: 758-767 [PMID: [29706374](#) DOI: [10.1016/S1470-2045\(18\)30188-8](#)]
- 93 **Maisonneuve P**, Marshall BC, Lowenfels AB. Risk of pancreatic cancer in patients with cystic fibrosis. *Gut* 2007; **56**: 1327-1328 [PMID: [17698876](#) DOI: [10.1136/gut.2007.125278](#)]
- 94 **Weinstein LS**. G(s)alpha mutations in fibrous dysplasia and McCune-Albright syndrome. *J Bone Miner Res* 2006; **21** Suppl 2: P120-P124 [PMID: [17229000](#) DOI: [10.1359/jbmr.06s223](#)]
- 95 **Majoer BC**, Boyce AM, Bovée JV, Smit VT, Collins MT, Cleton-Jansen AM, Dekkers OM, Hamdy NA, Dijkstra PS, Appelman-Dijkstra NM. Increased Risk of Breast Cancer at a Young Age in Women with Fibrous Dysplasia. *J Bone Miner Res* 2018; **33**: 84-90 [PMID: [28856726](#) DOI: [10.1002/jbmr.3286](#)]
- 96 **Vortmeyer AO**, Gläsker S, Mehta GU, Abu-Asab MS, Smith JH, Zhuang Z, Collins MT, Oldfield EH. Somatic GNAS mutation causes widespread and diffuse pituitary disease in acromegalic patients with McCune-Albright syndrome. *J Clin Endocrinol Metab* 2012; **97**: 2404-2413 [PMID: [22564667](#) DOI: [10.1210/jc.2012-1274](#)]
- 97 **Collins MT**, Sarlis NJ, Merino MJ, Monroe J, Crawford SE, Krakoff JA, Guthrie LC, Bonat S, Robey PG, Shenker A. Thyroid carcinoma in the McCune-Albright syndrome: contributory role of activating Gs alpha mutations. *J Clin Endocrinol Metab* 2003; **88**: 4413-4417 [PMID: [12970318](#) DOI: [10.1210/jc.2002-021642](#)]
- 98 **Nishikawa G**, Sekine S, Ogawa R, Matsubara A, Mori T, Taniguchi H, Kushima R, Hiraoka N,

- Tsuta K, Tsuda H, Kanai Y. Frequent GNAS mutations in low-grade appendiceal mucinous neoplasms. *Br J Cancer* 2013; **108**: 951-958 [PMID: 23403822 DOI: 10.1038/bjc.2013.47]
- 99 **Fragoso MC**, Latronico AC, Carvalho FM, Zerbini MC, Marcondes JA, Araujo LM, Lando VS, Frazzatto ET, Mendonca BB, Villares SM. Activating mutation of the stimulatory G protein (gsp) as a putative cause of ovarian and testicular human stromal Leydig cell tumors. *J Clin Endocrinol Metab* 1998; **83**: 2074-2078 [PMID: 9626141 DOI: 10.1210/jcem.83.6.4847]
- 100 **Robinson C**, Estrada A, Zaheer A, Singh VK, Wolfgang CL, Goggins MG, Hruban RH, Wood LD, Noë M, Montgomery EA, Guthrie LC, Lennon AM, Boyce AM, Collins MT. Clinical and Radiographic Gastrointestinal Abnormalities in McCune-Albright Syndrome. *J Clin Endocrinol Metab* 2018; **103**: 4293-4303 [PMID: 30124968 DOI: 10.1210/jc.2018-01022]
- 101 **Parvanescu A**, Cros J, Ronot M, Hentic O, Grybek V, Couvelard A, Levy P, Chanson P, Ruszniewski P, Sauvanet A, Gaujoux S. Lessons from McCune-Albright syndrome-associated intraductal papillary mucinous neoplasms: : GNAS-activating mutations in pancreatic carcinogenesis. *JAMA Surg* 2014; **149**: 858-862 [PMID: 24898823 DOI: 10.1001/jamasurg.2014.535]
- 102 **Tanaka M**. Controversies in the management of pancreatic IPMN. *Nat Rev Gastroenterol Hepatol* 2011; **8**: 56-60 [PMID: 21212775 DOI: 10.1038/nrgastro.2010.193]
- 103 **Pergolini I**, Sahara K, Ferrone CR, Morales-Oyarvide V, Wolpin BM, Mucci LA, Brugge WR, Mino-Kenudson M, Patino M, Sahani DV, Warshaw AL, Lillemoie KD, Fernández-Del Castillo C. Long-term Risk of Pancreatic Malignancy in Patients With Branch Duct Intraductal Papillary Mucinous Neoplasm in a Referral Center. *Gastroenterology* 2017; **153**: 1284-1294. e1 [PMID: 28739282 DOI: 10.1053/j.gastro.2017.07.019]
- 104 **Alhakim M**, Elshimy G, Vinales K, Correa R. SUN-324 Should We Screen for Pancreatic Cancer in Patient with Mccune Albright Syndrome? *J Endocr Soc* 2019; **3**: SUN-324 [DOI: 10.1210/js.2019-SUN-324]
- 105 **Kamilaris CDC**, Stratakis CA. Multiple Endocrine Neoplasia Type 1 (MEN1): An Update and the Significance of Early Genetic and Clinical Diagnosis. *Front Endocrinol (Lausanne)* 2019; **10**: 339 [PMID: 31263451 DOI: 10.3389/fendo.2019.00339]
- 106 **Jensen RT**, Norton JA. Treatment of Pancreatic Neuroendocrine Tumors in Multiple Endocrine Neoplasia Type 1: Some Clarity But Continued Controversy. *Pancreas* 2017; **46**: 589-594 [PMID: 28426491 DOI: 10.1097/MPA.0000000000000825]
- 107 **Concolino P**, Costella A, Capoluongo E. Multiple endocrine neoplasia type 1 (MEN1): An update of 208 new germline variants reported in the last nine years. *Cancer Genet* 2016; **209**: 36-41 [PMID: 26767918 DOI: 10.1016/j.cancergen.2015.12.002]
- 108 **Hannan FM**, Nesbit MA, Christie PT, Fratter C, Dudley NE, Sadler GP, Thakker RV. Familial isolated primary hyperparathyroidism caused by mutations of the MEN1 gene. *Nat Clin Pract Endocrinol Metab* 2008; **4**: 53-58 [PMID: 18084346 DOI: 10.1038/ncpendmet0718]
- 109 **Scarpa A**, Chang DK, Nones K, Corbo V, Patch AM, Bailey P, Lawlor RT, Johns AL, Miller DK, Mafficini A, Rusev B, Scardoni M, Antonello D, Barbi S, Sikora KO, Cingarlini S, Vicentini C, McKay S, Quinn MC, Bruxner TJ, Christ AN, Harliwong I, Idrisoglu S, McLean S, Nourse C, Nourbakhsh E, Wilson PJ, Anderson MJ, Fink JL, Newell F, Waddell N, Holmes O, Kazakoff SH, Leonard C, Wood S, Xu Q, Nagaraj SH, Amato E, Dalai I, Bersani S, Cataldo I, Dei Tos AP, Capelli P, Davi MV, Landoni L, Malpaga A, Miotto M, Whitehall VL, Leggett BA, Harris JL, Harris J, Jones MD, Humphris J, Chantrell LA, Chin V, Nagrial AM, Pajic M, Scarlett CJ, Pinho A, Rooman I, Toon C, Wu J, Pinese M, Cowley M, Barbour A, Mawson A, Humphrey ES, Colvin EK, Chou A, Lovell JA, Jamieson NB, Duthie F, Gingras MC, Fisher WE, Dagg RA, Lau LM, Lee M, Pickett HA, Reddel RR, Samra JS, Kench JG, Merrett ND, Epari K, Nguyen NQ, Zeps N, Falconi M, Simbolo M, Butturini G, Van Buren G, Partelli S, Fassan M; Australian Pancreatic Cancer Genome Initiative, Khanna KK, Gill AJ, Wheeler DA, Gibbs RA, Musgrove EA, Bassi C, Tortora G, Pederzoli P, Pearson JV, Biankin AV, Grimmond SM. Whole-genome landscape of pancreatic neuroendocrine tumours. *Nature* 2017; **543**: 65-71 [PMID: 28199314 DOI: 10.1038/nature21063]
- 110 **Thakker RV**, Newey PJ, Walls GV, Bilezikian J, Dralle H, Ebeling PR, Melmed S, Sakurai A, Tonelli F, Brandi ML; Endocrine Society. Clinical practice guidelines for multiple endocrine neoplasia type 1 (MEN1). *J Clin Endocrinol Metab* 2012; **97**: 2990-3011 [PMID: 22723327 DOI: 10.1210/jc.2012-1230]
- 111 **Findeis-Hosey JJ**, McMahon KQ, Findeis SK. Von Hippel-Lindau Disease. *J Pediatr Genet* 2016; **5**: 116-123 [PMID: 27617152 DOI: 10.1055/s-0036-1579757]
- 112 **Maher ER**, Neumann HP, Richard S. von Hippel-Lindau disease: a clinical and scientific review. *Eur J Hum Genet* 2011; **19**: 617-623 [PMID: 21386872 DOI: 10.1038/ejhg.2010.175]
- 113 **Lubensky IA**, Pack S, Ault D, Vortmeyer AO, Libutti SK, Choyke PL, Walther MM, Linehan WM, Zhuang Z. Multiple neuroendocrine tumors of the pancreas in von Hippel-Lindau disease patients: histopathological and molecular genetic analysis. *Am J Pathol* 1998; **153**: 223-231 [PMID: 9665483 DOI: 10.1016/S0002-9440(10)65563-0]
- 114 **Blansfield JA**, Choyke L, Morita SY, Choyke PL, Pingpank JF, Alexander HR, Seidel G, Shutack Y, Yuldasheva N, Eugeni M, Bartlett DL, Glenn GM, Middleton L, Linehan WM, Libutti SK. Clinical, genetic and radiographic analysis of 108 patients with von Hippel-Lindau disease (VHL) manifested by pancreatic neuroendocrine neoplasms (PNETs). *Surgery* 2007; **142**: 814-818; discussion 818 [PMID: 18063061 DOI: 10.1016/j.surg.2007.09.012]
- 115 **Tamura K**, Nishimori I, Ito T, Yamasaki I, Igarashi H, Shuin T. Diagnosis and management of

- pancreatic neuroendocrine tumor in von Hippel-Lindau disease. *World J Gastroenterol* 2010; **16**: 4515-4518 [PMID: 20857520 DOI: 10.3748/wjg.v16.i36.4515]
- 116 **Fang S**, Krahe R, Lozano G, Han Y, Chen W, Post SM, Zhang B, Wilson CD, Bachinski LL, Strong LC, Amos CI. Effects of MDM2, MDM4 and TP53 codon 72 polymorphisms on cancer risk in a cohort study of carriers of TP53 germline mutations. *PLoS One* 2010; **5**: e10813 [PMID: 20520810 DOI: 10.1371/journal.pone.0010813]
- 117 **Hwang SJ**, Lozano G, Amos CI, Strong LC. Germline p53 mutations in a cohort with childhood sarcoma: sex differences in cancer risk. *Am J Hum Genet* 2003; **72**: 975-983 [PMID: 12610779 DOI: 10.1086/374567]
- 118 **Gonzalez KD**, Noltner KA, Buzin CH, Gu D, Wen-Fong CY, Nguyen VQ, Han JH, Lowstuter K, Longmate J, Sommer SS, Weitzel JN. Beyond Li Fraumeni Syndrome: clinical characteristics of families with p53 germline mutations. *J Clin Oncol* 2009; **27**: 1250-1256 [PMID: 19204208 DOI: 10.1200/JCO.2008.16.6959]
- 119 **Mai PL**, Malkin D, Garber JE, Schiffman JD, Weitzel JN, Strong LC, Wyss O, Locke L, Means V, Achatz MI, Hainaut P, Frebourg T, Evans DG, Bleiker E, Patenaude A, Schneider K, Wilfond B, Peters JA, Hwang PM, Ford J, Tabori U, Ognjanovic S, Dennis PA, Wentzensen IM, Greene MH, Fraumeni JF Jr, Savage SA. Li-Fraumeni syndrome: report of a clinical research workshop and creation of a research consortium. *Cancer Genet* 2012; **205**: 479-487 [PMID: 22939227 DOI: 10.1016/j.cancergen.2012.06.008]
- 120 **Birch JM**, Hartley AL, Tricker KJ, Prosser J, Condie A, Kelsey AM, Harris M, Jones PH, Binchy A, Crowther D. Prevalence and diversity of constitutional mutations in the p53 gene among 21 Li-Fraumeni families. *Cancer Res* 1994; **54**: 1298-1304 [PMID: 8118819]
- 121 **Solomon S**, Das S, Brand R, Whitcomb DC. Inherited pancreatic cancer syndromes. *Cancer J* 2012; **18**: 485-491 [PMID: 23187834 DOI: 10.1097/PPO.0b013e318278c4a6]
- 122 **Brand RE**, Lerch MM, Rubinstein WS, Neoptolemos JP, Whitcomb DC, Hruban RH, Brentnall TA, Lynch HT, Canto MI; Participants of the Fourth International Symposium of Inherited Diseases of the Pancreas. Advances in counselling and surveillance of patients at risk for pancreatic cancer. *Gut* 2007; **56**: 1460-1469 [PMID: 17872573 DOI: 10.1136/gut.2006.108456]
- 123 **Brose MS**, Rebbeck TR, Calzone KA, Stopfer JE, Nathanson KL, Weber BL. Cancer risk estimates for BRCA1 mutation carriers identified in a risk evaluation program. *J Natl Cancer Inst* 2002; **94**: 1365-1372 [PMID: 12237282 DOI: 10.1093/jnci/94.18.1365]
- 124 **Kanda M**, Matthaai H, Wu J, Hong SM, Yu J, Borges M, Hruban RH, Maitra A, Kinzler K, Vogelstein B, Goggins M. Presence of somatic mutations in most early-stage pancreatic intraepithelial neoplasia. *Gastroenterology* 2012; **142**: 730-733. e9 [PMID: 22226782 DOI: 10.1053/j.gastro.2011.12.042]
- 125 **Brune KA**, Lau B, Palmisano E, Canto M, Goggins MG, Hruban RH, Klein AP. Importance of age of onset in pancreatic cancer kindreds. *J Natl Cancer Inst* 2010; **102**: 119-126 [PMID: 20068195 DOI: 10.1093/jnci/djp466]
- 126 **Kastrinos F**, Mukherjee B, Tayob N, Wang F, Sparr J, Raymond VM, Bandipalliam P, Stoffel EM, Gruber SB, Syngal S. Risk of pancreatic cancer in families with Lynch syndrome. *JAMA* 2009; **302**: 1790-1795 [PMID: 19861671 DOI: 10.1001/jama.2009.1529]
- 127 **Geary J**, Sasieni P, Houlston R, Izatt L, Eeles R, Payne SJ, Fisher S, Hodgson SV. Gene-related cancer spectrum in families with hereditary non-polyposis colorectal cancer (HNPCC). *Fam Cancer* 2008; **7**: 163-172 [PMID: 17939062 DOI: 10.1007/s10689-007-9164-6]

Application of artificial intelligence in preoperative imaging of hepatocellular carcinoma: Current status and future perspectives

Bing Feng, Xiao-Hong Ma, Shuang Wang, Wei Cai, Xia-Bi Liu, Xin-Ming Zhao

ORCID number: Bing Feng [0000-0003-1080-9551](https://orcid.org/0000-0003-1080-9551); Xiao-Hong Ma [0000-0002-9048-8374](https://orcid.org/0000-0002-9048-8374); Shuang Wang [0000-0001-9241-2018](https://orcid.org/0000-0001-9241-2018); Wei Cai [0000-0002-6273-3678](https://orcid.org/0000-0002-6273-3678); Xia-Bi Liu [0000-0003-1633-0648](https://orcid.org/0000-0003-1633-0648); Xin-Ming Zhao [0000-0001-7286-771X](https://orcid.org/0000-0001-7286-771X).

Author contributions: Feng B performed literature review and drafted the manuscript; Cai W contributed to data collection of the study; Wang S, Liu XB, and Zhao XM reviewed the manuscript; Ma XH contributed to conception and design of the study, and critically revised this manuscript; all authors have read and approved the final manuscript.

Supported by CAMS Innovation Fund for Medical Sciences (CIFMS), No. 2016-I2M-1-001; PUMC Youth Fund, No. 2017320010; Chinese Academy of Medical Sciences (CAMS) Research Fund, No. ZZ2016B01; Beijing HopeRun Special Fund of Cancer Foundation of China, No. LC2016B15; and PUMC Postgraduate Education and Teaching Reform Fund, No. 10023201900303.

Conflict-of-interest statement: The authors declare no conflict of interests for this article.

Open-Access: This article is an open-access article that was

Bing Feng, Xiao-Hong Ma, Shuang Wang, Wei Cai, Xin-Ming Zhao, Department of Diagnostic Radiology, National Cancer Center/National Clinical Research Center for Cancer/Cancer Hospital, Chinese Academy of Medical Sciences and Peking Union Medical College, Beijing 100021, China

Xia-Bi Liu, Beijing Laboratory of Intelligent Information Technology, School of Computer Science and Technology, Beijing Institute of Technology, Beijing 100081, China

Corresponding author: Xiao-Hong Ma, MD, Associate Professor, Doctor, Department of Diagnostic Radiology, National Cancer Center/National Clinical Research Center for Cancer/Cancer Hospital, Chinese Academy of Medical Sciences and Peking Union Medical College, No. 17 Panjiayuan Nanli, Chaoyang District, Beijing 100021, China.

maxiaohong@cicams.ac.cn

Abstract

Hepatocellular carcinoma (HCC) is the most common primary malignant liver tumor in China. Preoperative diagnosis of HCC is challenging because of atypical imaging manifestations and the diversity of focal liver lesions. Artificial intelligence (AI), such as machine learning (ML) and deep learning, has recently gained attention for its capability to reveal quantitative information on images. Currently, AI is used throughout the entire radiomics process and plays a critical role in multiple fields of medicine. This review summarizes the applications of AI in various aspects of preoperative imaging of HCC, including segmentation, differential diagnosis, prediction of histo-pathology, early detection of recurrence after curative treatment, and evaluation of treatment response. We also review the limitations of previous studies and discuss future directions for diagnostic imaging of HCC.

Key Words: Hepatocellular carcinoma; Radiomics; Artificial intelligence; Diagnosis; Treatment; Recurrence

©The Author(s) 2021. Published by Baishideng Publishing Group Inc. All rights reserved.

Core Tip: Hepatocellular carcinoma (HCC) threatens human health because of its high morbidity and recurrence rates. Patients with HCC may benefit from early diagnosis,

selected by an in-house editor and fully peer-reviewed by external reviewers. It is distributed in accordance with the Creative Commons Attribution NonCommercial (CC BY-NC 4.0) license, which permits others to distribute, remix, adapt, build upon this work non-commercially, and license their derivative works on different terms, provided the original work is properly cited and the use is non-commercial. See: <http://creativecommons.org/licenses/by-nc/4.0/>

Manuscript source: Invited manuscript

Specialty type: Gastroenterology and hepatology

Country/Territory of origin: China

Peer-review report's scientific quality classification

Grade A (Excellent): 0
Grade B (Very good): B
Grade C (Good): 0
Grade D (Fair): 0
Grade E (Poor): 0

Received: January 28, 2021

Peer-review started: January 28, 2021

First decision: March 29, 2021

Revised: April 15, 2021

Accepted: July 27, 2021

Article in press: July 27, 2021

Published online: August 28, 2021

P-Reviewer: Yang SS

S-Editor: Yan JP

L-Editor: Wang TQ

P-Editor: Liu JH



timely treatment, and appropriate follow-up strategies. In the era of big data, artificial intelligence (AI) provides critical information regarding the diagnosis, treatment, and prognosis of HCC. We herein discuss the role of AI in the following aspects of preoperative imaging: Segmentation, differential diagnosis, prediction of histopathology, early detection of recurrence after curative treatment, and evaluation of treatment response.

Citation: Feng B, Ma XH, Wang S, Cai W, Liu XB, Zhao XM. Application of artificial intelligence in preoperative imaging of hepatocellular carcinoma: Current status and future perspectives. *World J Gastroenterol* 2021; 27(32): 5341-5350

URL: <https://www.wjgnet.com/1007-9327/full/v27/i32/5341.htm>

DOI: <https://dx.doi.org/10.3748/wjg.v27.i32.5341>

INTRODUCTION

Hepatocellular carcinoma (HCC), which most often arises from chronic hepatitis B virus infection, is one of the main causes of cancer-related deaths worldwide, particularly in China[1]. HCC presents with characteristic radiological features and can be diagnosed without biopsy. Imaging is therefore crucial for diagnosis and management. Computed tomography (CT) is the most widely used method for HCC diagnosis, although magnetic resonance imaging (MRI) is the optimal diagnostic modality, owing to its multi-parameter imaging techniques. However, even with the application of dynamic contrast-enhanced MRI (DCE-MRI), the imaging diagnosis of HCC is challenging because of atypical imaging manifestations and liver tumor diversity.

A single clinical image contains a large amount of quantitative information that can provide crucial data for diagnostic and treatment purposes. This information can be processed using innovative methods. Radiomics has recently gained attention for its potential to further analyze images. It allows for the extraction of a large amount of quantitative objective data included in radiological images that could be explored for determining underlying biological processes[2]. The workflow of a radiomics study generally includes five stages: Image acquisition, segmentation, feature extraction, exploratory analysis, and modeling[3] (Figure 1). Every stage is closely related to artificial intelligence (AI). The concept of AI was first advocated in 1955 by McCarthy *et al*[4], who described AI as a computer program that attempts to simulate human cognitive functions. AI can learn and solve problems to improve itself.

Machine learning (ML) is at the core of AI and involves various techniques, such as artificial neural networks, support vector machines (SVM), and random forest (RF). Deep learning (DL) is an important branch of ML, and convolutional neural networks (CNNs) are a type of DL algorithm. The relationships among AI, ML, and DL are described in Figure 2. With technological advances and the use of AI, radiomics has rapidly developed in recent years, and all radiomics techniques have now been utilized in studies within the medical field. This review focuses on the application of AI for HCC imaging, including segmentation, differential diagnosis, prediction of histopathology, early detection of recurrence after curative treatment, and evaluation of treatment response.

SEGMENTATION OF HCC LESIONS

Although HCC segmentation is challenging, it is crucial for various medical imaging analyses. Manual and semi-manual segmentation are time-consuming and susceptible to interobserver variability, which might in turn lead to the biased results. In contrast, automatic segmentation based on an AI algorithm is more repeatable and efficient. CNNs have been successfully applied for the automatic segmentation of hepatic lesions in both CT and MRI. Chlebus *et al*[5] figured out a CNN model for the automatic segmentation of liver tumors on CT; however, with respect to tumor detection, the model performed poorly compared with human performance. Bousabarah *et al*[6] established a DL algorithm to automatically delineate the liver and HCC lesions on MRI. The model was a combination of a deep CNN, RF, and thresholding. The mean dice similarity coefficient between the DL model and manual



Figure 1 The five stages of a radiomics study where artificial intelligence can play a role.

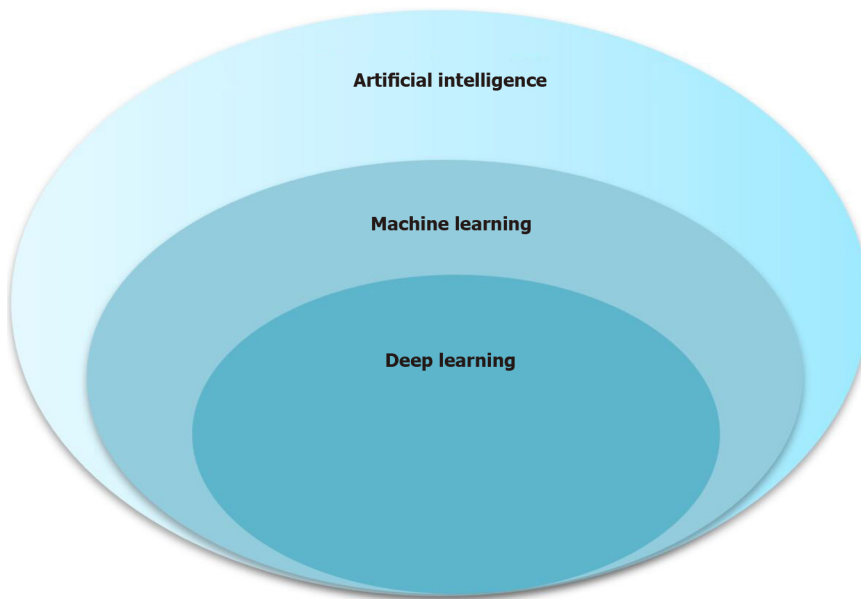


Figure 2 Relationship of artificial intelligence, machine learning, and deep learning.

segmentation was 0.64/0.68 (validation/test) for tumor segmentation and 0.91/0.91 for liver segmentations. Current methods do not achieve a comparably high level of performance in liver imaging for automatic tumor segmentation. This may be due to the heterogeneity of the liver parenchyma and the tumor itself. Larger datasets will be required to improve the accuracy of DL algorithms and will ensure optimal sensitivity and specificity.

DIFFERENTIAL DIAGNOSIS

Imaging-based differential diagnosis improves the accuracy of diagnosis. For HCC, the primary diagnostic modalities are CT and MRI. Radiomics with AI has been gradually applied in clinical research, as it can provide quantitative information, including additional differential characteristics not yet recognized in current radiological diagnosis. This could, in turn, help less-experienced radiologists diagnose focal liver lesions more accurately. Table 1 summarizes the studies on the differential diagnosis of HCC with AI.

CT

Some studies have applied conventional ML algorithms for the differentiation of liver masses. In the non-cirrhotic liver, Nie *et al*[7,8] reported CT-based radiomics nomograms for the preoperative differentiation of HCC from hepatocellular adenoma (HCA) and focal nodular hyperplasia (FNH). It showed good discrimination capability, with an area under the curve (AUC) of 0.96/0.94 and 0.979/0.917 (training/validation) for differentiating HCC from HCA and FNH, respectively. In patients with cirrhosis, ML techniques could classify indeterminate liver nodules as HCC or non-HCC based on triphasic CT scans, with an AUC of 0.70/0.66 (training/validation)[9]. Ponnoprat *et al*[10] developed an ML method to differentiate between HCC and intrahepatic cholangiocarcinoma (ICC), the two most common malignant liver tumors, based on multi-phase CT. They reported an 88% accuracy in HCC-ICC classification. DL with CNN for the differential diagnosis of liver lesions also showed relatively high diagnostic capability, reaching an AUC of 0.86-0.99[11-13].

Table 1 Summary of studies on differential diagnosis of hepatocellular carcinoma

| Ref. | Aim of the study | Modality | Patients | Method | AUC of the final model |
|-----------------------------|---|----------|----------|--------|------------------------|
| Nie <i>et al</i> [7] | Differentiation between HCC and HCA | CT | 131 | ML | T: 0.96, V: 0.94 |
| Nie <i>et al</i> [8] | Differentiation between HCC and FNH | CT | 156 | ML | T: 0.979, V: 0.917 |
| Mokrane <i>et al</i> [9] | Differentiation between HCC and non-HCC nodules | CT | 178 | ML | T: 0.70, V: 0.66 |
| Ponnoprat <i>et al</i> [10] | Differentiation between HCC and ICC | CT | 257 | ML | NA |
| Shi <i>et al</i> [11] | Differentiation of HCC from other FLLs | CT | 342 | DL | 0.925 |
| Yasaka <i>et al</i> [12] | Liver mass classification | CT | 560 | DL | 0.92 |
| Cao <i>et al</i> [13] | FLL classification | CT | 375 | DL | V: 0.88-0.99 |
| Jiang <i>et al</i> [14] | Comparing the diagnostic accuracies of EASL (v2018), LI-RADS criteria, and radiomics models for HCC | MRI | 211 | ML | T: 0.861, V: 0.810 |
| Zhen <i>et al</i> [15] | Classification of liver tumors | MRI | 1411 | DL | 0.963-0.998 |
| Liu <i>et al</i> [16] | Differentiation of cHCC-CC from CC and HCC | MRI | 85 | ML | 0.77 |
| Huang <i>et al</i> [17] | Diagnosis of DPHCC | MRI | 100 | ML | 0.784 |
| Jian <i>et al</i> [18] | Characterization of HCC | MRI | 112 | DL | NA |
| Wu <i>et al</i> [19] | Classification of HCC and hepatic hemangioma | MRI | 369 | ML | T: 0.86, V: 0.89 |

T: Training cohort; V: Validation cohort; NA: Not available; AUC: The area under the receiver operating characteristic curve; ML: Machine learning; DL: Deep learning; HCC: Hepatocellular carcinoma; HCA: Hepatocellular adenoma; FNH: Focal nodular hyperplasia; ICC: Intrahepatic cholangiocarcinoma; cHCC-CC: Combined hepatocellular cholangiocarcinoma; CC: Cholangiocarcinoma; DPHCC: Dual-phenotype hepatocellular carcinoma; FLL: Focal liver lesion.

MRI

MRI can provide more comprehensive information for differential diagnosis than CT because of its multi-parameter techniques and various tissue contrast mechanisms. Accurate diagnosis of HCC remains a challenge because of liver tumor diversity and relies on the experience of radiologists. Jiang *et al*[14] established a radiomics signature from multi-sequence MRI using the least absolute shrinkage and selection operator (LASSO) model and multivariate logistic regression analysis. The AUC of the radiomics signature was 0.810. It showed a comparable accuracy with the LI-RADS (0.841) and EASL criteria (0.811) for HCC diagnosis. Zhen *et al*[15] used CNNs to develop a DL model to classify liver tumors based on MR images. The CNN model combined with clinical data performed well in identifying HCC (AUC, 0.985; 95%CI: 0.960-1.000), metastatic tumors (AUC, 0.998; 95%CI: 0.989-1.000), and other primary malignancies (AUC, 0.963; 95%CI: 0.896-1.000). Some researchers have also applied ML algorithms to the differential diagnosis of primary liver cancer subtypes. Liu *et al*[16] reported an ML analysis of MRI radiomics features for the differentiation of combined hepatocellular cholangiocarcinoma (cHCC-CC) from HCC and cholangiocarcinoma. The model showed acceptable performance, with an AUC of 0.77. Huang *et al*[17] created a radiomics signature from Gd-EOB-DTPA-enhanced MRI for the diagnosis of dual-phenotype HCC (DPHCC). They used LASSO and four classifiers: Multi-layer perceptron, SVM, logistic regression, and K-nearest neighbor. The combination of different phases and classifiers achieved the best performance in the preoperative diagnosis of DPHCC. ML and DL algorithms can also be used in non-contrast MRI to increase the diagnostic accuracy of HCC[18,19]. This is beneficial for patients who cannot receive contrast injections.

CT- or MRI-based ML and DL models have demonstrated promising predictive performance and have reached a high level of accuracy similar to that of experienced radiologists. Accurate preoperative diagnosis of focal liver lesions can help clinicians make proper decisions, optimize patient management, and improve patient prognosis.

PREOPERATIVE PREDICTION OF HISTOPATHOLOGY

Grade

Histological grade represents the biological behavior and aggressiveness of tumors. The high recurrence rate of HCC is associated with its pathological grade. The pathological grade of HCC determined using imaging may provide valuable prognostic information. Mao *et al*[20] developed an ML model based on contrast-enhanced CT for preoperative prediction of the pathological grade of HCC. The model achieved an AUC of 0.8014 when combined with clinical factors. The radiomics signature based on T1WI, T2WI, and DCE-MRI was also found to be significantly related to the histopathological grade of HCC[21,22]. Yang *et al*[22] proposed a DL model with a multichannel fusion three-dimensional CNN (3D-CNN) based on DCE-MR to differentiate among pathological grades. The model reached an average accuracy of 0.7396 ± 0.0104 . Thus, further improvements are needed to achieve better diagnostic performance of radiomics models for histological grade.

Microvascular invasion

In addition to predicting the HCC grade, the prediction of microvascular invasion (MVI) has also become a common topic of study. MVI status is a crucial factor influencing treatment selection and follow-up planning; thus, it must be determined preoperatively[23,24]. Some studies have tried to predict MVI before surgery using radiological images and clinical factors. They found that MVI was closely related to several factors. Some studies used LASSO to construct radiomics signatures from CT and MRI and developed models with various conventional ML algorithms for the preoperative prediction of MVI[25-27]. The results showed favorable predictive accuracy for MVI status in HCC patients, especially when combined with clinical factors[28,29]. Jiang *et al*[30] figured out a CT-based model using eXtreme Gradient Boosting and DL algorithm with 3D-CNN to predict MVI preoperatively. The 3D-CNN model demonstrated high diagnostic capability, with an AUC of 0.980/0.906 (training/validation). However, different dimensionality reduction and modeling methods affect the diagnostic performance of the final models. Ni *et al*[31] retrospectively analyzed 206 HCC cases to explore the best radiomic-based diagnostic model. The LASSO + GBDT method showed better performance than the other methods, when the threshold probability was more than 0.22.

MVI usually occurs in the peritumoral region, but it is unclear whether including the features of the peritumoral region could improve predictive capability. Nebbia *et al* [32] developed an ML model for preoperative prediction of MVI status using multiparametric MRI. They found that radiomics features extracted from the tumor region had good diagnostic performance, with an AUC of 0.867. Radiomics features from the peritumoral region also showed an association with MVI; however, the AUC was slightly lower than that of intratumoral radiomics features. Although peritumoral enhancement pattern is reported to be a good predictor of MVI status[33], the usefulness of the features extracted from peritumoral regions for predicting MVI status needs further evaluation in larger populations.

Molecular profiling

HCC originates from hepatocytes and/or hepatic progenitor cells and can express various molecular phenotypes[34]. As such, prognosis varies even among patients with the same pathological grade. Molecular profiling is an important modality that may reflect the biological behavior and invasiveness of tumors. Several studies have used ML methods to identify the molecular phenotypes of HCC preoperatively. CK19 is a biliary-specific marker, and CK19 positivity is associated with a poor postoperative prognosis in HCC[35,36]. In a recent study, the radiomics signature derived from gadoxetic acid-enhanced MRI was used to predict CK19 status in HCC. The final model combined the radiomics signature and clinical factors and achieved a sensitivity of 0.818/0.769 (training/validation) and specificity of 0.974/0.818 (training/validation)[37].

Glypican 3 (GPC3), a type of heparan sulfate proteoglycan, is located on the cell surface. Previous studies have found that GPC3 is closely associated with postoperative metastasis and recurrence in patients with HCC[38]. Furthermore, GPC3 is considered a potential immunotherapeutic target for HCC therapy, especially in patients with unresectable HCC. Gu *et al*[39] constructed a radiomics signature from MRI and achieved good predictive efficacy, with an AUC of 0.879/0.871 (training/validation). Combining the radiomics signature with α -fetoprotein levels further improved the predictive performance, with an AUC of 0.926/0.914 (train-

ing/validation). Another molecular biomarker of HCC is the Ki-67 index. A high Ki-67 index is related to early recurrence and poor prognosis, thus making it a potential indicator of tumor aggressiveness. Recent studies have reported that the Ki-67 status can be predicted preoperatively using CT and MRI[40,41]. Prediction of molecular phenotypes *via* preoperative imaging can aid in the selection of individualized therapeutic strategies.

PREDICTION OF TREATMENT RESPONSE AND EARLY RECURRENCE AFTER CURATIVE TREATMENT

Individualized medical care depends on accurate risk stratification systems. These systems help select the proper treatment and evaluate treatment response. Pretreatment imaging acts as an important role in predicting the effects of treatment, helping clinicians choose the best individualized treatment strategy for patients.

Early recurrence, that is, recurrence within 1-2 years after resection or ablation, is a strong influencing factor of poor prognosis in patients with HCC. A radiomics nomogram derived from preoperative CT and MRI was established to predict early recurrence after surgery or curative ablation in HCC patients[42,43]. The radiomics nomogram comprising both the radiomics score and clinicoradiological risk factors demonstrated good performance, with an AUC of 0.785-0.844[44,45]. Prediction of early recurrence is critical for planning follow-up surveillance strategies and determining the necessity of further interventions after curative treatment. Wang *et al* [46] proposed a DL-based radiomics approach from multi-phase CT images to predict the early recurrence of HCC; it achieved an AUC of 0.825. Unfortunately, image-based radiomics models for early recurrent HCC have poor reproducibility among medical centers[47], limiting their application in clinical practice.

GUIDANCE OF TREATMENT SELECTION

Trans-arterial chemoembolization

Patients with unresectable HCC can undergo trans-arterial chemoembolization (TACE), local radiofrequency ablation, and systemic treatment with sorafenib. ML or DL models based on pretreatment CT or MRI have been recently considered as potential tools for predicting treatment response to TACE for HCC[48,49]. Morshid *et al*[50] used pretreatment quantitative CT image features and clinical factors to develop an ML model to predict treatment response to TACE; the model had an accuracy of 74.2%. Abajian *et al*[51] used MR imaging and clinical data to create an AI model for the prediction of TACE treatment response; the model had an overall accuracy of 78%. Similar results were obtained in other studies, confirming the usefulness of radiomics features extracted from pretreatment CT or MRI for the prediction of tumor response to TACE[52-54]. Peng *et al*[55] described a DL model of a residual CNN to predict the treatment response to TACE for HCC. The final model had a high accuracy in predicting four different therapy response types (complete response, partial response, stable disease, and progressive disease). Thus, it could help clinicians identify patients who will optimally benefit from TACE.

Immunotherapy

Immunotherapy has been shown to be a promising treatment for HCC; however, treatment response to immunotherapy remains low[56-58]. Therefore, it is necessary for clinicians to identify which patients will respond to immunotherapy. Treatment response to immunotherapy is highly dependent on the immune status of the tumor [59]. Tumor immunoprofiling is thus important in predicting its effect. A contrast-enhanced CT-based Rad score developed using the ML algorithm showed high predictive power for CD8⁺ T-cell infiltration, which is associated with the immunotherapy response[60]. Hectors *et al*[61] reported that MRI radiomics features were correlated with various immunohistochemical cell markers and the expression of certain immunotherapy targets. Chen *et al*[62] used clinical data and intratumoral and peritumoral radiomics features to build an ML model from Gd-EOB-DTPA-enhanced MRI. The model showed excellent performance in predicting the immunoscore, with an AUC of 0.926 (95%CI: 0.884-0.967). Collectively, these findings indicated that radiomics features extracted by ML methods might serve as noninvasive predictors of the immune characteristics of HCC and assist physicians in identifying patients who

will benefit from immunotherapy.

LIMITATIONS

The application of AI in different fields of medical research has demonstrated promising results; however, there are some limitations. First, nearly all the research was retrospective and included a relatively small sample size. Therefore, the performance of these predictive models should be validated in larger, multicenter, and prospective studies. Second, the predictive models had limited reproducibility for application in clinical practice, and image heterogeneity might be a significant influencing factor. Third, the AI calculation algorithm requires specialized software packages, leading to increased medical costs. The workflow includes imaging acquisition, segmentation, feature extraction, exploratory analysis, and modeling, making it complex and diverse, further limiting its clinical application.

While AI and radiomics have proven useful in various aspects of HCC, the underlying mechanisms have not been clearly stated, such as pathological correlation and relationship between radiomics and genomics. More research is needed to explore the relationships among imaging, pathophysiology, and prognosis.

CONCLUSION

AI has been applied in many studies on preoperative imaging of HCC. It can extract a large amount of quantitative information from images and reflect pathophysiological processes. Diagnostic and predictive models using AI algorithms have demonstrated promising results in the fields of segmentation, differential diagnosis, prediction of histology, and guidance for treatment selection. However, considering the limitations and complexity of AI, additional research is needed before it can be widely used in clinical practice. Some specific issues, such as reproducibility, heterogeneity of imaging acquisition, and lack of external multicenter validation, need to be considered. Further research will be crucial in improving the accuracy and reproducibility of diagnostic and predictive models, enabling their application for individualized treatment in patients with HCC.

REFERENCES

- Villanueva A.** Hepatocellular Carcinoma. *N Engl J Med* 2019; **380**: 1450-1462 [PMID: 30970190 DOI: 10.1056/NEJMra1713263]
- Gillies RJ, Kinahan PE, Hricak H.** Radiomics: Images Are More than Pictures, They Are Data. *Radiology* 2016; **278**: 563-577 [PMID: 26579733 DOI: 10.1148/radiol.2015151169]
- Lewis S, Hectors S, Taouli B.** Radiomics of hepatocellular carcinoma. *Abdom Radiol (NY)* 2021; **46**: 111-123 [PMID: 31925492 DOI: 10.1007/s00261-019-02378-5]
- McCarthy J, Minsky ML, Rochester N, Shannon CE.** A Proposal for the Dartmouth Summer Research Project on Artificial Intelligence. *AI Mag* 1955; **27**: 12-14
- Chlebus G, Schenk A, Moltz JH, van Ginneken B, Hahn HK, Meine H.** Automatic liver tumor segmentation in CT with fully convolutional neural networks and object-based postprocessing. *Sci Rep* 2018; **8**: 15497 [PMID: 30341319 DOI: 10.1038/s41598-018-33860-7]
- Bousabarah K, Letzen B, Tefera J, Savic L, Schobert I, Schlachter T, Staib LH, Kocher M, Chapiro J, Lin M.** Automated detection and delineation of hepatocellular carcinoma on multiphasic contrast-enhanced MRI using deep learning. *Abdom Radiol (NY)* 2021; **46**: 216-225 [PMID: 32500237 DOI: 10.1007/s00261-020-02604-5]
- Nie P, Wang N, Pang J, Yang G, Duan S, Chen J, Xu W.** CT-Based Radiomics Nomogram: A Potential Tool for Differentiating Hepatocellular Adenoma From Hepatocellular Carcinoma in the Noncirrhotic Liver. *Acad Radiol* 2021; **28**: 799-807 [PMID: 32386828 DOI: 10.1016/j.acra.2020.04.027]
- Nie P, Yang G, Guo J, Chen J, Li X, Ji Q, Wu J, Cui J, Xu W.** A CT-based radiomics nomogram for differentiation of focal nodular hyperplasia from hepatocellular carcinoma in the non-cirrhotic liver. *Cancer Imaging* 2020; **20**: 20 [PMID: 32093786 DOI: 10.1186/s40644-020-00297-z]
- Mokrane FZ, Lu L, Vavasseur A, Otal P, Peron JM, Luk L, Yang H, Ammari S, Saenger Y, Rousseau H, Zhao B, Schwartz LH, Derclé L.** Radiomics machine-learning signature for diagnosis of hepatocellular carcinoma in cirrhotic patients with indeterminate liver nodules. *Eur Radiol* 2020; **30**: 558-570 [PMID: 31444598 DOI: 10.1007/s00330-019-06347-w]
- Ponnoprat D, Inkeaw P, Chaijaruwanich J, Traisathit P, Sripan P, Inmutto N, Na Chiangmai W,**

- Pongnikorn D, Chitapanarux I. Classification of hepatocellular carcinoma and intrahepatic cholangiocarcinoma based on multi-phase CT scans. *Med Biol Eng Comput* 2020; **58**: 2497-2515 [PMID: 32794015 DOI: 10.1007/s11517-020-02229-2]
- 11 Shi W, Kuang S, Cao S, Hu B, Xie S, Chen S, Chen Y, Gao D, Zhu Y, Zhang H, Liu H, Ye M, Sirlin CB, Wang J. Deep learning assisted differentiation of hepatocellular carcinoma from focal liver lesions: choice of four-phase and three-phase CT imaging protocol. *Abdom Radiol (NY)* 2020; **45**: 2688-2697 [PMID: 32232524 DOI: 10.1007/s00261-020-02485-8]
 - 12 Yasaka K, Akai H, Abe O, Kiryu S. Deep Learning with Convolutional Neural Network for Differentiation of Liver Masses at Dynamic Contrast-enhanced CT: A Preliminary Study. *Radiology* 2018; **286**: 887-896 [PMID: 29059036 DOI: 10.1148/radiol.2017170706]
 - 13 Cao SE, Zhang LQ, Kuang SC, Shi WQ, Hu B, Xie SD, Chen YN, Liu H, Chen SM, Jiang T, Ye M, Zhang HX, Wang J. Multiphase convolutional dense network for the classification of focal liver lesions on dynamic contrast-enhanced computed tomography. *World J Gastroenterol* 2020; **26**: 3660-3672 [PMID: 32742134 DOI: 10.3748/wjg.v26.i25.3660]
 - 14 Jiang H, Liu X, Chen J, Wei Y, Lee JM, Cao L, Wu Y, Duan T, Li X, Ma L, Song B. Man or machine? *Cancer Imaging* 2019; **19**: 84 [PMID: 31806050 DOI: 10.1186/s40644-019-0266-9]
 - 15 Zhen SH, Cheng M, Tao YB, Wang YF, Juengpanich S, Jiang ZY, Jiang YK, Yan YY, Lu W, Lue JM, Qian JH, Wu ZY, Sun JH, Lin H, Cai XJ. Deep Learning for Accurate Diagnosis of Liver Tumor Based on Magnetic Resonance Imaging and Clinical Data. *Front Oncol* 2020; **10**: 680 [PMID: 32547939 DOI: 10.3389/fonc.2020.00680]
 - 16 Liu X, Khalvati F, Namdar K, Fischer S, Lewis S, Taouli B, Haider MA, Jhaveri KS. Can machine learning radiomics provide pre-operative differentiation of combined hepatocellular cholangiocarcinoma from hepatocellular carcinoma and cholangiocarcinoma to inform optimal treatment planning? *Eur Radiol* 2021; **31**: 244-255 [PMID: 32749585 DOI: 10.1007/s00330-020-07119-7]
 - 17 Huang X, Long L, Wei J, Li Y, Xia Y, Zuo P, Chai X. Radiomics for diagnosis of dual-phenotype hepatocellular carcinoma using Gd-EOB-DTPA-enhanced MRI and patient prognosis. *J Cancer Res Clin Oncol* 2019; **145**: 2995-3003 [PMID: 31664520 DOI: 10.1007/s00432-019-03062-3]
 - 18 Jian W, Ju H, Cen X, Cui M, Zhang H, Zhang L, Wang G, Gu L, Zhou W. Improving the malignancy characterization of hepatocellular carcinoma using deeply supervised cross modal transfer learning for non-enhanced MR. *Annu Int Conf IEEE Eng Med Biol Soc* 2019; **2019**: 853-856 [PMID: 31946029 DOI: 10.1109/EMBC.2019.8857467]
 - 19 Wu J, Liu A, Cui J, Chen A, Song Q, Xie L. Radiomics-based classification of hepatocellular carcinoma and hepatic haemangioma on precontrast magnetic resonance images. *BMC Med Imaging* 2019; **19**: 23 [PMID: 30866850 DOI: 10.1186/s12880-019-0321-9]
 - 20 Mao B, Zhang L, Ning P, Ding F, Wu F, Lu G, Geng Y, Ma J. Preoperative prediction for pathological grade of hepatocellular carcinoma via machine learning-based radiomics. *Eur Radiol* 2020; **30**: 6924-6932 [PMID: 32696256 DOI: 10.1007/s00330-020-07056-5]
 - 21 Wu M, Tan H, Gao F, Hai J, Ning P, Chen J, Zhu S, Wang M, Dou S, Shi D. Predicting the grade of hepatocellular carcinoma based on non-contrast-enhanced MRI radiomics signature. *Eur Radiol* 2019; **29**: 2802-2811 [PMID: 30406313 DOI: 10.1007/s00330-018-5787-2]
 - 22 Yang DW, Jia XB, Xiao YJ, Wang XP, Wang ZC, Yang ZH. Noninvasive Evaluation of the Pathologic Grade of Hepatocellular Carcinoma Using MCF-3DCNN: A Pilot Study. *Biomed Res Int* 2019; **2019**: 9783106 [PMID: 31183380 DOI: 10.1155/2019/9783106]
 - 23 Peng Z, Chen S, Xiao H, Wang Y, Li J, Mei J, Chen Z, Zhou Q, Feng S, Chen M, Qian G, Peng S, Kuang M. Microvascular Invasion as a Predictor of Response to Treatment with Sorafenib and Transarterial Chemoembolization for Recurrent Intermediate-Stage Hepatocellular Carcinoma. *Radiology* 2019; **292**: 237-247 [PMID: 31135299 DOI: 10.1148/radiol.2019181818]
 - 24 Tang A. Using MRI to Assess Microvascular Invasion in Hepatocellular Carcinoma. *Radiology* 2020; **297**: 582-583 [PMID: 32996872 DOI: 10.1148/radiol.2020203376]
 - 25 Zhang X, Ruan S, Xiao W, Shao J, Tian W, Liu W, Zhang Z, Wan D, Huang J, Huang Q, Yang Y, Yang H, Ding Y, Liang W, Bai X, Liang T. Contrast-enhanced CT radiomics for preoperative evaluation of microvascular invasion in hepatocellular carcinoma: A two-center study. *Clin Transl Med* 2020; **10**: e111 [PMID: 32567245 DOI: 10.1002/ctm2.111]
 - 26 Peng J, Zhang J, Zhang Q, Xu Y, Zhou J, Liu L. A radiomics nomogram for preoperative prediction of microvascular invasion risk in hepatitis B virus-related hepatocellular carcinoma. *Diagn Interv Radiol* 2018; **24**: 121-127 [PMID: 29770763 DOI: 10.5152/dir.2018.17467]
 - 27 Ma X, Wei J, Gu D, Zhu Y, Feng B, Liang M, Wang S, Zhao X, Tian J. Preoperative radiomics nomogram for microvascular invasion prediction in hepatocellular carcinoma using contrast-enhanced CT. *Eur Radiol* 2019; **29**: 3595-3605 [PMID: 30770969 DOI: 10.1007/s00330-018-5985-y]
 - 28 Yang L, Gu D, Wei J, Yang C, Rao S, Wang W, Chen C, Ding Y, Tian J, Zeng M. A Radiomics Nomogram for Preoperative Prediction of Microvascular Invasion in Hepatocellular Carcinoma. *Liver Cancer* 2019; **8**: 373-386 [PMID: 31768346 DOI: 10.1159/000494099]
 - 29 Zhang R, Xu L, Wen X, Zhang J, Yang P, Zhang L, Xue X, Wang X, Huang Q, Guo C, Shi Y, Niu T, Chen F. A nomogram based on bi-regional radiomics features from multimodal magnetic resonance imaging for preoperative prediction of microvascular invasion in hepatocellular carcinoma. *Quant Imaging Med Surg* 2019; **9**: 1503-1515 [PMID: 31667137 DOI: 10.21037/qims.2019.09.07]
 - 30 Jiang YQ, Cao SE, Cao S, Chen JN, Wang GY, Shi WQ, Deng YN, Cheng N, Ma K, Zeng KN, Yan XJ, Yang HZ, Huan WJ, Tang WM, Zheng Y, Shao CK, Wang J, Yang Y, Chen GH. Preoperative

- identification of microvascular invasion in hepatocellular carcinoma by XGBoost and deep learning. *J Cancer Res Clin Oncol* 2021; **147**: 821-833 [PMID: 32852634 DOI: 10.1007/s00432-020-03366-9]
- 31 Ni M, Zhou X, Lv Q, Li Z, Gao Y, Tan Y, Liu J, Liu F, Yu H, Jiao L, Wang G. Radiomics models for diagnosing microvascular invasion in hepatocellular carcinoma: which model is the best model? *Cancer Imaging* 2019; **19**: 60 [PMID: 31455432 DOI: 10.1186/s40644-019-0249-x]
 - 32 Nebbia G, Zhang Q, Arefan D, Zhao X, Wu S. Pre-operative Microvascular Invasion Prediction Using Multi-parametric Liver MRI Radiomics. *J Digit Imaging* 2020; **33**: 1376-1386 [PMID: 32495126 DOI: 10.1007/s10278-020-00353-x]
 - 33 Ahn SJ, Kim JH, Park SJ, Kim ST, Han JK. Hepatocellular carcinoma: preoperative gadoteric acid-enhanced MR imaging can predict early recurrence after curative resection using image features and texture analysis. *Abdom Radiol (NY)* 2019; **44**: 539-548 [PMID: 30229421 DOI: 10.1007/s00261-018-1768-9]
 - 34 Mishra L, Banker T, Murray J, Byers S, Thenappan A, He AR, Shetty K, Johnson L, Reddy EP. Liver stem cells and hepatocellular carcinoma. *Hepatology* 2009; **49**: 318-329 [PMID: 19111019 DOI: 10.1002/hep.22704]
 - 35 Lee SH, Lee JS, Na GH, You YK, Kim DG. Immunohistochemical markers for hepatocellular carcinoma prognosis after liver resection and liver transplantation. *Clin Transplant* 2017; **31** [PMID: 27653235 DOI: 10.1111/ctr.12852]
 - 36 Roncalli M, Park YN, Di Tommaso L. Histopathological classification of hepatocellular carcinoma. *Dig Liver Dis* 2010; **42** Suppl 3: S228-S234 [PMID: 20547308 DOI: 10.1016/S1590-8658(10)60510-5]
 - 37 Wang W, Gu D, Wei J, Ding Y, Yang L, Zhu K, Luo R, Rao SX, Tian J, Zeng M. A radiomics-based biomarker for cytokeratin 19 status of hepatocellular carcinoma with gadoteric acid-enhanced MRI. *Eur Radiol* 2020; **30**: 3004-3014 [PMID: 32002645 DOI: 10.1007/s00330-019-06585-y]
 - 38 Ning S, Bin C, Na H, Peng S, Yi D, Xiang-hua Y, Fang-yin Z, Da-yong Z, Rong-cheng L. Glypican-3, a novel prognostic marker of hepatocellular cancer, is related with postoperative metastasis and recurrence in hepatocellular cancer patients. *Mol Biol Rep* 2012; **39**: 351-357 [PMID: 21655958 DOI: 10.1007/s11033-011-0745-y]
 - 39 Gu D, Xie Y, Wei J, Li W, Ye Z, Zhu Z, Tian J, Li X. MRI-Based Radiomics Signature: A Potential Biomarker for Identifying Glypican 3-Positive Hepatocellular Carcinoma. *J Magn Reson Imaging* 2020; **52**: 1679-1687 [PMID: 32491239 DOI: 10.1002/jmri.27199]
 - 40 Ye Z, Jiang H, Chen J, Liu X, Wei Y, Xia C, Duan T, Cao L, Zhang Z, Song B. Texture analysis on gadoteric acid enhanced-MRI for predicting Ki-67 status in hepatocellular carcinoma: A prospective study. *Chin J Cancer Res* 2019; **31**: 806-817 [PMID: 31814684 DOI: 10.21147/j.issn.1000-9604.2019.05.10]
 - 41 Wu H, Han X, Wang Z, Mo L, Liu W, Guo Y, Wei X, Jiang X. Prediction of the Ki-67 marker index in hepatocellular carcinoma based on CT radiomics features. *Phys Med Biol* 2020; **65**: 235048 [PMID: 32756021 DOI: 10.1088/1361-6560/abac9c]
 - 42 Zhou Y, He L, Huang Y, Chen S, Wu P, Ye W, Liu Z, Liang C. CT-based radiomics signature: a potential biomarker for preoperative prediction of early recurrence in hepatocellular carcinoma. *Abdom Radiol (NY)* 2017; **42**: 1695-1704 [PMID: 28180924 DOI: 10.1007/s00261-017-1072-0]
 - 43 Yuan C, Wang Z, Gu D, Tian J, Zhao P, Wei J, Yang X, Hao X, Dong D, He N, Sun Y, Gao W, Feng J. Prediction early recurrence of hepatocellular carcinoma eligible for curative ablation using a Radiomics nomogram. *Cancer Imaging* 2019; **19**: 21 [PMID: 31027510 DOI: 10.1186/s40644-019-0207-7]
 - 44 Zhu HB, Zheng ZY, Zhao H, Zhang J, Zhu H, Li YH, Dong ZY, Xiao LS, Kuang JJ, Zhang XL, Liu L. Radiomics-based nomogram using CT imaging for noninvasive preoperative prediction of early recurrence in patients with hepatocellular carcinoma. *Diagn Interv Radiol* 2020; **26**: 411-419 [PMID: 32490826 DOI: 10.5152/dir.2020.19623]
 - 45 Zhang Z, Jiang H, Chen J, Wei Y, Cao L, Ye Z, Li X, Ma L, Song B. Hepatocellular carcinoma: radiomics nomogram on gadoteric acid-enhanced MR imaging for early postoperative recurrence prediction. *Cancer Imaging* 2019; **19**: 22 [PMID: 31088553 DOI: 10.1186/s40644-019-0209-5]
 - 46 Wang W, Chen Q, Iwamoto Y, Han X, Zhang Q, Hu H, Lin L, Chen YW. Deep Learning-Based Radiomics Models for Early Recurrence Prediction of Hepatocellular Carcinoma with Multi-phase CT Images and Clinical Data. *Annu Int Conf IEEE Eng Med Biol Soc* 2019; **2019**: 4881-4884 [PMID: 31946954 DOI: 10.1109/EMBC.2019.8856356]
 - 47 Hu HT, Shan QY, Chen SL, Li B, Feng ST, Xu EJ, Li X, Long JY, Xie XY, Lu MD, Kuang M, Shen JX, Wang W. CT-based radiomics for preoperative prediction of early recurrent hepatocellular carcinoma: technical reproducibility of acquisition and scanners. *Radiol Med* 2020; **125**: 697-705 [PMID: 32200455 DOI: 10.1007/s11547-020-01174-2]
 - 48 Kim J, Choi SJ, Lee SH, Lee HY, Park H. Predicting Survival Using Pretreatment CT for Patients With Hepatocellular Carcinoma Treated With Transarterial Chemoembolization: Comparison of Models Using Radiomics. *AJR Am J Roentgenol* 2018; **211**: 1026-1034 [PMID: 30240304 DOI: 10.2214/AJR.18.19507]
 - 49 Liu QP, Xu X, Zhu FP, Zhang YD, Liu XS. Prediction of prognostic risk factors in hepatocellular carcinoma with transarterial chemoembolization using multi-modal multi-task deep learning. *EClinicalMedicine* 2020; **23**: 100379 [PMID: 32548574 DOI: 10.1016/j.eclinm.2020.100379]
 - 50 Morshid A, Elsayes KM, Khalaf AM, Elmohr MM, Yu J, Kaseb AO, Hassan M, Mahvash A, Wang Z, Hazle JD, Fuentes D. A machine learning model to predict hepatocellular carcinoma response to

- transcatheter arterial chemoembolization. *Radiol Artif Intell* 2019; **1** [PMID: 31858078 DOI: 10.1148/ryai.2019180021]
- 51 **Abajian A**, Murali N, Savic LJ, Laage-Gaupp FM, Nezami N, Duncan JS, Schlachter T, Lin M, Geschwind JF, Chapiro J. Predicting Treatment Response to Intra-arterial Therapies for Hepatocellular Carcinoma with the Use of Supervised Machine Learning-An Artificial Intelligence Concept. *J Vasc Interv Radiol* 2018; **29**: 850-857.e1 [PMID: 29548875 DOI: 10.1016/j.jvir.2018.01.769]
 - 52 **Song W**, Yu X, Guo D, Liu H, Tang Z, Liu X, Zhou J, Zhang H, Liu Y. MRI-Based Radiomics: Associations With the Recurrence-Free Survival of Patients With Hepatocellular Carcinoma Treated With Conventional Transcatheter Arterial Chemoembolization. *J Magn Reson Imaging* 2020; **52**: 461-473 [PMID: 31675174 DOI: 10.1002/jmri.26977]
 - 53 **Abajian A**, Murali N, Savic LJ, Laage-Gaupp FM, Nezami N, Duncan JS, Schlachter T, Lin M, Geschwind JF, Chapiro J. Predicting Treatment Response to Image-Guided Therapies Using Machine Learning: An Example for Trans-Arterial Treatment of Hepatocellular Carcinoma. *J Vis Exp* 2018 [PMID: 30371657 DOI: 10.3791/58382]
 - 54 **Meng XP**, Wang YC, Ju S, Lu CQ, Zhong BY, Ni CF, Zhang Q, Yu Q, Xu J, Ji J, Zhang XM, Tang TY, Yang G, Zhao Z. Radiomics Analysis on Multiphase Contrast-Enhanced CT: A Survival Prediction Tool in Patients With Hepatocellular Carcinoma Undergoing Transarterial Chemoembolization. *Front Oncol* 2020; **10**: 1196 [PMID: 32850345 DOI: 10.3389/fonc.2020.01196]
 - 55 **Peng J**, Kang S, Ning Z, Deng H, Shen J, Xu Y, Zhang J, Zhao W, Li X, Gong W, Huang J, Liu L. Residual convolutional neural network for predicting response of transarterial chemoembolization in hepatocellular carcinoma from CT imaging. *Eur Radiol* 2020; **30**: 413-424 [PMID: 31332558 DOI: 10.1007/s00330-019-06318-1]
 - 56 **Yau T**, Kang YK, Kim TY, El-Khoueiry AB, Santoro A, Sangro B, Melero I, Kudo M, Hou MM, Matilla A, Tovoli F, Knox JJ, Ruth He A, El-Rayes BF, Acosta-Rivera M, Lim HY, Neely J, Shen Y, Wisniewski T, Anderson J, Hsu C. Efficacy and Safety of Nivolumab Plus Ipilimumab in Patients With Advanced Hepatocellular Carcinoma Previously Treated With Sorafenib: The CheckMate 040 Randomized Clinical Trial. *JAMA Oncol* 2020; **6**: e204564 [PMID: 33001135 DOI: 10.1001/jamaoncol.2020.4564]
 - 57 **Lee MS**, Ryoo BY, Hsu CH, Numata K, Stein S, Verret W, Hack SP, Spahn J, Liu B, Abdullah H, Wang Y, He AR, Lee KH; GO30140 investigators. Atezolizumab with or without bevacizumab in unresectable hepatocellular carcinoma (GO30140): an open-label, multicentre, phase 1b study. *Lancet Oncol* 2020; **21**: 808-820 [PMID: 32502443 DOI: 10.1016/S1470-2045(20)30156-X]
 - 58 **Finn RS**, Qin S, Ikeda M, Galle PR, Ducreux M, Kim TY, Kudo M, Breder V, Merle P, Kaseb AO, Li D, Verret W, Xu DZ, Hernandez S, Liu J, Huang C, Mulla S, Wang Y, Lim HY, Zhu AX, Cheng AL; IMbrave150 Investigators. Atezolizumab plus Bevacizumab in Unresectable Hepatocellular Carcinoma. *N Engl J Med* 2020; **382**: 1894-1905 [PMID: 32402160 DOI: 10.1056/NEJMoa1915745]
 - 59 **Chen DS**, Mellman I. Elements of cancer immunity and the cancer-immune set point. *Nature* 2017; **541**: 321-330 [PMID: 28102259 DOI: 10.1038/nature21349]
 - 60 **Liao H**, Zhang Z, Chen J, Liao M, Xu L, Wu Z, Yuan K, Song B, Zeng Y. Preoperative Radiomic Approach to Evaluate Tumor-Infiltrating CD8⁺ T Cells in Hepatocellular Carcinoma Patients Using Contrast-Enhanced Computed Tomography. *Ann Surg Oncol* 2019; **26**: 4537-4547 [PMID: 31520208 DOI: 10.1245/s10434-019-07815-9]
 - 61 **Hectors SJ**, Lewis S, Besa C, King MJ, Said D, Putra J, Ward S, Higashi T, Thung S, Yao S, Laface I, Schwartz M, Gnajatic S, Merad M, Hoshida Y, Taouli B. MRI radiomics features predict immunological characteristics of hepatocellular carcinoma. *Eur Radiol* 2020; **30**: 3759-3769 [PMID: 32086577 DOI: 10.1007/s00330-020-06675-2]
 - 62 **Chen S**, Feng S, Wei J, Liu F, Li B, Li X, Hou Y, Gu D, Tang M, Xiao H, Jia Y, Peng S, Tian J, Kuang M. Pretreatment prediction of immunoscore in hepatocellular cancer: a radiomics-based clinical model based on Gd-EOB-DTPA-enhanced MRI imaging. *Eur Radiol* 2019; **29**: 4177-4187 [PMID: 30666445 DOI: 10.1007/s00330-018-5986-x]

Artificial intelligence application in diagnostic gastrointestinal endoscopy - Deus ex machina?

Fábio Pereira Correia, Luís Carvalho Lourenço

ORCID number: Fábio Pereira Correia [0000-0001-6395-3405](https://orcid.org/0000-0001-6395-3405); Luís Carvalho Lourenço [0000-0002-2643-9359](https://orcid.org/0000-0002-2643-9359).

Author contributions: All authors contributed equally to this work, and have read and approved the final manuscript.

Conflict-of-interest statement: The authors declare that they have no conflicting interests

Open-Access: This article is an open-access article that was selected by an in-house editor and fully peer-reviewed by external reviewers. It is distributed in accordance with the Creative Commons Attribution NonCommercial (CC BY-NC 4.0) license, which permits others to distribute, remix, adapt, build upon this work non-commercially, and license their derivative works on different terms, provided the original work is properly cited and the use is non-commercial. See: <http://creativecommons.org/licenses/by-nc/4.0/>

Manuscript source: Invited manuscript

Specialty type: Gastroenterology and hepatology

Country/Territory of origin: Portugal

Fábio Pereira Correia, Luís Carvalho Lourenço, Department of Gastroenterology, Hospital Prof. Dr Fernando Fonseca, Lisbon 2720-276, Portugal

Corresponding author: Luís Carvalho Lourenço, MD, Attending Doctor, Department of Gastroenterology, Hospital Prof. Dr Fernando Fonseca, IC 19, Lisbon 2720-276, Portugal. luisclourenco@gmail.com

Abstract

The close relationship of medicine with technology and the particular interest in this symbiosis in recent years has led to the development of several computed artificial intelligence (AI) systems aimed at various areas of medicine. A number of studies have demonstrated that those systems allow accurate diagnoses with histological precision, thus facilitating decision-making by clinicians in real time. In the field of gastroenterology, AI has been applied in the diagnosis of pathologies of the entire digestive tract and their attached glands, and are increasingly accepted for the detection of colorectal polyps and confirming their histological classification. Studies have shown high accuracy, sensitivity, and specificity in relation to expert endoscopists, and mainly in relation to those with less experience. Other applications that are increasingly studied and with very promising results are the investigation of dysplasia in patients with Barrett's esophagus and the endoscopic and histological assessment of colon inflammation in patients with ulcerative colitis. In some cases AI is thus better than or at least equal to human abilities. However, additional studies are needed to reinforce the existing data, and mainly to determine the applicability of this technology in other indications. This review summarizes the state of the art of AI in gastroenterological pathology.

Key Words: Artificial intelligence; Computer-aided diagnosis; Deep learning; gastrointestinal endoscopy; Colorectal polyps; Dysplasia

©The Author(s) 2021. Published by Baishideng Publishing Group Inc. All rights reserved.

Core Tip: The uses of artificial intelligence (AI) in gastroenterology are growing from day to day. Many published studies have demonstrated the potential benefits of using this technology in clinical practice. We review here the most recent studies related to

Peer-review report's scientific quality classification

Grade A (Excellent): 0
 Grade B (Very good): B
 Grade C (Good): 0
 Grade D (Fair): 0
 Grade E (Poor): 0

Received: January 28, 2021

Peer-review started: January 28, 2021

First decision: May 2, 2021

Revised: May 15, 2021

Accepted: July 19, 2021

Article in press: July 19, 2021

Published online: August 28, 2021

P-Reviewer: Gora MJ

S-Editor: Ma YJ

L-Editor: Filipodia

P-Editor: Li JH



the major hot topics of AI in gastroenterology, namely colorectal polyps, dysplasia in Barrett's esophagus, and inflammation in ulcerative colitis. The machine seems to cooperate with the human, helping him to exceed his abilities and making the future of this symbiosis very promising.

Citation: Correia FP, Lourenço LC. Artificial intelligence application in diagnostic gastrointestinal endoscopy - Deus ex machina? *World J Gastroenterol* 2021; 27(32): 5351-5361

URL: <https://www.wjgnet.com/1007-9327/full/v27/i32/5351.htm>

DOI: <https://dx.doi.org/10.3748/wjg.v27.i32.5351>

INTRODUCTION

Artificial intelligence (AI) is a concept that involves the fields of science and engineering, and was defined by one of its founders, Alan Turing, as the ability of a computer to achieve human performance in cognitive tasks[1]. Machine Learning (ML) is an AI subfield that allows the identification of patterns that can be used to analyze a particular situation[2]. ML can "learn" and improve with experience gained from provided data sets and then apply that information to similar scenarios in the future [2]. Deep learning (DL) is an AI subfield that uses artificial neural networks that are similar to the human brain, and which the capacity to learn and make decisions on its own[2]. Since 1970, AI has been used in medicine for various purposes, including improving the effectiveness of diagnosis, facilitating therapeutic and disease monitoring, and improving overall patient outcomes[2,3].

Gastroenterology is a medical specialty with great potential for integrating AI technology, as the diagnosis of gastrointestinal conditions relies much on image-based investigations (endoscopy and radiology)[4]. Numerous recent studies have investigated the applicability of AI in such diverse areas of gastroenterology, as in the investigation of dysplasia in Barrett's esophagus (BE), diagnosis of gastroesophageal reflux disease, differentiation of acute and chronic pancreatitis, detection and classification of colorectal polyps, characterization of colonic inflammatory activity in patients with inflammatory bowel disease (IBD), among others[2].

In this review, we aimed to describe the latest uses of AI in gastroenterology and the evidence that allows understanding how far these developments can supplant human abilities. We conducted a search of several platforms (PubMed, MEDLINE and EMBASE), with no time limit for articles that compared the performance of these systems and endoscopists.

AI APPLICATIONS IN DIAGNOSTIC GASTROINTESTINAL ENDOSCOPY

AI for the detection of dysplasia in Barrett's esophagus

The epidemiology of esophageal cancer has changed over the years. The increasing incidence of esophageal adenocarcinoma since the 1970s, has made it the most common type of esophageal cancer, mainly in the western countries[5,6]. BE is considered a premalignant condition[5,6] with a risk of progression to esophageal adenocarcinoma of up to 0.3% per year[7]. Endoscopic surveillance programs are based on the fact that progression tends to occur gradually from low-grade to high-grade dysplasia and esophageal adenocarcinoma. The aim is to find premalignant and malignant lesions at an early stage[8].

Because of the possible impact on the survival of the patients, there has been a growing interest in the application of AI and ML in patients with BE[9]. Several studies have reported high rates of sensitivity, specificity and accuracy with computer-aided detection (CAD) systems in detecting and delineating dysplastic lesions in patients with BE[10-13]. In comparison with expert endoscopists, the CAD system had an accuracy of 88% vs 73%, sensitivity of 93% vs 72%, and specificity of 83% vs 74% [10]. In addition, the area of delineation of the lesion by the CAD system overlapped that of expert endoscopists (Figure 1)[10].

Despite the promising results and the data showing that the detection speed for dysplastic lesions was compatible with the real-time use of endoscopic surveillance,

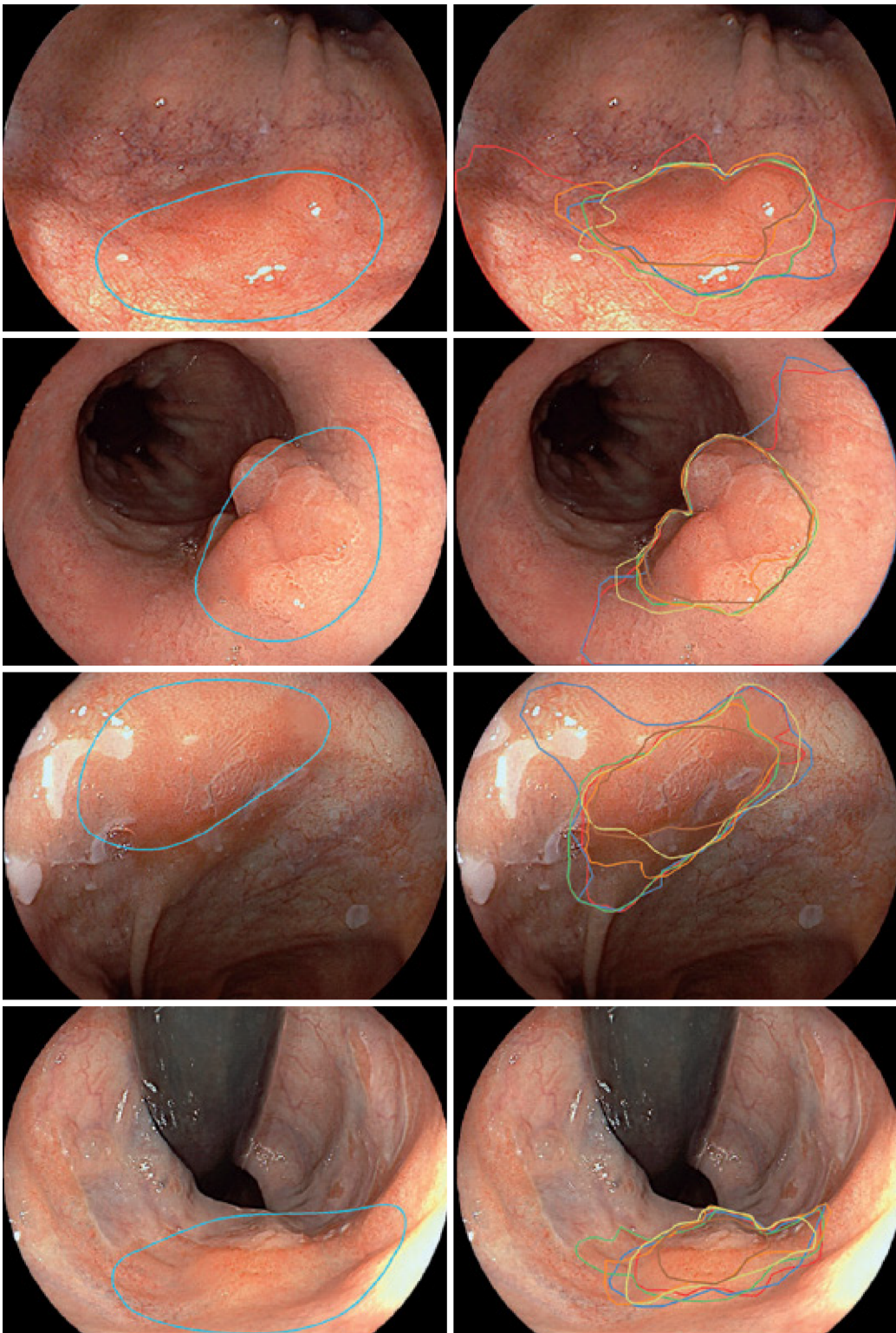


Figure 1 Delineation of Barrett's esophagus by computer-aided detection system and expert endoscopists. Images on the left are from a computer-aided detection system to identify and delineate dysplastic lesions in Barrett's esophagus with white-light imaging. Images on the right show the outlines of the same lesions made by expert endoscopists[13]. Citation: de Groof J, van der Sommen F, van der Putten J, Struyvenberg MR, Zinger S, Curvers WL, Pech O, Meining A, Neuhaus H, Bisschops R, Schoon E, With PH, Bergman JJ. The Argos project: The development of a computer-aided detection system to improve detection of Barrett's neoplasia on white-light endoscopy. *United European Gastroenterol J* 2019; 7: 538-47. Copyright © The Author(s) 2019. Published by SAGE Publications.

this application has only recently been tried in real time. Thus, Ebigbo *et al*[14] used the CAD system in 14 patients simultaneously with endoscopic examination by BE-expert endoscopists. The performance of the AI system was similar to that of the experienced endoscopists, with a sensitivity of 83.7%, a specificity of 100%, and an accuracy of 89.9%, suggesting its potential to improve endoscopic surveillance of BE,

mainly by nonexpert endoscopists.

Currently, there is no evidence that advanced imaging techniques, such as chromoendoscopy, autofluorescence endoscopy, or confocal laser endomicroscopy, offer advantages over high-definition white-light endoscopy (WLE)[7]. Volumetric laser endomicroscopy (VLE) is a recent endoscopic imaging technology that uses optical coherence tomography to produce high-resolution scans of 6-cm segments of the esophagus, with surface and subsurface image depth greater than 3 mm[15,16]. In this way, the real-time diagnosis of surface and subsurface lesions, as well as guiding their endoscopic treatment is possible[15,16]. VLE scans comprise a large amount of visual information with numerous gray-shade images that make interpretation complex and time consuming even by experts[17-19]. CAD systems have been developed that are better at identifying early BE neoplasia in *ex vivo* VLE images than VLE experts are[17], mainly when multiframe analysis is used[18]. However, further studies are needed to validate *in vivo* data. Trindade *et al*[19] also created AI image enhancement software called intelligent real-time image segmentation, that identifies three VLE features previously associated with histologic dysplasia (*i.e.* hyper-reflective surface, hyporeflective structures and lack of a layered architecture) and displays them as different colors superimposed over the VLE image to facilitate interpretation. Studies are underway to assess the effectiveness of this AI system.

AI in the detection of colorectal polyps

It is now known that colorectal cancer (CRC) surveillance with colonoscopy of both the right and left colon is associated with a reduction in CRC mortality[20-22]. The importance of a meticulous high-quality colonoscopy is a result of the inverse relationship that exists between the adenoma detection rate and the risk of interval CRC or advanced-stage CRC[23]. The high rate (up to 30%) of missed adenomas during screening colonoscopy led to the development of computer-aided detection (CADe) systems, which are programs based on DL, in an attempt to mitigate this problem[24]. The first study[25] on the use of CADe in the detection of colon polyps was published in 2003, and it demonstrated good results. However, only static images were used. Since then, several systems have been developed and used with real-time endoscopy. In recent systematic review and meta-analysis, Hassan *et al*[26] assessed the relationship between the increased detection of polyps and the main features of the detected lesions. The review included five randomized clinical trials with a total of 4354 patients (2163 in the CADe and 2191 in the control group). The highlight of the results was that the adenoma detection rate in the CADe group was significantly higher (36.6%) than that in the control group (25.2%) regardless of adenoma size, location, and morphology of the polyps. The rates of detection of advanced adenomas were not significantly different. The authors concluded that AI could benefit colorectal cancer surveillance, as the factors that affect the detection of lesions by human observers, such as size and morphology, do not interfere with detection by the AI system. In addition, the study shows that the AI system did not affect the efficiency of colonoscopy, maintaining similar withdrawal time in both groups. The results are supported by those in prospective study by Liu *et al*[27] in which the adenoma detection rate was higher in the CADe group than in the control group (29.01% *vs* 20.91%) and a meta-analysis by Barua *et al*[28] that found an absolute increase of 10.3% in the detection rate of adenomas. The increase was mainly the result of increased detection of nonadvanced diminutive adenomas, serrated adenomas, and hyperplastic polyps[26,27]. In addition to the smaller size, other characteristics of the polyps first detected by the CADe system were isochromia, flat shape, unclear boundary, partly behind colon folds, and at the edge of the visual field[27]. Thus, the features of the polyps seem to contribute to a higher probability of missed lesions, however Lui *et al* [29] found that 79% of missed lesions can be detected with AI support during the first examination and considered that the main cause of missed lesions was human error, such as less endoscopist experience or the presence of multiple polyps that can increase endoscopist distraction or fatigue. We did not find consistent evidence for the use of advanced imaging techniques in the detection of polyps by CAD systems.

AI in the histological characterization of colorectal polyps

One of the problems of CRC surveillance is the high cost of polypectomy and pathological examination, in particular given the high prevalence of diminutive polyps ≤ 5 mm[30]. It has been proven that a resect and discard strategy for diminutive polyps has an important economic impact, without losing efficacy in CRC surveillance[30]. An optical biopsy of diminutive polyps supported by image-enhanced endoscopic may be appropriate. The Preservation and Incorporation of Valuable endoscopic Innovations (PIVI) group of the American Society for Gastrointestinal Endoscopy (ASGE)[31]

recommends that for a “diagnose-and-leave” strategy, endoscopic diagnosis should provide a 90% or higher negative predictive value for adenomatous histology when used with high confidence. For a “resect and discard” strategy for adenomas ≤ 5 mm, it is recommended that an optical biopsy with high confidence, when combined with a histologic assessment of polyps larger than 5 mm, should provide $\geq 90\%$ agreement in the assignment of post polypectomy surveillance intervals compared with decisions based on pathological assessment of all identified polyps.

The optical diagnosis of colorectal polyps has not yet been widely implemented because of the lack of endoscopist experience and the considerable learning curve of advanced imaging modalities[32,33]. To overcome this problem, AI systems such as, computer-aided diagnostic (CADx) that help to predict the histology (*i.e.* neoplastic or non-neoplastic) of detected polyps (Figure 2) have been developed with the aim of avoiding unnecessary endoscopic biopsies or resection[33-35]. Yang *et al*[35] created DL models that classify colorectal lesions histologically using white-light colonoscopy images. They found an accuracy of 79.5% in distinguishing neoplastic and non-neoplastic lesions and 87.1% in distinguishing advanced and nonadvanced colorectal lesions. When comparing the performance of endoscopists and CADx for the classification of polyps, they found that CADx performed better than less experienced endoscopists, but not better than experts.

Combinations of advanced imaging modalities, such as narrow-band imaging (NBI) or endocytoscopy, and CAD systems improved the performance of AI-assisted optical biopsy[34]. Several studies have shown the potential of combining NBI with CADx in the classification of polyps[36-38]. Song *et al*[37] developed a DL model to predict colorectal polyp histology based on NBI near-focus images. Their study showed a good diagnostic accuracy (81.3%-82.4%) that was comparable to expert endoscopists and was significantly more accurate than trainee endoscopists. CADx performance was consistent regardless of polyp size, location, or morphology, with an average histological assessment time of 0.02-0.04 s. They concluded that an AI CAD system can help inexperienced endoscopists in the histological assessment of colorectal polyps and increase the confidence of experts regarding their assessments.

A recent systematic review and meta-analysis that included 18 studies (15 retrospective and three prospective) and 7680 images of colorectal polyps was performed to evaluate the prediction of histology[39]. AI had an accuracy of 0.96 (AUC), with a sensitivity of 92.3% and a specificity of 89.8%. Comparing studies that used NBI with those that used non-NBI techniques, they found a significantly better accuracy (AUC 0.98 *vs* 0.84) in the NBI studies. When they evaluated performance in the histological characterization of diminutive polyps, they found that the accuracy overlapped and that the pooled negative predictive value was 91.3%-95.1%, which complies with the threshold of the “resect and discard” strategy of the ASGE. The difference in the performance of AI and endoscopists was not significant except in studies that included nonexpert endoscopists, in which the performance AI was significantly better than that of nonexpert endoscopists.

Endocytoscopy (EC) is an advanced endoscopic technique in which a contact light microscopy system is integrated into the distal tip of a conventional colonoscope[40]. This technique has performed well in differentiating between diminutive neoplastic and non-neoplastic colorectal polyps both alone[41] and in combination with NBI (EC-NBI)[42]. The combined use of EC and CAD (EC-CAD) to classify the histology of colorectal polyps has been studied. According to Mori *et al*[40], this technology achieved a sensitivity of 92%, a specificity of 79.5%, and an accuracy of 89.2%. The performance was comparable to EC image evaluation by experts, but significantly better than evaluation by trainees for identifying neoplastic polyps.

AI in IBD

Ulcerative colitis (UC) is a chronic inflammatory disease, and the therapeutic goals have changed over the last decades, from the treatment of symptoms toward mucosal healing, with the aim of modifying the natural history of disease[43-45]. Mucosal healing can be defined by endoscopic evaluation because the inflammation is limited to the mucosal layer[44]. However, it is currently known that histological evidence of inflammation, even in patients with mucosal healing, is a prognostic marker of a two-to-three-fold increase in the risk of colitis relapse and colon cancer[44,45]. Consequently, assessment of inflammatory activity and severity are important for the choice of therapeutic and follow-up strategies. This supports performing colonoscopies with biopsies and visually interpretation of mucosal and histologic parameters of inflammation using standardized disease activity measures[46]. Visual interpretation is subject to bias, interobserver, and intraobserver variability. Histological evaluation requires time for processing and interpretation, which limits the ability to make

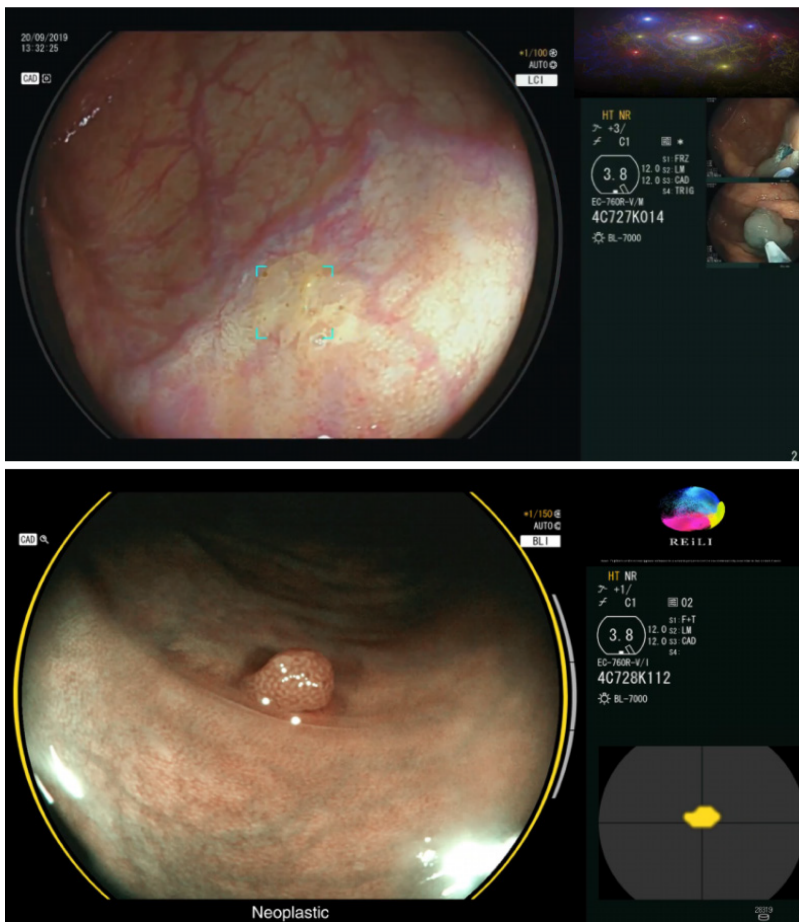


Figure 2 Computer-aided detection system for detecting and classifying colorectal polyps. The top image is a polypoid lesion (delimited by blue marks) identified by a CADe system. The bottom image is a lesion classified as neoplastic by the CADx system with a high degree of confidence (three gray bars on the right side of the image)[33]. Citation: Mori Y, Neumann H, Misawa M, Kudo SE, Bretthauer M. Artificial intelligence in colonoscopy - Now on the market. What's next? *J Gastroenterol Hepatol* 2021; 36(1): 7-11. Copyright © The Author(s) 2020. Published by Journal of Gastroenterology and Hepatology Foundation and John Wiley & Sons Australia, Ltd.

decisions in real time[46].

Several studies have used AI for the macroscopic and histological characterization of colic mucosa in UC. Takenaka *et al*[47] developed a deep neural network for evaluation of UC with the aim of predicting endoscopic remission, a UC endoscopic index of severity score of 0; and histologic remission, a Geboes score of ≤ 3 points using endoscopic images. In the training set, they used 40,758 images of colonoscopies and the histologic results of 6885 biopsies from the same patients. They validated the results in a prospective study of 875 patients with 4187 endoscopic images and 4104 biopsy specimens. In the validation phase, the AI system was able to identify patients with endoscopic remission with 90.1% of accuracy and histologic remission with 92.9% of accuracy using only endoscopic images. The results suggest that computer-aided diagnosis can reliably assist endoscopic and histologic disease activity in UC without the need for mucosal biopsies. It should be noted that the study used only white-light images (WLIs). Chromoendoscopy was not used after WLI evaluation.

However, there are doubts that conventional WLI can reliably identify persistent histologic inflammation. Alternatives such as NBI, confocal laser endomicroscopy, or EC have emerged[48]. Despite their excellent diagnostic performance, these techniques are highly dependent on experienced endoscopists[48]. Maeda *et al*[48] developed a CAD system that used AI and EC to predict persistent histologic inflammation (Figure 3). It was used to retrospectively evaluate 12900 EC images for ML and 9935 EC images for validation, in addition assessment of biopsy samples by experienced pathologists blinded to the endoscopy results. The algorithm had 74% sensitivity, 97% specificity, and 91% accuracy in identifying histologic inflammation, and perfect reproducibility. The results are promising, and the authors concluded that the symbiosis achieved with the CAD system and EC has the potential to support immediate intervention and ultimately reduce the number of required biopsy samples.

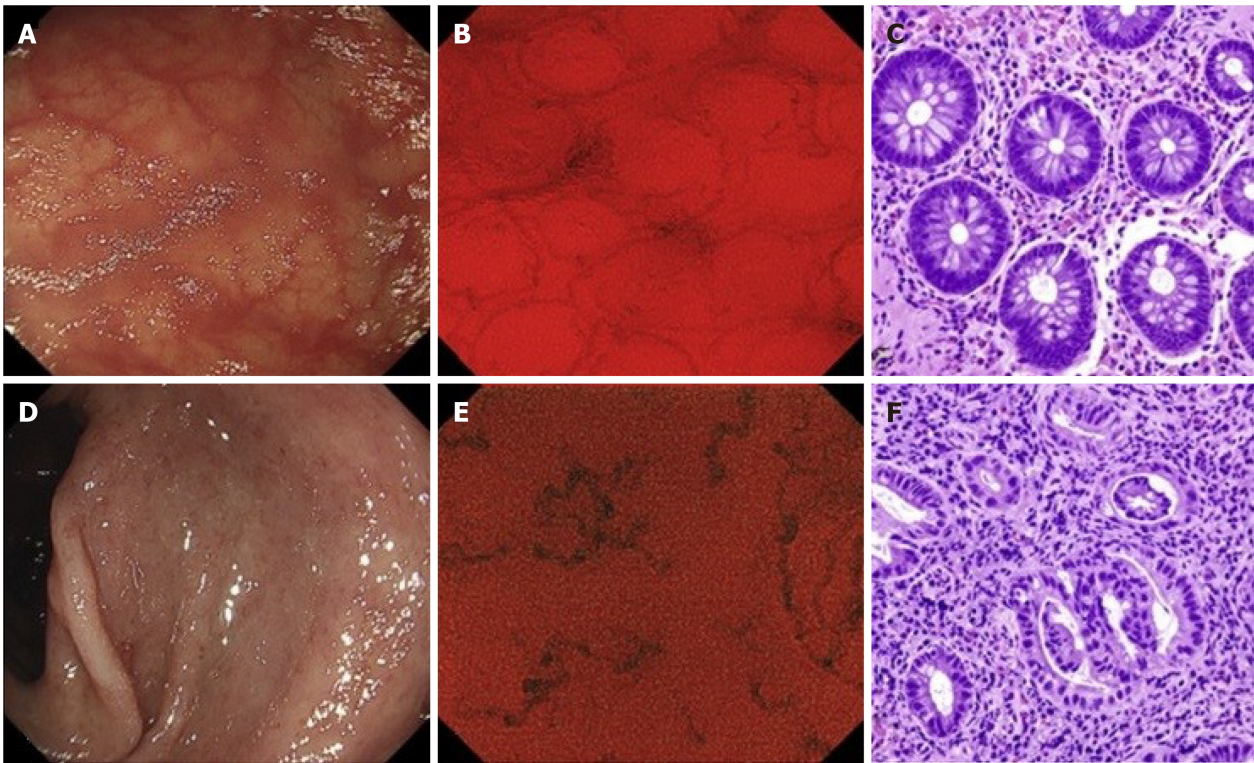


Figure 3 Application of computer-aided detection systems to endocytoscopy. A, D: Conventional endoscopic images in WLI; B, E: Endocytoscopic images; C, F: Histological images. A CAD system evaluated the endocytoscopy image B: “healing” and E: active inflammation. The classifications were later confirmed by the pathologist[48]. Citation: Maeda Y, Kudo SE, Mori Y, Misawa M, Ogata N, Sasanuma S, Wakamura K, Oda M, Mori K, Ohtsuka K. Fully automated diagnostic system with artificial intelligence using endocytoscopy to identify the presence of histologic inflammation associated with ulcerative colitis (with video). *Gastrointest Endosc* 2019; 89(2): 408-415. Copyright © The Author(s) 2019 by the American Society for Gastrointestinal Endoscopy. Published by Elsevier, Inc.

There is a lack of published studies of the potential benefit of AI in assessment of disease activity in Crohn’s disease. Evidence of the applicability of AI to the surveillance of dysplasia in patients with IBD is still lacking. Maeda *et al*[49] described a case in which an AI system assisted in the detection of dysplastic lesions in a patient with UC. They concluded that AI may have potential in this context, especially for nonexpert endoscopists.

CONCLUSION

The evidence for a role of AI in diagnostic endoscopy is growing, with increasing supporting evidence in dysplasia detection in BE, identification and assessment of colorectal polyps, and characterization of colonic mucosa in UC. A number of possible applications are still under evaluation (Table 1)[50-58]. *Deus ex machina* is a Latin expression meaning “God from the machine”. The term was coined from the conventions of ancient Greek theatre, where actors who were playing gods were brought onto stage using a machine[59]. Later it was used in the story plots of theatre plays and movies to describe an unexpected and sudden solution to resolve main issues or tragedies. AI is currently being developed for use in endoscopy daily practice. It seems to be a quick solution of the long-standing problems of the interobserver agreement and the subjective “feeling” and accuracy of the endoscopist in diagnostic exams. Apart from the complexity of improving or overcoming human evaluation, there are also availability issues that will limit the access to this new technology.

In the meantime, the added value of electronic systems to human practice must not be underrated as they would definitely contribute to the standardization of diagnostic endoscopy worldwide. Apart from that, savings in the time, effort, economic, and human resources needed for diagnostic exams, would make room for improvements in endoscopic therapeutic procedures, which are growing in complexity over time.

In conclusion, AI is currently used to optimize diagnostic endoscopy procedures, with growing indications and evidence over time. Although it may not be ready for

Table 1 Potential applications of artificial intelligence in gastrointestinal pathology (under evaluation)

| Disease | Detection | Ref. |
|---|--|---|
| Esophageal squamous cell carcinoma (ESCC) | Detection of early ESCC | Yang <i>et al</i> [50] Kumagai <i>et al</i> [51] |
| <i>Helicobacter pylori</i> infection | Diagnosis of <i>Helicobacter pylori</i> infection | Mohan <i>et al</i> [52] |
| Gastric cancer (GC) | Detection of preneoplastic lesions and early gastric cancer Prediction the invasion depth of GC | Anta <i>et al</i> [53] Nagao <i>et al</i> [54] |
| Celiac disease | Early detection of celiac disease | Sana <i>et al</i> [55] |
| Gastrointestinal bleeding | Detection of small bowel bleeding with wireless capsule endoscopic | Aoki <i>et al</i> [56] Tsuboi <i>et al</i> [57] |
| Pancreatic lesions | Differentiation of pancreatic cancer from chronic pancreatitis and normal pancreas | Tonozuka <i>et al</i> [58] |

prime-time use worldwide, the future of AI is near. It will depend on us, human endoscopists, to define how far these machines can help us with (and solve?) our naturally imperfect issues.

REFERENCES

- 1 **Ramesh AN**, Kambhampati C, Monson JR, Drew PJ. Artificial intelligence in medicine. *Ann R Coll Surg Engl* 2004; **86**: 334-338 [PMID: 15333167 DOI: 10.1308/147870804290]
- 2 **Kaul V**, Enslin S, Gross SA. History of artificial intelligence in medicine. *Gastrointest Endosc* 2020; **92**: 807-812 [PMID: 32565184 DOI: 10.1016/j.gie.2020.06.040]
- 3 **Liu R**, Rong Yan, Peng Z. A review of medical artificial intelligence. *Global Health J* 2020; **4**: 42-45 [DOI: 10.1016/j.glojh.2020.04.002]
- 4 **Sung JJ**, Poon NC. Artificial intelligence in gastroenterology: where are we heading? *Front Med* 2020; **14**: 511-517 [PMID: 32458189 DOI: 10.1007/s11684-020-0742-4]
- 5 **Shaheen NJ**, Falk GW, Iyer PG, Gerson LB; American College of Gastroenterology. ACG Clinical Guideline: Diagnosis and Management of Barrett's Esophagus. *Am J Gastroenterol* 2016; **111**: 30-50; quiz 51 [PMID: 26526079 DOI: 10.1038/ajg.2015.322]
- 6 **Maitra I**, Date RS, Martin FL. Towards screening Barrett's oesophagus: current guidelines, imaging modalities and future developments. *Clin J Gastroenterol* 2020; **13**: 635-649 [PMID: 32495144 DOI: 10.1007/s12328-020-01135-2]
- 7 **Weusten B**, Bisschops R, Coron E, Dinis-Ribeiro M, Dumonceau JM, Esteban JM, Hassan C, Pech O, Repici A, Bergman J, di Pietro M. Endoscopic management of Barrett's esophagus: European Society of Gastrointestinal Endoscopy (ESGE) Position Statement. *Endoscopy* 2017; **49**: 191-198 [PMID: 28122386 DOI: 10.1055/s-0042-122140]
- 8 **Sharma P**, Shaheen NJ, Katzka D, Bergman JJGHM. AGA Clinical Practice Update on Endoscopic Treatment of Barrett's Esophagus With Dysplasia and/or Early Cancer: Expert Review. *Gastroenterology* 2020; **158**: 760-769 [PMID: 31730766 DOI: 10.1053/j.gastro.2019.09.051]
- 9 **de Souza LA Jr**, Palm C, Mendel R, Hook C, Ebigbo A, Probst A, Messmann H, Weber S, Papa JP. A survey on Barrett's esophagus analysis using machine learning. *Comput Biol Med* 2018; **96**: 203-213 [PMID: 29626734 DOI: 10.1016/j.combiomed.2018.03.014]
- 10 **de Groof AJ**, Struyvenberg MR, van der Putten J, van der Sommen F, Fockens KN, Curvers WL, Zinger S, Pouw RE, Coron E, Baldaque-Silva F, Pech O, Weusten B, Meining A, Neuhaus H, Bisschops R, Dent J, Schoon EJ, de With PH, Bergman JJ. Deep-Learning System Detects Neoplasia in Patients With Barrett's Esophagus With Higher Accuracy Than Endoscopists in a Multistep Training and Validation Study With Benchmarking. *Gastroenterology* 2020; **158**: 915-929.e4 [PMID: 31759929 DOI: 10.1053/j.gastro.2019.11.030]
- 11 **Hashimoto R**, Requa J, Dao T, Ninh A, Tran E, Mai D, Lugo M, El-Hage Chehade N, Chang KJ, Karnes WE, Samarasena JB. Artificial intelligence using convolutional neural networks for real-time detection of early esophageal neoplasia in Barrett's esophagus (with video). *Gastrointest Endosc* 2020; **91**: 1264-1271.e1 [PMID: 31930967 DOI: 10.1016/j.gie.2019.12.049]
- 12 **Lui TKL**, Tsui VWM, Leung WK. Accuracy of artificial intelligence-assisted detection of upper GI lesions: a systematic review and meta-analysis. *Gastrointest Endosc* 2020; **92**: 821-830.e9 [PMID: 32562608 DOI: 10.1016/j.gie.2020.06.034]
- 13 **de Groof J**, van der Sommen F, van der Putten J, Struyvenberg MR, Zinger S, Curvers WL, Pech O, Meining A, Neuhaus H, Bisschops R, Schoon EJ, de With PH, Bergman JJ. The Argos project: The development of a computer-aided detection system to improve detection of Barrett's neoplasia on

- white light endoscopy. *United European Gastroenterol J* 2019; **7**: 538-547 [PMID: 31065371 DOI: 10.1177/2050640619837443]
- 14 **Ebigbo A**, Mendel R, Probst A, Manzeneder J, Prinz F, de Souza LA Jr, Papa J, Palm C, Messmann H. Real-time use of artificial intelligence in the evaluation of cancer in Barrett's oesophagus. *Gut* 2020; **69**: 615-616 [PMID: 31541004 DOI: 10.1136/gutjnl-2019-319460]
 - 15 **Wolfsen HC**. Volumetric Laser Endomicroscopy in Patients With Barrett Esophagus. *Gastroenterol Hepatol (N Y)* 2016; **12**: 719-722 [PMID: 28035200]
 - 16 **Wolfsen HC**, Sharma P, Wallace MB, Leggett C, Tearney G, Wang KK. Safety and feasibility of volumetric laser endomicroscopy in patients with Barrett's esophagus (with videos). *Gastrointest Endosc* 2015; **82**: 631-640 [PMID: 25956472 DOI: 10.1016/j.gie.2015.03.1968]
 - 17 **Swager AF**, van der Sommen F, Klomp SR, Zinger S, Meijer SL, Schoon EJ, Bergman JJGHM, de With PH, Curvers WL. Computer-aided detection of early Barrett's neoplasia using volumetric laser endomicroscopy. *Gastrointest Endosc* 2017; **86**: 839-846 [PMID: 28322771 DOI: 10.1016/j.gie.2017.03.011]
 - 18 **Struyvenberg MR**, van der Sommen F, Swager AF, de Groof AJ, Rikos A, Schoon EJ, Bergman JJ, de With PHN, Curvers WL. Improved Barrett's neoplasia detection using computer-assisted multiframe analysis of volumetric laser endomicroscopy. *Dis Esophagus* 2020; **33** [PMID: 31364700 DOI: 10.1093/dote/doz065]
 - 19 **Trindade AJ**, McKinley MJ, Fan C, Leggett CL, Kahn A, Pleskow DK. Endoscopic Surveillance of Barrett's Esophagus Using Volumetric Laser Endomicroscopy With Artificial Intelligence Image Enhancement. *Gastroenterology* 2019; **157**: 303-305 [PMID: 31078625 DOI: 10.1053/j.gastro.2019.04.048]
 - 20 **Pan J**, Xin L, Ma YF, Hu LH, Li ZS. Colonoscopy Reduces Colorectal Cancer Incidence and Mortality in Patients With Non-Malignant Findings: A Meta-Analysis. *Am J Gastroenterol* 2016; **111**: 355-365 [PMID: 26753884 DOI: 10.1038/ajg.2015.418]
 - 21 **Niikura R**, Hirata Y, Suzuki N, Yamada A, Hayakawa Y, Suzuki H, Yamamoto S, Nakata R, Komatsu J, Okamoto M, Kodaira M, Shinozaki T, Fujishiro M, Watanabe T, Koike K. Colonoscopy reduces colorectal cancer mortality: A multicenter, long-term, colonoscopy-based cohort study. *PLoS One* 2017; **12**: e0185294 [PMID: 28957370 DOI: 10.1371/journal.pone.0185294]
 - 22 **Doubeni CA**, Corley DA, Quinn VP, Jensen CD, Zauber AG, Goodman M, Johnson JR, Mehta SJ, Becerra TA, Zhao WK, Schottinger J, Doria-Rose VP, Levin TR, Weiss NS, Fletcher RH. Effectiveness of screening colonoscopy in reducing the risk of death from right and left colon cancer: a large community-based study. *Gut* 2018; **67**: 291-298 [PMID: 27733426 DOI: 10.1136/gutjnl-2016-312712]
 - 23 **Corley DA**, Jensen CD, Marks AR, Zhao WK, Lee JK, Doubeni CA, Zauber AG, de Boer J, Fireman BH, Schottinger JE, Quinn VP, Ghai NR, Levin TR, Quesenberry CP. Adenoma detection rate and risk of colorectal cancer and death. *N Engl J Med* 2014; **370**: 1298-1306 [PMID: 24693890 DOI: 10.1056/NEJMoa1309086]
 - 24 **Wang P**, Liu P, Glissen Brown JR, Berzin TM, Zhou G, Lei S, Liu X, Li L, Xiao X. Lower Adenoma Miss Rate of Computer-Aided Detection-Assisted Colonoscopy vs Routine White-Light Colonoscopy in a Prospective Tandem Study. *Gastroenterology* 2020; **159**: 1252-1261.e5 [PMID: 32562721 DOI: 10.1053/j.gastro.2020.06.023]
 - 25 **Karkanis SA**, Iakovidis DK, Maroulis DE, Karras DA, Tzivras M. Computer-aided tumor detection in endoscopic video using color wavelet features. *IEEE Trans Inf Technol Biomed* 2003; **7**: 141-152 [PMID: 14518727 DOI: 10.1109/TITB.2003.813794]
 - 26 **Hassan C**, Spadaccini M, Iannone A, Maselli R, Jovani M, Chandrasekar VT, Antonelli G, Yu H, Areia M, Dinis-Ribeiro M, Bhandari P, Sharma P, Rex DK, Rösch T, Wallace M, Repici A. Performance of artificial intelligence in colonoscopy for adenoma and polyp detection: a systematic review and meta-analysis. *Gastrointest Endosc* 2021; **93**: 77-85.e6 [PMID: 32598963 DOI: 10.1016/j.gie.2020.06.059]
 - 27 **Liu P**, Wang P, Glissen Brown JR, Berzin TM, Zhou G, Liu W, Xiao X, Chen Z, Zhang Z, Zhou C, Lei L, Xiong F, Li L, Liu X. The single-monitor trial: an embedded CAde system increased adenoma detection during colonoscopy: a prospective randomized study. *Therap Adv Gastroenterol* 2020; **13**: 1756284820979165 [PMID: 33403003 DOI: 10.1177/1756284820979165]
 - 28 **Barua I**, Vinsard DG, Jodal HC, Løberg M, Kalager M, Holme Ø, Misawa M, Bretthauer M, Mori Y. Artificial intelligence for polyp detection during colonoscopy: a systematic review and meta-analysis. *Endoscopy* 2021; **53**: 277-284 [PMID: 32557490 DOI: 10.1055/a-1201-7165]
 - 29 **Lui TKL**, Hui CKY, Tsui VWM, Cheung KS, Ko MKL, Foo DCC, Mak LY, Yeung CK, Lui TH, Wong SY, Leung WK. New insights on missed colonic lesions during colonoscopy through artificial intelligence-assisted real-time detection (with video). *Gastrointest Endosc* 2021; **93**: 193-200.e1 [PMID: 32376335 DOI: 10.1016/j.gie.2020.04.066]
 - 30 **Hassan C**, Pickhardt PJ, Rex DK. A resect and discard strategy would improve cost-effectiveness of colorectal cancer screening. *Clin Gastroenterol Hepatol* 2010; **8**: 865-869, 869.e1 [PMID: 20621680 DOI: 10.1016/j.cgh.2010.05.018]
 - 31 **ASGE Technology Committee**, Abu Dayyeh BK, Thosani N, Konda V, Wallace MB, Rex DK, Chauhan SS, Hwang JH, Komanduri S, Manfredi M, Maple JT, Murad FM, Siddiqui UD, Banerjee S. ASGE Technology Committee systematic review and meta-analysis assessing the ASGE PIVI thresholds for adopting real-time endoscopic assessment of the histology of diminutive colorectal polyps. *Gastrointest Endosc* 2015; **81**: 502.e1-502.e16 [PMID: 25597420 DOI: 10.1016/j.gie.2015.03.011]

- 10.1016/j.gie.2014.12.022]
- 32 **Castela J**, Mão de Ferro S, Rosa I, Lage P, Ferreira S, Pereira Silva J, Cortez Pinto J, Vale Rodrigues R, Moleiro J, Claro I, Esteves S, Dias Pereira A. Real-Time Optical Diagnosis of Colorectal Polyps in the Routine Clinical Practice Using the NICE and WASP Classifications in a Nonacademic Setting. *GE Port J Gastroenterol* 2019; **26**: 314-323 [PMID: 31559322 DOI: 10.1159/000495258]
 - 33 **Mori Y**, Neumann H, Misawa M, Kudo SE, Bretthauer M. Artificial intelligence in colonoscopy - Now on the market. What's next? *J Gastroenterol Hepatol* 2021; **36**: 7-11 [PMID: 33179322 DOI: 10.1111/jgh.15339]
 - 34 **Mori Y**, Kudo SE, Berzin TM, Misawa M, Takeda K. Computer-aided diagnosis for colonoscopy. *Endoscopy* 2017; **49**: 813-819 [PMID: 28561195 DOI: 10.1055/s-0043-109430]
 - 35 **Yang YJ**, Cho BJ, Lee MJ, Kim JH, Lim H, Bang CS, Jeong HM, Hong JT, Baik GH. Automated Classification of Colorectal Neoplasms in White-Light Colonoscopy Images via Deep Learning. *J Clin Med* 2020; **9** [PMID: 32456309 DOI: 10.3390/jcm9051593]
 - 36 **Byrne MF**, Chapados N, Soudan F, Oertel C, Linares Pérez M, Kelly R, Iqbal N, Chandelier F, Rex DK. Real-time differentiation of adenomatous and hyperplastic diminutive colorectal polyps during analysis of unaltered videos of standard colonoscopy using a deep learning model. *Gut* 2019; **68**: 94-100 [PMID: 29066576 DOI: 10.1136/gutjnl-2017-314547]
 - 37 **Song EM**, Park B, Ha CA, Hwang SW, Park SH, Yang DH, Ye BD, Myung SJ, Yang SK, Kim N, Byeon JS. Endoscopic diagnosis and treatment planning for colorectal polyps using a deep-learning model. *Sci Rep* 2020; **10**: 30 [PMID: 31913337 DOI: 10.1038/s41598-019-56697-0]
 - 38 **Rodriguez-Diaz E**, Baffy G, Lo WK, Mashimo H, Vidyarthi G, Mohapatra SS, Singh SK. Real-time artificial intelligence-based histologic classification of colorectal polyps with augmented visualization. *Gastrointest Endosc* 2021; **93**: 662-670 [PMID: 32949567 DOI: 10.1016/j.gie.2020.09.018]
 - 39 **Lui TKL**, Guo CG, Leung WK. Accuracy of artificial intelligence on histology prediction and detection of colorectal polyps: a systematic review and meta-analysis. *Gastrointest Endosc* 2020; **92**: 11-22.e6 [PMID: 32119938 DOI: 10.1016/j.gie.2020.02.033]
 - 40 **Mori Y**, Kudo SE, Wakamura K, Misawa M, Ogawa Y, Kutsukawa M, Kudo T, Hayashi T, Miyachi H, Ishida F, Inoue H. Novel computer-aided diagnostic system for colorectal lesions by using endocytoscopy (with videos). *Gastrointest Endosc* 2015; **81**: 621-629 [PMID: 25440671 DOI: 10.1016/j.gie.2014.09.008]
 - 41 **Utsumi T**, Sano Y, Iwatate M, Sunakawa H, Teramoto A, Hirata D, Hattori S, Sano W, Hasuike N, Ichikawa K, Fujimori T. Prospective real-time evaluation of diagnostic performance using endocytoscopy in differentiating neoplasia from non-neoplasia for colorectal diminutive polyps (≤ 5 mm). *World J Gastrointest Oncol* 2018; **10**: 96-102 [PMID: 29666668 DOI: 10.4251/wjgo.v10.i4.96]
 - 42 **Kataoka S**, Kudo SE, Misawa M, Nakamura H, Takeda K, Toyoshima N, Mori Y, Ogata N, Kudo T, Hisayuki T, Hayashi T, Wakamura K, Baba T, Ishida F. Endocytoscopy with NBI has the potential to correctly diagnose diminutive colorectal polyps that are difficult to diagnose using conventional NBI. *Endosc Int Open* 2020; **8**: E360-E367 [PMID: 32118108 DOI: 10.1055/a-1068-9228]
 - 43 **Danese S**, Roda G, Peyrin-Biroulet L. Evolving therapeutic goals in ulcerative colitis: towards disease clearance. *Nat Rev Gastroenterol Hepatol* 2020; **17**: 1-2 [PMID: 31520081 DOI: 10.1038/s41575-019-0211-1]
 - 44 **Chateau T**, Feakins R, Marchal-Bressenot A, Magro F, Danese S, Peyrin-Biroulet L. Histological Remission in Ulcerative Colitis: Under the Microscope Is the Cure. *Am J Gastroenterol* 2020; **115**: 179-189 [PMID: 31809296 DOI: 10.14309/ajg.0000000000000437]
 - 45 **Peyrin-Biroulet L**, Bressenot A, Kampman W. Histologic remission: the ultimate therapeutic goal in ulcerative colitis? *Clin Gastroenterol Hepatol* 2014; **12**: 929-34.e2 [PMID: 23911875 DOI: 10.1016/j.cgh.2013.07.022]
 - 46 **Holmer AK**, Dulai PS. Using Artificial Intelligence to Identify Patients With Ulcerative Colitis in Endoscopic and Histologic Remission. *Gastroenterology* 2020; **158**: 2045-2047 [PMID: 32289374 DOI: 10.1053/j.gastro.2020.04.011]
 - 47 **Takenaka K**, Ohtsuka K, Fujii T, Negi M, Suzuki K, Shimizu H, Oshima S, Akiyama S, Motobayashi M, Nagahori M, Saito E, Matsuoka K, Watanabe M. Development and Validation of a Deep Neural Network for Accurate Evaluation of Endoscopic Images From Patients With Ulcerative Colitis. *Gastroenterology* 2020; **158**: 2150-2157 [PMID: 32060000 DOI: 10.1053/j.gastro.2020.02.012]
 - 48 **Maeda Y**, Kudo SE, Mori Y, Misawa M, Ogata N, Sasanuma S, Wakamura K, Oda M, Mori K, Ohtsuka K. Fully automated diagnostic system with artificial intelligence using endocytoscopy to identify the presence of histologic inflammation associated with ulcerative colitis (with video). *Gastrointest Endosc* 2019; **89**: 408-415 [PMID: 30268542 DOI: 10.1016/j.gie.2018.09.024]
 - 49 **Maeda Y**, Kudo SE, Ogata N, Misawa M, Mori Y, Mori K, Ohtsuka K. Can artificial intelligence help to detect dysplasia in patients with ulcerative colitis? *Endoscopy* 2021; **53**: E273-E274 [PMID: 33003217 DOI: 10.1055/a-1261-2944]
 - 50 **Yang XX**, Li Z, Shao XJ, Ji R, Qu JY, Zheng MQ, Sun YN, Zhou RC, You H, Li LX, Feng J, Yang XY, Li YQ, Zuo XL. Real-time artificial intelligence for endoscopic diagnosis of early esophageal squamous cell cancer (with video). *Dig Endosc* 2020 [PMID: 33275789 DOI: 10.1111/den.13908]
 - 51 **Kumagai Y**, Takubo K, Kawada K, Aoyama K, Endo Y, Ozawa T, Hirasawa T, Yoshio T, Ishihara S, Fujishiro M, Tamaru JI, Mochiki E, Ishida H, Tada T. Diagnosis using deep-learning artificial intelligence based on the endocytoscopic observation of the esophagus. *Esophagus* 2019; **16**: 180-187

- [PMID: 30547352 DOI: 10.1007/s10388-018-0651-7]
- 52 **Mohan BP**, Khan SR, Kassab LL, Ponnada S, Mohy-Ud-Din N, Chandan S, Dulai PS, Kochhar GS. Convolutional neural networks in the computer-aided diagnosis of *Helicobacter pylori* infection and non-causal comparison to physician endoscopists: a systematic review with meta-analysis. *Ann Gastroenterol* 2021; **34**: 20-25 [PMID: 33414617 DOI: 10.20524/aog.2020.0542]
- 53 **Arribas Anta J**, Dinis-Ribeiro M. Early gastric cancer and Artificial Intelligence: Is it time for population screening? *Best Pract Res Clin Gastroenterol* 2021; **52-53**: 101710 [PMID: 34172244 DOI: 10.1016/j.bpg.2020.101710]
- 54 **Nagao S**, Tsuji Y, Sakaguchi Y, Takahashi Y, Minatsuki C, Niimi K, Yamashita H, Yamamichi N, Seto Y, Tada T, Koike K. Highly accurate artificial intelligence systems to predict the invasion depth of gastric cancer: efficacy of conventional white-light imaging, nonmagnifying narrow-band imaging, and indigo-carmin dye contrast imaging. *Gastrointest Endosc* 2020; **92**: 866-873.e1 [PMID: 32592776 DOI: 10.1016/j.gie.2020.06.047]
- 55 **Sana MK**, Hussain ZM, Shah PA, Maqsood MH. Artificial intelligence in celiac disease. *Comput Biol Med* 2020; **125**: 103996 [PMID: 32979542 DOI: 10.1016/j.combiomed.2020.103996]
- 56 **Aoki T**, Yamada A, Aoyama K, Saito H, Tsuboi A, Nakada A, Niikura R, Fujishiro M, Oka S, Ishihara S, Matsuda T, Tanaka S, Koike K, Tada T. Automatic detection of erosions and ulcerations in wireless capsule endoscopy images based on a deep convolutional neural network. *Gastrointest Endosc* 2019; **89**: 357-363.e2 [PMID: 30670179 DOI: 10.1016/j.gie.2018.10.027]
- 57 **Tsuboi A**, Oka S, Aoyama K, Saito H, Aoki T, Yamada A, Matsuda T, Fujishiro M, Ishihara S, Nakahori M, Koike K, Tanaka S, Tada T. Artificial intelligence using a convolutional neural network for automatic detection of small-bowel angiectasia in capsule endoscopy images. *Dig Endosc* 2020; **32**: 382-390 [PMID: 31392767 DOI: 10.1111/den.13507]
- 58 **Tonozuka R**, Itoi T, Nagata N, Kojima H, Sofuni A, Tsuchiya T, Ishii K, Tanaka R, Nagakawa Y, Mukai S. Deep learning analysis for the detection of pancreatic cancer on endosonographic images: a pilot study. *J Hepatobiliary Pancreat Sci* 2021; **28**: 95-104 [PMID: 32910528 DOI: 10.1002/jhbp.825]
- 59 **Chondros T**, Milidonis K, Vitzilaios G, Vaitis J. "Deus-Ex-Machina" reconstruction in the Athens theater of Dionysus. *Mech Mach Theory* 2013; **67**: 172-191 [DOI: 10.1016/j.mechmachtheory.2013.04.010]

Faecal microbiota transplantation enhances efficacy of immune checkpoint inhibitors therapy against cancer

Yong-Bo Kang, Yue Cai

ORCID number: Yong-Bo Kang 0000-0002-1584-5546; Yue Cai 0000-0001-6314-0463.

Author contributions: Kang YB collected the data and wrote most of the manuscript with help from Cai Y; Kang YB and Cai Y contributed equally to this study.

Supported by Science Research Start-up Fund for Doctor of Shanxi Medical University, No. XD1807; Science Research Start-up Fund for Doctor of Shanxi Province, No. SD1807; Scientific and Technological Innovation Programs of Higher Education Institutions in Shanxi, No. 2019L0425; and Shanxi Province Science Foundation for Youths, No. 201901D211314.

Conflict-of-interest statement: The authors report no conflicts of interest relevant to this manuscript.

Open-Access: This article is an open-access article that was selected by an in-house editor and fully peer-reviewed by external reviewers. It is distributed in accordance with the Creative Commons Attribution NonCommercial (CC BY-NC 4.0) license, which permits others to distribute, remix, adapt, build upon this work non-commercially, and license their derivative works

Yong-Bo Kang, Yue Cai, Department of Microbiology and Immunology, School of Basic Medical Sciences, Shanxi Medical University, Jinzhong 030600, Shanxi Province, China

Corresponding author: Yong-Bo Kang, PhD, Associate Professor, Department of Microbiology and Immunology, School of Basic Medical Sciences, Shanxi Medical University, Zhongdu Campus, Yuci District, Jinzhong 030600, Shanxi Province, China. 657151276@qq.com

Abstract

Even though immune checkpoint inhibitors (ICIs) are effective on multiple cancer types, there are still many non-responding patients. A possible factor put forward that may influence the efficacy of ICIs is the gut microbiota. Additionally, faecal microbiota transplantation may enhance efficacy of ICIs. Nevertheless, the data available in this field are insufficient, and relevant scientific work has just commenced. As a result, the current work reviewed the latest research on the association of gut microbiota with ICI treatments based on anti-programmed cell death protein 1 antibody and anti-cytotoxic T-lymphocyte-associated protein 4 antibody and explored the therapeutic potential of faecal microbiota transplantation in combination with ICI therapy in the future.

Key Words: Gut microbiome; Immunotherapy; Programmed cell death protein 1/programmed cell death protein ligand 1; Cytotoxic T-lymphocyte-associated protein 4; Immune checkpoint inhibitors resistance; Faecal microbiota transplantation

©The Author(s) 2021. Published by Baishideng Publishing Group Inc. All rights reserved.

Core Tip: Gut microbiota composition is closely associated with the efficacy of immune checkpoint inhibitors (ICIs). Specific species among the intestinal commensal bacteria may play a key role in the efficacy of ICIs against cancer. Faecal microbiota transplantation may enhance efficacy of ICIs.

Citation: Kang YB, Cai Y. Faecal microbiota transplantation enhances efficacy of immune checkpoint inhibitors therapy against cancer. *World J Gastroenterol* 2021; 27(32): 5362-5375

URL: <https://www.wjgnet.com/1007-9327/full/v27/i32/5362.htm>

DOI: <https://dx.doi.org/10.3748/wjg.v27.i32.5362>

on different terms, provided the original work is properly cited and the use is non-commercial. See: <http://creativecommons.org/licenses/by-nc/4.0/>

Manuscript source: Unsolicited manuscript

Specialty type: Gastroenterology and hepatology

Country/Territory of origin: China

Peer-review report's scientific quality classification

Grade A (Excellent): A

Grade B (Very good): 0

Grade C (Good): 0

Grade D (Fair): 0

Grade E (Poor): 0

Received: March 2, 2021

Peer-review started: March 2, 2021

First decision: June 3, 2021

Revised: July 3, 2021

Accepted: July 12, 2021

Article in press: July 12, 2021

Published online: August 28, 2021

P-Reviewer: Mazilu L

S-Editor: Fan JR

L-Editor: Filipodia

P-Editor: Liu JH



INTRODUCTION

Immune checkpoint molecules can modulate the immune system in the host *via* the transduction of immunosuppressive co-signals into the immunocompetent cells[1-5]. Typically, Programmed cell death protein 1 (PD-1)/programmed cell death protein ligand 1 (PD-L1) (CD274), PD-L2 (CD273), and cytotoxic T-lymphocyte-associated protein 4 (CTLA-4, CD152) are the most well-known examples[6-13]. These molecules are expressed in suitable cells at the suitable timing to exert their vital parts in the prevention of over-activated immune system in the host and the maintenance of immunological tolerance and homeostasis[1,2,5]. At the same time, immune checkpoint molecules show abnormal expression within tumour tissues[3,14-16]. Therefore, a strong immunosuppressive environment will be produced within tumour tissues, leading to resistance to treatment of numerous cancers. Immune checkpoint inhibitors (ICIs) mainly function to alleviate or destroy the immunosuppression mechanisms involved in tumour microenvironment (TME) by the use of inhibitory agents targeting the immune checkpoint molecules[2,5,17]. At present, anti-CTLA-4 (like ipilimumab), anti-PD-1 (such as pembrolizumab, nivolumab, and anti-PD-L1 (such as atezolizumab, durvalumab, avelumab) antibodies have been applied in treating several cancers in the world[18-23].

At present, checkpoint blockade still shows high effectiveness on certain cases, but just about 10%-30% cancers can achieve treatment responses. The combined used of ICIs is associated with a higher response rate and greater toxicity[24], regardless of the limited research on the ICI treatment. There are several ICI resistance mechanisms related to the low response rate, which are low PD-L1 expression, low tumour mutational burden, local immunosuppression, weak tumour cell antigenicity, tumour-infiltrating lymphocytes (TILs) functional exhaustion, no priming, and defected antigen presentation in the process of priming[25].

In addition, gut microbiome is suggested to be the potential factor that determines ICI efficacy. There are more than 100 trillion bacteria in the human gut, among which 500-1000 bacterial species have been identified to affect the mucosal immune system and exert vital parts in immune system operation under the normal or disease state [26]. Intestinal symbiotic bacteria may exert inflammatory or beneficial function while interacting with host immune system in intestinal lymphoid tissues. Therefore, faecal microbiota transplantation (FMT) can potentially improve the ICI efficacy. Nonetheless, there is only limited information on this topic, and related scientific work is merely at the beginning stage. The emergence of novel techniques has made it possible to investigate systemically the gut microbiota, which also sheds more light on the gut microbial compositions and their pathological variance. The present work aimed to review the latest research on the associations of gut microbiota with immune systems and ICI treatments based on anti-PD-1 antibody (Ab) and anti-CTLA-4 Ab and to explore the therapeutic potential of FMT combined with ICI therapy in the future.

ICIS

Two steps are necessary to activate tumour-specific T cells. Firstly, the selective binding of T cell receptor (TCR) to major histocompatibility complex I that has antigen-anchoring peptides[27]. Secondly, further amplification of the activation signal of TCR/CD3 complex is performed after the synergistic effect with co-stimulatory signals like OX40, CD28, and inducible T cell co-stimulator, which finally results in T cell priming and activation[27]. By contrast, co-inhibitory signals (also known as the immune checkpoints), including PD-1, CTLA-4, T cell immunoglobulin domain, mucin domain-3, and lymphocyte activation gene-3, inhibit T cell activation *via* offsetting CD28- or TCR/CD3-mediated tyrosine phosphorylation through the intracellular immunoreceptor tyrosine-based inhibition motif[28-30]. Tumour cells are likely to enhance the co-inhibitory signalling pathway activity for the sake of immune escape [31,32]. ICIs can decrease the tumour antigen immune tolerance and restore the anticancer response. Anti-CTLA-4 and anti-PD-1/PD-L1 are used to treat several cancers[33-38]. Nevertheless, there is a great potential to enhance the anticancer effect of ICI.

EFFECT OF GUT MICROBIOME ON THE EFFICACY OF ICIS

It has been recognized that gut microbiome is involved in cancer genesis and the immune surveillance that suppresses tumour progression[39-42]. Certain commensals may display the synergetic effects with treatments such as surgery, chemotherapy, radiotherapy, and immunotherapy after affecting the immune homeostasis in the intestine and immune adjustment of secondary immune organs[43-52]. ICIs can regulate tumour regression through enhancing the immune activation in the host. A series of studies suggested that gut microbiota composition shows close association with the efficacy of ICIs (Tables 1 and 2). At the same time, we revealed the potential mechanisms by which gut microbiome may be involved in the ICI efficacy (Figures 1 and 2).

Effect of gut microbiota on anti-PD-1/PD-L1 therapy

The PD-1/PD-L1 blockage treatment blocks the negative signals transduced by the PD-1 intracellular domains (like immunoreceptor tyrosine-based inhibition motif, immunoreceptor tyrosine-based switch motif)[53]. Typically, PD-1/PD-L1 blockage has been identified to promote T cell activation resulting from CD28 and TCR/CD3 while promoting T cell growth and survival by the activation of Ras-Raf-mitogen activated protein kinase and phosphatidylinositol 3 kinase-AKT signalling[54,55]. The PD-1/PD-L1 blockage treatment has been approved to treat certain malignant tumours, including non-small cell lung cancer (NSCLC), colorectal cancer (CRC), kidney cell cancer, and melanoma[56,57]. Biomarkers that contain the TIL status, PD-L1 expression, or deficiency of the mismatch repair system are tightly associated with the efficacy of PD-1/PD-L1 blockage treatment[58]. Besides those above-mentioned factors, gut microbiota contributes to difference in treatment responses as well[59].

In 2015, some investigators discover the relationship of gut microbiota with the efficacy of anti-PD-1 therapy using a mouse model[60]. Sivan *et al*[60] explored the therapeutic effect of anti-PD-1 therapy on C57BL/6 mice with genetic similarity, mice bearing the subcutaneous B16. SIY melanoma were obtained from two distinct mouse facilities [namely, Taconic Farms (TAC) and Jackson Laboratory (JAX)], which had markedly heterogeneous gut microbial compositions[60]. As a result, among the JAX populations, tumour growth was slower with higher sensitivity to the PD-1 blockage treatment. Such difference might be associated with the immune response. To be specific, JAX mice showed markedly enhanced CD8⁺ T cell aggregation within the tumour and tumour-specific T cell responses compared with the TAC counterparts. Further study suggested that the difference was abrogated by cohousing. In addition, when faecal microbiome was transferred from JAX to TAC, specific TILs increased and tumour development was suppressed. It was interesting that, in TAC, just the faecal microbiome transferred from JAX was able to suppress tumour development in the same degree with PD-1 blockage therapy, and it had synergistically regressed tumour development with PD-1 blockade therapy[60]. Gut microbiome analysis demonstrated that the abundance of *Bifidobacterium* was markedly increased in JAX. Meanwhile, the abundance of *Bifidobacterium* was significantly related to tumour specific immune cytotoxicity[60]. Administrating the commercial *Bifidobacterium* cocktail (namely, *Bifidobacterium longum* and *Bifidobacterium breve*) significantly suppressed tumour growth, particularly when it was used in combination with the PD-1 blockage treatment[60]. It was suggested that such increased anticancer activity was associated with the higher interferon (IFN)- γ production, greater tumour-specific CD8⁺ T cell proportion, and alterations of dendritic cell (DC) functions[60].

Xu *et al*[61] investigated the roles of gut microbiome within the MSS-type mice bearing CRC that received diverse antibiotic treatments in the response to PD-1 Ab therapy. Following PD-1 Ab therapy, injecting antibiotics offset the therapeutic effect of PD-1 Ab on suppressing tumour development relative to control group[61]. Besides, control group showed enrichment of *Bacteroidales_S24-7* and *Bacteroides_sp._CAG:927*. At the same time, mice receiving colistin treatment showed enrichment of *Bacteroides_sp._CAG:927*, *Bacteroides* and *Prevotella_sp._CAG: 1031*, whereas mice receiving vancomycin treatment showed enrichment of *Akkermansia_muciniphila* and *Prevotella_sp._CAG:485*. For mice receiving vancomycin treatment, most metabolites were associated with the glycerophospholipid metabolic pathway, confirming to the metagenomic prediction pathway. Additionally, *Akkermansia* and *Prevotella_sp._CAG:485* contributed to maintaining the therapeutic effect of PD-1 Ab through impacting glycerophospholipid metabolism[61]. Gut microbial alteration resulted in alterations of the glycerophospholipid metabolism degree, thereby affecting immune cytokine expression [such as interleukin (IL)-2 and IFN- γ] within TME, giving rise to the diverse PD-1 Ab efficacy[61]. The above results reveal that gut microbial alter-

Table 1 Changes in microbiota composition associated with anti-programmed cell death protein 1/programmed cell death protein ligand 1 treatment efficacy against cancer and potential strategies for improving efficacy

| Models | Disease | Implicated microbiota | New strategies | Implicated microbiota | Ref. |
|--------|---------------------------|---|---|--|--|
| Mice | Melanoma | <i>Bifidobacterium</i> ↑ | (1) FMT; and (2) Commercial cocktail of <i>Bifidobacterium</i> including <i>Bifidobacterium breve</i> and <i>B. longum</i> | NO | Sivan <i>et al</i> [60], 2015 |
| Mice | CRC | <i>Bacteroides</i> _sp._CAG:927↑, <i>Bacteroidales</i> _S24-7↑, <i>Akkermansia muciniphila</i> ↑ | NO | NO | Xu <i>et al</i> [61], 2020 |
| Mice | CT26 tumours | NO | GQD | <i>s__Bacteroides acidifaciens</i> ↑, <i>s__uncultured_organism_g__norank_f__Bacteroidales_S24-7</i> ↑ | Lv <i>et al</i> [62], 2019 |
| Mice | RCC | NO | (1) FMT; (2) <i>A. muciniphila</i> ; and (3) <i>Bacteroides salyersiae</i> | NO | Derosa <i>et al</i> [66], 2020 |
| Mice | Melanoma | NO | FMT | NO | Matson <i>et al</i> [68], 2018 |
| Mice | MCA-205 sarcoma | NO | (1) FMT; (2) <i>A. muciniphila</i> ; and (3) <i>A. muciniphila</i> with <i>Enterococcus hirae</i> ; <i>Alistipes indistinctus</i> | NO | Routy <i>et al</i> [69], 2018 |
| Mice | (1) RET; and (2) Melanoma | NO | (1) <i>A. muciniphila</i> ; and (2) <i>A. muciniphila</i> with <i>Enterococcus hirae</i> ; | NO | Routy <i>et al</i> [69], 2018 |
| Human | NSCLC | <i>Parabacteroides</i> ↑, <i>Methanobrevibacter</i> ↑, <i>Veillonella</i> ↓, <i>Selenomonadales</i> ↓, <i>Negativicutes</i> ↓ | NO | NO | Song <i>et al</i> [63], 2020 |
| Human | NSCLC | Gut microbial diversity↑, <i>Alistipes putredinis</i> ↑, <i>B. longum</i> ↑, <i>Prevotella copri</i> ↑, <i>Ruminococcus unclassified</i> ↓ | NO | NO | Jin <i>et al</i> [64], 2019 |
| Human | NSCLC | Altered gut microbiota metabolome | NO | NO | Botticelli <i>et al</i> [65], 2020 |
| Human | RCC | <i>A. muciniphila</i> ↑, <i>Bacteroides salyersiae</i> ↑, <i>Clostridium hathewayi</i> ↓ | NO | NO | Derosa <i>et al</i> [66], 2020 |
| Human | Melanoma | Gut microbial diversity↑, <i>Clostridiales/Ruminococcaceae</i> ↑, <i>Faecalibacterium</i> ↑, <i>Anaerotruncus colihominis</i> ↓, <i>Bacteroides thetaiotaomicron</i> ↓, <i>Escherichia coli</i> ↓ | NO | NO | Gopalakrishnan <i>et al</i> [67], 2018 |
| Human | Melanoma | <i>Bifidobacterium adolescentis</i> ↑, <i>B. longum</i> ↑, <i>Collinsella aerofaciens</i> ↑, <i>Enterococcus faecium</i> ↑, <i>Klebsiella pneumoniae</i> ↑, <i>Lactobacillus species</i> ↑, <i>Parabacteroides merdae</i> ↑, <i>Veillonella parvula</i> ↑, <i>Ruminococcus obeum</i> ↓, <i>Roseburia intestinalis</i> ↓ | NO | NO | Matson <i>et al</i> [68], 2018 |
| Human | NSCLC and RCC | <i>A. muciniphila</i> ↑ | NO | NO | Routy <i>et al</i> [69], 2018 |
| Human | Melanoma | NO | FMT | NO | Baruch <i>et al</i> [83], 2021 |

NO: No test or no research; FMT: Faecal microbiota transplantation; CRC: Colorectal cancer; RCC: Renal cell carcinoma; NSCLC: Non-small cell lung cancer; GQD: Gegen Qinlian decoction.

ations have certain impacts on the glycerophospholipid metabolic pathway, thus modulating the efficacy of PD-1 Ab immunotherapy in treating MSS-type mice bearing CRC.

Table 2 Changes in microbiota composition associated with anti-cytotoxic T-lymphocyte-associated protein 4 efficacy treatment against cancer and potential strategies for improving efficacy

| Models | Disease | Implicated microbiota | New strategies | Implicated microbiota | Ref. |
|--------|-----------------|---|--|-----------------------|---------------------------------|
| Mice | MCA205 sarcomas | <i>Clostridiales</i> ↑, <i>Bacteroides thetaiotaomicron</i> ↑, <i>B. uniformis</i> ↑, <i>Bacteroidales</i> ↓, <i>Burkholderiales</i> ↓, | (1) <i>B. thetaiotaomicron</i> ; (2) <i>B. fragilis</i> ; and (3) <i>Burkholderia cepacia</i> | NO | Vétizou <i>et al</i> [70], 2015 |
| Mice | CRC | NO | <i>Lactobacillus acidophilus</i> cell lysates | NO | Zhuo <i>et al</i> [73], 2019 |
| Mice | CRC | NO | (1) <i>Bifidobacterium pseudolongum</i> ; (2) <i>Lactobacillus johnsonii</i> ; (3) <i>Olsenella spp</i> ; and (4) Metabolite inosine | NO | Mager <i>et al</i> [74], 2020 |
| Huamn | Melanoma | <i>Faecalibacterium genus</i> ↑, unclassified <i>Ruminococcus</i> ↑, <i>Lachnospiraceae genus</i> ↑, <i>Clostridium XIVa</i> ↑, <i>Blautia</i> ↑, Butyrate producing bacterium↑, <i>Gemmiger formicilis</i> ↑, <i>Bacteroides</i> ↓, <i>B. fragilis</i> ↓, <i>B. thetaiotaomicron</i> ↓ | NO | NO | Chaput <i>et al</i> [72], 2017 |

NO: No test or no research; CRC: Colorectal cancer.

Recently, Lv *et al*[62] discovered that when Gegen Qinlian decoction (GQD) (one of the representative traditional Chinese medicine prescriptions) was used in conjunction with the anti-mouse PD-1 therapy in the xenograft model, it had potent effect on suppressing CT26 tumour growth. Besides, analysis on the gut microbiota also suggested that GQD used in combination with anti-mouse PD-1 therapy markedly enriched *s__uncultured_organism_g__norank_f__Bacteroidales_S24-7_and_s__Bacteroides_acidifaciens* group[62]. As indicated by metabolomic analysis results, metabolites with profound changes were detected in the combined treatment group [62]. Furthermore, the sphingolipid metabolism and glycerophospholipid metabolism metabolic pathways were examined[62]. Particularly, GQD combined with anti-mouse PD-1 treatment markedly promoted the fraction of CD8⁺ T cell subset within tumour tissue and peripheral blood samples and up-regulated IFN- γ level (an important factor of the anticancer immunotherapy)[62]. Moreover, GQD combined with anti-mouse PD-1 treatment decreased PD-1 expression while increasing IL-2 expression, revealing that such combined treatment suppressed the inhibitory checkpoints to restore efficiently T-cell functions[62]. Taken together, such findings revealed that GQD remodels gut microbiota to promote the anti-CRC efficacy of PD-1 blockade, and microsatellite stability was achieved.

Inspired by these results obtained from mouse models, many articles have been conducted to examine the association of gut microbiota with anti-PD-1 therapy among cancer cases. Song *et al*[63] explored the association of gut microbial structure and metabolomic features in the context of NSCLC with the anti-PD-1 therapy efficacy. According to analysis results of gut microbiome, cases from progression-free survival (PFS) \geq 6-mo group showed markedly increased β -diversity within gut microbiota relative to that of PFS < 6-mo group[63]. Besides, those from PFS \geq 6-mo group showed enrichment of *Methanobrevibacter* and *Parabacteroides*, whereas those from PFS < 6-mo group showed enrichment of *Selenomonadales*, *Negativicutes*, and *Veillonella*[63]. Furthermore, the protein families of function groups were studied using the COG, CAZy, and KO databases. As a result, 264, 859, and 390 functional groups were enriched in the above three databases, respectively, and significant differences were detected between the two groups. As revealed by analysis on bacterial metabolites, differences in the metabolic potentials of methane and methanol were significant between the two groups[63].

Jin *et al*[64] examined the association of gut microbiome with the clinical outcomes among the Chinese NSCLC cases receiving the anti-PD-1 therapy. Thereafter, patients were grouped as non-responder and responder groups based on the clinical response evaluated by the Response Evaluation Criteria in Solid Tumor version 1.1[64]. As a result, responders showed a greater gut microbial diversity at the beginning and stable composition in the process of treatment[64]. Besides, those showing higher microbial diversity were associated with the remarkably longer PFS in comparison with patients showing a lower diversity[64]. Differences in composition were detected between both groups, among which, *Alistipes putredinis*, *Prevotella copri*, and *Bifidobacterium longum* were enriched in responder group, while *Ruminococcus unclassified* was enriched in non-responder group[64]. In addition, the author applied multicolor flow cytometry to

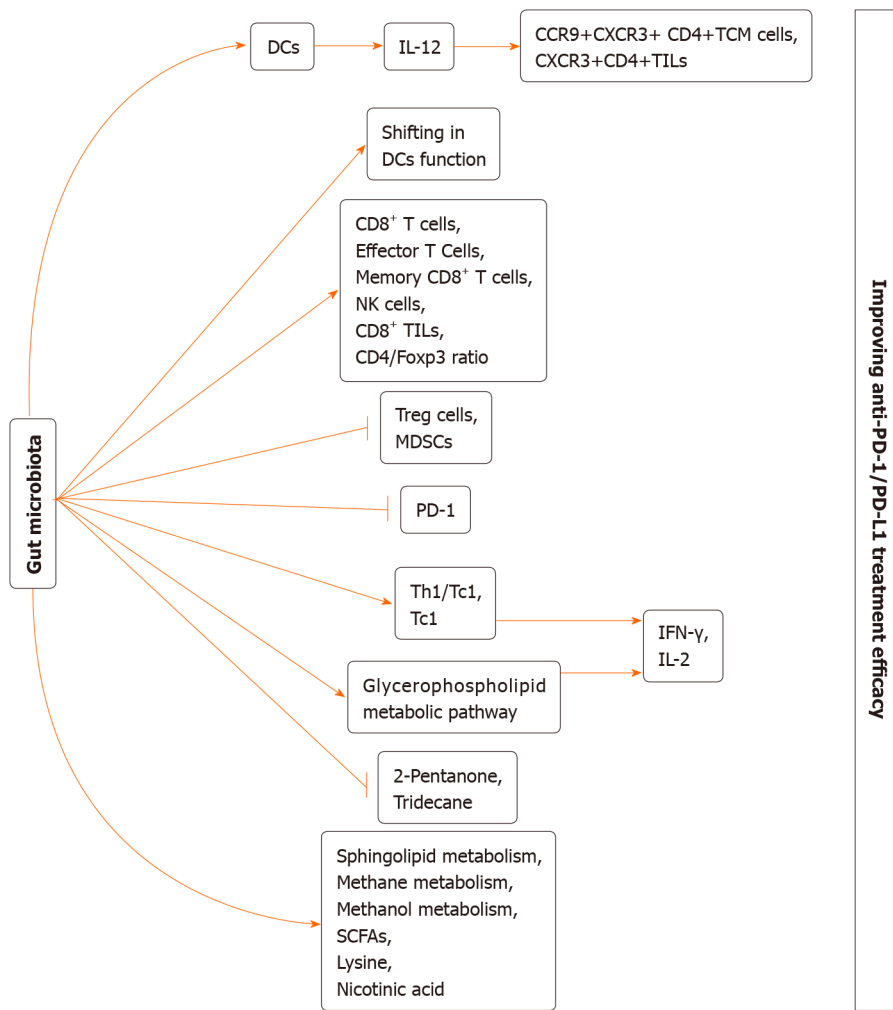


Figure 1 The potential mechanism of gut microbiome regulating anti-programmed cell death protein 1/programmed cell death protein ligand 1 treatment efficacy. (1) Gut microbiota may increase interleukin (IL)-12 production by dendritic cells (DCs), thereby increasing the CCR9⁺CXCR3⁺CD4⁺ central memory T cells and CXCR3⁺CD4⁺ tumour-infiltrating lymphocytes (TILs); (2) Gut microbiota may shift in the function of DCs; (3) Gut microbiota may increase CD8⁺ T cells, effector T Cells, memory CD8⁺ T cells, natural killer cells, CD8⁺ TILs, and CD4/Foxp3 ratio; (4) Gut microbiota may decrease numbers of regulatory T cells and myeloid-derived suppressor cells; gut microbiota may downregulate programmed cell death protein 1 expression; (5) Gut microbiota may induce Th1/Tc1 and Tc1 immune response, thereby increasing the interferon- γ and IL-2 secretion; (6) Gut microbiota may enhance glycerophospholipid metabolic pathway, thereby increasing the interferon- γ and IL-2 secretion; (7) Gut microbiota may decrease 2-pentanone and tridecane production; and (8) Gut microbiota may increase sphingolipid metabolism, methane metabolism, methanol metabolism, short chain fatty acids production, lysine production and nicotinic acid production. Altogether, all of these approaches may eventually improve anti-programmed cell death protein 1-1/programmed cell death protein ligand 1 treatment efficacy. DCs: Dendritic cells; T_{CM}: Central memory T; Treg: Regulatory T; MDSCs: Myeloid-derived suppressor cells; SCFAs: Short chain fatty acids; PD-1: Programmed cell death protein 1; IFN- γ : Interferon.

analyzed the systemic immune responses, which suggested that patients showing a greater gut microbial diversity were associated with higher proportions of peripheral blood natural killer cell and unique memory CD8⁺ T cell subsets upon anti-PD-1 treatment[64]. Botticelli and coworkers[65] also investigated the impact of gut microbial metabolome on anti-PD-1 therapy efficacy among NSCLC cases. As a result, 36% cases presented early progression, whereas the rest 64% showed progression at 12 mo later[65]. Besides, as revealed by gut microbiota metabolomic profiling, tridecane (alkane) and 2-Pentanone (ketone) were tightly related to early progression; by contrast, nicotinic acid, lysine and short chain fatty acids (namely, butyrate, propionate) were closely related to long-term benefits[65].

Recently, Derosa *et al*[66] assessed the significance of faecal bacterial composition in the anti-PD-1 treatment effect among patients with advanced renal cell carcinoma (RCC). Relative to RCC cases who received PD-1 blockage treatment with no use of antibiotics, RCC cases who received anti-PD-1 treatment in the presence of antibiotic treatment had evidently decreased objective response rates, which remarkably impacted the microbial composition. As a result, certain species like *Clostridium hathewayi* were dominant, and their abundances were higher in faecal samples of RCC cases relative to normal subjects. Tyrosine kinase inhibitors administered before

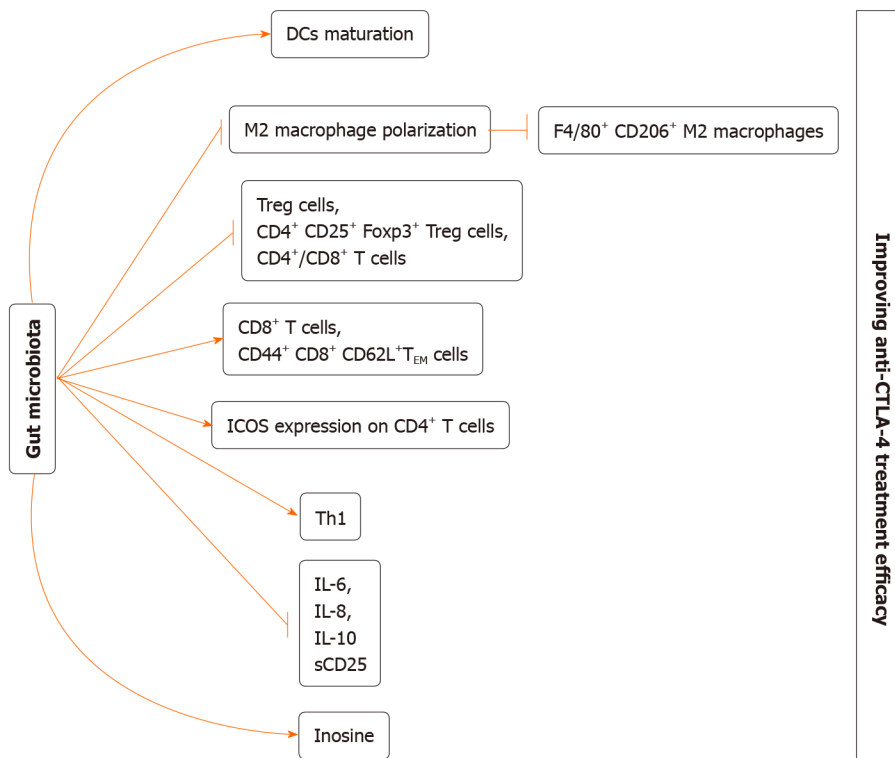


Figure 2 The potential mechanism of gut microbiome regulating anti-cytotoxic T-lymphocyte-associated protein 4 treatment efficacy. (1) Gut microbiota may induce dendritic cells maturation; (2) Gut microbiota may inhibit the M2 polarization, thereby decreasing M2 macrophages (F4/80⁺CD206⁺); (3) Gut microbiota may decrease regulatory T cells, CD4⁺CD25⁺Foxp3⁺ regulatory T cells, and CD4⁺/CD8⁺ T cells; (4) Gut microbiota increase CD8⁺ T cells and CD44⁺CD8⁺CD62L⁺ effector memory T cells; (5) Gut microbiota may increase inducible T cell co-stimulator expression on CD4⁺ T cells; (6) Gut microbiota may induce T helper 1 immune response; (7) Gut microbiota may reduce interleukin (IL)-6; IL-8; IL-10, and sCD25 level; and (8) Gut microbiota may increase inosine production. Altogether, all of these approaches may eventually improve anti-cytotoxic T-lymphocyte-associated protein 4 treatment efficacy. DCs: Dendritic cells; Treg: Regulatory T; T_{EM}: Effector memory T cells; ICOS: Inducible T cell co-stimulator; sCD25: Soluble CD25; IL: Interleukin.

nivolumab were related to the shift of microbial composition. For establishing the cause-effect relation of gut microbial composition with the anti-PD-1 therapy efficacy, some preclinical studies discovered that RCC-bearing mice receiving FMT from RCC cases developed resistance to anti-PD-1 therapy (NR-FMT). At the same time, both beneficial commensals (*Bacteroides salyersiae* and *A. muciniphila*) verified through whole genome sequencing and FMT successfully compensated the NR-FMT mice.

Conforming to the above results, Gopalakrishnan *et al*[67] evaluated the gut microbiota in melanoma cases who received the PD-1 blockage treatment (faecal samples from 43 cases, including 13 non-responders and 30 responders). As a result, responders exhibited a greater gut microbial diversity. Besides, in faecal samples, α -diversity showed positive correlation with PFS[67]. Further analysis indicated that the level of Clostridiales/Ruminococcaceae, *Faecalibacterium* (belonging to the Ruminococcaceae family, Clostridiales order) was higher in responders, while *Anaerotruncus colihominis*, *Bacteroides thetaiotaomicron* (belonging to Bacteroidales order), and *Escherichia coli* were significantly enriched in non-responders[67]. Additionally, the abundance of *Faecalibacterium* and Bacteroidales showed positive and negative relationships with tumour infiltrating CD8⁺ T cell level, respectively. The high abundances of *Faecalibacterium*, Ruminococcaceae, and Clostridiales in peripheral blood were accompanied with the increased effector T cell proportion, whereas Bacteroidales abundance showed positive relationship with regulatory T cells (Tregs) and myeloid-derived suppressor cell proportions. As revealed by multiple immunohistochemistry analyses, there were greater abundances of immune markers enriched in *Faecalibacterium* of the melanoma cases[67]. Such conclusions were verified by FMT experiments carried out in mouse models[67]. Matson *et al*[68] also found that gut microbiota affected anti-PD-1 therapy efficacy among the melanoma cases who developed metastasis. Meanwhile, as suggested by gut microbial analysis, the abundances of *B. longum*, *Bifidobacterium adolescentis*, *Enterococcus faecium*, *Collinsella aerofaciens*, *Lactobacillus* species, *Klebsiella pneumoniae*, *Veillonella parvula*, and *Parabacteroides merdae* were higher among responders, whereas those of *Roseburia intestinalis* and *Ruminococcus obeum* were significantly higher among the non-responders[68]. In addition, germ-free (GF) mice

subjected to gavage with responders-derived faecal materials showed significantly elevated IFN- γ and CD8⁺TIL levels and suppressed tumour growth, which facilitated to form the immunosupportive microenvironment[68]. Meanwhile, Routy *et al*[69] suggested that gut microbiota played a certain role in the resistance to anti-PD-1 therapy. Investigators discovered that, cancer cases who received anti-PD-1 therapy with antibiotics treatment had markedly reduced overall survival and PFS relative to those with no antibiotic treatment.

For investigating the association of antibiotic-induced dysbiosis with the reduced efficacy, investigators compared the compositions of gut microbiota in responders with those in non-responders[69]. Across the enriched bacterial species in the responders, *A. muciniphila* showed the highest correlation with the response rate of patients[69]. In addition, the IFN- γ production-induced immune reactions between Tc1 and *Enterococcus hirae* as well as between Th1/Tc1 and *Akkermansia muciniphila* predicted better patient survival[69]. In addition, clinical trial conducted using the mouse model suggested that mice that received FMT from responders showed superior response to the anti-PD-1 therapy and had higher proportion of CXCR3⁺CD4⁺TILs, whereas those that received FMT from non-responders, underwent antibiotic treatments and those in the GF status developed resistance to anti-PD-1 therapy[69]. Interestingly, antibiotic treatment reversed the efficacy of PD-1 blockade treatment through *A. muciniphila* recolonization in the presence or absence of *Enterococcus hirae*. Administration of *E. hirae* and *A. muciniphila* through oral gavage can increase CCR9⁺CXCR3⁺CD4⁺central memory T cells, promote IL-12 and IFN- γ secretion, and increase the CD4/Foxp3 ratio within tumour bed[69].

Role of gut commensals in the anti-CTLA-4 therapy

CTLA-4 is also a research hotspot apart from PD-1/PD-L1. The anti-CTLA-4 therapy can reverse the CTLA-4-hijacked activity of the co-stimulatory signal transduction pathway (CD28-CD80/86). Therefore, it is important to identify factors that modulate the anti-CTLA-4 therapy efficacy, so as to mitigate drug resistance and promote the treatment response.

Vétizou *et al*[70] carried out a trial for investigating the gut microbial impact on the efficacy of anti-CTLA-4 therapy[70]. In the mouse model of MCA205 sarcomas, compared with GF mice and those receiving broad-spectrum antibiotic treatment, specific pathogen-free mice showed higher efficacy in anti-CTLA-4 therapy[70], and commensal flora perturbation was observed after anti-CTLA-4 therapy. For certain species (*B. uniformis* and *Bacteroides thetaiotaomicron*), their abundances increased, while those of *Burkholderiales* and *Bacteroidales* declined[70]. Notably, *Bacteroides fragilis*, which was verified to be the immune-modulating bacteria, remained almost unchanged in the process of treatment[70,71]. Additionally, *B. thetaiotaomicron*, *Burkholderia cepacian*, and *B. fragilis* recolonization in GF mice or those receiving antibiotic treatment reversed the resistance to anti-CTLA-4 therapy[70]. Moreover, it was further detected that *B. fragilis* administered by oral gavage promoted DC maturation and elicited Th1 immune response within the tumour-draining lymph nodes[70]. Furthermore, adoptive Th1 cell transfer of cells specific to *B. fragilis* reversed the anti-CTLA-4 sensitivity in GF mice or those receiving antibiotic treatment to some extent[70]. In addition to the promoted anti-CTLA-4 effect, the treatment-related colitis was also alleviated by recolonizing *Burkholderia cepacia* and *B. fragilis* [70]. By FMT from melanoma cases, investigators discovered that the high abundance of *B. fragilis* was associated with tumour regression[70]. In addition, it was interesting to find that vancomycin treatment enhanced the ipilimumab efficacy, while alleviating side reactions that were not parallel to the promoted efficacy. To explore the reason, vancomycin might show indirect effect on promoting the abundance of *Bacteroidales* through suppressing *Clostridiales* proliferation[70].

Nonetheless, another trial examining the association of baseline gut microbiome with the clinical outcomes among the melanoma cases who developed metastasis came to different results from those obtained by Marie Vétizou[72]. Different from the results obtained from the clinical trial on mouse models, the low baseline abundances of *B. thetaiotaomicron* and *B. fragilis* but high abundance of *Bacteroides* were detected among the enrolled cases, which restricted the anticancer activity of CTLA-4. In addition, certain Firmicutes species, such as unclassified *Ruminococcus*, *Faecalibacterium* genus, *Clostridium XIVa*, *Lachnospiraceae* genus, *Gemmiger formicilis*, butyrate producing bacterium, and *Blautia* were associated with the increased response rates and superior clinical outcomes (prolonged overall survival and PFS). For exploring the underlying mechanisms, parameters associated with the immune status were analyzed, which suggested that cases exhibiting increased response to treatment had reduced baseline proportions of systemic proinflammatory cytokines (sCD25, IL-6, IL-8), CD4⁺/CD8⁺ T

cells, and Tregs while increased inducible T cell co-stimulator level in CD4⁺ T cells. Different from the above-mentioned clinical trials, antibiotic treatment made no difference to the composition of predominant microbiota or bacteria that potentially affected the efficacy[72]. It was previously suggested that antibiotic treatment reduced the efficacy of ICI treatment, and such findings should be further investigated. Such different results among different trials might be associated with certain factors such as the heterogeneities between human and mouse models and the bias in FMT.

Recently, Zhuo *et al*[73] assessed the protection of anti-CTLA-4 blocking Ab (CTLA-4 mAb) in combination with *Lactobacillus acidophilus* cell lysates in the syngeneic BALB/c mouse model with CRC. Compared with CTLA-4 mAb monotherapy, the body weight loss was mitigated by *L. acidophilus* lysates. Meanwhile, CRC growth was suppressed in mice receiving combined administration, suggesting the effect of lysates on enhancing the anticancer effect of CTLA-4 mAb detected using the mouse model [73]. Such improved therapeutic effect was related to the higher proportions of effector memory T cells (CD44⁺CD8⁺CD62L⁺) and CD8⁺ T cells, but the lower proportions of M2 macrophages (F4/80⁺CD206⁺) and Treg (CD4⁺CD25⁺Foxp3⁺) cells within TME[73]. Additionally, *L. acidophilus* lysates showed a certain immunomodulatory activity by inhibiting IL-10 expression in lipopolysaccharide-activated Raw264.7 macrophages and M2 polarization[73]. Finally, faecal microbiota was subjected to 16S ribosomal RNA gene sequencing, demonstrating that combined administration markedly suppressed the abnormally increased proteobacteria abundance and partially offset the CRC-caused dysbiosis among the model mice[73]. Consistently, Mager *et al*[74] isolated three bacterial species—*Bifidobacterium pseudolongum*, *Lactobacillus johnsonii*, and *Olsenella* species—that significantly enhanced the efficacy of anti-CTLA-4 treatment in CRC mouse models. Based on further research, intestinal *B. pseudolongum* improved immunotherapy response by producing the metabolite inosine. Decreased gut barrier function induced by immunotherapy enlarged systemic translocation of inosine and activated antitumour T cells. The effect of inosine relied on T cell expression of the adenosine A2A receptor as well as the required co-stimulation.

In general, alterations of intestinal bacteria exert a significant influence in ensuring the efficacy of cancer with ICIs treatments, with specific changes of the commensal microbes standing for a potential way that can be used to improve or to weaken ICIs efficacy. As a result, manipulating gut microbiota composition may provide a direct and effective method to strengthen the therapeutic effect of cancer ICIs.

FUTURE PROSPECTS OF FMT COMBINED WITH ICIS THERAPY IN CANCER TREATMENT

FMT refers to the process where the faecal suspension obtained from a normal subject is injected to the gastrointestinal tract of another subject for the sake of curing a certain disease. FMT is a direct and superior approach to enhance the efficacy of ICIs through modulating the gut microbiota in human beings. FMT has been adopted for more than 50 years. Faeces was initially adopted by Ge Hong in China in the 14th century to treat various conditions, such as diarrhea[75]. Eiseman *et al*[76] adopted faecal enemas to treat pseudomembranous colitis in 1958 [probably because of *Clostridium difficile* infection (CDI)], and this was also the first time to introduce FMT to the mainstream medicine. Thereafter, FMT has become more and more popular because of its simple use and effects on treating CDI. In recent years, FMT has been investigated in numerous other fields[77]. FMT has been found to be effective on certain disorders, like irritable bowel syndrome, inflammatory bowel disease, anorexia nervosa, metabolic disorders, multiple sclerosis, autoimmune disorders cancer, cardiovascular diseases, and neuropsychiatric disorders[78-82]. Similarly, FMT may represent an efficient approach to increase response rate in ICIs therapy. Currently, only a few clinical trials have studied the effects of FMT on PD-1 Ab immunotherapy response in cancer patients. Recently, Baruch *et al*[83] carried out one phase I trial for evaluating whether it was safe and feasible to perform FMT and re-induction of PD-1 blockage treatment among 10 melanoma cases who developed PD-1-refractory metastases (Table 2). Clinical responses were detected among 3 cases, including 2 with partial responses and 1 with complete response[83]. Obviously, treatment with FMT showed association with favorable changes in immune cell infiltrates and gene expression profiles in both the gut lamina propria and the TME[83]. Additionally, an ongoing single-center phase 2 clinical trial (NCT03341143) investigates the therapeutic effect of FMT combined with pembrolizumab on melanoma patients who develop resistance to the anti-PD-1 treatment[84]. However, results are not reported at present. In

conclusion, such preliminary results shed more lights on the effect of FMT on anticancer treatment. As a result, FMT combined with ICIs has been regarded as the potential anticancer treatment.

CONCLUSION

Accumulating evidence has demonstrated the shift in gut microbiome composition influencing ICIs efficacy. Nevertheless, it obviously shows that in-depth studies on the mechanism(s) of interaction between gut microbiota and ICI efficacy need to be performed in different cancer populations. Additionally, FMT combined with ICIs may serve as a new anticancer treatment that requires more investigation. Scientific research in this field is just at the beginning stage, and more relevant information is needed. To this end, first of all, it is of great importance to determine the mechanism by which FMT re-establishes the balanced gut microbiota, finally achieving the remarkable cure rate among cancer cases who receive ICI therapy. Secondly, well-designed randomized controlled trials are required to ensure the safety and efficacy of FMT for cancer patients with ICIs treatment. Besides, additional high-quality data (e.g., longitudinal study) are also necessary to explore potential adverse effects. Moreover, it is of importance to study the composition of the small intestinal and faecal microbiota before and after FMT. These studies can contribute to better understanding the mechanisms of this therapy as well as identify microbes and their products involved in the pathogenesis of cancer. Thirdly, the best gut microbiota composition to enhance ICIs efficiency need to be recognized. On this basis, it is important to choose the right donors. Finally, FMT represents a relatively simple procedure during short duration. Compared with the repeated hospitalization and conventional therapy, FMT has low costs. Thus, the most appropriate method and duration for FMT needs to be determined. For this reason, besides conventional approaches, FMT is promising as an alternative therapy for cancer in the future.

ACKNOWLEDGEMENTS

I owe my parents (Kang WL and Feng QH) a great deal because they have devoted most of their time and energy to cultivating me. I am very grateful to my wife and mother-in-law (Zheng LB) for taking good care of our family.

REFERENCES

- 1 **Chen L**, Flies DB. Molecular mechanisms of T cell co-stimulation and co-inhibition. *Nat Rev Immunol* 2013; **13**: 227-242 [PMID: [23470321](#) DOI: [10.1038/nri3405](#)]
- 2 **Adachi K**, Tamada K. Immune checkpoint blockade opens an avenue of cancer immunotherapy with a potent clinical efficacy. *Cancer Sci* 2015; **106**: 945-950 [PMID: [25981182](#) DOI: [10.1111/cas.12695](#)]
- 3 **Postow MA**, Callahan MK, Wolchok JD. Immune Checkpoint Blockade in Cancer Therapy. *J Clin Oncol* 2015; **33**: 1974-1982 [PMID: [25605845](#) DOI: [10.1200/JCO.2014.59.4358](#)]
- 4 **Nirschl CJ**, Drake CG. Molecular pathways: coexpression of immune checkpoint molecules: signaling pathways and implications for cancer immunotherapy. *Clin Cancer Res* 2013; **19**: 4917-4924 [PMID: [23868869](#) DOI: [10.1158/1078-0432.CCR-12-1972](#)]
- 5 **Baumeister SH**, Freeman GJ, Dranoff G, Sharpe AH. Coinhibitory Pathways in Immunotherapy for Cancer. *Annu Rev Immunol* 2016; **34**: 539-573 [PMID: [26927206](#) DOI: [10.1146/annurev-immunol-032414-112049](#)]
- 6 **Ishida Y**, Agata Y, Shibahara K, Honjo T. Induced expression of PD-1, a novel member of the immunoglobulin gene superfamily, upon programmed cell death. *EMBO J* 1992; **11**: 3887-3895 [PMID: [1396582](#)]
- 7 **Nishimura H**, Nose M, Hiai H, Minato N, Honjo T. Development of lupus-like autoimmune diseases by disruption of the PD-1 gene encoding an ITIM motif-carrying immunoreceptor. *Immunity* 1999; **11**: 141-151 [PMID: [10485649](#) DOI: [10.1016/s1074-7613\(00\)80089-8](#)]
- 8 **Nishimura H**, Okazaki T, Tanaka Y, Nakatani K, Hara M, Matsumori A, Sasayama S, Mizoguchi A, Hiai H, Minato N, Honjo T. Autoimmune dilated cardiomyopathy in PD-1 receptor-deficient mice. *Science* 2001; **291**: 319-322 [PMID: [11209085](#) DOI: [10.1126/science.291.5502.319](#)]
- 9 **Dong H**, Zhu G, Tamada K, Chen L. B7-H1, a third member of the B7 family, co-stimulates T-cell proliferation and interleukin-10 secretion. *Nat Med* 1999; **5**: 1365-1369 [PMID: [10581077](#) DOI: [10.1038/70932](#)]
- 10 **Tamura H**, Dong H, Zhu G, Sica GL, Flies DB, Tamada K, Chen L. B7-H1 costimulation

- preferentially enhances CD28-independent T-helper cell function. *Blood* 2001; **97**: 1809-1816 [PMID: 11238124 DOI: 10.1182/blood.v97.6.1809]
- 11 **Dong H**, Zhu G, Tamada K, Flies DB, van Deursen JM, Chen L. B7-H1 determines accumulation and deletion of intrahepatic CD8(+) T lymphocytes. *Immunity* 2004; **20**: 327-336 [PMID: 15030776 DOI: 10.1016/s1074-7613(04)00050-0]
 - 12 **Latchman Y**, Wood CR, Chernova T, Chaudhary D, Borde M, Chernova I, Iwai Y, Long AJ, Brown JA, Nunes R, Greenfield EA, Bourque K, Bousiotis VA, Carter LL, Carreno BM, Malenkovich N, Nishimura H, Okazaki T, Honjo T, Sharpe AH, Freeman GJ. PD-L2 is a second ligand for PD-1 and inhibits T cell activation. *Nat Immunol* 2001; **2**: 261-268 [PMID: 11224527 DOI: 10.1038/85330]
 - 13 **Wang S**, Bajorath J, Flies DB, Dong H, Honjo T, Chen L. Molecular modeling and functional mapping of B7-H1 and B7-DC uncouple costimulatory function from PD-1 interaction. *J Exp Med* 2003; **197**: 1083-1091 [PMID: 12719480 DOI: 10.1084/jem.20021752]
 - 14 **Pardoll DM**. The blockade of immune checkpoints in cancer immunotherapy. *Nat Rev Cancer* 2012; **12**: 252-264 [PMID: 22437870 DOI: 10.1038/nrc3239]
 - 15 **Leach DR**, Krummel MF, Allison JP. Enhancement of antitumor immunity by CTLA-4 blockade. *Science* 1996; **271**: 1734-1736 [PMID: 8596936 DOI: 10.1126/science.271.5256.1734]
 - 16 **Dong H**, Strome SE, Salomao DR, Tamura H, Hirano F, Flies DB, Roche PC, Lu J, Zhu G, Tamada K, Lennon VA, Celis E, Chen L. Tumor-associated B7-H1 promotes T-cell apoptosis: a potential mechanism of immune evasion. *Nat Med* 2002; **8**: 793-800 [PMID: 12091876 DOI: 10.1038/nm730]
 - 17 **Ribas A**, Wolchok JD. Cancer immunotherapy using checkpoint blockade. *Science* 2018; **359**: 1350-1355 [PMID: 29567705 DOI: 10.1126/science.aar4060]
 - 18 **Topalian SL**, Hodi FS, Brahmer JR, Gettinger SN, Smith DC, McDermott DF, Powderly JD, Carvajal RD, Sosman JA, Atkins MB, Leming PD, Spigel DR, Antonia SJ, Horn L, Drake CG, Pardoll DM, Chen L, Sharfman WH, Anders RA, Taube JM, McMiller TL, Xu H, Korman AJ, Jure-Kunkel M, Agrawal S, McDonald D, Kollia GD, Gupta A, Wigginton JM, Sznol M. Safety, activity, and immune correlates of anti-PD-1 antibody in cancer. *N Engl J Med* 2012; **366**: 2443-2454 [PMID: 22658127 DOI: 10.1056/NEJMoa1200690]
 - 19 **Hamid O**, Robert C, Daud A, Hodi FS, Hwu WJ, Kefford R, Wolchok JD, Hersey P, Joseph RW, Weber JS, Dronca R, Gangadhar TC, Patnaik A, Zarour H, Joshua AM, Gergich K, Ellassaiss-Schaap J, Algazi A, Mateus C, Boasberg P, Tumeah PC, Chmielowski B, Ebbinghaus SW, Li XN, Kang SP, Ribas A. Safety and tumor responses with lambrolizumab (anti-PD-1) in melanoma. *N Engl J Med* 2013; **369**: 134-144 [PMID: 23724846 DOI: 10.1056/NEJMoa1305133]
 - 20 **Powles T**, Eder JP, Fine GD, Braithel FS, Loriot Y, Cruz C, Bellmunt J, Burris HA, Petrylak DP, Teng SL, Shen X, Boyd Z, Hegde PS, Chen DS, Vogelzang NJ. MPDL3280A (anti-PD-L1) treatment leads to clinical activity in metastatic bladder cancer. *Nature* 2014; **515**: 558-562 [PMID: 25428503 DOI: 10.1038/nature13904]
 - 21 **Kaufman HL**, Russell J, Hamid O, Bhatia S, Terheyden P, D'Angelo SP, Shih KC, Lebbé C, Linette GP, Milella M, Brownell I, Lewis KD, Lorch JH, Chin K, Mahnke L, von Heydebreck A, Cuillerot JM, Nghiem P. Avelumab in patients with chemotherapy-refractory metastatic Merkel cell carcinoma: a multicentre, single-group, open-label, phase 2 trial. *Lancet Oncol* 2016; **17**: 1374-1385 [PMID: 27592805 DOI: 10.1016/S1470-2045(16)30364-3]
 - 22 **Massard C**, Gordon MS, Sharma S, Raffi S, Wainberg ZA, Luke J, Curiel TJ, Colon-Otero G, Hamid O, Sanborn RE, O'Donnell PH, Drakaki A, Tan W, Kurland JF, Rebelatto MC, Jin X, Blake-Haskins JA, Gupta A, Segal NH. Safety and Efficacy of Durvalumab (MEDI4736), an Anti-Programmed Cell Death Ligand-1 Immune Checkpoint Inhibitor, in Patients With Advanced Urothelial Bladder Cancer. *J Clin Oncol* 2016; **34**: 3119-3125 [PMID: 27269937 DOI: 10.1200/JCO.2016.67.9761]
 - 23 **Hodi FS**, O'Day SJ, McDermott DF, Weber RW, Sosman JA, Haanen JB, Gonzalez R, Robert C, Schadendorf D, Hassel JC, Akerley W, van den Eertwegh AJ, Lutzky J, Lorigan P, Vaubel JM, Linette GP, Hogg D, Ottensmeier CH, Lebbé C, Peschel C, Quirt J, Clark JI, Wolchok JD, Weber JS, Tian J, Yellin MJ, Nichol GM, Hoos A, Urba WJ. Improved survival with ipilimumab in patients with metastatic melanoma. *N Engl J Med* 2010; **363**: 711-723 [PMID: 20525992 DOI: 10.1056/NEJMoa1003466]
 - 24 **Kourie HR**, Klastersky JA. Side-effects of checkpoint inhibitor-based combination therapy. *Curr Opin Oncol* 2016; **28**: 306-313 [PMID: 27136134 DOI: 10.1097/CCO.0000000000000295]
 - 25 **Jenkins RW**, Barbie DA, Flaherty KT. Mechanisms of resistance to immune checkpoint inhibitors. *Br J Cancer* 2018; **118**: 9-16 [PMID: 29319049 DOI: 10.1038/bjc.2017.434]
 - 26 **Ivanov II**, Honda K. Intestinal commensal microbes as immune modulators. *Cell Host Microbe* 2012; **12**: 496-508 [PMID: 23084918 DOI: 10.1016/j.chom.2012.09.009]
 - 27 **Kumar S**, Leigh ND, Cao X. The Role of Co-stimulatory/Co-inhibitory Signals in Graft-vs.-Host Disease. *Front Immunol* 2018; **9**: 3003 [PMID: 30627129 DOI: 10.3389/fimmu.2018.03003]
 - 28 **Jiang X**, Wang J, Deng X, Xiong F, Ge J, Xiang B, Wu X, Ma J, Zhou M, Li X, Li Y, Li G, Xiong W, Guo C, Zeng Z. Role of the tumor microenvironment in PD-L1/PD-1-mediated tumor immune escape. *Mol Cancer* 2019; **18**: 10 [PMID: 30646912 DOI: 10.1186/s12943-018-0928-4]
 - 29 **Long J**, Lin J, Wang A, Wu L, Zheng Y, Yang X, Wan X, Xu H, Chen S, Zhao H. PD-1/PD-L1 blockade in gastrointestinal cancers: lessons learned and the road toward precision immunotherapy. *J Hematol Oncol* 2017; **10**: 146 [PMID: 28774337 DOI: 10.1186/s13045-017-0511-2]
 - 30 **Marin-Acevedo JA**, Dholaria B, Soyano AE, Knutson KL, Chumsri S, Lou Y. Next generation of immune checkpoint therapy in cancer: new developments and challenges. *J Hematol Oncol* 2018; **11**: 39 [PMID: 29544515 DOI: 10.1186/s13045-018-0582-8]

- 31 **Dyck L**, Mills KHG. Immune checkpoints and their inhibition in cancer and infectious diseases. *Eur J Immunol* 2017; **47**: 765-779 [PMID: [28393361](#) DOI: [10.1002/eji.201646875](#)]
- 32 **Ren B**, Cui M, Yang G, Wang H, Feng M, You L, Zhao Y. Tumor microenvironment participates in metastasis of pancreatic cancer. *Mol Cancer* 2018; **17**: 108 [PMID: [30060755](#) DOI: [10.1186/s12943-018-0858-1](#)]
- 33 **Horn L**, Mansfield AS, Szczesna A, Havel L, Krzakowski M, Hochmair MJ, Huemer F, Losonczy G, Johnson ML, Nishio M, Reck M, Mok T, Lam S, Shames DS, Liu J, Ding B, Lopez-Chavez A, Kabbinavar F, Lin W, Sandler A, Liu SV; IMpower133 Study Group. First-Line Atezolizumab plus Chemotherapy in Extensive-Stage Small-Cell Lung Cancer. *N Engl J Med* 2018; **379**: 2220-2229 [PMID: [30280641](#) DOI: [10.1056/NEJMoa1809064](#)]
- 34 **Migden MR**, Rischin D, Schmuits CD, Guminski A, Hauschild A, Lewis KD, Chung CH, Hernandez-Aya L, Lim AM, Chang ALS, Rabinowitz G, Thai AA, Dunn LA, Hughes BGM, Khushalani NI, Modi B, Schadendorf D, Gao B, Seebach F, Li S, Li J, Mathias M, Booth J, Mohan K, Stankevich E, Babiker HM, Brana I, Gil-Martin M, Homsí J, Johnson ML, Moreno V, Niu J, Owonikoko TK, Papadopoulos KP, Yancopoulos GD, Lowy I, Fury MG. PD-1 Blockade with Cemiplimab in Advanced Cutaneous Squamous-Cell Carcinoma. *N Engl J Med* 2018; **379**: 341-351 [PMID: [29863979](#) DOI: [10.1056/NEJMoa1805131](#)]
- 35 **Eggermont AMM**, Blank CU, Mandala M, Long GV, Atkinson V, Dalle S, Haydon A, Lichinitser M, Khattak A, Carlino MS, Sandhu S, Larkin J, Puig S, Ascierto PA, Rutkowski P, Schadendorf D, Koornstra R, Hernandez-Aya L, Maio M, van den Eertwegh AJM, Grob JJ, Gutzmer R, Jamal R, Lorigan P, Ibrahim N, Marreaud S, van Akkooi ACJ, Suciú S, Robert C. Adjuvant Pembrolizumab versus Placebo in Resected Stage III Melanoma. *N Engl J Med* 2018; **378**: 1789-1801 [PMID: [29658430](#) DOI: [10.1056/NEJMoa1802357](#)]
- 36 **Forde PM**, Chaft JE, Smith KN, Anagnostou V, Cottrell TR, Hellmann MD, Zahurak M, Yang SC, Jones DR, Broderick S, Battafarano RJ, Velez MJ, Rekhtman N, Olah Z, Naidoo J, Marrone KA, Verde F, Guo H, Zhang J, Caushi JX, Chan HY, Sidhom JW, Scharpf RB, White J, Gabrielson E, Wang H, Rosner GL, Rusch V, Wolchok JD, Merghoub T, Taube JM, Velculescu VE, Topalian SL, Brahmer JR, Pardoll DM. Neoadjuvant PD-1 Blockade in Resectable Lung Cancer. *N Engl J Med* 2018; **378**: 1976-1986 [PMID: [29658848](#) DOI: [10.1056/NEJMoa1716078](#)]
- 37 **Garassino MC**, Cho BC, Kim JH, Mazières J, Vansteenkiste J, Lena H, Corral Jaime J, Gray JE, Powderly J, Chouaid C, Bidoli P, Wheatley-Price P, Park K, Soo RA, Huang Y, Wadsworth C, Dennis PA, Rizvi NA; ATLANTIC Investigators. Durvalumab as third-line or later treatment for advanced non-small-cell lung cancer (ATLANTIC): an open-label, single-arm, phase 2 study. *Lancet Oncol* 2018; **19**: 521-536 [PMID: [29545095](#) DOI: [10.1016/S1470-2045\(18\)30144-X](#)]
- 38 **Xue S**, Hu M, Iyer V, Yu J. Blocking the PD-1/PD-L1 pathway in glioma: a potential new treatment strategy. *J Hematol Oncol* 2017; **10**: 81 [PMID: [28388955](#) DOI: [10.1186/s13045-017-0455-6](#)]
- 39 **Zitvogel L**, Galluzzi L, Viaud S, Vétizou M, Daillère R, Merad M, Kroemer G. Cancer and the gut microbiota: an unexpected link. *Sci Transl Med* 2015; **7**: 271ps1 [PMID: [25609166](#) DOI: [10.1126/scitranslmed.3010473](#)]
- 40 **Sears CL**, Garrett WS. Microbes, microbiota, and colon cancer. *Cell Host Microbe* 2014; **15**: 317-328 [PMID: [24629338](#) DOI: [10.1016/j.chom.2014.02.007](#)]
- 41 **Brennan CA**, Garrett WS. Gut Microbiota, Inflammation, and Colorectal Cancer. *Annu Rev Microbiol* 2016; **70**: 395-411 [PMID: [27607555](#) DOI: [10.1146/annurev-micro-102215-095513](#)]
- 42 **Hold GL**. Gastrointestinal Microbiota and Colon Cancer. *Dig Dis* 2016; **34**: 244-250 [PMID: [27028619](#) DOI: [10.1159/000443358](#)]
- 43 **Viaud S**, Saccheri F, Mignot G, Yamazaki T, Daillère R, Hannani D, Enot DP, Pfirschke C, Engblom C, Pittet MJ, Schlitzer A, Ginhoux F, Apetoh L, Chachaty E, Woerther PL, Eberl G, Bérard M, Ecobichon C, Clermont D, Bizet C, Gaboriau-Routhiau V, Cerf-Bensussan N, Opolon P, Yessaad N, Vivier E, Ryffel B, Elson CO, Doré J, Kroemer G, Lepage P, Boneca IG, Ghiringhelli F, Zitvogel L. The intestinal microbiota modulates the anticancer immune effects of cyclophosphamide. *Science* 2013; **342**: 971-976 [PMID: [24264990](#) DOI: [10.1126/science.1240537](#)]
- 44 **Mima K**, Nakagawa S, Sawayama H, Ishimoto T, Imai K, Iwatsuki M, Hashimoto D, Baba Y, Yamashita YI, Yoshida N, Chikamoto A, Baba H. The microbiome and hepatobiliary-pancreatic cancers. *Cancer Lett* 2017; **402**: 9-15 [PMID: [28527946](#) DOI: [10.1016/j.canlet.2017.05.001](#)]
- 45 **Roy S**, Trinchieri G. Microbiota: a key orchestrator of cancer therapy. *Nat Rev Cancer* 2017; **17**: 271-285 [PMID: [28303904](#) DOI: [10.1038/nrc.2017.13](#)]
- 46 **Alexander JL**, Wilson ID, Teare J, Marchesi JR, Nicholson JK, Kinross JM. Gut microbiota modulation of chemotherapy efficacy and toxicity. *Nat Rev Gastroenterol Hepatol* 2017; **14**: 356-365 [PMID: [28270698](#) DOI: [10.1038/nrgastro.2017.20](#)]
- 47 **Vétizou M**, Daillère R, Zitvogel L. [The role of intestinal microbiota in the response to anti-tumor therapies]. *Med Sci (Paris)* 2016; **32**: 974-982 [PMID: [28008838](#) DOI: [10.1051/medsci/20163211013](#)]
- 48 **Pitt JM**, Vétizou M, Waldschmitt N, Kroemer G, Chamaillard M, Boneca IG, Zitvogel L. Fine-Tuning Cancer Immunotherapy: Optimizing the Gut Microbiome. *Cancer Res* 2016; **76**: 4602-4607 [PMID: [27474734](#) DOI: [10.1158/0008-5472.CAN-16-0448](#)]
- 49 **Honda K**, Littman DR. The microbiota in adaptive immune homeostasis and disease. *Nature* 2016; **535**: 75-84 [PMID: [27383982](#) DOI: [10.1038/nature18848](#)]
- 50 **Spranger S**, Sivan A, Corrales L, Gajewski TF. Tumor and Host Factors Controlling Antitumor Immunity and Efficacy of Cancer Immunotherapy. *Adv Immunol* 2016; **130**: 75-93 [PMID: [26923000](#)]

- DOI: [10.1016/bs.ai.2015.12.003](https://doi.org/10.1016/bs.ai.2015.12.003)]
- 51 **West NR**, Powrie F. Immunotherapy Not Working? *Cancer Cell* 2015; **28**: 687-689 [PMID: [26678336](https://pubmed.ncbi.nlm.nih.gov/26678336/) DOI: [10.1016/j.ccell.2015.11.010](https://doi.org/10.1016/j.ccell.2015.11.010)]
 - 52 **Hefazi M**, Patnaik MM, Hogan WJ, Litzow MR, Pardi DS, Khanna S. Safety and Efficacy of Fecal Microbiota Transplant for Recurrent *Clostridium difficile* Infection in Patients With Cancer Treated With Cytotoxic Chemotherapy: A Single-Institution Retrospective Case Series. *Mayo Clin Proc* 2017; **92**: 1617-1624 [PMID: [29101931](https://pubmed.ncbi.nlm.nih.gov/29101931/) DOI: [10.1016/j.mayocp.2017.08.016](https://doi.org/10.1016/j.mayocp.2017.08.016)]
 - 53 **Parry RV**, Chemnitz JM, Frauwirth KA, Lanfranco AR, Braunstein I, Kobayashi SV, Linsley PS, Thompson CB, Riley JL. CTLA-4 and PD-1 receptors inhibit T-cell activation by distinct mechanisms. *Mol Cell Biol* 2005; **25**: 9543-9553 [PMID: [16227604](https://pubmed.ncbi.nlm.nih.gov/16227604/) DOI: [10.1128/MCB.25.21.9543-9553.2005](https://doi.org/10.1128/MCB.25.21.9543-9553.2005)]
 - 54 **Bardhan K**, Anagnostou T, Boussiotis VA. The PD1:PD-L1/2 Pathway from Discovery to Clinical Implementation. *Front Immunol* 2016; **7**: 550 [PMID: [28018338](https://pubmed.ncbi.nlm.nih.gov/28018338/) DOI: [10.3389/fimmu.2016.00550](https://doi.org/10.3389/fimmu.2016.00550)]
 - 55 **Patsoukis N**, Brown J, Petkova V, Liu F, Li L, Boussiotis VA. Selective effects of PD-1 on Akt and Ras pathways regulate molecular components of the cell cycle and inhibit T cell proliferation. *Sci Signal* 2012; **5**: ra46 [PMID: [22740686](https://pubmed.ncbi.nlm.nih.gov/22740686/) DOI: [10.1126/scisignal.2002796](https://doi.org/10.1126/scisignal.2002796)]
 - 56 **Somasundaram A**, Burns TF. The next generation of immunotherapy: keeping lung cancer in check. *J Hematol Oncol* 2017; **10**: 87 [PMID: [28434399](https://pubmed.ncbi.nlm.nih.gov/28434399/) DOI: [10.1186/s13045-017-0456-5](https://doi.org/10.1186/s13045-017-0456-5)]
 - 57 **Ohaegbulam KC**, Assal A, Lazar-Molnar E, Yao Y, Zang X. Human cancer immunotherapy with antibodies to the PD-1 and PD-L1 pathway. *Trends Mol Med* 2015; **21**: 24-33 [PMID: [25440090](https://pubmed.ncbi.nlm.nih.gov/25440090/) DOI: [10.1016/j.molmed.2014.10.009](https://doi.org/10.1016/j.molmed.2014.10.009)]
 - 58 **Yi M**, Jiao D, Xu H, Liu Q, Zhao W, Han X, Wu K. Biomarkers for predicting efficacy of PD-1/PD-L1 inhibitors. *Mol Cancer* 2018; **17**: 129 [PMID: [30139382](https://pubmed.ncbi.nlm.nih.gov/30139382/) DOI: [10.1186/s12943-018-0864-3](https://doi.org/10.1186/s12943-018-0864-3)]
 - 59 **Yi M**, Yu S, Qin S, Liu Q, Xu H, Zhao W, Chu Q, Wu K. Gut microbiome modulates efficacy of immune checkpoint inhibitors. *J Hematol Oncol* 2018; **11**: 47 [PMID: [29580257](https://pubmed.ncbi.nlm.nih.gov/29580257/) DOI: [10.1186/s13045-018-0592-6](https://doi.org/10.1186/s13045-018-0592-6)]
 - 60 **Sivan A**, Corrales L, Hubert N, Williams JB, Aquino-Michaels K, Earley ZM, Benyamin FW, Lei YM, Jabri B, Alegre ML, Chang EB, Gajewski TF. Commensal *Bifidobacterium* promotes antitumor immunity and facilitates anti-PD-L1 efficacy. *Science* 2015; **350**: 1084-1089 [PMID: [26541606](https://pubmed.ncbi.nlm.nih.gov/26541606/) DOI: [10.1126/science.aac4255](https://doi.org/10.1126/science.aac4255)]
 - 61 **Xu X**, Lv J, Guo F, Li J, Jia Y, Jiang D, Wang N, Zhang C, Kong L, Liu Y, Zhang Y, Li Z. Gut Microbiome Influences the Efficacy of PD-1 Antibody Immunotherapy on MSS-Type Colorectal Cancer via Metabolic Pathway. *Front Microbiol* 2020; **11**: 814 [PMID: [32425919](https://pubmed.ncbi.nlm.nih.gov/32425919/) DOI: [10.3389/fmicb.2020.00814](https://doi.org/10.3389/fmicb.2020.00814)]
 - 62 **Lv J**, Jia Y, Li J, Kuai W, Li Y, Guo F, Xu X, Zhao Z, Lv J, Li Z. Gegen Qinlian decoction enhances the effect of PD-1 blockade in colorectal cancer with microsatellite stability by remodelling the gut microbiota and the tumour microenvironment. *Cell Death Dis* 2019; **10**: 415 [PMID: [31138779](https://pubmed.ncbi.nlm.nih.gov/31138779/) DOI: [10.1038/s41419-019-1638-6](https://doi.org/10.1038/s41419-019-1638-6)]
 - 63 **Song P**, Yang D, Wang H, Cui X, Si X, Zhang X, Zhang L. Relationship between intestinal flora structure and metabolite analysis and immunotherapy efficacy in Chinese NSCLC patients. *Thorac Cancer* 2020; **11**: 1621-1632 [PMID: [32329229](https://pubmed.ncbi.nlm.nih.gov/32329229/) DOI: [10.1111/1759-7714.13442](https://doi.org/10.1111/1759-7714.13442)]
 - 64 **Jin Y**, Dong H, Xia L, Yang Y, Zhu Y, Shen Y, Zheng H, Yao C, Wang Y, Lu S. The Diversity of Gut Microbiome is Associated With Favorable Responses to Anti-Programmed Death 1 Immunotherapy in Chinese Patients With NSCLC. *J Thorac Oncol* 2019; **14**: 1378-1389 [PMID: [31026576](https://pubmed.ncbi.nlm.nih.gov/31026576/) DOI: [10.1016/j.jtho.2019.04.007](https://doi.org/10.1016/j.jtho.2019.04.007)]
 - 65 **Botticelli A**, Vernocchi P, Marini F, Quagliariello A, Cerbelli B, Reddel S, Del Chierico F, Di Pietro F, Giusti R, Tomassini A, Giampaoli O, Miccheli A, Zizzari IG, Nuti M, Putignani L, Marchetti P. Gut metabolomics profiling of non-small cell lung cancer (NSCLC) patients under immunotherapy treatment. *J Transl Med* 2020; **18**: 49 [PMID: [32014010](https://pubmed.ncbi.nlm.nih.gov/32014010/) DOI: [10.1186/s12967-020-02231-0](https://doi.org/10.1186/s12967-020-02231-0)]
 - 66 **Derosa L**, Routy B, Fidelle M, Iebba V, Alla L, Pasolli E, Segata N, Desnoyer A, Pietrantonio F, Ferrere G, Fahrner JE, Le Chatellier E, Pons N, Galleron N, Roume H, Duong CPM, Mondragón L, Iribarren K, Bonvalet M, Terrisse S, Rauber C, Goubet AG, Daillère R, Lemaître F, Reni A, Casu B, Alou MT, Alves Costa Silva C, Raoult D, Fizazi K, Escudier B, Kroemer G, Albiges L, Zitvogel L. Gut Bacteria Composition Drives Primary Resistance to Cancer Immunotherapy in Renal Cell Carcinoma Patients. *Eur Urol* 2020; **78**: 195-206 [PMID: [32376136](https://pubmed.ncbi.nlm.nih.gov/32376136/) DOI: [10.1016/j.eururo.2020.04.044](https://doi.org/10.1016/j.eururo.2020.04.044)]
 - 67 **Gopalakrishnan V**, Spencer CN, Nezi L, Reuben A, Andrews MC, Karpinetz TV, Prieto PA, Vicente D, Hoffman K, Wei SC, Cogdill AP, Zhao L, Hudgens CW, Hutchinson DS, Manzo T, Petaccia de Macedo M, Cotechini T, Kumar T, Chen WS, Reddy SM, Szczepaniak Sloane R, Galloway-Pena J, Jiang H, Chen PL, Shpall EJ, Rezvani K, Alousi AM, Chemaly RF, Shelburne S, Vence LM, Okhuysen PC, Jensen VB, Swennes AG, McAllister F, Marcelo Riquelme Sanchez E, Zhang Y, Le Chatelier E, Zitvogel L, Pons N, Austin-Breneman JL, Haydu LE, Burton EM, Gardner JM, Sirmans E, Hu J, Lazar AJ, Tsujikawa T, Diab A, Tawbi H, Glitza IC, Hwu WJ, Patel SP, Woodman SE, Amaria RN, Davies MA, Gershenwald JE, Hwu P, Lee JE, Zhang J, Coussens LM, Cooper ZA, Futreal PA, Daniel CR, Ajami NJ, Petrosino JF, Tetzlaff MT, Sharma P, Allison JP, Jenq RR, Wargo JA. Gut microbiome modulates response to anti-PD-1 immunotherapy in melanoma patients. *Science* 2018; **359**: 97-103 [PMID: [29097493](https://pubmed.ncbi.nlm.nih.gov/29097493/) DOI: [10.1126/science.aan4236](https://doi.org/10.1126/science.aan4236)]
 - 68 **Matson V**, Fessler J, Bao R, Chongsuwat T, Zha Y, Alegre ML, Luke JJ, Gajewski TF. The commensal microbiome is associated with anti-PD-1 efficacy in metastatic melanoma patients.

- Science* 2018; **359**: 104-108 [PMID: 29302014 DOI: 10.1126/science.aao3290]
- 69 **Routy B**, Le Chatelier E, Derosa L, Duong CPM, Alou MT, Daillère R, Fluckiger A, Messaoudene M, Rauber C, Roberti MP, Fidelle M, Flament C, Poirier-Colame V, Opolon P, Klein C, Iribarren K, Mondragón L, Jacquilot N, Qu B, Ferrere G, Clémenson C, Mezquita L, Masip JR, Naltet C, Brosseau S, Kaderbhai C, Richard C, Rizvi H, Levenez F, Galleron N, Quinquis B, Pons N, Ryffel B, Minard-Colin V, Gonin P, Soria JC, Deutsch E, Loriot Y, Ghiringhelli F, Zalcman G, Goldwasser F, Escudier B, Hellmann MD, Eggermont A, Raoult D, Albiges L, Kroemer G, Zitvogel L. Gut microbiome influences efficacy of PD-1-based immunotherapy against epithelial tumors. *Science* 2018; **359**: 91-97 [PMID: 29097494 DOI: 10.1126/science.aan3706]
- 70 **Vétizou M**, Pitt JM, Daillère R, Lepage P, Waldschmitt N, Flament C, Rusakiewicz S, Routy B, Roberti MP, Duong CP, Poirier-Colame V, Roux A, Becharef S, Formenti S, Golden E, Cording S, Eberl G, Schlitzer A, Ginhoux F, Mani S, Yamazaki T, Jacquilot N, Enot DP, Bérard M, Nigou J, Opolon P, Eggermont A, Woerther PL, Chachaty E, Chaput N, Robert C, Mateus C, Kroemer G, Raoult D, Boneca IG, Carbonnel F, Chamillard M, Zitvogel L. Anticancer immunotherapy by CTLA-4 blockade relies on the gut microbiota. *Science* 2015; **350**: 1079-1084 [PMID: 26541610 DOI: 10.1126/science.aad1329]
- 71 **Irrazabal T**, Martin A. T Regulatory Cells Gone Bad: An Oncogenic Immune Response against Enterotoxigenic *B. fragilis* Infection Leads to Colon Cancer. *Cancer Discov* 2015; **5**: 1021-1023 [PMID: 26429936 DOI: 10.1158/2159-8290.CD-15-0987]
- 72 **Chaput N**, Lepage P, Coutzac C, Soularue E, Le Roux K, Monot C, Boselli L, Routier E, Cassard L, Collins M, Vaysse T, Marthey L, Eggermont A, Asvatourian V, Lanoy E, Mateus C, Robert C, Carbonnel F. Baseline gut microbiota predicts clinical response and colitis in metastatic melanoma patients treated with ipilimumab. *Ann Oncol* 2017; **28**: 1368-1379 [PMID: 28368458 DOI: 10.1093/annonc/mdx108]
- 73 **Zhuo Q**, Yu B, Zhou J, Zhang J, Zhang R, Xie J, Wang Q, Zhao S. Lysates of *Lactobacillus acidophilus* combined with CTLA-4-blocking antibodies enhance antitumor immunity in a mouse colon cancer model. *Sci Rep* 2019; **9**: 20128 [PMID: 31882868 DOI: 10.1038/s41598-019-56661-y]
- 74 **Mager LF**, Burkhard R, Pett N, Cooke NCA, Brown K, Ramay H, Paik S, Stagg J, Groves RA, Gallo M, Lewis IA, Geuking MB, McCoy KD. Microbiome-derived inosine modulates response to checkpoint inhibitor immunotherapy. *Science* 2020; **369**: 1481-1489 [PMID: 32792462 DOI: 10.1126/science.abc3421]
- 75 **Zhang F**, Luo W, Shi Y, Fan Z, Ji G. Should we standardize the 1,700-year-old fecal microbiota transplantation? *Am J Gastroenterol* 2012; **107**: 1755; author reply p.1755-1755; author reply p.1756 [PMID: 23160295 DOI: 10.1038/ajg.2012.251]
- 76 **Eiseman B**, Silen W, Bascom GS, Kauvar AJ. Fecal enema as an adjunct in the treatment of pseudomembranous enterocolitis. *Surgery* 1958; **44**: 854-859 [PMID: 13592638]
- 77 **Kang Y**, Cai Y. Altered Gut Microbiota in HIV Infection: Future Perspective of Fecal Microbiota Transplantation Therapy. *AIDS Res Hum Retroviruses* 2019; **35**: 229-235 [PMID: 29877092 DOI: 10.1089/AID.2017.0268]
- 78 **Kang Y**, Cai Y. Gut microbiota and obesity: implications for fecal microbiota transplantation therapy. *Hormones (Athens)* 2017; **16**: 223-234 [PMID: 29278509 DOI: 10.14310/horm.2002.1742]
- 79 **Kang YB**, Cai Y, Zhang H. Gut microbiota and allergy/asthma: From pathogenesis to new therapeutic strategies. *Allergol Immunopathol (Madr)* 2017; **45**: 305-309 [PMID: 28029408 DOI: 10.1016/j.aller.2016.08.004]
- 80 **Di Bella S**, Drapeau C, García-Almodóvar E, Petrosillo N. Fecal microbiota transplantation: the state of the art. *Infect Dis Rep* 2013; **5**: e13 [PMID: 24470963 DOI: 10.4081/idr.2013.e13]
- 81 **Smits LP**, Bouter KE, de Vos WM, Borody TJ, Nieuwdorp M. Therapeutic potential of fecal microbiota transplantation. *Gastroenterology* 2013; **145**: 946-953 [PMID: 24018052 DOI: 10.1053/j.gastro.2013.08.058]
- 82 **Vrieze A**, de Groot PF, Kootte RS, Knaapen M, van Nood E, Nieuwdorp M. Fecal transplant: a safe and sustainable clinical therapy for restoring intestinal microbial balance in human disease? *Best Pract Res Clin Gastroenterol* 2013; **27**: 127-137 [PMID: 23768558 DOI: 10.1016/j.bpg.2013.03.003]
- 83 **Baruch EN**, Youngster I, Ben-Betzalel G, Ortenberg R, Lahat A, Katz L, Adler K, Dick-Necula D, Raskin S, Bloch N, Rotin D, Anafi L, Avivi C, Melnichenko J, Steinberg-Silman Y, Mamtani R, Harati H, Asher N, Shapira-Frommer R, Brosh-Nissimov T, Eshet Y, Ben-Simon S, Ziv O, Khan MAW, Amit M, Ajami NJ, Barshack I, Schachter J, Wargo JA, Koren O, Markel G, Boursi B. Fecal microbiota transplant promotes response in immunotherapy-refractory melanoma patients. *Science* 2021; **371**: 602-609 [PMID: 33303685 DOI: 10.1126/science.abb5920]
- 84 **ClinicalTrials.gov**. Fecal microbiota transplant (FMT) in melanoma patients. [cited 16 January 2019]. Available from: <https://www.clinicaltrials.gov/ct2/show/NCT03341143>

Immune checkpoint inhibitor-related hepatotoxicity: A review

Devika Remash, David S Prince, Catriona McKenzie, Simone I Strasser, Steven Kao, Ken Liu

ORCID number: Devika Remash 0000-0002-0262-6870; David S Prince 0000-0001-8087-0548; Catriona McKenzie 0000-0002-6452-4976; Simone I Strasser 0000-0001-6374-1525; Steven Kao 0000-0003-4531-7397; Ken Liu 0000-0002-0453-3168.

Author contributions: McKenzie C, Kao S, Strasser SI and Liu K were involved in the conception of the review, and critically revised the article; Remash D, Prince DS and Liu K performed the literature review, and drafted the article; all authors have read and approved the final version.

Conflict-of-interest statement:

Authors declare no conflict of interests for this article.

Open-Access: This article is an open-access article that was selected by an in-house editor and fully peer-reviewed by external reviewers. It is distributed in accordance with the Creative Commons Attribution NonCommercial (CC BY-NC 4.0) license, which permits others to distribute, remix, adapt, build upon this work non-commercially, and license their derivative works on different terms, provided the original work is properly cited and the use is non-commercial. See: <http://creativecommons.org/licenses/by-nc/4.0/>

Manuscript source: Invited manuscript

Devika Remash, David S Prince, Catriona McKenzie, Simone I Strasser, Ken Liu, AW Morrow Gastroenterology and Liver Centre, Royal Prince Alfred Hospital, Sydney 2050, NSW, Australia

Catriona McKenzie, Simone I Strasser, Steven Kao, Ken Liu, Sydney Medical School, University of Sydney, Sydney 2006, NSW, Australia

Catriona McKenzie, Tissue Pathology and Diagnostic Oncology, Royal Prince Alfred Hospital, Sydney 2050, NSW, Australia

Catriona McKenzie, New South Wales Health Pathology, New South Wales Health, Sydney 2050, NSW, Australia

Steven Kao, Medical Oncology, Chris O'Brien Lifehouse, Sydney 2050, NSW, Australia

Corresponding author: Ken Liu, BSc, FRACP, MBBS, Consultant Physician-Scientist, Senior Lecturer, Staff Physician, AW Morrow Gastroenterology and Liver Centre, Royal Prince Alfred Hospital, Missenden Road, Camperdown, Sydney 2050, NSW, Australia.

ken.liu@health.nsw.gov.au

Abstract

The application of immune checkpoint inhibitors (ICI) in advanced cancer has been a major development in the last decade. The indications for ICIs are constantly expanding into new territory across different cancers, disease stages and lines of therapy. With this increased use, adverse events including immune checkpoint inhibitor-related hepatotoxicity (ICH) have emerged as an important clinical problem. This along with the introduction of ICI as first- and second-line treatments for advanced hepatocellular carcinoma makes ICH very relevant to gastroenterologists and hepatologists. The incidence of ICH varies between 1%-20% depending on the number, type and dose of ICI received. Investigation and management generally involve excluding differential diagnoses and following a stepwise escalation of withholding or ceasing ICI, corticosteroid treatment and adding other immunosuppressive agents depending on the severity of toxicity. The majority of patients with ICH recover and some may even safely recommence ICI therapy. Guideline recommendations are largely based on evidence derived from retrospective case series which highlights a priority for future research.

Key Words: Immunotherapy; Immune checkpoint inhibitors; Hepatitis; Adverse drug event; Drug-induced liver injury; Immunosuppression

Specialty type: Gastroenterology and hepatology

Country/Territory of origin:
Australia

Peer-review report's scientific quality classification

Grade A (Excellent): 0
Grade B (Very good): B, B
Grade C (Good): 0
Grade D (Fair): 0
Grade E (Poor): 0

Received: March 31, 2021

Peer-review started: March 31, 2021

First decision: June 23, 2021

Revised: June 28, 2021

Accepted: August 3, 2021

Article in press: August 3, 2021

Published online: August 28, 2021

P-Reviewer: Sachu A, Zou Z

S-Editor: Fan JR

L-Editor: A

P-Editor: Yuan YY



©The Author(s) 2021. Published by Baishideng Publishing Group Inc. All rights reserved.

Core Tip: Immune checkpoint inhibitor (ICI)-related hepatotoxicity (ICH) is an increasingly encountered clinical problem for gastroenterologists. Although the diagnosis should be suspected in patients receiving ICI with liver function test derangements, a thorough history, examination and targeted liver investigations including cross-sectional imaging should be performed to exclude differential diagnoses. Once ICH is confirmed, its severity should be graded which then guides management. Management of ICH follows a stepwise approach beginning with cessation of ICI, followed by corticosteroids and other immunosuppressants with close monitoring after each step. The decision to recommence ICI after recovery is made on a case-by-case basis.

Citation: Remash D, Prince DS, McKenzie C, Strasser SI, Kao S, Liu K. Immune checkpoint inhibitor-related hepatotoxicity: A review. *World J Gastroenterol* 2021; 27(32): 5376-5391

URL: <https://www.wjgnet.com/1007-9327/full/v27/i32/5376.htm>

DOI: <https://dx.doi.org/10.3748/wjg.v27.i32.5376>

INTRODUCTION

Immunological recognition of cancer cells involves an antigen presenting cell binding and presenting tumor antigens to a T cell *via* its T-cell receptor. The ensuing immune response depends on the presence of either co-stimulatory molecules (which results in immune activation) or inhibitory molecules (which results in immune downregulation and exhaustion). These inhibitory (so called checkpoint) molecules exist as a 'brake' to prevent excessive immune activation or autoimmunity. However, they are also exploited by tumor cells to evade detection by the immune system and facilitate tumor progression[1].

Immunotherapy has recently revolutionized the treatment of advanced malignancy. It involves the use of monoclonal antibodies to inhibit these immune checkpoint molecules leading to immune activation against cancer cells. The main immune checkpoint molecules currently targeted by immunotherapy are the programmed cell death protein 1 (PD-1), programmed death-ligand 1 (PD-L1), and cytotoxic T-lymphocyte-associated protein 4 (CTLA-4). Since the CTLA-4 inhibitor ipilimumab was approved for the treatment of metastatic melanoma in 2011[2], immunotherapies have been trialled in many other malignancies with varying success. With their increased use, the toxicities of immunotherapies have also emerged as an important clinical problem. As expected, the side effect of enhancing the body's immune response to cancer is unwanted inflammation. These immune related adverse events (irAEs) can affect almost any organ but most commonly the skin, liver, gastrointestinal tract and endocrine glands. Treatment of irAEs may require temporary or permanent cessation of immunotherapy with or without commencement of immunosuppression which is suboptimal (at least theoretically) in terms of anti-cancer effect.

For gastroenterologists and hepatologists, immunotherapy-related hepatotoxicity deserves special mention as it is commonly encountered. Furthermore, checkpoint inhibitors have recently been added to first- and second-line treatment options for advanced hepatocellular carcinoma (HCC) after promising clinical trial results[3-5]. These patients tend to have relatively limited liver reserve since most HCCs occur on a background of liver cirrhosis[6]. Thus, immunotherapy-related hepatotoxicity can result in liver failure and even death.

In this review, we summarize the latest literature on epidemiology, pathophysiology, diagnosis, assessment and management of immune checkpoint inhibitors (ICI)-induced hepatotoxicity (ICH).

EPIDEMIOLOGY OF ICH

Incidence

Although ICH is primarily considered a 'hepatitis' presenting with elevated transam-

inases, cases of immune-mediated ‘cholangitis’ with elevated biliary enzymes are generally also included in its definition. Further complicating the diagnosis of ICH (and therefore measurement of its incidence) is that ICI is increasingly being used in combination with other chemotherapies and targeted therapies which can themselves cause hepatotoxicity. Indeed, distinguishing between ICH and drug-induced liver injury (DILI) secondary to co-administered therapy can be difficult.

The reported incidence of ICH depends on the severity grade [according to common terminology criteria for adverse events (CTCAE), discussed further below], type and dose of ICI and if it was used as monotherapy or in combination with another ICI. The reported incidence of all ICH (any grade) varies widely between 0%-30% while only 0%-20% experience severe ICH (grade 3 or 4) (Table 1). Fulminant hepatic failure and death following ICI has also been reported with an incidence of up to 0.4%, particularly with CTLA-4 inhibitors[7]. Indeed, ICH is overrepresented in cases of severe irAEs and accounts for 16% of all immunotherapy-related fatalities[8].

Among patients receiving monotherapy, CTLA-4 inhibitors (ipilimumab and tremelimumab) have the highest rate of hepatotoxicity[9]. The incidence of ICH following CTLA-4 inhibitor monotherapy ranges between mostly between 0%-30% (mostly 3%-15%) with 1%-20% (mostly 1%-10%) being grade 3/4 in severity[2,10-12]. The frequency of ICH appears to increase when higher doses of CTLA-4 inhibitors are administered. For ipilimumab, reported rates of hepatitis (any grade) were only 3%-5% in patients treated with standard doses (3 mg/kg) compared to 15%-16% in those treated with high dose (10 mg/kg)[13,14].

In large trials of PD-L1 inhibitors (*e.g.*, atezolizumab, durvalumab, avelumab) patients exhibited rates of ICH similar to those observed for CTLA-4 inhibitors (1%-17% overall, 3%-5% grade 3/4)[15-17]. In contrast, monotherapy with PD-1 inhibitors (*e.g.*, nivolumab, pembrolizumab) results in the lowest incidence of ICH with rates consistently reported between 0%-3% (mostly 1%-2%) and very few grade 3/4 reactions (< 1%) (Table 1). Unlike CTLA-4 inhibitors, the incidence of irAEs secondary to PD-1 and PD-L1 inhibitors does not appear to be dose-related[18].

Combination therapy with CTLA-4 and PD-1 blockade has been shown to have synergistic anti-tumor effect in advanced melanoma[19]. As expected, combination therapy also results in higher rates of irAEs including ICH. In this group, ICH of any grade occurs in 18%-22% overall with 8%-11% having severe hepatitis (Table 1).

As experience with ICI increases, real-world observational data on ICH have emerged and the incidence appears to be comparable to rates reported in clinical trials[20, 21].

Other risk factors

The type of underlying malignancy appears to impact on the risk of developing ICH. A meta-analysis of 17 phase II and III trials of ICI in advanced cancer found a higher likelihood of hepatotoxicity in melanoma patients compared to other types of cancer (odds ratio 5.66 *vs* 2.71, respectively)[22].

A small study of patients with pre-existing autoimmune disease observed high rates of irAEs (33% experienced grade 3-5 events) and exacerbations of autoimmune disease (27% experienced flares requiring treatment) following ipilimumab treatment[23]. However, none of these patients had autoimmune liver conditions nor experienced ICH. In a larger study of patients with pre-existing autoimmune conditions receiving anti-PD-1 therapy, rates of ICH were similar to those reported in studies of general patients (3% overall, 2% grade 3/4)[24]. Again, none of these patients had a liver-specific autoimmune condition. Unsurprisingly, irAEs are common when a patient with previous irAEs is rechallenged. However, irAE encountered after one ICI does not seem to predict the same irAEs when switching to a different class of ICI[24].

From trials in advanced HCC, ICI appears to be generally well-tolerated in patients with underlying liver disease. Although elevated aspartate aminotransferase (AST) and/or alanine aminotransferase (ALT) were commonly reported adverse events in this population (15%-23% any grade, 6%-13% grade 3/4), the proportion attributable to ICH were similar to those seen in trials of patients without liver disease[3-5]. However, trials in patients with liver disease included primarily those with compensated (Child-Pugh class A) cirrhosis, thus limiting the generalizability of these findings to sicker patients. Reassuringly, sub-analyses of a small number of patients with Child-Pugh class B7-8 (decompensated) cirrhosis in the Checkmate-040 study (*n* = 49) revealed overall ICH rates of 8% following nivolumab treatment[25]. Thus, from limited initial data of patients with Child-Pugh class A or early Child-Pugh class B cirrhosis, the incidence of ICH does not appear to be significantly higher than in those without liver disease.

Table 1 Incidence of severe hepatotoxicity by immunotherapy agent used as reported in key phase II and III clinical trials

| Class | Agent | Ref. | Indication | Incidence of hepatotoxicity (all grades) % (no. of patients) | Incidence of \geq grade 3 hepatotoxicity % (no. of patients) | |
|--------------------------------|---|-----------------------------------|----------------------------------|--|--|-------------|
| CTLA-4 | Ipilimumab (standard dose) 3 mg/kg | Hodi <i>et al</i> [71], 2018 | Melanoma | 0.3 (1/311) | 0 (0/311) | |
| | | Weber <i>et al</i> [72], 2009 | Melanoma | 15.5 (9/58) | 10.3 (6/58) | |
| | | Hodi <i>et al</i> [2], 2010 | Melanoma | 3.8 (5/131) | 0 (0/131) | |
| | | | Melanoma | 2.1 (8/380) | 1.1 (4/380) | |
| | | Wolchok <i>et al</i> [73], 2010 | Melanoma | 26.4% (19/72) | 0 (0/72) | |
| | Robert <i>et al</i> [74], 2011 | Melanoma | 29.1 (72/247) | 20.6 (51/247) | | |
| | Ipilimumab (high dose) 10 mg/kg | Wolchok <i>et al</i> [73], 2010 | Melanoma | 70.4 (50/71) | 15.5 (11/71) | |
| Anti-PD-1 | Nivolumab | Ribas <i>et al</i> [75], 2013 | Melanoma | 0.6 (2/325) | 0.6 (2/325) | |
| | | Hodi <i>et al</i> [71], 2018 | Melanoma | 0.3 (1/313) | 0.3 (1/313) | |
| | | Weber <i>et al</i> [76], 2017 | Melanoma | 1.9 (11/576) | 0.7 (4/576) | |
| | | Brahmer <i>et al</i> [77], 2015 | Squamous cell NSCLC | 1.5 (2/131) | 0 (0/131) | |
| | | Borghaei <i>et al</i> [78], 2015 | Non-squamous NSCLC | 3.1 (9/287) | 0 (0/287) | |
| | Robert <i>et al</i> [79], 2014 | Melanoma | 1.1 (1/89) | 1.1 (1/89) | | |
| | Pembrolizumab | Robert <i>et al</i> [79], 2014 | Melanoma | 0 (0/84) | 0 (0/84) | |
| Anti-PD-L1 | Atezolizumab | Eggermont <i>et al</i> [80], 2018 | Melanoma | 1.8 (9/509) | 1.4 (7/509) | |
| | | Jotte <i>et al</i> [82], 2020 | Squamous NSCLC | 17.4 (58/334) | 5.4 (18/334) | |
| | Atezolizumab + Bevacizumab (anti-VEGF antibody) | Finn <i>et al</i> [3], 2020 | HCC | 33.4 (110/329) | 10.6 (35/329) | |
| | Avelumab | D'Angelo <i>et al</i> [83], 2020 | Metastatic Merkel cell carcinoma | 1.1 (1/88) | 1.1 (1/88) | |
| | Durvalumab | Garassino <i>et al</i> [84], 2018 | Advanced NSCLC | 0.2 (1/444) | 0.2 (1/444) | |
| | Combination Therapy | Ipilimumab + Nivolumab | Migden <i>et al</i> [81], 2018 | Cutaneous Squamous-Cell Carcinoma | 8.5 (5/59) | 0 (0/59) |
| | | | Hodi <i>et al</i> [71], 2018 | Melanoma | 3.2 (10/313) | 2.6 (8/313) |
| Postow <i>et al</i> [85], 2015 | | | Melanoma | 22.3 (21/94) | 10.6 (10/94) | |
| Larkin <i>et al</i> [86], 2015 | | | Melanoma | 17.6 (55/313) | 8.3 (26/313) | |
| | Wolchok <i>et al</i> [73], 2010 | Melanoma | 20.8 (11/53) | 11.3 (6/53) | | |

Grading of severity is according to common terminology criteria for adverse events. CTLA-4: Cytotoxic T-lymphocyte-associated protein 4; HCC: Hepatocellular carcinoma; no. of: Number of; NSCLC: Non-small cell lung cancer; PD-1: Programmed cell death protein 1; PD-L1: Programmed death-

ligand 1; VEGF: Vascular endothelial growth factor.

High rates of allograft rejection and graft failure have been described in solid organ transplant recipients[26]. In particular, ICI treatment may be a consideration in liver transplant recipients for recurrent HCC or other malignancies (*e.g.*, melanoma). Liver injury (due to allograft rejection, not ICH) has been reported in 29%-37% of liver transplant patients in small series ($n = 11-19$)[26-28]. Of concern, a high proportion (3/4, 75%) of these rejections were fatal, although patient numbers were small[26,28].

PATHOGENESIS OF ICH

The exact pathogenesis of ICH is not fully understood but likely to be multifactorial. The general theory is that ICI-induced immune activation leads to not only a tumor-specific T cell response but also loss of peripheral tolerance against the patient's own cells[29]. In the case of ICH, immune activation against hepatocytes leads to a T-cell mediated hepatitis and hepatocyte death.

Mechanistically, proposed processes involved in irAEs include: T cell reactions to shared antigens expressed on both tumors and target organs, development of auto-antibodies, of ICI antibodies directly binding to target organs and/or overactivation of immune cells leading to excessive cytokine secretion[29]. The precise mechanism(s) underlying ICH development has not been elucidated.

It also remains unclear why certain patients develop ICH but not others. It has been proposed that genetic factors play an important role, however, no obvious high-risk genetic loci have been identified to date. Although it is a focus of active research, there are currently no reliable biomarkers to predict ICH in routine clinical use.

CLINICAL FEATURES

Presentation

ICH is usually asymptomatic and detected incidentally on routine liver function tests (LFTs) performed during monitoring after ICI treatment. The median time to onset of ICH is most commonly reported as 8-12 wk[14,30,31], however it can manifest as early as 2-3 wk after initiating ICI treatment[14,32-34]. Patients with more severe disease can present clinically with fever, jaundice, right-sided abdominal pain, dark urine and easy bruising. As aforementioned, acute liver failure (encephalopathy and coagulopathy) is rare, especially as the initial presentation[35]. Clinical presentations may vary depending on the class of ICI with fever found to be a more prominent feature in ICH secondary to CTLA-4 inhibitors compared to anti-PD-1 or anti-PD-L1 antibodies in one study[36].

A hepatocellular pattern of LFTs elevation (or transaminitis) is the most common pattern seen with ALT typically being higher than AST[36]. However, a cholestatic or mixed pattern of LFTs derangement is more common with PD-1/PD-L1 inhibitors compared to CTLA-4 inhibitors[36,37]. Rarely, cases of immune-mediated cholangiopathy (discussed further below) have also been described particularly with PD-1/PD-L1 inhibitors[38]. Elevations in total bilirubin can also be seen which reflects either prolonged injury or a sign of more severe disease.

Diagnosis, differentials and work-up

Although clinicians should be vigilant in looking for ICH in patients receiving ICI, not all cases of newly deranged LFTs are due to ICH. Indeed, a diagnosis of ICH only accounts for a fraction (less than 20%-30%) of all patients who were reported to have elevated AST and/or ALT as an adverse event in clinical trials[4,5,39]. Therefore, ICH is a diagnosis of exclusion and it is still important to conduct a thorough assessment to exclude other common differentials. A list of differential diagnoses with suggested investigations (or 'liver screen') is shown in [Table 2](#).

A few key differential diagnoses deserve mention. Liver function abnormalities are more common when ICI are used in combination with other systemic chemotherapies such as dacarbazine or vemurafenib in melanoma[32], paclitaxel and carboplatin in lung cancer[40,41], or bevacizumab in HCC[3]. Furthermore, patients should be asked about other recent medications including non-prescription treatments (over-the-

Table 2 Differential diagnosis and suggested investigations

| System | Differential diagnosis | Investigations |
|---------------------------|--|---|
| Drug-induced liver injury | (1) Other co-administered anti-cancer drugs; (2) Alcohol related liver disease; and (3) Acetaminophen toxicity | Medication history |
| Tumor-related | Metastatic disease | Abdominal imaging with ultrasound, CT or MRCP |
| Infectious | (1) Sepsis; (2) Acute HAV infection; (3) Acute HBV or flare of chronic HBV; (4) Chronic HCV; (5) Acute HEV; (6) Acute CMV or reactivation; and (7) Acute EBV | (1) Septic screen as appropriate; (2) Anti-HAV (IgM); (3) HBsAg, Anti-HBc IgG, IgM, ± HBV DNA; (4) Anti-HCV ± HCV RNA; (5) Anti-HEV (IgM); (6) CMV IgM and IgG ± CMV DNA; and (7) EBV IgM and IgG |
| Biliary disease | (1) Cholecystitis; (2) Cholangitis; and (3) Pancreatitis | (1) Abdominal imaging; and (2) Serum lipase |
| Autoimmune | Autoimmune hepatitis ¹ | ANA, Anti-SMA, Anti-LKM1, serum IgG levels |
| Musculoskeletal | (1) Myositis (potentially an irAEs); and (2) Rhabdomyolysis | Serum CK |
| Metabolic | Underlying NASH | (1) Metabolic risk factors; and (2) Abdominal imaging for hepatic steatosis |
| Vascular | (1) Portal-vein/hepatic vein thrombosis; and (2) Ischemic hepatitis | Abdominal imaging and clinical history |

¹Although anti-nuclear antibodies is frequently positive at low-titres in IC (< 1:80), specific auto-antibodies seen in autoimmune hepatitis are usually negative.

ANA: Anti-nuclear antibodies; Anti-HBc: Anti-Hepatitis B core antibody; anti-LKM1: Anti-liver-kidney microsomal 1 antibody; Anti-SMA: Anti-smooth muscle antibody; CK: Creatine kinase; CMV: Cytomegalovirus; CT: Computed tomography; EBV: Epstein-Barr virus; HAV: Hepatitis A virus; HBsAg: Hepatitis B surface antigen; HBV: Hepatitis B virus; HCV: Hepatitis C virus; HEV: Hepatitis E virus; irAEs: Immune-related adverse events; MRCP: Magnetic resonance cholangiopancreatography; NASH: Non-alcoholic steatohepatitis.

counter, complementary and herbal medications) and their alcohol intake. All the above can cause a non-immune mediated (direct or idiosyncratic) DILI. Hence, a detailed medication history should be performed. Practically, it can be difficult differentiating between ICH *vs* non-ICI mediated DILI and further investigations such as liver biopsy may not reliably separate these entities.

Patients with malignancy can also have direct tumor spread to the liver or regional lymph nodes which can lead to LFTs derangement from either biliary obstruction by bulky metastases or widespread infiltration of the liver. One study of 70 patients with liver injury after receiving pembrolizumab (mainly for melanoma) found the cause of liver injury as determined by 'expert adjudication' was due to progressive hepatic metastases or malignant biliary obstruction in 60% of cases (double the number of cases judged to be due to ICH)[39]. Cross-sectional imaging with either abdominal ultrasound or more commonly computed tomography scan can be useful to identify biliary obstruction and the extent of liver metastases. As advanced cancer patients tend to get regular scans to monitor response to therapy, there may be a recent scan for review or comparison. Otherwise, imaging findings in patients with ICH are mild and non-specific even in severe cases and may include hepatomegaly, periportal edema, or periportal lymphadenopathy[42]. Extensive bone metastases can draw attention to the liver by causing elevations in total alkaline phosphatase (without a rise in gamma-glutamyl transferase)[43], which can be clarified by checking the bone-specific isoform (ostase).

Patients receiving certain systemic chemotherapies are at increased risk of reactivation of chronic hepatitis B. Although hepatitis B reactivation is very rare (< 1%) with ICI therapy[44], it can also occur with other co-administered chemotherapies or during treatment of ICH with corticosteroids. Therefore, patients should have their hepatitis B status checked routinely prior to commencing treatment with ICIs[45] and be considered for prophylactic antiviral therapy. Although a flare of hepatitis C virus (HCV) secondary to ICI therapy has not been previously reported[4,5], patients with untreated HCV should have close monitoring of their viral load and LFTs, which may both fluctuate during treatment[46]. Indeed, anti-PD1 treatment has been shown to facilitate control of chronic HCV infection[47] with some patients achieving dramatic reductions in their viral load and normalization of their ALT[46].

Role of liver biopsy

Although a liver biopsy is useful to exclude differential diagnoses and assess the degree of liver inflammation, it is usually not necessary in the work-up and ma-

agement of ICH. Its invasive nature and cost, means it is generally reserved for situations when the diagnosis is unclear despite non-invasive investigations or the clinical course is atypical and not responding to standard treatments. Histological findings in ICH is variable but typically demonstrate lobular and/or periportal inflammation[36]. Centrilobular necrosis and central endothelialitis may also be present. Some distinct phenotypes may exist with granulomatous hepatitis reported in patients treated with CTLA-4 inhibitors, and a lobular, non-granulomatous hepatitis in those treated with anti-PD-1/anti-PD-L1 antibodies. Inflammatory infiltrates in ICH are predominantly activated T-lymphocytes (mainly CD8+) and histiocytes with few or no plasma cells[36]. Comparatively, patients with autoimmune hepatitis flares have proportionately more CD20+ B lymphocytes and CD4+ T-lymphocytes[48]. **Figure 1** presents two distinct histologic presentations of ICI-induced hepatotoxicity.

Assessing causality and grading severity

Establishing causality for ICI causing hepatotoxicity begins with excluding differential diagnoses as outlined above. Formal scoring systems such as the Roussel Uclaf Causality Assessment Method (RUCAM) provide a useful framework and are often used in the DILI research setting but less so in clinical practice[49]. One problem with RUCAM is the difficulty in achieving scores to classify patients as having 'definite' or 'highly probable' DILI without rechallenging the patient with ICI which is not always safe to do. Instead the majority of patients are labelled as 'probable' DILI[39].

Once a diagnosis of ICH is judged to be the likely cause of the patient's deranged LFTs, the severity of hepatotoxicity should be graded as it determines the treatment. Most oncology clinical trials report the severity of liver injury according to the CTCAE whereas the DILI Network (DILIN) severity index is commonly used for grading DILI severity. Both grading systems take into account the patient's symptoms, degree of liver enzyme and bilirubin derangement and/or international normalized ratio (DILIN only) (**Table 3**). It should be noted that neither CTCAE nor DILIN systems were devised specifically for grading ICH, but rather for raised LFTs secondary to any anti-cancer therapy.

MANAGEMENT OF ICH

As ICH is a relatively new entity, there have been no prospective randomized controlled trials evaluating different treatment recommendations. Thus, current international treatment guidelines are all based on low level evidence (case series and expert opinion). **Table 4** outlines treatment recommendations from major oncology and hepatology societies for each CTCAE grade of ICH. Importantly, treatment should be patient-centred with their active involvement in decision making throughout.

As with any other DILI, temporary or permanent discontinuation of the culprit agent should be the first step and is recommended by all society guidelines for moderate (\geq grade 2) ICH. Therefore, LFTs should be checked at baseline and prior to each dose of ICI. Since the pathogenesis of hepatotoxicity is immune-mediated, immunosuppression is the other mainstay of treatment. Although minor differences exist between guidelines, they generally all follow a stepwise algorithm involving withholding or ceasing ICI, followed by corticosteroid treatment [oral prednisolone or intravenous (IV) methylprednisolone] and further immunosuppression [mycophenolate mofetil (MMF), calcineurin inhibitors and anti-thymocyte antibodies *etc.*] depending on the initial severity and response to subsequent treatment.

Withdrawal of ICI

A considerable proportion of patients can undergo resolution of ICH without need for immunosuppressive therapy. At least three small case series ($n = 6-16$) have reported ICH resolution rates of 38%-50% by simply withholding the ICI even in those with grade 3/4 disease[36,50,51]. However, most society guidelines recommend starting corticosteroids for patients with \geq grade 2 ICH, highlighting that guideline recommendations should always be applied in the appropriate clinical context. Therefore, a period of close LFTs monitoring after withholding ICI (daily to weekly depending on severity of ICH) may be useful in helping some patients avoid unnecessary immunosuppression and their related side effects. This period of observation is particularly important in cases where ICI has been co-administered with other potentially hepatotoxic drugs. Cessation of these drugs (without immunosuppression) may lead to recovery if they were the main culprit for the liver injury. Whether ICI therapy should be temporarily or permanently ceased will be discussed later.

Table 3 Comparison of common grading systems for inhibitor-related hepatotoxicity

| Grade | | Grade 1 | Grade 2 | Grade 3 | Grade 4 | Grade 5 |
|------------|--|--|---|--|--|---------|
| CTCAE [87] | (1) Asymptomatic; (2) AST or ALT > 1-3 × more than ULN; and (3) T. Bil > 1-1.5 × more than ULN | (1) Asymptomatic; (2) AST or ALT > 3-5 × more than ULN; and (3) T. Bil > 1.5-3 × more than ULN | (1) Symptomatic liver dysfunction; (2) Fibrosis on biopsy; (3) Compensated cirrhosis; (4) Reactivation of chronic hepatitis; (5) AST or ALT > 5-20 × more than ULN; and (6) T. Bil > 3-10 × more than ULN | (1) Decompensated liver function (<i>e.g.</i> , ascites, coagulopathy, encephalopathy, coma); (2) AST or ALT > 20 × more than ULN; and (3) T. Bil > 10 × more than ULN | Death due to hepatotoxicity | |
| DILIN [73] | (1) Elevations in serum ALT and/or ALP levels; (2) T. Bil < 2.5 ULN; (3) INR < 1.5; and (4) Present with or without symptoms (fatigue, asthenia, nausea, anorexia, RUQ pain, jaundice, pruritus, rashes, or weight loss) | (1) Elevated serum ALT and/or ALP; (2) T. Bil ≥ 2.5 ULN or INR ≥ 1.5; and (3) Symptoms may become aggravated | (1) Elevated serum ALT and/or ALP; (2) T. Bil ≥ 5 ULN ± INR ≥ 1.5; (3) Symptoms are further aggravated; (4) Indication for hospitalization; and (5) No evidence of hepatic encephalopathy | (1) Coagulation abnormality indicated by INR ≥ 1.5; (2) Signs of hepatic encephalopathy; (3) T. Bil ≥ 10 ULN or daily elevation ≥ 1.0 mg/dL in 26 wk after the DILI onset; and (4) Ascites and DILI-related dysfunction of another organ | (1) Death due to DILI; and (2) Or need to receive liver transplantation for survival | |

ALT: Alanine Aminotransferase; AST: Aspartate aminotransferase; CTCAE: Common terminology criteria for adverse events; DILI: Drug induced liver injury; DILIN: Drug-induced Liver Injury Network; ICH: Immune checkpoint inhibitor-induced hepatotoxicity; INR: International normalized ratio; RUQ: Right upper quadrant; T. Bil: Total bilirubin; ULN: Upper limit of normal.

Corticosteroids

As discussed above, commencement of corticosteroids is not essential but something to be considered depending on the severity of ICH and initial response in LFTs after withholding ICI. Oral prednisolone at a dose of 0.5-1 mg/kg of body weight is the recommended for patients with grade 2 hepatotoxicity and IV boluses of methylprednisolone 1-2 mg/kg of body weight for patients with grade 3/4 toxicity. It is important to note these dosing regimens are not derived from comparative studies but were instead extrapolated from treatment of other irAEs or autoimmune hepatitis. Indeed, higher doses of corticosteroids (> 60 mg daily of oral prednisolone) has not been shown to confer additional benefit in time to hepatitis resolution compared to lower doses[20]. A therapeutic response and eventual resolution of ICH is achieved in the majority of patients by withholding ICI and commencing corticosteroids[36]. This should be evident after 2-3 d of treatment[52]. Once a response is seen, steroids should then be tapered gradually over at least 4 wk to minimize the risk of rebound hepatitis [53]. As for other conditions, patients receiving systemic corticosteroids should be monitored for its complications including infection, hyperglycemia, and psychosis.

Refractory disease

A minority of patients either do not respond or fail to normalize their LFTs back to baseline despite corticosteroid treatment. If there is no response with oral prednisolone, IV methylprednisolone can be considered. In the setting ICH that is refractory to both oral and IV corticosteroids, MMF has been the preferred second-line agent at a dose of 500-1000 mg twice daily (Table 4). Azathioprine is the first-line steroid-sparing agent used in autoimmune hepatitis. Although its use has been reported in ICH, it is usually not favored because its immunosuppressive effect takes several months to peak and its metabolites can cause hepatotoxicity[54-56]. The main side effects from MMF are gastrointestinal upset (abdominal pain, nausea, vomiting and diarrhea) and cytopenia.

For ICH refractory to corticosteroids and MMF, collective experience is limited to case reports. Calcineurin inhibitors (tacrolimus and cyclosporine) have been used with varying success in autoimmune hepatitis and form the backbone of liver transplant rejection treatment[57]. Their mechanism of action against T cell mediated liver inflammation makes them a logical choice in treatment-refractory ICH. Calcineurin inhibitors [20,56] along with other agents including anti-thymocyte globulin therapy[58], tocilizumab[59], plasma exchange[60] and even infliximab have all been used successfully to treat steroid-refractory ICH[61]. However, infliximab is not recommended by most guidelines since it can cause an autoimmune phenotype DILL, albeit rarely[62]. If not done prior, a liver biopsy should be strongly considered before commencing these third-line immunosuppressive agents.

Table 4 Comparison of management recommendations for inhibitor-related hepatotoxicity by major expert societies

| Grade | FDA[88] | Society of Immunotherapy of Cancer[89] | American Society of Clinical Oncology [90] | European Society for Medical Oncology[91] | Australian (eVIQ Guidelines)[53] | European Association for the Study of Liver[52] |
|---------|--|---|--|--|--|---|
| Grade 1 | (1) Monitor closely; (2) Continue ICI; and (3) Investigate for other causes of hepatitis | (1) Monitor closely; (2) Continue ICI; and (3) Investigate for other causes of hepatitis | (1) Monitor closely; (2) Continue ICI; (3) Check LFTs twice a week; and (4) Investigate for other causes of hepatitis | (1) Monitor closely; (2) Continue ICI; (3) Check LFTs weekly; and (4) Investigate for other causes of hepatitis | (1) Continue ICI; (2) Monitor LFTs more closely; and (3) Investigate for other causes of hepatitis | If irAEs are excluded (unlikely or unrelated) continue therapy with close follow-up. Start symptomatic treatment |
| Grade 2 | (1) Withhold ICI; (2) Investigate for other causes of hepatitis; (3) Start prednisone 0.5–1 mg/kg/d of prednisone Po until LFTs improve to < Grade 1 then wean steroids; and (4) Consider restarting when on less than equivalent of prednisone 7.5 mg/d | (1) Withhold ICI; (2) Investigate for other causes of hepatitis; (3) Start prednisone 0.5–1 mg/kg/d Po (or equivalent) with a 4-wk taper; (4) Monitor LFTs twice a week; (5) Liver biopsy optional; and (6) Resume ICI when steroids tapered to 10 mg/d and liver enzymes are grade 1 level or better | (1) Withhold ICI; (2) Investigate for other causes of hepatitis; (3) Monitor LFTs every 3 d and if no improvement start prednisone 0.5–1 mg/kg/d Po (or equivalent); and (4) Resume ICI when LFTs grade 1 level while on less than prednisolone 10 mg/d (taper over a month) | (1) Withhold ICI; (2) Investigate for other causes of hepatitis; (3) Recheck LFTs/INR every 3 d; (4) If LFTs increase on subsequent check after stopping checkpoint inhibitor, start oral prednisolone 1 mg/kg/d; (5) Once LFTs return to grade 1, start weaning steroids; and (6) Resume ICI when liver enzymes are grade 1 level or better while on less than prednisolone 10 mg/d | (1) Withhold ICI; (2) Monitor LFTs every 3 d; (3) Investigate for other causes of hepatitis; (4) Consider corticosteroid therapy for patients who are symptomatic or worsening LFTs; and (5) Resume ICI treatment once corticosteroid treatment is complete and tapered over 4 wk | (1) Skip dose and monitor liver parameters, INR and albumin twice weekly; (2) Start symptomatic treatment; (3) If abnormal liver parameters persist longer than 2 wk, start immunosuppression and discontinue the drug; and (4) Upon improvement immunotherapy could be resumed after corticosteroid tapering |
| Grade 3 | (1) Permanently cease ICI; (2) Start prednisone at 1–2 mg/kg/d Po (or equivalent); (3) Consider imaging and liver biopsy while assessing for alternative causes of hepatitis | (1) Permanently cease ICI; (2) Monitor complete metabolic panel every 1–2 d; (3) Start prednisone at 1–2 mg/kg/d (or equivalent); (4) If refractory to steroids, consider adding MMF. Once LFTs improve, taper over 4 wk; and (5) Consider liver biopsy | (1) Permanently discontinue medication; (2) Consider hospitalization and start IV 1–2 mg/kg/d methylprednisolone; (3) If no improvement in 3 d consider adding secondary agent; (4) Monitor LFTs daily/every other day; (5) Once LFTs improve will need to wean steroids over 4–6 wk; and (6) Do not offer infliximab | (1) Withhold ICI; (2) Investigate for other causes of hepatitis; (3) Recheck LFTs/INR daily; (4) Consider hospitalization; (5) Start prednisolone 1 mg/kg/d Po if ALT/AST < 400 U/L and normal bilirubin/albumin/INR OR start IV methylprednisolone 2 mg/kg/d if ALT/AST > 400 U/L or elevated bilirubin/INR or decreased albumin; (6) Once LFTs improve to grade 2, can switch to PO steroids and wean over 4 wk; (7) Consider rechallenge at discretion of consultant; (8) If no improvement on steroids, consider adding mycophenolate and/or tacrolimus; and (9) Do not offer infliximab | (1) Permanently discontinue treatment; (2) Investigate for other causes of hepatitis; (3) Consider liver biopsy; (4) Hospitalize patient if unwell; (5) Urgent administration of start IV 1–2 mg/kg/d methylprednisolone For 3 d, following high dose oral prednisolone; and (6) If no improvement on steroids, urgent referral to a gastroenterologist to prescribe other steroid-sparing agents | (1) Discontinue immunotherapy and monitor liver parameters. Consider permanent discontinuation of immunotherapy; (2) Start corticosteroids (methylprednisolone or equivalent) at a dose of 1–2 mg/kg/d depending on severity; (3) If there is no response to corticosteroids within 2–3 d, MMF should be added at 1000 mg twice daily; (4) Further immunosuppression: MMF, cyclosporine, tacrolimus, anti-thymocyte antibodies; and (5) Infliximab is not recommended |
| Grade 4 | (1) Permanently cease ICI; (2) Start prednisone at 1–2 mg/kg/d Po (or equivalent); and (3) Consider imaging and liver biopsy while assessing for alternative causes of hepatitis | (1) Permanently cease ICI; (2) Start prednisone at 1–2 mg/kg/d Po (or equivalent); (3) Monitor complete metabolic panel every 1–2 d; (4) If refractory to steroids, consider adding MMF. LFTs improve, taper over 4 wk; and (5) Consider liver biopsy | (1) Permanently discontinue medication; (2) Consider hospitalization and start IV 2 mg/kg/d methylprednisolone; (3) Add MMF if no improvement in 72 h; (4) Consider transfer to tertiary center with hepatology consultation if no improvement; (5) Do not offer infliximab; and (6) If LFTs improve, will need steroid wean over 4–6 wk | (1) Permanently discontinue medication; (2) Consider hospitalization and start IV methylprednisolone 2 mg/kg/d; (3) Formal hepatology consultation; (4) Consider liver biopsy; (5) If no improvement on IV steroids, add MMF and/or tacrolimus; (6) Do not offer infliximab; and (7) Once LFTs improve to > grade 2, can switch to oral steroids and wean over 4 wk | (1) Permanently discontinue treatment; (2) Investigate for other causes of hepatitis; (3) Consider liver biopsy; (4) Hospitalize patient if unwell; (5) Urgent administration of start IV 1–2 mg/kg/d Methylprednisolone. For 3 d, following high dose oral prednisolone; and (6) If no improvement on steroids, urgent referral to a gastroenterologist to prescribe other steroid-sparing agents | |

Grading of severity is according to common terminology criteria for adverse events. ALT: Alanine aminotransferase; AST: Aspartate aminotransferase; FDA: United States Food and Drug Administration; ICI: Immune checkpoint inhibitor; INR: International normalized ratio; irAEs: Immune-related adverse events; IV: Intravenous; LFTs: Liver function tests; MMF: Mycophenolate mofetil; PO: Per oral.

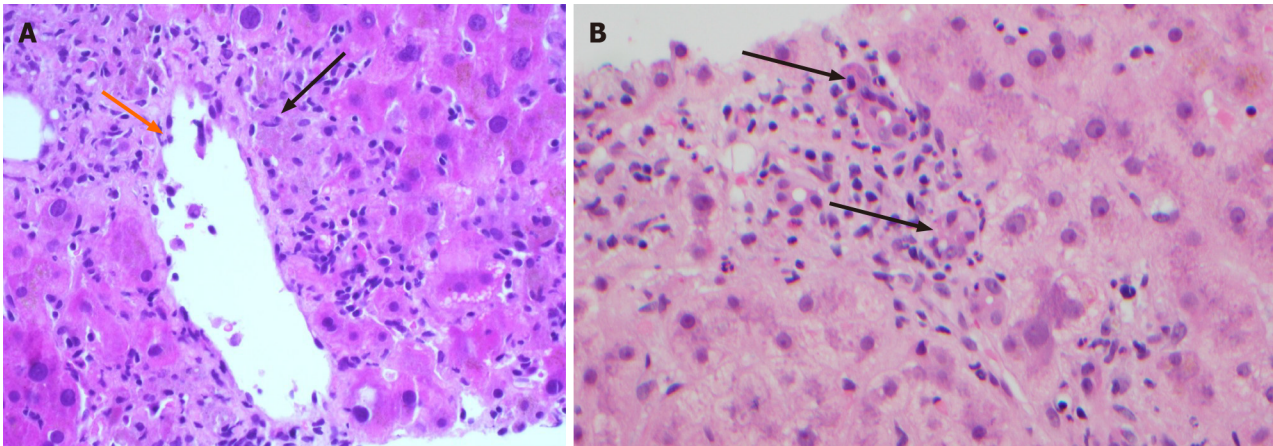


Figure 1 Histopathological changes of inhibitor-related hepatotoxicity. A: Prominent perivenulitis (black arrow) with endothelialitis (orange arrow) in a case of ipilimumab related hepatotoxicity (hematoxylin and eosin, 400 ×); B: Lymphocytic cholangitis with prominent duct damage secondary to nivolumab (black arrows; hematoxylin and eosin, 400 ×).

As aforementioned, ICH can also present as an immune-mediated cholangiopathy, especially in those receiving PD-1/PD-L1 inhibitors. In this entity, the inflammation is centred around the biliary tree with CD8+ T cell infiltration seen on liver biopsy. Characteristically has a moderate to poor response to steroid therapy[63] and the addition of ursodeoxycholic acid to immunosuppression may be helpful[64].

Ongoing monitoring and prognosis

Once a response is achieved, patients should have ongoing monitoring for clinical signs and symptoms and LFTs. The monitoring frequency (between daily to weekly) is titrated according to the severity of ICH and rate of improvement after commencing treatment[53]. Subsequent LFTs also help guide decisions regarding weaning of immunosuppression. Importantly, LFTs monitoring (fortnightly to monthly) should continue after apparent resolution of ICH and completion of immunosuppression as rebound hepatitis has been reported in up to a third of patients[65].

Although the majority of ICH patients recover and deaths due to hepatitis very rarely occur, the impact of ICH and its treatment on cancer outcomes is unclear. In a study of 491 pembrolizumab-treated patients, Tsung *et al*[39] demonstrated that development of liver injury portended worse overall survival compared to those without liver injury[39]. On sub-analysis, patients with liver injury due to 'probable' ICH exhibited significantly better survival compared to those with other causes of liver injury (*e.g.*, hepatic metastases). In contrast, corticosteroid treatment in melanoma patients with irAEs (including ICH) after CTLA-4 blockade did not impact on treatment response or survival[66,67].

As patients receiving ICI typically have advanced (incurable) malignancy, referral to palliative care services should be considered if not already done so. Palliative care services may assist clinicians and patients with managing the symptoms arising from irAEs, making treatment decisions (including when to cease therapy), and future planning. Early referral to palliative care has been shown to significantly improve patient physical and psychological symptoms, quality of life, and treatment satisfaction[68].

Restarting vs permanently ceasing ICI

The decision on whether to restart or permanently cease ICI is a difficult one. Although current guidelines recommend temporarily withholding ICI in grade 2 ICH and permanently ceasing in grade 3/4 (Table 4), the decision is often more challenging and involves weighing up the ICH (its severity and response to immunosuppression) against the advanced cancer (its current activity, response to ICI and other available treatment options). Furthermore, multiple case reports have described successful

reintroduction of ICI without ICH recurrence despite initial grade 3/4 hepatotoxicity. Other promising strategies include co-administration of budesonide (corticosteroid with high first-pass metabolism) when rechallenging with ICI[69] or resuming anti-PD-1 monotherapy in patients with severe toxicity from combination ICI therapy[70]. However, these approaches need confirmatory study before they can be widely adopted. At present, the decision to rechallenge with ICI should still be determined on a case-by-case basis through multidisciplinary discussion.

FUTURE DIRECTIONS

As the indications and frequency of ICI use expand, recognition and management of ICH will be an increasingly important issue. Current guideline recommendations are based on experience found in retrospective case series due to relatively low numbers of patients developing ICH overall (especially those who are steroid refractory). In order to strengthen the evidence base in this area, clearly both prospective large observational registries and eventually randomized controlled trials are needed. This would almost certainly involve collaborations across many centers for patient recruitment. Our rudimentary knowledge of the pathobiology behind ICH also limits our ability to predict which patients will develop it and who will respond to treatment. Therefore, efforts at the basic science level to study the genetic and immune profile of ICH patients are equally important. As our knowledge and experience increases, ICI selection may be personalized to each individual in the future not only with regards to their cancer response but also their risk of developing ICH and how best to treat it.

CONCLUSION

In summary, we have arrived at a new era of cancer therapy where ICI will form the backbone of many regimens. Uncommonly, these treatments are complicated by ICH which can be severe. After excluding key differential diagnoses, the management algorithm follows a stepwise escalation in immunosuppression. The majority of patients recover with some being able to recommence ICI therapy. Future studies are needed to boost the evidence base and hence confidence behind current treatment recommendations.

REFERENCES

- 1 **Xu W**, Liu K, Chen M, Sun JY, McCaughan GW, Lu XJ, Ji J. Immunotherapy for hepatocellular carcinoma: recent advances and future perspectives. *Ther Adv Med Oncol* 2019; **11**: 1758835919862692 [PMID: 31384311 DOI: 10.1177/1758835919862692]
- 2 **Hodi FS**, O'Day SJ, McDermott DF, Weber RW, Sosman JA, Haanen JB, Gonzalez R, Robert C, Schadendorf D, Hassel JC, Akerley W, van den Eertwegh AJ, Lutzky J, Lorigan P, Vaubel JM, Linette GP, Hogg D, Ottensmeier CH, Lebbé C, Peschel C, Quirt I, Clark JI, Wolchok JD, Weber JS, Tian J, Yellin MJ, Nichol GM, Hoos A, Urba WJ. Improved survival with ipilimumab in patients with metastatic melanoma. *N Engl J Med* 2010; **363**: 711-723 [PMID: 20525992 DOI: 10.1056/NEJMoa1003466]
- 3 **Finn RS**, Qin S, Ikeda M, Galle PR, Ducreux M, Kim TY, Kudo M, Breder V, Merle P, Kaseb AO, Li D, Verret W, Xu DZ, Hernandez S, Liu J, Huang C, Mulla S, Wang Y, Lim HY, Zhu AX, Cheng AL; IMbrave150 Investigators. Atezolizumab plus Bevacizumab in Unresectable Hepatocellular Carcinoma. *N Engl J Med* 2020; **382**: 1894-1905 [PMID: 32402160 DOI: 10.1056/NEJMoa1915745]
- 4 **El-Khoueiry AB**, Sangro B, Yau T, Crocenzi TS, Kudo M, Hsu C, Kim TY, Choo SP, Trojan J, Welling TH Rd, Meyer T, Kang YK, Yeo W, Chopra A, Anderson J, Dela Cruz C, Lang L, Neely J, Tang H, Dastani HB, Melero I. Nivolumab in patients with advanced hepatocellular carcinoma (CheckMate 040): an open-label, non-comparative, phase 1/2 dose escalation and expansion trial. *Lancet* 2017; **389**: 2492-2502 [PMID: 28434648 DOI: 10.1016/S0140-6736(17)31046-2]
- 5 **Finn RS**, Ryoo BY, Merle P, Kudo M, Bouattour M, Lim HY, Breder V, Edeline J, Chao Y, Ogasawara S, Yau T, Garrido M, Chan SL, Knox J, Daniele B, Ebbinghaus SW, Chen E, Siegel AB, Zhu AX, Cheng AL; KEYNOTE-240 investigators. Pembrolizumab As Second-Line Therapy in Patients With Advanced Hepatocellular Carcinoma in KEYNOTE-240: A Randomized, Double-Blind, Phase III Trial. *J Clin Oncol* 2020; **38**: 193-202 [PMID: 31790344 DOI: 10.1200/JCO.19.01307]
- 6 **Liu K**, Zhang X, Xu W, Chen J, Yu J, Gamble JR, McCaughan GW. Targeting the vasculature in hepatocellular carcinoma treatment: Starving vs normalizing blood supply. *Clin Transl Gastroenterol*

- 2017; **8**: e98 [DOI: [10.1038/ctg.2017.28](https://doi.org/10.1038/ctg.2017.28)]
- 7 **Wang DY**, Salem JE, Cohen JV, Chandra S, Menzer C, Ye F, Zhao S, Das S, Beckermann KE, Ha L, Rathmell WK, Ancell KK, Balko JM, Bowman C, Davis EJ, Chism DD, Horn L, Long GV, Carlino MS, Lebrun-Vignes B, Eroglu Z, Hassel JC, Menzies AM, Sosman JA, Sullivan RJ, Moslehi JJ, Johnson DB. Fatal Toxic Effects Associated With Immune Checkpoint Inhibitors: A Systematic Review and Meta-analysis. *JAMA Oncol* 2018; **4**: 1721-1728 [PMID: [30242316](https://pubmed.ncbi.nlm.nih.gov/30242316/) DOI: [10.1001/jamaoncol.2018.3923](https://doi.org/10.1001/jamaoncol.2018.3923)]
 - 8 **Sznol M**, Ferrucci PF, Hogg D, Atkins MB, Wolter P, Guidoboni M, Lebbé C, Kirkwood JM, Schachter J, Daniels GA, Hassel J, Cebon J, Gerritsen W, Atkinson V, Thomas L, McCaffrey J, Power D, Walker D, Bhorre R, Jiang J, Hodi FS, Wolchok JD. Pooled Analysis Safety Profile of Nivolumab and Ipilimumab Combination Therapy in Patients With Advanced Melanoma. *J Clin Oncol* 2017; **35**: 3815-3822 [PMID: [28915085](https://pubmed.ncbi.nlm.nih.gov/28915085/) DOI: [10.1200/JCO.2016.72.1167](https://doi.org/10.1200/JCO.2016.72.1167)]
 - 9 **Topalian SL**, Sznol M, McDermott DF, Kluger HM, Carvajal RD, Sharfman WH, Brahmer JR, Lawrence DP, Atkins MB, Powderly JD, Leming PD, Lipson EJ, Puzanov I, Smith DC, Taube JM, Wigginton JM, Kollia GD, Gupta A, Pardoll DM, Sosman JA, Hodi FS. Survival, durable tumor remission, and long-term safety in patients with advanced melanoma receiving nivolumab. *J Clin Oncol* 2014; **32**: 1020-1030 [PMID: [24590637](https://pubmed.ncbi.nlm.nih.gov/24590637/) DOI: [10.1200/JCO.2013.53.0105](https://doi.org/10.1200/JCO.2013.53.0105)]
 - 10 **Sharpe AH**. Introduction to checkpoint inhibitors and cancer immunotherapy. *Immunol Rev* 2017; **276**: 5-8 [PMID: [28258698](https://pubmed.ncbi.nlm.nih.gov/28258698/) DOI: [10.1111/imr.12531](https://doi.org/10.1111/imr.12531)]
 - 11 **Chascsa DM**, Rakela J. Knowns and unknowns: the safety and efficacy of cancer immunotherapy in chronic liver disease. *Curr Hepatol Rep* 2018; **17**: 153-155 [DOI: [10.1007/s11901-018-0408-8](https://doi.org/10.1007/s11901-018-0408-8)]
 - 12 **Weber JS**, Hodi FS, Wolchok JD, Topalian SL, Schadendorf D, Larkin J, Sznol M, Long GV, Li H, Waxman IM, Jiang J, Robert C. Safety Profile of Nivolumab Monotherapy: A Pooled Analysis of Patients With Advanced Melanoma. *J Clin Oncol* 2017; **35**: 785-792 [PMID: [28068177](https://pubmed.ncbi.nlm.nih.gov/28068177/) DOI: [10.1200/JCO.2015.66.1389](https://doi.org/10.1200/JCO.2015.66.1389)]
 - 13 **Ascierto PA**, Del Vecchio M, Robert C, Mackiewicz A, Chiarion-Sileni V, Arance A, Lebbé C, Bastholt L, Hamid O, Rutkowski P, McNeil C, Garbe C, Loquai C, Dreno B, Thomas L, Grob JJ, Liszkay G, Nyakas M, Gutzmer R, Pikiel J, Grange F, Hoeller C, Ferraresi V, Smylie M, Schadendorf D, Mortier L, Svane IM, Hennicken D, Qureshi A, Maio M. Ipilimumab 10 mg/kg versus ipilimumab 3 mg/kg in patients with unresectable or metastatic melanoma: a randomised, double-blind, multicentre, phase 3 trial. *Lancet Oncol* 2017; **18**: 611-622 [PMID: [28359784](https://pubmed.ncbi.nlm.nih.gov/28359784/) DOI: [10.1016/S1470-2045\(17\)30231-0](https://doi.org/10.1016/S1470-2045(17)30231-0)]
 - 14 **Lewis AM**, Croughan WD, Aranibar N, Lee AG, Warrack B, Abu-Absi NR, Patel R, Drew B, Borys MC, Reily MD, Li ZJ. Understanding and Controlling Sialylation in a CHO Fc-Fusion Process. *PLoS One* 2016; **11**: e0157111 [PMID: [27310468](https://pubmed.ncbi.nlm.nih.gov/27310468/) DOI: [10.1371/journal.pone.0157111](https://doi.org/10.1371/journal.pone.0157111)]
 - 15 **Highlights of prescribing information.** Imfinzi (Durvalumab). [cited 20 January 2021]. Available from: https://www.accessdata.fda.gov/drugsatfda_docs/label/2020/761069s0181bl.pdf
 - 16 **Highlights of prescribing information.** Tecentriq (Atezolizumab). [cited 20 January 2021]. Available from: https://www.accessdata.fda.gov/drugsatfda_docs/label/2020/761034s0281bl.pdf
 - 17 **Lanitis T**, Proskorovsky I, Ambavane A, Hunger M, Zheng Y, Bharmal M, Phatak H. Survival Analysis in Patients with Metastatic Merkel Cell Carcinoma Treated with Avelumab. *Adv Ther* 2019; **36**: 2327-2341 [PMID: [31350728](https://pubmed.ncbi.nlm.nih.gov/31350728/) DOI: [10.1007/s12325-019-01034-0](https://doi.org/10.1007/s12325-019-01034-0)]
 - 18 **Wang PF**, Chen Y, Song SY, Wang TJ, Ji WJ, Li SW, Liu N, Yan CX. Immune-Related Adverse Events Associated with Anti-PD-1/PD-L1 Treatment for Malignancies: A Meta-Analysis. *Front Pharmacol* 2017; **8**: 730 [PMID: [29093678](https://pubmed.ncbi.nlm.nih.gov/29093678/) DOI: [10.3389/fphar.2017.00730](https://doi.org/10.3389/fphar.2017.00730)]
 - 19 **Intlekofer AM**, Thompson CB. At the bench: preclinical rationale for CTLA-4 and PD-1 blockade as cancer immunotherapy. *J Leukoc Biol* 2013; **94**: 25-39 [PMID: [23625198](https://pubmed.ncbi.nlm.nih.gov/23625198/) DOI: [10.1189/jlb.1212621](https://doi.org/10.1189/jlb.1212621)]
 - 20 **Cheung V**, Gupta T, Payne M, Middleton MR, Collier JD, Simmons A, Klenerman P, Brain O, Cobbold JF. Immunotherapy-related hepatitis: real-world experience from a tertiary centre. *Frontline Gastroenterol* 2019; **10**: 364-371 [PMID: [31656561](https://pubmed.ncbi.nlm.nih.gov/31656561/) DOI: [10.1136/flgastro-2018-101146](https://doi.org/10.1136/flgastro-2018-101146)]
 - 21 **Mizuno K**, Ito T, Ishigami M, Ishizu Y, Kuzuya T, Honda T, Kawashima H, Inukai Y, Toyoda H, Yokota K, Hase T, Maeda O, Kiyoi H, Nagino M, Hibi H, Kodera Y, Fujimoto Y, Sone M, Gotoh M, Ando Y, Akiyama M, Hasegawa Y, Fujishiro M. Real world data of liver injury induced by immune checkpoint inhibitors in Japanese patients with advanced malignancies. *J Gastroenterol* 2020; **55**: 653-661 [PMID: [32124082](https://pubmed.ncbi.nlm.nih.gov/32124082/) DOI: [10.1007/s00535-020-01677-9](https://doi.org/10.1007/s00535-020-01677-9)]
 - 22 **Wang W**, Lie P, Guo M, He J. Risk of hepatotoxicity in cancer patients treated with immune checkpoint inhibitors: A systematic review and meta-analysis of published data. *Int J Cancer* 2017; **141**: 1018-1028 [PMID: [28263392](https://pubmed.ncbi.nlm.nih.gov/28263392/) DOI: [10.1002/ijc.30678](https://doi.org/10.1002/ijc.30678)]
 - 23 **Johnson DB**, Sullivan RJ, Ott PA, Carlino MS, Khushalani NI, Ye F, Guminski A, Puzanov I, Lawrence DP, Buchbinder EI, Mudigonda T, Spencer K, Bender C, Lee J, Kaufman HL, Menzies AM, Hassel JC, Mehnert JM, Sosman JA, Long GV, Clark JI. Ipilimumab Therapy in Patients With Advanced Melanoma and Preexisting Autoimmune Disorders. *JAMA Oncol* 2016; **2**: 234-240 [PMID: [26633184](https://pubmed.ncbi.nlm.nih.gov/26633184/) DOI: [10.1001/jamaoncol.2015.4368](https://doi.org/10.1001/jamaoncol.2015.4368)]
 - 24 **Menzies AM**, Johnson DB, Ramanujam S, Atkinson VG, Wong ANM, Park JJ, McQuade JL, Shoushtari AN, Tsai KK, Eroglu Z, Klein O, Hassel JC, Sosman JA, Guminski A, Sullivan RJ, Ribas A, Carlino MS, Davies MA, Sandhu SK, Long GV. Anti-PD-1 therapy in patients with advanced melanoma and preexisting autoimmune disorders or major toxicity with ipilimumab. *Ann Oncol* 2017; **28**: 368-376 [PMID: [27687304](https://pubmed.ncbi.nlm.nih.gov/27687304/) DOI: [10.1093/annonc/mdw443](https://doi.org/10.1093/annonc/mdw443)]
 - 25 **Kudo M**, Matilla A, Santoro A, Melero I, Sangro B. Checkmate-040: Nivolumab (NIVO) in patients

- (pts) with advanced hepatocellular carcinoma (aHCC) and Child-Pugh B (CPB) status. *J Clin Oncol* 2019; **37**: 327 [DOI: [10.1200/JCO.2019.37.4_suppl.327](https://doi.org/10.1200/JCO.2019.37.4_suppl.327)]
- 26 **Abdel-Wahab N**, Safa H, Abudayyeh A, Johnson DH, Trinh VA, Zobniw CM, Lin H, Wong MK, Abdelrahim M, Gaber AO, Suarez-Almazor ME, Diab A. Checkpoint inhibitor therapy for cancer in solid organ transplantation recipients: an institutional experience and a systematic review of the literature. *J Immunother Cancer* 2019; **7**: 106 [PMID: [30992053](https://pubmed.ncbi.nlm.nih.gov/30992053/) DOI: [10.1186/s40425-019-0585-1](https://doi.org/10.1186/s40425-019-0585-1)]
 - 27 **Kumar V**, Shinagare AB, Rennke HG, Ghai S, Lorch JH, Ott PA, Rahma OE. The Safety and Efficacy of Checkpoint Inhibitors in Transplant Recipients: A Case Series and Systematic Review of Literature. *Oncologist* 2020; **25**: 505-514 [PMID: [32043699](https://pubmed.ncbi.nlm.nih.gov/32043699/) DOI: [10.1634/theoncologist.2019-0659](https://doi.org/10.1634/theoncologist.2019-0659)]
 - 28 **Munker S**, De Toni EN. Use of checkpoint inhibitors in liver transplant recipients. *United European Gastroenterol J* 2018; **6**: 970-973 [PMID: [30228883](https://pubmed.ncbi.nlm.nih.gov/30228883/) DOI: [10.1177/2050640618774631](https://doi.org/10.1177/2050640618774631)]
 - 29 **König D**, Läubli H. Mechanisms of Immune-Related Complications in Cancer Patients Treated with Immune Checkpoint Inhibitors. *Pharmacology* 2021; **106**: 123-136 [PMID: [32721966](https://pubmed.ncbi.nlm.nih.gov/32721966/) DOI: [10.1159/000509081](https://doi.org/10.1159/000509081)]
 - 30 **Alessandrino F**, Tirumani SH, Krajewski KM, Shinagare AB, Jagannathan JP, Ramaiya NH, Di Salvo DN. Imaging of hepatic toxicity of systemic therapy in a tertiary cancer centre: chemotherapy, haematopoietic stem cell transplantation, molecular targeted therapies, and immune checkpoint inhibitors. *Clin Radiol* 2017; **72**: 521-533 [PMID: [28476244](https://pubmed.ncbi.nlm.nih.gov/28476244/) DOI: [10.1016/j.crad.2017.04.003](https://doi.org/10.1016/j.crad.2017.04.003)]
 - 31 **Weber JS**, Kähler KC, Hauschild A. Management of immune-related adverse events and kinetics of response with ipilimumab. *J Clin Oncol* 2012; **30**: 2691-2697 [PMID: [22614989](https://pubmed.ncbi.nlm.nih.gov/22614989/) DOI: [10.1200/JCO.2012.41.6750](https://doi.org/10.1200/JCO.2012.41.6750)]
 - 32 **Fashoyin-Aje L**, Donoghue M, Chen H, He K, Veeraraghavan J, Goldberg KB, Keegan P, McKee AE, Pazdur R. FDA Approval Summary: Pembrolizumab for Recurrent Locally Advanced or Metastatic Gastric or Gastroesophageal Junction Adenocarcinoma Expressing PD-L1. *Oncologist* 2019; **24**: 103-109 [PMID: [30120163](https://pubmed.ncbi.nlm.nih.gov/30120163/) DOI: [10.1634/theoncologist.2018-0221](https://doi.org/10.1634/theoncologist.2018-0221)]
 - 33 **Ready N**, Farago AF, de Braud F, Atmaca A, Hellmann MD, Schneider JG, Spigel DR, Moreno V, Chau I, Hann CL, Eder JP, Steele NL, Pieters A, Fairchild J, Antonia SJ. Third-Line Nivolumab Monotherapy in Recurrent SCLC: CheckMate 032. *J Thorac Oncol* 2019; **14**: 237-244 [PMID: [30316010](https://pubmed.ncbi.nlm.nih.gov/30316010/) DOI: [10.1016/j.jtho.2018.10.003](https://doi.org/10.1016/j.jtho.2018.10.003)]
 - 34 **Suzman DL**, Pelosof L, Rosenberg A, Avigan MI. Hepatotoxicity of immune checkpoint inhibitors: An evolving picture of risk associated with a vital class of immunotherapy agents. *Liver Int* 2018; **38**: 976-987 [PMID: [29603856](https://pubmed.ncbi.nlm.nih.gov/29603856/) DOI: [10.1111/liv.13746](https://doi.org/10.1111/liv.13746)]
 - 35 **Jennings JJ**, Mandaliya R, Nakshabandi A, Lewis JH. Hepatotoxicity induced by immune checkpoint inhibitors: a comprehensive review including current and alternative management strategies. *Expert Opin Drug Metab Toxicol* 2019; **15**: 231-244 [PMID: [30677306](https://pubmed.ncbi.nlm.nih.gov/30677306/) DOI: [10.1080/17425255.2019.1574744](https://doi.org/10.1080/17425255.2019.1574744)]
 - 36 **De Martin E**, Michot JM, Papouin B, Champiat S, Mateus C, Lambotte O, Roche B, Antonini TM, Coilly A, Laghouati S, Robert C, Marabelle A, Guettier C, Samuel D. Characterization of liver injury induced by cancer immunotherapy using immune checkpoint inhibitors. *J Hepatol* 2018; **68**: 1181-1190 [PMID: [29427729](https://pubmed.ncbi.nlm.nih.gov/29427729/) DOI: [10.1016/j.jhep.2018.01.033](https://doi.org/10.1016/j.jhep.2018.01.033)]
 - 37 **Imoto K**, Kohjima M, Hioki T, Kurashige T, Kurokawa M, Tashiro S, Suzuki H, Kuwano A, Tanaka M, Okada S, Kato M, Ogawa Y. Clinical Features of Liver Injury Induced by Immune Checkpoint Inhibitors in Japanese Patients. *Can J Gastroenterol Hepatol* 2019; **2019**: 6391712 [PMID: [31929981](https://pubmed.ncbi.nlm.nih.gov/31929981/) DOI: [10.1155/2019/6391712](https://doi.org/10.1155/2019/6391712)]
 - 38 **Fouchard M**, Jantzen H, Quere G, Descourt R, Robinet G, Poureau PG. Three cases of immune cholangitis related to anti-programmed cell death and programmed cell death ligand agents for the treatment of non-small cell lung cancer. *Eur J Cancer* 2019; **115**: 107-110 [PMID: [31132740](https://pubmed.ncbi.nlm.nih.gov/31132740/) DOI: [10.1016/j.ejca.2019.04.022](https://doi.org/10.1016/j.ejca.2019.04.022)]
 - 39 **Tsung I**, Dolan R, Lao CD, Fecher L, Riggenbach K, Yeboah-Korang A, Fontana RJ. Liver injury is most commonly due to hepatic metastases rather than drug hepatotoxicity during pembrolizumab immunotherapy. *Aliment Pharmacol Ther* 2019; **50**: 800-808 [PMID: [31309615](https://pubmed.ncbi.nlm.nih.gov/31309615/) DOI: [10.1111/apt.15413](https://doi.org/10.1111/apt.15413)]
 - 40 **Lynch TJ**, Bondarenko I, Luft A, Serwatowski P, Barlesi F, Chacko R, Sebastian M, Neal J, Lu H, Cuillerot JM, Reck M. Ipilimumab in combination with paclitaxel and carboplatin as first-line treatment in stage IIIB/IV non-small-cell lung cancer: results from a randomized, double-blind, multicenter phase II study. *J Clin Oncol* 2012; **30**: 2046-2054 [PMID: [22547592](https://pubmed.ncbi.nlm.nih.gov/22547592/) DOI: [10.1200/JCO.2011.38.4032](https://doi.org/10.1200/JCO.2011.38.4032)]
 - 41 **Reck M**, Bondarenko I, Luft A, Serwatowski P, Barlesi F, Chacko R, Sebastian M, Lu H, Cuillerot JM, Lynch TJ. Ipilimumab in combination with paclitaxel and carboplatin as first-line therapy in extensive-disease-small-cell lung cancer: results from a randomized, double-blind, multicenter phase 2 trial. *Ann Oncol* 2013; **24**: 75-83 [PMID: [22858559](https://pubmed.ncbi.nlm.nih.gov/22858559/) DOI: [10.1093/annonc/mds213](https://doi.org/10.1093/annonc/mds213)]
 - 42 **Kim KW**, Ramaiya NH, Krajewski KM, Jagannathan JP, Tirumani SH, Srivastava A, Ibrahim N. Ipilimumab associated hepatitis: imaging and clinicopathologic findings. *Invest New Drugs* 2013; **31**: 1071-1077 [PMID: [23408334](https://pubmed.ncbi.nlm.nih.gov/23408334/) DOI: [10.1007/s10637-013-9939-6](https://doi.org/10.1007/s10637-013-9939-6)]
 - 43 **Fohr B**, Dunstan CR, Seibel MJ. Clinical review 165: Markers of bone remodeling in metastatic bone disease. *J Clin Endocrinol Metab* 2003; **88**: 5059-5075 [PMID: [14602728](https://pubmed.ncbi.nlm.nih.gov/14602728/) DOI: [10.1210/jc.2003-030910](https://doi.org/10.1210/jc.2003-030910)]
 - 44 **Wong GL**, Wong VW, Hui VW, Yip TC, Tse YK, Liang LY, Lui RN, Mok TS, Chan HL, Chan SL. Hepatitis Flare During Immunotherapy in Patients With Current or Past Hepatitis B Virus Infection.

- Am J Gastroenterol* 2021; **116**: 1274-1283 [PMID: 33560651 DOI: 10.14309/ajg.0000000000001142]
- 45 **Hwang JP**, Feld JJ, Hammond SP, Wang SH, Alston-Johnson DE, Cryer DR, Hershman DL, Locher AP, Sabichi AL, Symington BE, Terrault N, Wong ML, Somerfield MR, Artz AS. Hepatitis B Virus Screening and Management for Patients With Cancer Prior to Therapy: ASCO Provisional Clinical Opinion Update. *J Clin Oncol* 2020; **38**: 3698-3715 [PMID: 32716741 DOI: 10.1200/JCO.20.01757]
- 46 **Jang S**, Venna S. Antitumor and Anti-Hepatitis C Viral Response After Administration of the Anti-Programmed Death 1 Antibody Pembrolizumab. *J Oncol Pract* 2017; **13**: 462-464 [PMID: 28562196 DOI: 10.1200/JOP.2016.019224]
- 47 **Fuller MJ**, Callendret B, Zhu B, Freeman GJ, Hasselschwert DL, Satterfield W, Sharpe AH, Dustin LB, Rice CM, Grakoui A, Ahmed R, Walker CM. Immunotherapy of chronic hepatitis C virus infection with antibodies against programmed cell death-1 (PD-1). *Proc Natl Acad Sci USA* 2013; **110**: 15001-15006 [PMID: 23980172 DOI: 10.1073/pnas.1312772110]
- 48 **Zen Y**, Yeh MM. Hepatotoxicity of immune checkpoint inhibitors: a histology study of seven cases in comparison with autoimmune hepatitis and idiosyncratic drug-induced liver injury. *Mod Pathol* 2018; **31**: 965-973 [PMID: 29403081 DOI: 10.1038/s41379-018-0013-y]
- 49 **Danan G**, Benichou C. Causality assessment of adverse reactions to drugs--I. A novel method based on the conclusions of international consensus meetings: application to drug-induced liver injuries. *J Clin Epidemiol* 1993; **46**: 1323-1330 [PMID: 8229110 DOI: 10.1016/0895-4356(93)90101-6]
- 50 **Bernardo SG**, Moskalenko M, Pan M, Shah S, Sidhu HK, Sicular S, Harcharik S, Chang R, Friedlander P, Saenger YM. Elevated rates of transaminitis during ipilimumab therapy for metastatic melanoma. *Melanoma Res* 2013; **23**: 47-54 [PMID: 23262440 DOI: 10.1097/CMR.0b013e32835c7e68]
- 51 **Gauci ML**, Baroudjian B, Zeboulon C, Pages C, Poté N, Roux O, Bouattour M, Lebbé C; PATIO group. Immune-related hepatitis with immunotherapy: Are corticosteroids always needed? *J Hepatol* 2018; **69**: 548-550 [PMID: 29747956 DOI: 10.1016/j.jhep.2018.03.034]
- 52 **European Association for the Study of the Liver**; Clinical Practice Guideline Panel: Chair; Panel members; EASL Governing Board representative. EASL Clinical Practice Guidelines: Drug-induced liver injury. *J Hepatol* 2019; **70**: 1222-1261 [PMID: 30926241 DOI: 10.1016/j.jhep.2019.02.014]
- 53 **eviQ**. Management of immune-related adverse events 2020. [cited 1 March 2021]. Available from: <https://www.eviq.org.au/clinical-resources/side-effect-and-toxicity-management/immunological/1993-management-of-immune-related-adverse-events#hepatotoxicity>
- 54 **Iwamoto K**, Ishitsuka Y, Tanaka R, Sekine I, Fujimoto M. Azathioprine combination therapy for steroid-refractory hepatic immune system-related adverse events. *Eur J Dermatol* 2017; **27**: 301-303 [PMID: 28468733 DOI: 10.1684/ejd.2017.2973]
- 55 **Cheng R**, Cooper A, Kench J, Watson G, Bye W, McNeil C, Shackel N. Ipilimumab-induced toxicities and the gastroenterologist. *J Gastroenterol Hepatol* 2015; **30**: 657-666 [PMID: 25641691 DOI: 10.1111/jgh.12888]
- 56 **Huffman BM**, Kottschade LA, Kamath PS, Markovic SN. Hepatotoxicity After Immune Checkpoint Inhibitor Therapy in Melanoma: Natural Progression and Management. *Am J Clin Oncol* 2018; **41**: 760-765 [PMID: 28749795 DOI: 10.1097/COC.0000000000000374]
- 57 **Mack CL**, Adams D, Assis DN, Kerkar N, Manns MP, Mayo MJ, Vierling JM, Alsawas M, Murad MH, Czaja AJ. Diagnosis and Management of Autoimmune Hepatitis in Adults and Children: 2019 Practice Guidance and Guidelines From the American Association for the Study of Liver Diseases. *Hepatology* 2020; **72**: 671-722 [PMID: 31863477 DOI: 10.1002/hep.31065]
- 58 **Chmiel KD**, Suan D, Liddle C, Nankivell B, Ibrahim R, Bautista C, Thompson J, Fulcher D, Kefford R. Resolution of severe ipilimumab-induced hepatitis after antithymocyte globulin therapy. *J Clin Oncol* 2011; **29**: e237-e240 [PMID: 21220617 DOI: 10.1200/JCO.2010.32.2206]
- 59 **Stroud CR**, Hegde A, Cherry C, Naqash AR, Sharma N, Addepalli S, Cherukuri S, Parent T, Hardin J, Walker P. Tocilizumab for the management of immune mediated adverse events secondary to PD-1 blockade. *J Oncol Pharm Pract* 2019; **25**: 551-557 [PMID: 29207939 DOI: 10.1177/1078155217745144]
- 60 **Riveiro-Barciela M**, Muñoz-Couselo E, Fernandez-Sojo J, Diaz-Mejia N, Parra-López R, Buti M. Acute liver failure due to immune-mediated hepatitis successfully managed with plasma exchange: New settings call for new treatment strategies? *J Hepatol* 2019; **70**: 564-566 [PMID: 30503040 DOI: 10.1016/j.jhep.2018.10.020]
- 61 **Corrigan M**, Haydon G, Thompson F, Rajoriya N, Peplow CL, Hubscher SG, Steven N, Hirschfield GM, Armstrong MJ. Infliximab for the treatment of refractory immune-related hepatitis secondary to checkpoint inhibitors: A case report. *JHEP Rep* 2019; **1**: 66-69 [PMID: 32039353 DOI: 10.1016/j.jhepr.2019.02.001]
- 62 **Ghabril M**, Bonkovsky HL, Kum C, Davern T, Hayashi PH, Kleiner DE, Serrano J, Rochon J, Fontana RJ, Bonacini M; US Drug-Induced Liver Injury Network. Liver injury from tumor necrosis factor- α antagonists: analysis of thirty-four cases. *Clin Gastroenterol Hepatol* 2013; **11**: 558-564.e3 [PMID: 23333219 DOI: 10.1016/j.cgh.2012.12.025]
- 63 **Kawakami H**, Tanizaki J, Tanaka K, Haratani K, Hayashi H, Takeda M, Kamata K, Takenaka M, Kimura M, Chikugo T, Sato T, Kudo M, Ito A, Nakagawa K. Imaging and clinicopathological features of nivolumab-related cholangitis in patients with non-small cell lung cancer. *Invest New Drugs* 2017; **35**: 529-536 [PMID: 28317087 DOI: 10.1007/s10637-017-0453-0]
- 64 **Teplý BA**, Lipson EJ. Identification and management of toxicities from immune checkpoint-blocking

- drugs. *Oncology (Williston Park)* 2014; **28** Suppl 3: 30-38 [PMID: 25384885]
- 65 **Riveiro-Barciela M**, Barreira-Díaz A, Vidal-González J, Muñoz-Couselo E, Martínez-Valle F, Viladomiu L, Mínguez B, Ortiz-Velez C, Castells L, Esteban R, Buti M. Immune-related hepatitis related to checkpoint inhibitors: Clinical and prognostic factors. *Liver Int* 2020; **40**: 1906-1916 [PMID: 32329119 DOI: 10.1111/liv.14489]
- 66 **Downey SG**, Klapper JA, Smith FO, Yang JC, Sherry RM, Royal RE, Kammula US, Hughes MS, Allen TE, Levy CL, Yellin M, Nichol G, White DE, Steinberg SM, Rosenberg SA. Prognostic factors related to clinical response in patients with metastatic melanoma treated by CTL-associated antigen-4 blockade. *Clin Cancer Res* 2007; **13**: 6681-6688 [PMID: 17982122 DOI: 10.1158/1078-0432.CCR-07-0187]
- 67 **Horvat TZ**, Adel NG, Dang TO, Momtaz P, Postow MA, Callahan MK, Carvajal RD, Dickson MA, D'Angelo SP, Woo KM, Panageas KS, Wolchok JD, Chapman PB. Immune-Related Adverse Events, Need for Systemic Immunosuppression, and Effects on Survival and Time to Treatment Failure in Patients With Melanoma Treated With Ipilimumab at Memorial Sloan Kettering Cancer Center. *J Clin Oncol* 2015; **33**: 3193-3198 [PMID: 26282644 DOI: 10.1200/JCO.2015.60.8448]
- 68 **Laube R**, Sabih AH, Strasser SI, Lim L, Cigolini M, Liu K. Palliative care in hepatocellular carcinoma. *J Gastroenterol Hepatol* 2021; **36**: 618-628 [PMID: 32627853 DOI: 10.1111/jgh.15169]
- 69 **Ziemer M**, Koukouloti E, Beyer S, Simon JC, Berg T. Managing immune checkpoint-inhibitor-induced severe autoimmune-like hepatitis by liver-directed topical steroids. *J Hepatol* 2017; **66**: 657-659 [PMID: 27908801 DOI: 10.1016/j.jhep.2016.11.015]
- 70 **Pollack MH**, Betof A, Dearden H, Rapazzo K, Valentine I, Brohl AS, Ancell KK, Long GV, Menzies AM, Eroglu Z, Johnson DB, Shoushtari AN. Safety of resuming anti-PD-1 in patients with immune-related adverse events (irAEs) during combined anti-CTLA-4 and anti-PD1 in metastatic melanoma. *Ann Oncol* 2018; **29**: 250-255 [PMID: 29045547 DOI: 10.1093/annonc/mdx642]
- 71 **Hodi FS**, Chiarion-Sileni V, Gonzalez R, Grob JJ, Rutkowski P, Cowey CL, Lao CD, Schadendorf D, Waggstaff J, Dummer R, Ferrucci PF, Smylie M, Hill A, Hogg D, Marquez-Rodas I, Jiang J, Rizzo J, Larkin J, Wolchok JD. Nivolumab plus ipilimumab or nivolumab alone versus ipilimumab alone in advanced melanoma (CheckMate 067): 4-year outcomes of a multicentre, randomised, phase 3 trial. *Lancet Oncol* 2018; **19**: 1480-1492 [PMID: 30361170 DOI: 10.1016/S1470-2045(18)30700-9]
- 72 **Weber J**, Thompson JA, Hamid O, Minor D, Amin A, Ron I, Ridolfi R, Assi H, Maraveyas A, Berman D, Siegel J, O'Day SJ. A randomized, double-blind, placebo-controlled, phase II study comparing the tolerability and efficacy of ipilimumab administered with or without prophylactic budesonide in patients with unresectable stage III or IV melanoma. *Clin Cancer Res* 2009; **15**: 5591-5598 [PMID: 19671877 DOI: 10.1158/1078-0432.CCR-09-1024]
- 73 **Wolchok JD**, Neyns B, Linette G, Negrier S, Lutzky J, Thomas L, Waterfield W, Schadendorf D, Smylie M, Guthrie T Jr, Grob JJ, Chesney J, Chin K, Chen K, Hoos A, O'Day SJ, Lebbé C. Ipilimumab monotherapy in patients with pretreated advanced melanoma: a randomised, double-blind, multicentre, phase 2, dose-ranging study. *Lancet Oncol* 2010; **11**: 155-164 [PMID: 20004617 DOI: 10.1016/S1470-2045(09)70334-1]
- 74 **Robert C**, Thomas L, Bondarenko I, O'Day S, Weber J, Garbe C, Lebbe C, Baurain JF, Testori A, Grob JJ, Davidson N, Richards J, Maio M, Hauschild A, Miller WH Jr, Gascon P, Lotem M, Harmankaya K, Ibrahim R, Francis S, Chen TT, Humphrey R, Hoos A, Wolchok JD. Ipilimumab plus dacarbazine for previously untreated metastatic melanoma. *N Engl J Med* 2011; **364**: 2517-2526 [PMID: 21639810 DOI: 10.1056/NEJMoa1104621]
- 75 **Ribas A**, Kefford R, Marshall MA, Punt CJ, Haanen JB, Marmol M, Garbe C, Gogas H, Schachter J, Linette G, Lorigan P, Kendra KL, Maio M, Trefzer U, Smylie M, McArthur GA, Dreno B, Nathan PD, Mackiewicz J, Kirkwood JM, Gomez-Navarro J, Huang B, Pavlov D, Hauschild A. Phase III randomized clinical trial comparing tremelimumab with standard-of-care chemotherapy in patients with advanced melanoma. *J Clin Oncol* 2013; **31**: 616-622 [PMID: 23295794 DOI: 10.1200/JCO.2012.44.6112]
- 76 **Weber J**, Mandala M, Del Vecchio M, Gogas HJ, Arance AM, Cowey CL, Dalle S, Schenker M, Chiarion-Sileni V, Marquez-Rodas I, Grob JJ, Butler MO, Middleton MR, Maio M, Atkinson V, Queirolo P, Gonzalez R, Kudchadkar RR, Smylie M, Meyer N, Mortier L, Atkins MB, Long GV, Bhatia S, Lebbé C, Rutkowski P, Yokota K, Yamazaki N, Kim TM, de Pril V, Sabater J, Qureshi A, Larkin J, Ascierto PA; CheckMate 238 Collaborators. Adjuvant Nivolumab versus Ipilimumab in Resected Stage III or IV Melanoma. *N Engl J Med* 2017; **377**: 1824-1835 [PMID: 28891423 DOI: 10.1056/NEJMoa1709030]
- 77 **Brahmer J**, Reckamp KL, Baas P, Crinò L, Eberhardt WE, Poddubskaya E, Antonia S, Pluzanski A, Vokes EE, Holgado E, Waterhouse D, Ready N, Gainor J, Arén Frontera O, Havel L, Steins M, Garassino MC, Aerts JG, Domine M, Paz-Ares L, Reck M, Baudelet C, Harbison CT, Lestini B, Spigel DR. Nivolumab vs Docetaxel in Advanced Squamous-Cell Non-Small-Cell Lung Cancer. *N Engl J Med* 2015; **373**: 123-135 [DOI: 10.1056/nejmoa1504627]
- 78 **Borghaei H**, Paz-Ares L, Horn L, Spigel DR, Steins M, Ready NE, Chow LQ, Vokes EE, Felip E, Holgado E, Barlesi F, Kohlhäufel M, Arrieta O, Burgio MA, Fayette J, Lena H, Poddubskaya E, Gerber DE, Gettinger SN, Rudin CM, Rizvi N, Crinò L, Blumenschein GR Jr, Antonia SJ, Dorange C, Harbison CT, Graf Finckenstein F, Brahmer JR. Nivolumab vs Docetaxel in Advanced Nonsquamous Non-Small-Cell Lung Cancer. *N Engl J Med* 2015; **373**: 1627-1639 [DOI: 10.1056/nejmoa1507643]
- 79 **Robert C**, Ribas A, Wolchok JD, Hodi FS, Hamid O, Kefford R, Weber JS, Joshua AM, Hwu WJ,

- Gangadhar TC, Patnaik A, Dronca R, Zarour H, Joseph RW, Boasberg P, Chmielowski B, Mateus C, Postow MA, Gergich K, Elassaiss-Schaap J, Li XN, Iannone R, Ebbinghaus SW, Kang SP, Daud A. Anti-programmed-death-receptor-1 treatment with pembrolizumab in ipilimumab-refractory advanced melanoma: a randomised dose-comparison cohort of a phase 1 trial. *Lancet* 2014; **384**: 1109-1117 [PMID: 25034862 DOI: 10.1016/S0140-6736(14)60958-2]
- 80 **Eggermont AMM**, Blank CU, Mandala M, Long GV, Atkinson V, Dalle S, Haydon A, Lichinitser M, Khattak A, Carlino MS, Sandhu S, Larkin J, Puig S, Ascierto PA, Rutkowski P, Schadendorf D, Koornstra R, Hernandez-Aya L, Maio M, van den Eertwegh AJM, Grob JJ, Gutzmer R, Jamal R, Lorigan P, Ibrahim N, Marreaud S, van Akkooi ACJ, Suci S, Robert C. Adjuvant Pembrolizumab versus Placebo in Resected Stage III Melanoma. *N Engl J Med* 2018; **378**: 1789-1801 [PMID: 29658430 DOI: 10.1056/NEJMoa1802357]
- 81 **Migden MR**, Rischin D, Schmults CD, Guminski A, Hauschild A, Lewis KD, Chung CH, Hernandez-Aya L, Lim AM, Chang ALS, Rabinowits G, Thai AA, Dunn LA, Hughes BGM, Khushalani NI, Modi B, Schadendorf D, Gao B, Seebach F, Li S, Li J, Mathias M, Booth J, Mohan K, Stankevich E, Babiker HM, Brana I, Gil-Martin M, Homs J, Johnson ML, Moreno V, Niu J, Owonikoko TK, Papadopoulos KP, Yancopoulos GD, Lowy I, Fury MG. PD-1 Blockade with Cemiplimab in Advanced Cutaneous Squamous-Cell Carcinoma. *N Engl J Med* 2018; **379**: 341-351 [PMID: 29863979 DOI: 10.1056/NEJMoa1805131]
- 82 **Jotte R**, Cappuzzo F, Vynnychenko I, Stroyakovskiy D, Rodríguez-Abreu D, Hussein M, Soo R, Conter HJ, Kozuki T, Huang KC, Graupner V, Sun SW, Hoang T, Jessop H, McClelland M, Ballinger M, Sandler A, Socinski MA. Atezolizumab in Combination With Carboplatin and Nab-Paclitaxel in Advanced Squamous NSCLC (IMpower131): Results From a Randomized Phase III Trial. *J Thorac Oncol* 2020; **15**: 1351-1360 [PMID: 32302702 DOI: 10.1016/j.jtho.2020.03.028]
- 83 **D'Angelo SP**, Bhatia S, Brohl AS, Hamid O, Mehnert JM, Terheyden P, Shih KC, Brownell I, Lebbé C, Lewis KD, Linette GP, Milella M, Georges S, Shah P, Eilers-Lenz B, Bajars M, Güzel G, Nghiem PT. Avelumab in patients with previously treated metastatic Merkel cell carcinoma: long-term data and biomarker analyses from the single-arm phase 2 JAVELIN Merkel 200 trial. *J Immunother Cancer* 2020; **8** [PMID: 32414862 DOI: 10.1136/jitc-2020-000674]
- 84 **Garassino MC**, Cho BC, Kim JH, Mazières J, Vansteenkiste J, Lena H, Corral Jaime J, Gray JE, Powderly J, Chouaid C, Bidoli P, Wheatley-Price P, Park K, Soo RA, Huang Y, Wadsworth C, Dennis PA, Rizvi NA; ATLANTIC Investigators. Durvalumab as third-line or later treatment for advanced non-small-cell lung cancer (ATLANTIC): an open-label, single-arm, phase 2 study. *Lancet Oncol* 2018; **19**: 521-536 [PMID: 29545095 DOI: 10.1016/S1470-2045(18)30144-X]
- 85 **Postow MA**, Chesney J, Pavlick AC, Robert C, Grossmann K, McDermott D, Linette GP, Meyer N, Giguere JK, Agarwala SS, Shaheen M, Ernstoff MS, Minor D, Salama AK, Taylor M, Ott PA, Rollin LM, Horak C, Gagnier P, Wolchok JD, Hodi FS. Nivolumab and ipilimumab vs ipilimumab in untreated melanoma. *N Engl J Med* 2015; **372**: 2006-2017 [DOI: 10.1056/nejmoa1414428]
- 86 **Larkin J**, Chiarion-Sileni V, Gonzalez R, Grob JJ, Cowey CL, Lao CD, Schadendorf D, Dummer R, Smylie M, Rutkowski P, Ferrucci PF, Hill A, Wagstaff J, Carlino MS, Haanen JB, Maio M, Marquez-Rodas I, McArthur GA, Ascierto PA, Long GV, Callahan MK, Postow MA, Grossmann K, Sznol M, Dreno B, Bastholt L, Yang A, Rollin LM, Horak C, Hodi FS, Wolchok JD. Combined Nivolumab and Ipilimumab or Monotherapy in Untreated Melanoma. *N Engl J Med* 2015; **373**: 23-34 [PMID: 26027431 DOI: 10.1056/NEJMoa1504030]
- 87 **Colevas A**, Setser A. The NCI Common Terminology Criteria for Adverse Events (CTCAE) v 3.0 is the new standard for oncology clinical trials. *J Clin Oncol* 2004; **22**: 6098 [DOI: 10.1200/jco.2004.22.90140.6098]
- 88 **US Food & Drug Administration**. Silver Spring (MD): FDA. [cited 1 March 2021]. Available from: <https://www.fda.gov/Drugs/default.htm>
- 89 **Puzanov I**, Diab A, Abdallah K, Bingham CO 3rd, Brogdon C, Dadu R, Hamad L, Kim S, Lacouture ME, LeBoeuf NR, Lenihan D, Onofrei C, Shannon V, Sharma R, Silk AW, Skondra D, Suarez-Almazor ME, Wang Y, Wiley K, Kaufman HL, Ernstoff MS; Society for Immunotherapy of Cancer Toxicity Management Working Group. Managing toxicities associated with immune checkpoint inhibitors: consensus recommendations from the Society for Immunotherapy of Cancer (SITC) Toxicity Management Working Group. *J Immunother Cancer* 2017; **5**: 95 [PMID: 29162153 DOI: 10.1186/s40425-017-0300-z]
- 90 **Brahmer JR**, Lacchetti C, Schneider BJ, Atkins MB, Brassil KJ, Caterino JM, Chau I, Ernstoff MS, Gardner JM, Ginex P, Hallmeyer S, Holter Chakrabarty J, Leighl NB, Mammen JS, McDermott DF, Naing A, Nastoupil LJ, Phillips T, Porter LD, Puzanov I, Reichner CA, Santomaso BD, Seigel C, Spira A, Suarez-Almazor ME, Wang Y, Weber JS, Wolchok JD, Thompson JA; National Comprehensive Cancer Network. Management of Immune-Related Adverse Events in Patients Treated With Immune Checkpoint Inhibitor Therapy: American Society of Clinical Oncology Clinical Practice Guideline. *J Clin Oncol* 2018; **36**: 1714-1768 [PMID: 29442540 DOI: 10.1200/JCO.2017.77.6385]
- 91 **Haanen JBAG**, Carbonnel F, Robert C, Kerr KM, Peters S, Larkin J, Jordan K; ESMO Guidelines Committee. Management of toxicities from immunotherapy: ESMO Clinical Practice Guidelines for diagnosis, treatment and follow-up. *Ann Oncol* 2017; **28**: iv119-iv142 [PMID: 28881921 DOI: 10.1093/annonc/mdx225]

Basic Study

Therapeutic effect of *Cistanche deserticola* on defecation in senile constipation rat model through stem cell factor/C-kit signaling pathway

Xia Zhang, Fa-Juan Zheng, Zhen Zhang

ORCID number: Xia Zhang [0000-0002-1855-9940](https://orcid.org/0000-0002-1855-9940); Fa-Juan Zheng [0000-0002-3538-699X](https://orcid.org/0000-0002-3538-699X); Zhen Zhang [0000-0001-9948-9034](https://orcid.org/0000-0001-9948-9034).

Author contributions: Zhang Z designed the study; Zhang X and Zhang Z wrote the manuscript and were involved in revision, editing and review; Zhang X reformatted the manuscript; Zheng FJ was involved in the animal experiment process and data collation and input; All authors read and approved the final manuscript.

Supported by Natural Science Foundation of Chongqing, No. cstc2017jcyjAX0306.

Institutional animal care and use committee statement: The study was reviewed and approved by the Chongqing Hospital of Traditional Chinese Medicine Ethics Committee, No. Cstc2017jcyjAX0306.

Conflict-of-interest statement: There is no conflict of interest associated with any of the senior author or other coauthors contributed their efforts in this manuscript.

Data sharing statement: Technical appendix, statistical code, and

Xia Zhang, Fa-Juan Zheng, Department of Science and Education, Chongqing Hospital of Traditional Chinese Medicine, Chongqing 400021, China

Zhen Zhang, Department of Anorectal, Chongqing Hospital of Traditional Chinese Medicine, Chongqing 400021, China

Corresponding author: Zhen Zhang, MD, Deputy Director, Department of Anorectal, Chongqing Hospital of Traditional Chinese Medicine, No. 6 Seventh Branch of Panxi Road, Jiangbei District, Chongqing 400021, China. zhangzhen@cdutcm.edu.cn

Abstract

BACKGROUND

Constipation is one of the chronic gastrointestinal functional diseases. It seriously affects the quality of life. *Cistanche deserticola* (*C. deserticola*) can treat constipation obviously, but its mechanism has not been clarified. We supposed that mechanism of it improved the intestinal motility by stimulating interstitial Cajal cells (ICC). Activation of the C-kit receptor on the surface of ICC is closely related to ICC function, and the stem cell factor (SCF)/C-kit signaling pathways plays an important role on it. To investigate the mechanism of how *C. deserticola* treats constipation, this study aimed to establish a constipation model in rats and explore the role of SCF/C-kit signaling pathway in the treatment.

AIM

To explore the SCF/C-kit signaling pathways in the role of *C. deserticola* for treatment of constipation by a constipation rat model.

METHODS

Forty-eight 8-mo-old Sprague–Dawley rats were divided into 4 groups by random weight method: Normal group ($n = 12$), model group ($n = 12$), *C. deserticola* group ($n = 12$) and blocker group ($n = 12$). The normal group received normal saline by gavage; the model group received loperamide by gavage; the blocker group received loperamide and *C. deserticola* by gavage, and STI571 was injected by intraperitoneally. During treatment, the weight, fecal granules and fecal quality were recorded every 10 d. On day 20 after model induction, the colon tissues of each group were removed. Hematoxylin and eosin staining was used to observe pathological changes. Expression levels of SCF, C-kit and *Aquaporin* genes were

dataset available from the corresponding author at zhangzhen@cdutcm.edu.cn.

Participants gave informed consent for data sharing.

ARRIVE guidelines statement: The authors have read the ARRIVE guidelines, and the manuscript was prepared and revised according to the ARRIVE guidelines.

Open-Access: This article is an open-access article that was selected by an in-house editor and fully peer-reviewed by external reviewers. It is distributed in accordance with the Creative Commons Attribution NonCommercial (CC BY-NC 4.0) license, which permits others to distribute, remix, adapt, build upon this work non-commercially, and license their derivative works on different terms, provided the original work is properly cited and the use is non-commercial. See: <http://creativecommons.org/licenses/by-nc/4.0/>

Manuscript source: Unsolicited manuscript

Specialty type: Gastroenterology and hepatology

Country/Territory of origin: China

Peer-review report's scientific quality classification

Grade A (Excellent): 0
Grade B (Very good): 0
Grade C (Good): C
Grade D (Fair): 0
Grade E (Poor): 0

Received: April 7, 2021

Peer-review started: April 7, 2021

First decision: May 27, 2021

Revised: June 3, 2021

Accepted: July 20, 2021

Article in press: July 20, 2021

Published online: August 28, 2021

P-Reviewer: Rangel-Corona R

S-Editor: Wu YXJ

L-Editor: Filipodia

P-Editor: Li JH



detected by immunohistochemistry, western blotting, and real-time-quantitative polymerase chain reaction. The colonic epithelial mitochondria and goblet cells were observed by transmission electron microscopy.

RESULTS

Compared with the normal group, as treatment progressed, the weight of rats in the model and blocker groups decreased significantly, the stool weight decreased, and the stool quality was dry ($P < 0.05$). *C. deserticola* reversed the decrease in body weight and stool weight and improved stool quality. Histopathological analysis indicated that the colonic mucosal epithelium in the model group was incomplete, and the arrangement of the glands was irregular or damaged. Treatment with *C. deserticola* improved the integrity and continuity of the epithelial cells and regular arrangement of the glands. The blocking agents inhibited the effects of *C. deserticola*. Immunohistochemistry and real-time-quantitative polymerase chain reaction showed that expression of SCF and C-kit protein or genes in the colonic tissue of the model group was decreased ($P < 0.05$), while treatment with *C. deserticola* increased protein or gene expression ($P < 0.05$). Western blotting showed that expression of aquaporin APQ3 was increased, while the expression of Cx43 decreased in the model group. Treatment with *C. deserticola* inhibited expression of APQ3 and promoted expression of Cx43. Transmission electron microscopy showed that the mitochondria of the colonic epithelium in the model group were swollen and arranged disorderly, and microvilli were sparse. The condition was better in the *C. deserticola* group. Mice treated with STI571 blocker confirmed that blocking the SCF/C-kit pathway inhibited the improvement of constipation by *C. deserticola*.

CONCLUSION

C. deserticola improved defecation in rats with constipation, and the SCF/C-kit signaling pathway, which is a key link of ICC function, played an important role of the treatment.

Key Words: *Cistanche deserticola*; Senile constipation; Stem cell factors; C-kit

©The Author(s) 2021. Published by Baishideng Publishing Group Inc. All rights reserved.

Core Tip: We studied a possible mechanism of *Cistanche deserticola* (*C. deserticola*) in the treatment of constipation. The mechanism might improve colon motility through stem cell factor (SCF)/C-kit signaling pathway in colon Cajal stromal cells. Therefore, the constipation rat model was replicated, and then rats were treated by direct administration of *C. deserticola* and specific blocking of the SCF/C-kit signaling pathway. The defecation of rats, changes of colonic pathology and ultrastructure as well as the protein expression related to the SCF/C-kit signaling pathway were observed. Our results support that the SCF/C-kit signaling pathway plays an important mechanism on the therapeutic effect of *C. deserticola*.

Citation: Zhang X, Zheng FJ, Zhang Z. Therapeutic effect of *Cistanche deserticola* on defecation in senile constipation rat model through stem cell factor/C-kit signaling pathway. *World J Gastroenterol* 2021; 27(32): 5392-5403

URL: <https://www.wjgnet.com/1007-9327/full/v27/i32/5392.htm>

DOI: <https://dx.doi.org/10.3748/wjg.v27.i32.5392>

INTRODUCTION

Senile constipation (SC) is one of the common chronic gastrointestinal functional diseases in geriatric patients, which induces or aggravates cerebrovascular events and other diseases and seriously affects the quality of life of the elderly population[1,2]. According to traditional Chinese medicine, the main etiology and pathogenesis of SC are gastrointestinal heat, deficiency of Yin and Jin and intestinal de-wetting[3,4], while

Cistanche deserticola (*C. deserticola*) can warm the kidneys and relax the bowels. Researchers have reported that the effect of intestinal motility improvement and treatment of SC is clear, but its mechanism has not been clarified[5,6]. Interstitial Cajal cells (ICCs) are a special type of mesenchymal cells in the gastrointestinal tract. Activation of the C-kit receptor on the surface of ICCs is closely related to cell proliferation, differentiation and function. ICCs participate in the pathogenesis of many gastrointestinal motor dysfunctions[7,8]. Activation of C-kit depends on the binding of its ligand stem cell factor (SCF)[9]. To investigate the effect and mechanism of action of *C. deserticola* on SC, this study aimed to establish an SC model in rats induced by loperidol to explore the role of the SCF/C-kit signaling pathway in the treatment of constipation by *C. deserticola*.

MATERIALS AND METHODS

Experimental materials

Experimental animals: The experimental animals were 48 male 8-mo-old Sprague-Dawley rats weighing 500-550 g; all purchased from Changsha Tianqin Biotechnology Co. Ltd. Rats were raised in the animal laboratory of Chongqing Weisiteng Biomedical Technology Co. Ltd., given normal day and night light, food and drink. All procedures complied with the management guidelines issued by the Ethics Committee of Chongqing Traditional Chinese Medicine Hospital.

Primary reagents: The primary reagents included loperamide (Sigma, St. Louis, MO, United States), *C. deserticola* from Hubei Jurui Traditional Chinese Medicine Decoction Co. Ltd., STI571 from Chinese Selleck Co. Ltd., and SCF, C-kit, connexin 43 (Cx43), aquaporin 3 (AQP3) and β -actin antibodies (Abcam, Cambridge, MA, United States), PrimeScript II 1st Strand cDNA Synthesis Kit and Premix Taq™ (Ex Taq™ Version 2.0) (Takara Co. Ltd., Japan).

Methods

SC model preparation and grouping: To avoid the influence of confounding factors such as body weight on the experimental results, the rats were randomly grouped by the block random grouping method. Forty-eight rats were fed adaptively for 1 wk, and the rats were numbered in order of weight from light to heavy. According to the order of body weight, the rats were divided into 12 zones (the weight of rats in each zone was similar), with 4 rats in each zone. The 12 zones were divided into 4 groups of 12 (normal, model, *C. deserticola* and blocker). Rats in the model group were given loperamide (0.0625/100 g, 10 mL/kg) by gavage. The first gavage dose was doubled, and the drug was given at 10:00 every day, once a day for 20 consecutive days. The normal group was given the same amount of normal saline by gavage. In addition, the model group was treated with *C. deserticola* (0.156 g/100 g, 10 mL/kg) by gavage. The blocker group was given *C. deserticola* (0.156 g/100 g, 10 mL/kg) by gavage and STI571 (25 mg/mL, 1 mL/kg) by intraperitoneal injection. During the experiment, body weight, stool weight and stool condition were recorded every 10 d. No accidental death occurred in any of the rats. Twenty days later, the rats were killed, and the colonic tissue was removed for examination and liquid nitrogen preservation. The remaining parts were fixed and embedded.

Histopathological analysis: The rats fasted overnight were anesthetized by intraperitoneal injection with 7% chloral hydrate (5 mL/kg) on the next day. The abdomen was opened to separate the colonic tissue, and 8-10 mm of colon was removed. The intestinal contents were removed by gently shaking in precooled polybutylene succinate and fixed for 24 h in 4% paraformaldehyde fixative solution. Conventional paraffin embedding was performed. Tissue sections (5 μ m) were removed for hematoxylin and eosin staining, and the histopathological morphology was observed under a microscope.

Detection of expression of SCF and C-kit by immunohistochemical staining: The paraffin tissues examined by histopathology above were sectioned, rehydrated with sectioned xylene dewaxed gradient ethanol, antigen remedied by heat and sealed for 1 h with goat serum at room temperature. SCF and C-kit primary antibodies were added dropwise, and tissues were kept overnight at 4 °C. After rinsing with polybutylene succinate, horseradish peroxidase was dropped to label secondary antibody, rinsed with polybutylene succinate for 5 min, drop 2,4-diaminobutyric acid chromogen solution, re-dye with hematoxylin, reverse gradient alcohol dehydration, transpar-

entized by xylene and neutral resin seal. Microscopically, the nuclei were purplish blue, and the positive result products were brownish yellow or yellow particles.

Detection of expression of *C-kit* mRNA in colonic tissue by real-time-quantitative polymerase chain reaction (RT-qPCR): Frozen rat colonic tissue was ground by homogenizer, and 1 mL RNAiso Plus was added. Total RNA of colonic tissue was extracted by chloroform/isopropanol method, and the RNA quality was detected by gel electrophoresis. After identified by Bio-Rad gel imager, 1 µg RNA was reverse transcribed into cDNA by Takara PrimeScript II 1st Strand cDNA Synthesis Kit. According to NCBI database Gene ID: 64030, the CDS region of the *C-kit* gene was found and combined with NCBI Primer-Blast design Primer sequence, which was synthesized by Sangon Biotech Co. Ltd, *C-kit* primer sequence sense strand 5'-AGGTGTACCGTTCCTGTCCC-3', antisense strand 5'-GGCTGGATTGCTCTTTGCTGT-3', β -*actin* sense strand 5'-CTTCCTTCCTGGGTATGGAATC-3', antisense strand 5'-CTGTGTTGGCATAGAGGTCTT-3'. PCR amplification was performed on a Bio-Rad CFX90 Real-Time PCR instrument. The conditions for PCR assay were initial denaturation at 95 °C for 5 min, 30 cycles of 95 °C for 30 s, 60 °C for 30 s and 72 °C for 1 min followed by final extension at 72 °C for 10 min. $2^{-\Delta\Delta Ct}$ ($\Delta Ct = Ct \text{ value} - \beta\text{-actin } Ct \text{ value}$) was taken to analyze relative gene expression.

Detection of protein expression level of Cx43 and AQP3 in colonic tissue by Western blotting: About 1 cm of frozen colonic tissue was collected and lysed with RIPA strong pyrolysis liquid (100 µL). The tissue was homogenized with a glass homogenizer 20 times and transferred to a 1.5 mL centrifuge tube. The supernatant was extracted after centrifugation at 12000 rpm at 4 °C for 5 min, and the concentration of total protein in the supernatant was determined by BCA method. We removed 25 µg denatured protein to perform sodium dodecyl sulfate-polyacrylamide gel electrophoresis and then transferred the proteins in the gel to polyvinylidene fluoride membrane at a constant current of 200 mA then sealed by 5% skim milk confining liquid for 2 h at room temperature. Corresponding primary antibodies were diluted with sealing fluid, incubated at 4 °C overnight, then washed the membrane resistance and added second antibodies. After adding ECL fluid, they were put under the exposure meter for test by optical density analysis.

Transmission electron microscopy: We took about 1 cm of proximal colonic tissue, fixed it in 2.5% glutaraldehyde for 24 h, dehydrated it with graded acetone, embedded it in Epon812 and cut 50 nm ultrathin sections on an ultramicrotome. The sections were stained with uranium dioxide acetate and lead citrate dyeing liquid at room temperature for 10 min. We observed colonic villi, epithelial cell mitochondria and goblet cells under a Philips Tecnai-10 transmission electron microscope.

Statistical analysis

SPSS 19.0 software was used for data analysis, and GraphPad Prism8.4 software was used for plotting the results. The Shapiro-Wilk's test was used for normality testing. Data with normal distribution were represented by mean \pm SD. Error items were used to represent the mean \pm SD of hemoglobin after treatment. Student's *t*-test was used for comparison between two groups. Analysis of variance was used for comparison between multiple groups. The Student-Newman-Keuls method was used for comparison between multiple groups in pairs, and Dunnett's test was used to measure the differences between each experimental group and control group in sequence. Associated data were measured by multiple time point, and repeated measurement data analysis of variance was conducted. If the sphericity test showed $P > 0.05$, repeated measurement data analysis of variance was used. If $P < 0.05$, the generalized estimation equation was taken. Data that did not conform to a normal distribution were represented by M (P25, P75), and the Kruskal-Wallis *H* rank sum test was used for comparison between groups. The χ^2 test was used to compare between groups when the data was unordered data, and Pearson's χ^2 test was used if the proportion of cells with theoretical frequency < 5 was $< 20\%$. If the proportion of cells with theoretical frequency < 5 was $\geq 20\%$, Fisher's exact test was used. $P < 0.05$ was used to determine that the difference was statistically significant.

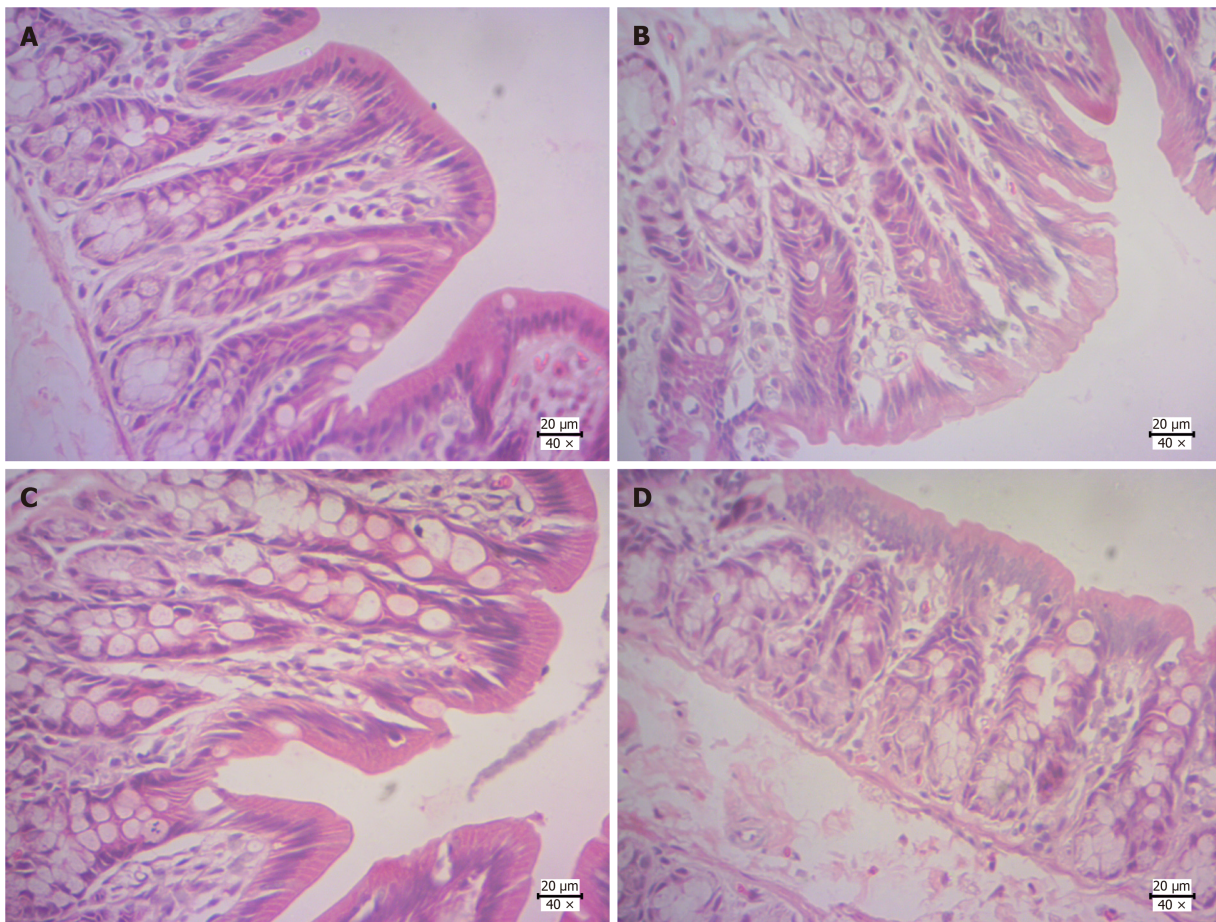


Figure 1 Colonic histopathological changes. A: Normal group; B: Model group; C: *Cistanche deserticola* group; D: Blocker group. Magnification: $\times 40$; Scale bar: 20 μm .

RESULTS

General conditions

One day after gavage of loperamide compared with the normal group, the body weight and stool weight in the model group were significantly decreased ($P < 0.05$), but there was no significant difference in stool quality score ($P > 0.05$). *C. deserticola* treatment in the model group slowed the decrease in body weight and stool weight ($P < 0.05$), but the body weight in the blocker group was not significantly reduced. After 10 d of treatment, compared with the normal group, the body weight and stool volume of rats in the model group were further significantly reduced, and the stools were dry and almost contained no water ($P < 0.05$). The body weight loss of rats was also significantly reduced by treatment with *C. deserticola* ($P < 0.05$). The body weight of rats in the blocker group was not significantly different from that in the model group ($P > 0.05$). On day 20 before sampling, the body weight of rats in the model group was significantly lower than that in the normal group, and the stool quality score was significantly increased ($P < 0.05$), while the weight loss caused by constipation was inhibited by *C. deserticola* treatment, and the stool quality score was decreased ($P < 0.05$).

Colonic histopathology

Hematoxylin and eosin staining of colonic tissue of rats is shown in Figure 1. In the normal group, intestinal villi were intact, intestinal mucosa was intact and continuous, cells and glands were arranged regularly. Mucosa and submucosa were not infiltrated by inflammatory cells, and tissue structure was normal. In the model group, intestinal villi and mucosa were largely destroyed, local villi were shed and loosely arranged, and part of the glandular structure disappeared. In the *C. deserticola* group, histopathological staining was less than that of the model group, but there was necrosis in some goblet cells. After intraperitoneal injection in the blocker group, compared with the *C. deserticola* group, there was still local loss of intestinal villi, and there was fracture and

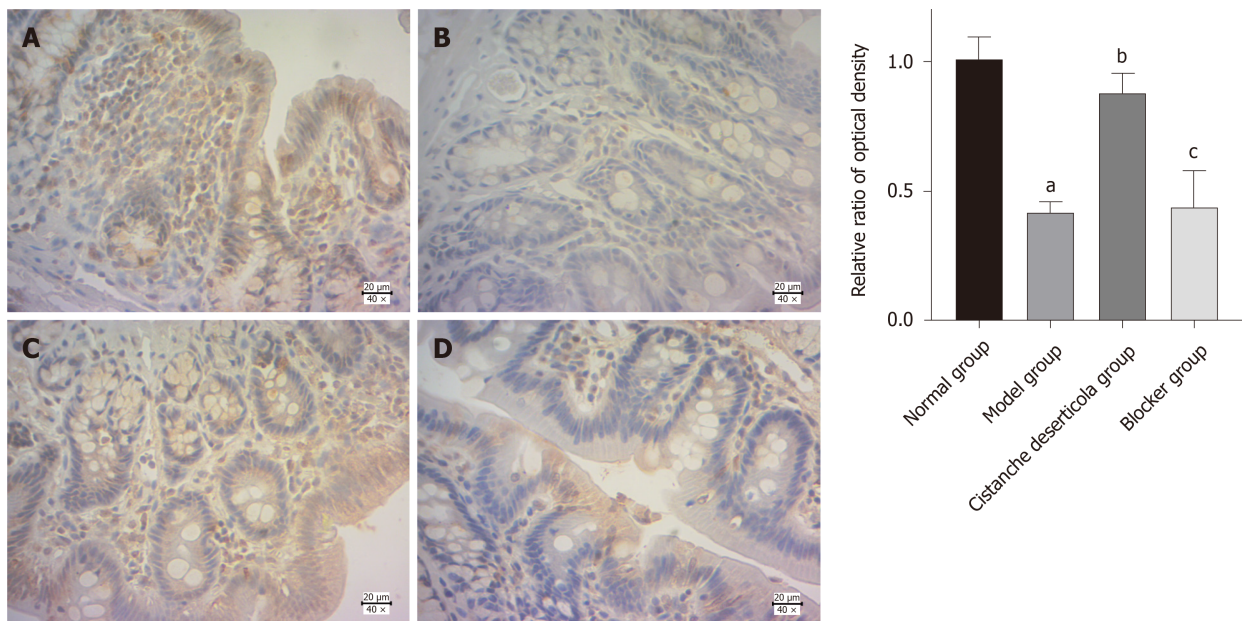


Figure 2 Expression of stem cell factor and relative optical density ratio in colonic tissue by immunohistochemical detection. A: Normal group; B: Model group; C: *Cistanche deserticola* group; D: Blocker group. Magnification: $\times 40$; Scale bar: 20 μm . ^a $P < 0.05$, the expressions of stem cell factor and C-kit in colon tissue of the model group were both significantly decreased compared with the normal group; ^b $P < 0.05$, the expression of stem cell factor and C-kit in the colon tissue of rats in the *Cistanche deserticola* group was significantly increased compared with model group. There was no difference in the expression of stem cell factor and C-kit in the colon tissue of rats between the blocker group and the model group.

loss of intestinal mucosa.

Detection of expression of stem cell factor and C-kit protein by immunohistochemical staining

Immunohistochemical staining showed that SCF and C-kit were expressed in the colon of the control group. Compared with the control group, expression of SCF and C-kit in the model group was significantly decreased ($P < 0.05$). Compared with the model group, expression of SCF and C-kit in the *C. deserticola* group was significantly increased ($P < 0.05$). There was no difference in expression of SCF and C-kit between the blocker and model groups ($P < 0.05$, Figures 2 and 3).

RT-qPCR

RT-qPCR showed that expression of *C-kit* mRNA in the model group was significantly lower than in the normal group (Figure 4, $P < 0.05$). Compared with the model group, *C-kit* in the *C. deserticola* group was significantly increased ($P < 0.05$). There was no significant difference in *C-kit* mRNA level between the model and blocker groups ($P > 0.05$). These results indicated that *C-kit* expression adjusted by *C. deserticola* participated in the improvement of constipation, and blockers inhibited the efficacy of *C. deserticola*.

Western blotting

Western blotting showed that AQP3 protein was expressed at a low level in the normal control group, while it was significantly increased in the model group compared with the control group (Figure 5) ($P < 0.05$). Expression of AQP3 protein was decreased after treatment with *C. deserticola*, and the inhibitory effect of *C. deserticola* on the expression of AQP3 was inhibited by blocker treatment ($P < 0.05$). Expression of Cx43 was the opposite of that of AQP3. These results suggested that the pharmacology effect of *C. deserticola* on rats with SC was achieved by promoting expression of Cx43 and inhibiting expression of AQP3 (Figures 5-7).

Transmission electron microscopy

After loperamide induction, mitochondrial swelling and autophagy occurred in some of the colonic mucosal epithelial cells in the model group. The number and length of intestinal microvilli decreased, and goblet cell pyknosis occurred (Figure 8). After treatment with *C. deserticola*, the number of intestinal microvilli increased. The microvilli were arranged neatly, and the structure was complete. The goblet cells

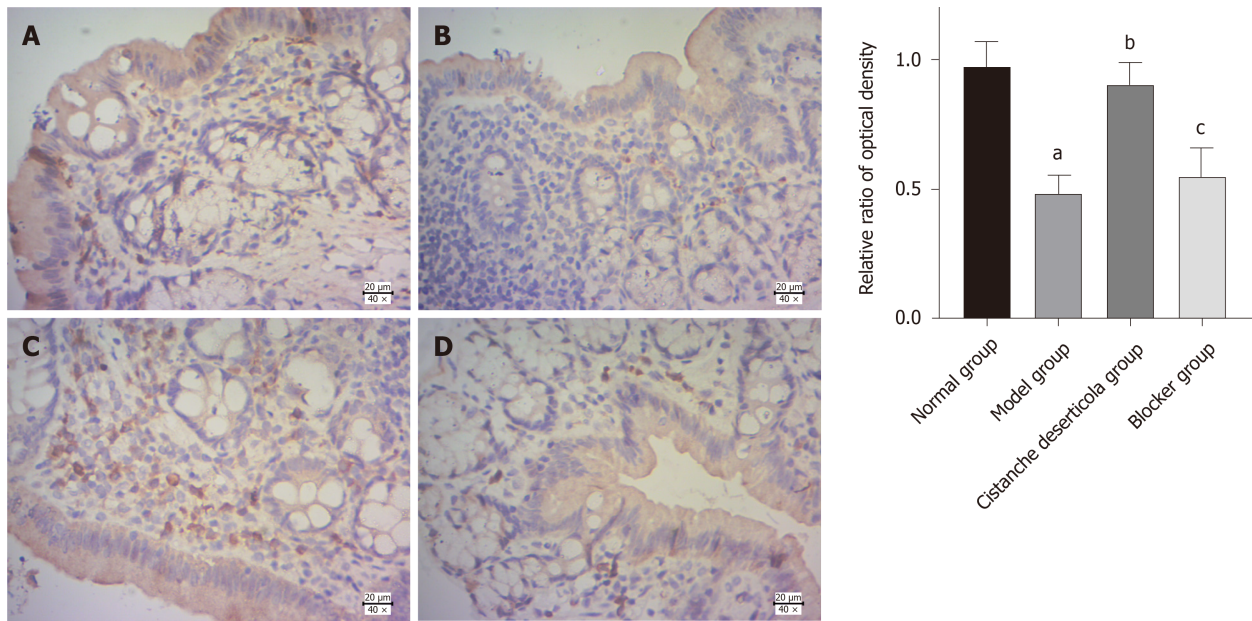


Figure 3 Expression of C-kit and relative optical density ratio in colonic tissue by immunohistochemical detection. A: Normal group; B: Model group; C: *Cistanche deserticola* group; D: Blocker group. Magnification: $\times 40$; Scale bar: 20 μm . ^a $P < 0.05$, compared with normal group; ^b $P < 0.05$, compared with model group; ^c $P > 0.05$, compared with model group.

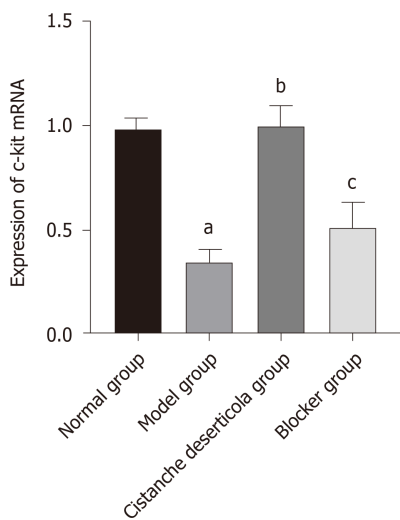


Figure 4 Expression of C-kit mRNA in colon tissue of rats in each group. ^a $P < 0.05$, compared with normal group; ^b $P < 0.05$, compared with model group; ^c $P > 0.05$, compared with model group.

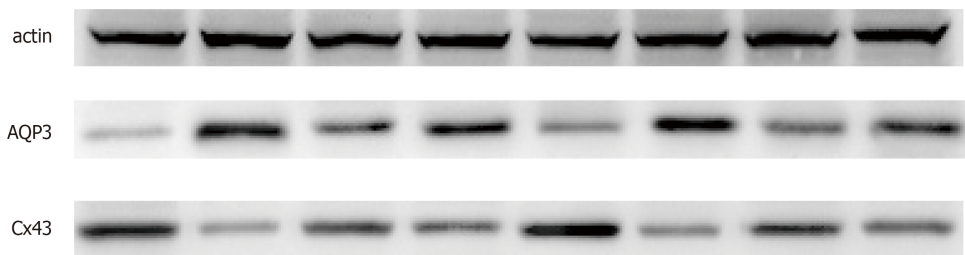


Figure 5 Connexin 43 and aquaporin 3 protein expression detected by western blotting. AQP3: Aquaporin 3; Cx43: Connexin 43.

regained some structural integrity but still did not return to normal length. After inhibitor treatment, the number of microvilli in colonic epithelial cells decreased significantly compared with those in the *C. deserticola* group, with loose arrangement,

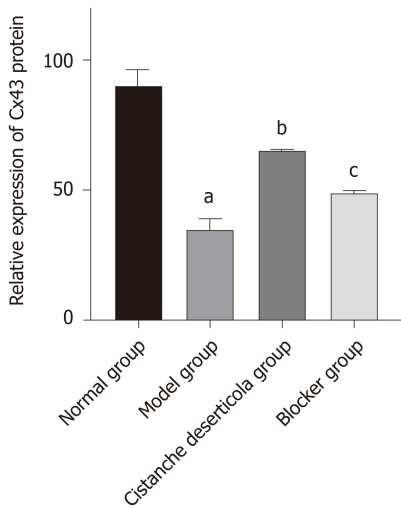


Figure 6 Relative expression of connexin 43 protein. ^a $P < 0.05$, compared with normal group; ^b $P < 0.05$, compared with model group; ^c $P > 0.05$, compared with model group. Cx43: Connexin 43.

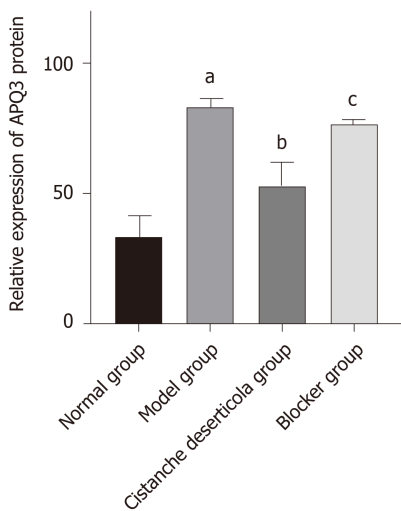


Figure 7 Relative expression of aquaporin 3 protein. ^a $P < 0.05$, compared with normal group; ^b $P < 0.05$, compared with model group; ^c $P > 0.05$, compared with model group. AQP3: Aquaporin 3.

shorter length, irregular morphology of mitochondria and severe pyknosis of goblet cells.

DISCUSSION

Constipation is common in the elderly population and is one of the common symptoms that affect the health status and quality of life of elderly people[10,11]. In terms of traditional Chinese medicine, Bai *et al*[12] believed that the basic pathogenesis of SC was dysfunction of large intestine conduction function, senile body failure, gradual loss of liver and kidney functions, lack of qi and blood and loss of body fluid, which led to dry stools, resulting in constipation[13]. SC puts pressure on patients and their families in many aspects, and it is important to explore its pathogenesis.

C. deserticola has the functions of tonifying kidney Yang, benefiting blood and regulating body immunity[14]. *C. deserticola* and Chinese herbal decoction containing *C. deserticola* have been widely used in the treatment of constipation, and the clinical effect is remarkable. Du *et al*[15] found in a rat model of Yang deficiency and constipation that *C. deserticola* improved the contraction amplitude of isolated colon, strengthened the contractility of the intestinal tract and returned the level of gastrointestinal hormones to normal. In addition, dietary fiber of *C. deserticola*, a

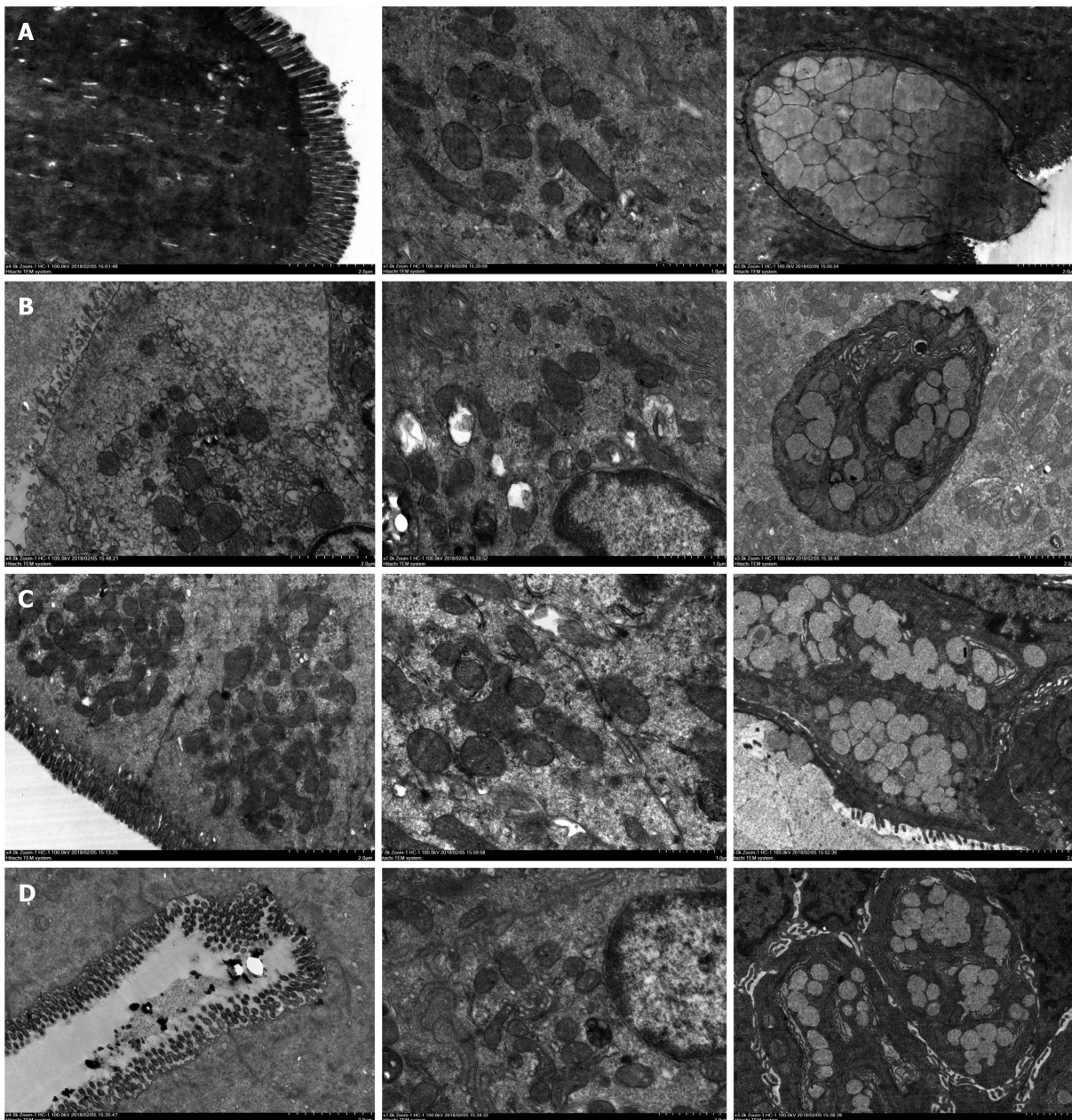


Figure 8 Observation of colonic villi, mitochondria of colonic epithelial cells and goblet cells by transmission electron microscopy. A: Normal group; B: Model group; C: *Cistanche deserticola* group; D: Blocker group.

processing byproduct of *C. deserticola*, improves the water-holding capacity of feces and has the advantage of low dose and good effect in nourishing intestines and improving defecation[16]. Our study found that *C. deserticola* treatment improved fecal moisture and colonic histopathology of rats with constipation.

ICCs are found throughout the intestinal tract and play a vital role in the neural control of intestinal movement as pacemakers and intestinal nerve transmission[17]. Proto-oncogene coding receptor tyrosine kinase, C-kit, is expressed by ICCs, and SCF is a ligand of C-kit[18]. The SCF/C-kit system is crucial in the development of ICCs. The SCF/C-kit signaling pathway has been analyzed during treatment of slow transfer constipation in rats by acupuncture[19]. Electroacupuncture at Tianshu point increased the number of colon ICCs in ACK2-treated mice, upregulated expression of SCF and C-kit proteins and reversed the phenotype of ICC. Prescription for invigorating qi and spleen can increase expression of ICC in colonic tissue and upregulate expression of *C-kit* and *SCF* mRNA, thus improving constipation symptoms[20]. In our study, immunohistochemistry showed that *C. deserticola* significantly upregulated expression of SCF and C-kit protein in a rat model of SC, and RT-qPCR showed that *C. deserticola* significantly upregulated expression of *C-kit* mRNA. C-kit blocker inhibited the upregulation of SCF and C-kit expression induced

by *C. deserticola*.

Fecal water content and colonic water transport are closely related to AQPs, which play an important role in intestinal water metabolism[21]. In a study of rats with slow transport constipation, Defecation decoction significantly improved constipation symptoms by regulating intestinal water absorption through downregulating AQP3 and AQP4[22]. In a rat model of functional constipation, the treatment mechanism of Oral Xiaofu Tongjie Fluid for functional constipation may be realized by regulating expression of vasoactive intestinal polypeptide and AQP3 in the colon[23]. Gap junctions play an essential role in mediating synchronous contraction of smooth muscle cells. Cx43 is the most important protein during that process[24]. Loss of Cx43 expression may be partially responsible for smooth muscle motor dysfunction[25]. Repair of the intestinal nervous system network structure in rats with slow transit constipation can improve the expression of Cx43 etc. and constipation symptoms[26]. These results indicate that the increased expression of AQP3 decreases fecal water content, leading to constipation, which may be an important mechanism of constipation. Expression of Cx43 may be related to contraction of intestinal smooth muscle and reduce the occurrence of constipation. In our study, western blotting showed that Cx43 expression was increased and AQP3 expression was inhibited by *C. deserticola* treatment, which resulted in increased smooth muscle contraction and decreased water absorption, and blocker treatment reversed these effects.

CONCLUSION

In conclusion, *C. deserticola* can inhibit expression of AQP3 and promote expression of Cx43 through the SCF/C-kit pathway, thereby improving the constipation induced by loperamine and reducing colonic tissue damage in aged rats. This study provided a good theoretical basis for clinical use of *C. deserticola*.

ARTICLE HIGHLIGHTS

Research background

Chronic constipation is a common functional gastrointestinal disease that seriously affects the quality of life, especially for senile patients. *Cistanche deserticola* (*C. deserticola*) is one kind of herb that can improve constipation obviously, but the mechanism of it is unclear. Since it increases the frequency of defecation, we suppose that its therapeutic effect is due to increased intestinal motility by an important signaling pathway, stem cell factor (SCF)/C-kit, located on the surface of interstitial Cajal cells.

Research motivation

The treatment of chronic constipation is not encouraging, and the available drugs cannot meet the clinical needs. New drugs are needed to safely increase intestinal motility and improve symptoms. New drugs should be based on in-depth studies of the mechanisms of some foods that are currently widely and safely used. *C. deserticola* is one kind of herb that has been used for thousands of years in Traditional Chinese Medicine for constipation. Benefits would be evident from more studies about the treatment mechanisms.

Research objectives

To investigate the mechanism of how *C. deserticola* treats constipation, this study aimed to establish a constipation model in rats and explore the role of the SCF/C-kit signaling pathway in the treatment.

Research methods

In the case of blank control group, a constipation rat model was first established. While these rats were treated with *C. deserticola*, a group of rats were specifically blocked from the target signaling pathway. The symptoms and defecation of these different groups of rats were observed, and the tissue and gene expression in which the target signaling pathway was located were observed to explain whether the SCF/C-kit signaling pathway plays a key role in the therapeutic effect of *C. deserticola*.

- 10.1113/jphysiol.2003.058792]
- 18 **Torihashi S**, Ward SM, Nishikawa S, Nishi K, Kobayashi S, Sanders KM. c-kit-dependent development of interstitial cells and electrical activity in the murine gastrointestinal tract. *Cell Tissue Res* 1995; **280**: 97-111 [PMID: 7538451 DOI: 10.1007/BF00304515]
 - 19 HX. Discussions on regulation of acupuncture on SCF/c-kit signaling pathway and mechanism of treatment of slow transverse constipation. *Nanjing: Nanjing University of Traditional Chinese Medicine* 2012
 - 20 **Wang JM**, Li M, Tang R, Wang PS, Xu LJ, Zhang R, Han Y. Effects of Recipe for invigorating qi, invigorating spleen and relieving constipation on ICC and SCF/ C-KIT signal pathway in colonic tissue of rats with slow transmission constipation. *Zhonghua Zhongyiyao Xuekan* 2019; **37**: 156-160+264
 - 21 **Ding YR**, Zheng PY, Li FG, Mei L, Huang H, Bai LM, Liu SM. Effects of Lactitol and Bifidobacterium infantis on AQP3 and ICC in rats with constipation. *Zhonghua Weishengwuxue He Mianyixue Zazhi* 2015; **35**: 890-895
 - 22 **Ji TL**. Effect of Defaecation Decoction on AQP3 and AQP4 in rats with slow transit constipation. *Nanjing: Nanjing University of Traditionl Chinese Medicine* 2017
 - 23 **Wang YJ**, Zhou YX, Zhang H, Yan SG, Xie P, Man SY, Li S. Effects of N Oral Xiaofu Tongjie Decoction on the Expression of VIP and AQP3 in Colonic Tissue of Rats with Functional Constipation. *Zhongguo Shiyen Fangjixue Zazhi* 2015; **9**: 116-119
 - 24 **Yu W**, Zeidel ML, Hill WG. Cellular expression profile for interstitial cells of cajal in bladder-a cell often misidentified as myocyte or myofibroblast. *PLoS One* 2012; **7**: e48897 [PMID: 23145014 DOI: 10.1371/journal.pone.0048897]
 - 25 **Nemeth L**, Maddur S, Puri P. Immunolocalization of the gap junction protein Connexin43 in the interstitial cells of Cajal in the normal and Hirschsprung's disease bowel. *J Pediatr Surg* 2000; **35**: 823-828 [PMID: 10873019 DOI: 10.1053/jpsu.2000.6851]
 - 26 **Kong JY**. Experimental study on the effect of Oral Xiaofu Tongjie Fluid on the repair of intestinal nervous system network structure in rats with slow transit constipation. *Chengdu Zongyiyao Daxue Xuebao* 2019

Basic Study

Recombinant angiotensin-like protein 4 attenuates intestinal barrier structure and function injury after ischemia/reperfusion

Zi-Yi Wang, Jian-Yu Lin, Yang-Rong Feng, De-Shun Liu, Xu-Zi Zhao, Tong Li, Si-Yuan Li, Jing-Chao Sun, Shu-Feng Li, Wen-Yan Jia, Hui-Rong Jing

ORCID number: Zi-Yi Wang 0000-0003-4119-6858; Jian-Yu Lin 0000-0002-7937-0324; Yang-Rong Feng 0000-0001-7893-0994; De-Shun Liu 0000-0002-9026-117X; Xu-Zi Zhao 0000-0002-2803-3256; Tong Li 0000-0002-9987-8256; Si-Yuan Li 0000-0003-0588-3191; Jing-Chao Sun 0000-0002-8370-4817; Shu-Feng Li 0000-0002-9626-681X; Wen-Yan Jia 0000-0002-5334-7628; Hui-Rong Jing 0000-0003-2725-1785.

Author contributions: Wang ZY, Jing HR and Lin JY designed the study; Jing HR and Wang ZY supervised the study; Liu DS, Zhao XZ and Sun JC collected and analyzed the data; Li SY and Feng YR performed the R Script; Lin JY and Li SF and Jia WY prepared the figures and drafted the manuscript; Jing HR and Li Tong revised the manuscript for important intellectual content; Jing HR and Jia WY contributed equally as co-corresponding authors; all authors read and approved the final manuscript.

Supported by the National Natural Science Foundation of China, No. 81600446; the Science and Technology of Traditional Chinese Medicine Foundation in Qingdao, No. 2021-zyyz03; and the Science and technology development of Medicine and health Foundation in

Zi-Yi Wang, Emergent Intensive Care Unit, The Second Affiliated Hospital of Dalian Medical University, Dalian 116023, Liaoning Province, China

Jian-Yu Lin, Department of Gastrointestinal Surgery, Weihai Central Hospital, Weihai 264200, Shandong Province, China

Yang-Rong Feng, Graduate College, Shandong First Medical University, Jinan 271000, Shandong Province, China

De-Shun Liu, Department of General Surgery, The Second Affiliated Hospital of Dalian Medical University, Dalian 116027, Liaoning Province, China

Xu-Zi Zhao, Department of Pharmacology, Dalian Medical University, Dalian 116044, Liaoning Province, China

Tong Li, Department of General Surgery, Peking Union Medical College Hospital, Chinese Academy of Medical Sciences & Peking Union Medical College, Beijing 100000, China

Si-Yuan Li, Jing-Chao Sun, Shu-Feng Li, Hui-Rong Jing, Department of General Surgery, Qingdao Municipal Hospital, Qingdao University, Qingdao 266071, Shandong Province, China

Wen-Yan Jia, Physiological Examination Center, The Affiliated Hospital of Qingdao University, Qingdao 266000, Shandong Province, China

Corresponding author: Hui-Rong Jing, MD, PhD, Associate Professor, Surgeon, Department of General Surgery, Qingdao Municipal Hospital, Qingdao University, No. 5 Donghai Middle Road, Southern District, Qingdao 266071, Shandong Province, China. jhrdlmu_edu@126.com

Abstract**BACKGROUND**

Intestinal barrier breakdown, a frequent complication of intestinal ischemia-reperfusion (I/R) including dysfunction and the structure changes of the intestine, is characterized by a loss of tight junction and enhanced permeability of the intestinal barrier and increased mortality. To develop effective and novel therapeutics is important for the improvement of outcome of patients with intestinal barrier deterioration. Recombinant human angiotensin-like protein 4 (rhANGPTL4) is reported to protect the blood-brain barrier when administered

Shandong Province, China, No. 202004010508.

Institutional animal care and use committee statement: The study was reviewed and approved by the Dalian Medical University Institutional Review Board (Approval No. L20190232).

Conflict-of-interest statement: The authors declare that they have no competing interests.

Data sharing statement: No additional data are available.

ARRIVE guidelines statement: The authors have read the ARRIVE Guidelines, and the manuscript was prepared and revised according to the ARRIVE Guidelines.

Open-Access: This article is an open-access article that was selected by an in-house editor and fully peer-reviewed by external reviewers. It is distributed in accordance with the Creative Commons Attribution NonCommercial (CC BY-NC 4.0) license, which permits others to distribute, remix, adapt, build upon this work non-commercially, and license their derivative works on different terms, provided the original work is properly cited and the use is non-commercial. See: <http://creativecommons.org/licenses/by-nc/4.0/>

Manuscript source: Unsolicited manuscript

Specialty type: Gastroenterology and hepatology

Country/Territory of origin: China

Peer-review report's scientific quality classification

Grade A (Excellent): A, A
Grade B (Very good): 0
Grade C (Good): 0
Grade D (Fair): D
Grade E (Poor): 0

Received: April 24, 2021

Peer-review started: April 24, 2021

First decision: June 3, 2021

Revised: June 17, 2021

Accepted: July 30, 2021

exogenously, and endogenous ANGPTL4 deficiency deteriorates radiation-induced intestinal injury.

AIM

To identify whether rhANGPTL4 may protect intestinal barrier breakdown induced by I/R.

METHODS

Intestinal I/R injury was elicited through clamping the superior mesenteric artery for 60 min followed by 240 min reperfusion. Intestinal epithelial (Caco-2) cells and human umbilical vein endothelial cells were challenged by hypoxia/reoxygenation to mimic I/R *in vitro*.

RESULTS

Indicators including fluorescein isothiocyanate-conjugated dextran (4 kilodaltons; FD-4) clearance, ratio of phosphorylated myosin light chain/total myosin light chain, myosin light chain kinase and loss of zonula occludens-1, claudin-2 and VE-cadherin were significantly increased after intestinal I/R or cell hypoxia/reoxygenation. rhANGPTL4 treatment significantly reversed these indicators, which were associated with inhibiting the inflammatory and oxidative cascade, excessive activation of cellular autophagy and apoptosis and improvement of survival rate. Similar results were observed *in vitro* when cells were challenged by hypoxia/reoxygenation, whereas rhANGPTL4 reversed the indicators close to normal level in Caco-2 cells and human umbilical vein endothelial cells significantly.

CONCLUSION

rhANGPTL4 can function as a protective agent against intestinal injury induced by intestinal I/R and improve survival *via* maintenance of intestinal barrier structure and functions.

Key Words: Angiotensin-like protein 4; Intestinal ischemia/reperfusion; COVID-19; Myosin light chain kinase; Intestinal barrier breakdown

©The Author(s) 2021. Published by Baishideng Publishing Group Inc. All rights reserved.

Core Tip: Improving therapy on intestinal barrier dysfunction induced by ischemia/reperfusion is still challenging. Most recently, studies indicated that patients who suffered from coronavirus disease 2019 are associated with intestinal hypoperfusion. We investigated the effect of recombinant human angiotensin-like protein 4 on intestinal barrier structure and function deterioration using intestinal ischemia/reperfusion models in rats as well as hypoxia/reoxygenation models in cells. Intestinal barrier indicators associated with the inflammatory and oxidative cascade, excessive activation of cellular autophagy and apoptosis were compared. Our results indicated that recombinant human angiotensin-like protein 4 behaved as a promising therapeutic agent for intestinal ischemia/reperfusion-induced intestine injury.

Citation: Wang ZY, Lin JY, Feng YR, Liu DS, Zhao XZ, Li T, Li SY, Sun JC, Li SF, Jia WY, Jing HR. Recombinant angiotensin-like protein 4 attenuates intestinal barrier structure and function injury after ischemia/reperfusion. *World J Gastroenterol* 2021; 27(32): 5404-5423

URL: <https://www.wjgnet.com/1007-9327/full/v27/i32/5404.htm>

DOI: <https://dx.doi.org/10.3748/wjg.v27.i32.5404>

INTRODUCTION

Intestinal barrier dysfunction induced by ischemia/reperfusion (I/R) and atopic dermatitis is frequently observed in clinical practice. Hospital mortality due to acute mesenteric ischemia remains high, ranging from 60% to 90% over the past few decades [1]. Reperfusion following intestinal ischemia promotes extensive activation of inflam-

Article in press: July 30, 2021**Published online:** August 28, 2021**P-Reviewer:** Delgado-Gallegos JL,
Katada K**S-Editor:** Zhang H**L-Editor:** Filipodia**P-Editor:** Li JH

matory response and oxidative stress, autophagy and apoptosis, leading to a dreadful illness, such as multiple organ dysfunction syndromes (MODS), especially breakdown of the intestinal barrier[2,3]. Recent studies have indicated that coronavirus disease 2019 associated with intestinal hypoperfusion may further deteriorate barrier dysfunction and acute lung injury *via* a positive feedback mechanism[4]. Although remarkable progress has been made, there is no widely accepted therapy to prevent I/R associated intestinal barrier dysfunction.

Integrity of the intestinal mucosal barrier is retained by the critical factors of tight junctions and intercellular junctions, including transmembrane proteins such as zonula occludens (ZO), claudins (CLDN) and junctional adhesion molecule. These consist of a complex that forms a selectively permeable seal between adjacent epithelial cells, which is a key element in the paradigm of gut-origin MODS[5,6]. Myosin light chain (MLC) phosphorylation *via* MLC kinase (MLCK) is critical in pathophysiological modulation of intestinal mucosal barrier breakdown. ZO-1 and CLDN-2 behaved specifically as loss and redistribution in intestinal mucosal barrier breakdown and may be regulated *via* an MLCK-dependent MLC phosphorylation signaling pathway[6-8]. Another critical factor is vascular leakage, which contributes to the intestinal barrier dysfunction after I/R. Microvascular endothelial cell layer including VE-cadherin (VE-cad) creates a semi-permeable barrier between tissue and blood for the transport of lipids, proteins and electrolytes. Microvascular barrier dysfunction is crucial in the initiation and progression of vascular barrier disruption after I/R[5,9,10].

Angiopoietin-like 4 (ANGPTL4) was identified by three independent research groups simultaneously and named ANGPTL4 by The HUGO Gene Nomenclature Committee in 2000[11]. Extensive investigations have been carried out over the past decades and found that this molecule is a remarkably dynamic entity that participates in a variety of pathophysiological conditions. The functions of ANGPTL4 have been involved in energy homeostasis, wound healing, anoikis resistance, retinopathy angiogenesis and corneal epithelium repair as well as ischemic and barrier regulation [12]. Recent studies have reported that ANGPTL4 is a therapeutic agent in vasculoprotection and counteracting permeability of the blood-brain barrier in ischemic stroke [13]. Others also reported that ANGPTL4 blocked reactive oxygen species (ROS)-induced anoikis in cholangiocarcinoma cells[14]. It is postulated that ANGPTL4 may play a role in intestinal barrier integrity after intestinal I/R.

Here, we show that treatment with recombinant human ANGPTL4 (rhANGPTL4), in a rat model of intestinal I/R and intestinal epithelial (Caco-2) cells and human umbilical vein endothelial cells (HUVECs) with hypoxia/reoxygenation (H/R) *in vitro*, improves intestinal histopathology injury and attenuates the intestinal mucosa inflammatory and oxidant response. rhANGPTL4 counteracts the autophagy and apoptosis of the intestine and consequently diminishes the increase of permeability and loss of tight junction proteins of the intestine. Similar effects were also observed in intestinal epithelial cells and vascular endothelial cells. We provide the first empirical evidence that ANGPTL4 protects intestinal mucosa barrier integrity and confers intestine protection. ANGPTL4 might, therefore, constitute a relevant novel therapeutic approach for intestinal mucosa after I/R.

MATERIALS AND METHODS

Animals and ethics statement

Male Wistar rats weighing 180-220 g were purchased from Dalian Medical University Animal Experimental Center (Dalian, China, institutional protocol number: SCXK 2008-0002) and preserved under qualified experimental conditions with laboratory water and food. They were accommodated with an equipment shelter and kept at 25 °C and humidity of 40%-50% with a 12 h light-12 h dark cycle. Rats were acclimatized for 1 wk prior to experimentation. All steps were executed in line with the institutional animal care guiding principles and approved by the Institutional Ethics Committee.

Intestinal ischemia and reperfusion experiment

Intestinal I/R models were established according to the methods reported previously [15]. In brief, superior mesenteric artery was isolated following laparotomy and blocked softly using a non-invasive microvascular clip for 60 min. Occlusion was affirmed while the vessel beats paused and intestinal color faded, then clips were removed, and the procedure lasted 240 min. Sham animals received laparotomy and superior mesenteric artery identification but without clamping.

Animal treatment

Animals were randomly divided into 3 groups with 8 rats in each: (1) sham group; (2) vehicle (normal saline) + I/R group; and (3) I/R + rhANGPTL4 group. In group 3, rats were treated (*via* intravenous injection through tail vein) with rhANGPTL4 (28 mg/kg body weight in 0.5 mL normal saline) at the beginning of reperfusion. Rats in sham and I/R groups received normal saline with the same volume. All rats were sacrificed, and samples were collected for further investigation.

Collection of specimens

Blood samples of 5-6 mL were collected from the abdominal aorta at the end of reperfusion. They were preserved for 30 min at room temperature and centrifuged at 4 °C (3000 rpm for 15 min). The isolated serum was frozen at -80 °C. The supernatant was placed in a sterilized Eppendorf tube (Eppendorf Company, Limited, Shanghai, China) at -80 °C. Three centimeter proximal jejunum and distal ileum was separated after animals were sacrificed and then placed at -80 °C for further investigation.

Assessment of intestinal permeability

Intestinal mucosal barrier function was assessed by mucosal-to-serosal clearance of fluorescein isothiocyanate-conjugated dextran (4 kilodaltons; FD-4) in everted ileal sacs incubated *ex vivo* as previously described[16]. Intestinal microvascular permeability was investigated using VE-cad as the indicator.

Serum lactate dehydrogenase assay

Serum lactate dehydrogenase (LDH) was determined by a kinetic assay as previously described[16].

Histological examination

The jejunum segments were collected and embedded in 4% paraformaldehyde for histological evaluation. Tissues were dehydrated in graded ethanol, paraffin-embedded and sliced. Slices were prepared and stained using hematoxylin-eosin. The intestinal mucosal injury was assessed using a light microscope following the criteria described by Chiu *et al*[17].

TUNEL staining

TUNEL staining was performed following the manufacturer's instructions (In Situ Cell Death Detection Kit; Roche, Germany) and previously described method[18]. TUNEL positive cells were counted under a microscope ($\times 400$), and the apoptotic cells in each slice were counted in seven independent areas followed by averaging.

Cell culture and H/R incubation

Caco-2 cells were acquired from the American Type Culture Collection (ATCC, Rockville, MD, United States). Cells were cultured in a humidified atmosphere of 5% CO₂ at 37 °C in Dulbecco's Modified Eagle Medium added with 1% nonessential amino acids, 10% fetal bovine serum and 1% glutamine (Gibco, CA, United States). In order to mimic intestinal I/R *in vivo*, Caco-2 cells were subjected to hypoxia for 1 h and reoxygenation for 4 h on passages 25-35 using microaerophilic equipment (Thermo Fisher Scientific, United States). Both small interfering RNA (siRNA) control and siRNA ANGPTL4 cells treated with H/R and vehicle were included. After H/R, supernatants were obtained from the monolayers and centrifuged at 1300 rpm for 10 min at 4 °C. The apoptosis of Caco-2 monolayers was determined instantly. Supernatants were preserved at -80 °C for further enzyme-linked immunosorbent assay. HUVECs (Lonza; passages 3-6) were seeded and grown in endothelial growth medium (EGM bullet kit; Thermo fisher, Shanghai, China) containing 10% (vol/vol) fetal bovine serum at 37 °C. H/R was performed as that for intestinal epithelium cells.

Transient transfection of siRNA

For siRNA transfection, 1×10^5 Caco-2 cells were seeded on six-well plates and transfected at the time of 70%-80% confluence with an ANGPTL4 siRNA or non-binding control siRNA using Lipofectamin 2000 (Invitrogen, Karlsruhe, Germany): siRNA ANGPTL4 sense 5'-AAAGCTGCAAGATGACCTCAGATGGAGGCTG-3'; anti-sense 5'-AAAAGGCTTAAGAAGGGAATCTTCTGGAAGAC-3'; siRNA control sense 5'-AAAGCTGTCTTCAAGATTGATATCGAAGACTA-3'; and anti-sense 5'-AAAATAGTCTTCGATATCAAGCTTGAAGAC A-3'. After 24 h incubation, the cells were washed, and fresh Dulbecco's Modified Eagle Medium containing 10% fetal

bovine serum was supplemented.

Expression and purification of rhANGPTL4 proteins

Full-length rhANGPTL4 was purchased from ProSpec-Tany TechnoGene Ltd. (Rehovot, Israel).

Measurement of intracellular reactive oxygen species ROS accumulation

Fluorescent probe DCFH-DA (Sigma Aldrich, United States) was used to observe the intracellular accumulation of ROS. After exchanging the proper medium, cells (5×10^5 cells/mL) were incubated in 10 μ M DCFH-DA solution at 37 °C for 30 min and were examined using a confocal microscope outfitted with an argon laser (488 nm, 200 mW) as previously studied[19].

Detection of intestinal tissue and cell cytokines

Interleukin (IL)-6, tumor necrosis factor α (TNF- α) and IL-1 β were quantified using rat enzyme-linked immunosorbent assay kits (BOSTER Bioengineering Co. Ltd., Wuhan, China) in intestinal tissues. Intestinal tissues were collected and coagulated on ice for 2 h. Intestinal samples were acquired and homogenized using a tissue homogenizer (IKA T10 Basic, Staufen, Germany) in 1 mL lysis buffer containing 150 mmol/L NaCl, 0.5% Triton \times 100, 1 mmol/L CaCl₂, 15 mmol/L Tris and 1 mmol/L MgCl₂, pH 7.4. Homogenates were centrifuged at 10000 \times g for 10 min. Supernatants were preserved at -80 °C for further investigation.

Intestinal epithelial cells were stimulated with H/R *in vitro* and treated with or without rhANGPTL4 as described above. Supernatants of cell homogenates were harvested after treatment and transferred to a -80 °C refrigerator for further analysis. TNF- α , IL-6 and IL-1 β of the cell homogenate supernatants were determined using the enzyme-linked immunosorbent assay (Bender Med Systems, San Diego, CA, United States) and quantified according to the standard curve method.

Western blotting analysis

For detecting ANGPTL4, MLCK, phosphorylated MLC (p-MLC), MLC, ZO-1, CLDN-2, VE-cad, microtubule-associated protein light chain 3 (LC3)-I, LC3-II, p62, beclin-1 and caspase-3 content in the intestine and Caco-2 cells, 30 μ g protein was extracted using 12% and 15% SDS-PAGE (Bio-Rad, Hercules, CA, United States), and moved to a polyvinylidene difluoride membrane (Millipore, Bedford, MA, United States). Membranes were incubated with primary anti-ANGPTL4 antibody (Abcam Ltd., Cambridge, United Kingdom), anti-MLCK antibody (Abcam Ltd., Hong Kong, United Kingdom), p-MLC and MLC antibody (Cell Signaling Technology, Beverly, MA, United States), anti-ZO-1 and CLDN-2 antibody and anti-VE-cad (Santa Cruz Biotechnology, United States), anti-LC3-I, anti-LC3-II, anti-p62, anti-Beclin-1 antibody (Santa Cruz Biotechnology, United States), anti-caspase-3 and anti-cleaved-caspase-3 antibody (Bioss, Minneapolis, MN, United States) or anti- β -actin antibody in Tris-phosphate-buffered solution overnight at 4 °C in 5% skimmed milk. The membranes were co-incubated with biotinylated secondary antibody and diluted 1:1000 in PBST containing 5% skimmed milk at 37 °C for 2 h after washing 3 times in TBS containing 0.1% Tween 20. Then membranes underwent large-scale elution with TBS containing 0.1% Tween and exposed using an enhanced chemiluminescence kit (Beyotime Institute of Biotechnology, Hangzhou, China).

Quantitative real-time polymerase chain reaction

Total RNA was collected from animals with Trizol kits (Invitrogen, Carlsbad, CA, United States) in line with the manufacturer's instructions. Reverse transcription into complementary DNA was executed using a TaKaRa RNA polymerase chain reaction (PCR) Kit (avian myeloblastosis virus) Version 3.0 (TaKaRa, Dalian, China) for PCR analysis; primers were described as follows: ANGPTL4 sense: 5'-AGACCCGAAG-GATAGAGTCCC-3' (forward), antisense: 5'-CCTTCTGGAACAGTTGCTGG-3' (reverse); β -actin sense: 5'-AGAGGGAAATCGTGCGTGAC-3' (forward), antisense: 5'-CAATAGTGATGACCTGGCCGT-3' (reverse). SYBR Premix Ex Taq kit (Takara, China) was used to perform quantitative real-time PCR, and ABI 7500 Fast Real-Time PCR System (Applied Biosystems) was used for fluorescence determination during amplification. PCR cycling was performed as follows: Initial annealing at 95 for 30 s, and 40 cycles at 95 °C for 5 s, 60 °C for 34 s and 72 °C for 30 s.

Statistical analysis

All measurements were calculated using mean \pm SD. A one-way analysis of variance was used to compare the average values of all groups. The Student-Newman-Keuls/least significant difference test was used to compare the mean of all pairs. Student's *t* test was used for the comparison of two groups. Kaplan-Meier log-rank test was applied to analyze the survival. A *P* value less than 0.05 was considered statistically significant. All statistical analyses were performed using SPSS 18.0 statistical software package (SPSS, Chicago, IL, United States).

RESULTS

Intestinal I/R induces endogenous ANGPTL4 expression

It has been reported that ANGPTL4 is induced in a mouse model of ischemic stroke and severe intestinal inflammation. We wondered whether ANGPTL4 might be expressed in the intestine after I/R in rats. Intestinal I/R injury markedly promoted the mRNA and protein expression of endogenous ANGPTL4 ($P < 0.05$; **Figure 1**). These findings indicate that endogenous ANGPTL4 is involved in intestinal I/R. Having shown that ANGPTL4 is expressed upon intestinal I/R, we then sought to investigate its effect on intestinal I/R.

rhANGPTL4 improves intestinal histopathologic injury and decreases LDH level after intestinal I/R

To illustrate the effect of extrinsic administration of ANGPTL4 on intestinal I/R injury, rhANGPTL4 (28 mg/kg body weight) was administered *via* the tail vein at the initiation of reperfusion. Intestinal I/R caused generalized and macroscopic necrosis with severe intestinal mucosal injury in intestinal areas paratactic to the macroscopically ischemic intestine ($P < 0.01$; **Figure 2A**). Similarly, serum LDH, a biochemical marker of tissue damage, was significantly elevated *vs* the sham group ($P < 0.01$; **Figure 2B**), suggesting the generalized tissue injury induced during this pathological process. Administration of rhANGPTL4 alleviated intestinal I/R injury significantly. Histopathologically, most parts of the intestine were free of secondary mucosal injury after treatment ($P < 0.01$; **Figure 2A**). Furthermore, LDH levels in rhANGPTL4-treated rats were significantly lower than in the sham group after I/R ($P < 0.01$; **Figure 2B**). This indicates that ANGPTL4 treatment alleviates the severity of reperfusion.

rhANGPTL4 regulates the intestinal permeability barrier and MLCK-tight junction pathway-related proteins in vivo

To elucidate the role of rhANGPTL4 in intestinal barrier structure and function, we evaluated intestinal permeability of FD-4, MLCK, p-MLC/MLC, ZO-1 and CLDN-2 protein expression in intestinal mucosa, and the well-established and the recently confirmed methods were used for evaluation of intestinal barrier function. In vehicle-treated animals, I/R caused obvious destruction of intestinal barrier function manifested as increased FD-4 clearance *vs* the sham group ($P < 0.01$; **Figure 3A**). Meanwhile, MLCK and p-MLC/total MLC were also increased coupled with a decrease of ZO-1 and CLDN-2 in vehicle-treated I/R animals. rhANGPTL4 treatment resulted in marked recovery of FD-4 clearance and changes of MLCK, p-MLC/total MLC, ZO-1 and CLDN-2 protein levels 4 h after I/R, close to normal levels compared with vehicle animals ($P < 0.01$; **Figure 3B**). This indicates that rhANGPTL4 administration improves both structural and functional repair of the intestinal barrier dysfunction induced by I/R. In addition, ANGPTL4 is involved in the changes of intestinal I/R-induced mucosal barrier structure (MLCK-tight junction protein signaling pathway) and function (FD4 clearance rate in intestinal permeability). rhANGPTL4 confers intestinal mucosal barrier protection by altering the structure and function of the intestinal mucosal barrier. In this process, the MLCK-regulated tight junction signaling pathway may be a potential mechanism. We further investigated the possible mechanism that is involved in the process of intestinal mucosa barrier function regulation.

rhANGPTL4 suppresses the intestinal inflammatory response and oxidative stress after intestinal I/R

Proinflammatory cytokines are main contributing factors for the disruption of intestinal barrier dysfunction after I/R. We evaluated whether the intestinal cytokines

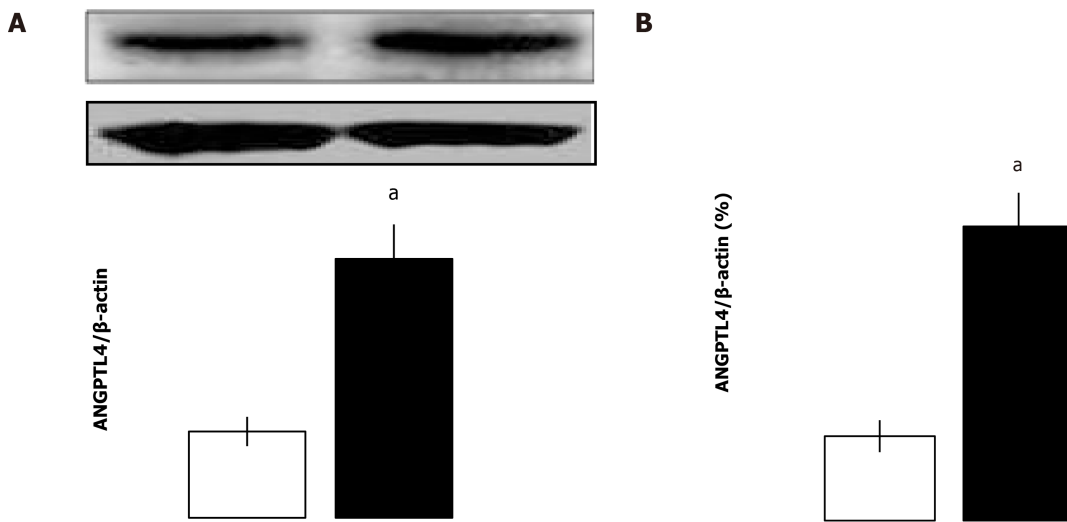


Figure 1 Intestinal angiotensin-like protein 4 level after intestinal ischemia-reperfusion in different groups (mean ± SD, *n* = 8). A: Angiotensin-like protein 4 protein levels were assessed by western blot; B: Angiotensin-like protein 4 mRNA levels in the intestine were measured by quantitative real-time polymerase chain reaction. ^a*P* < 0.05 vs sham by Student's *t* test. ANGPTL4: Angiotensin-like protein 4.

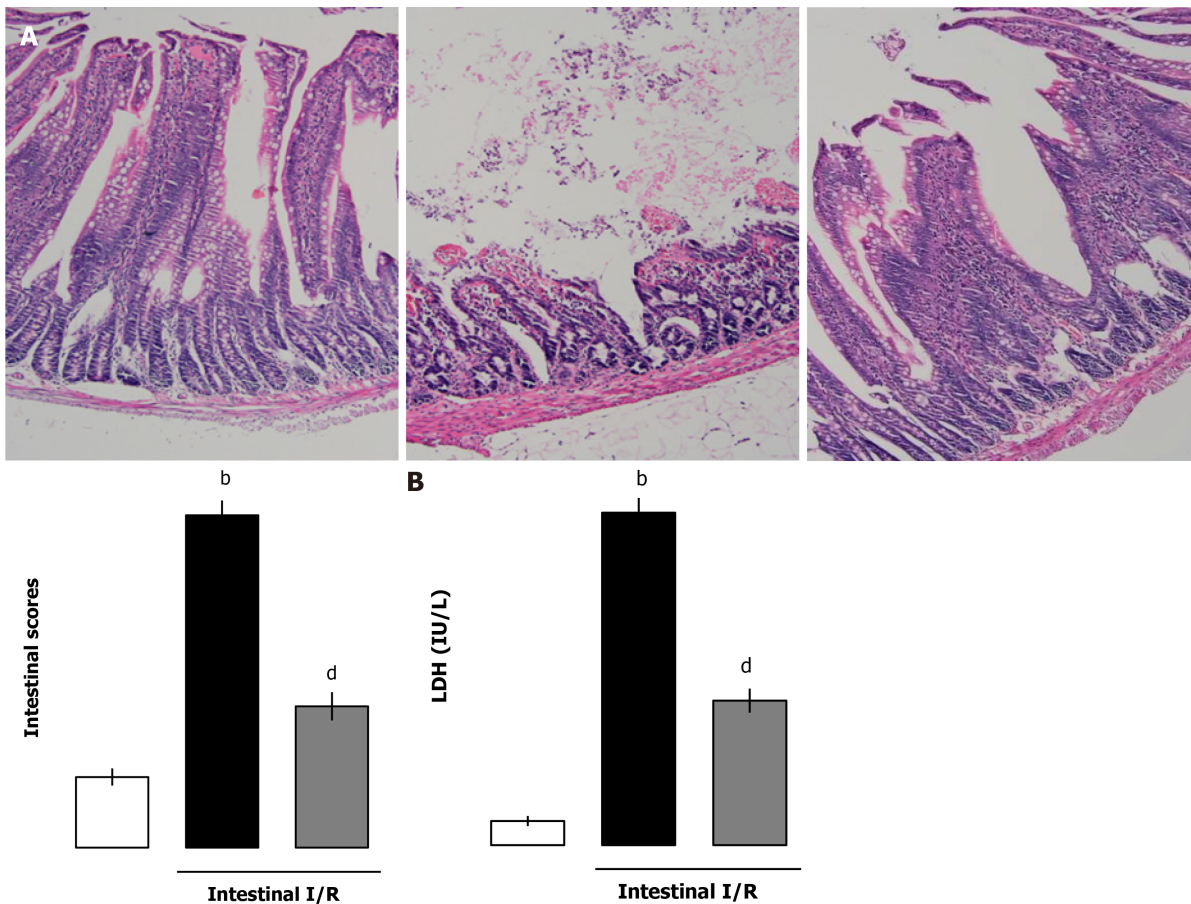


Figure 2 Recombinant human angiotensin-like protein 4 improved ischemia-reperfusion-induced intestinal histopathologically and serum lactate dehydrogenase. A and B: Pathologic changes of intestine (scale bar = 100 μm) of (A) tissue and (B) serum lactate dehydrogenase (LDH) in different groups (mean ± SD, *n* = 8). ^b*P* < 0.01 vs sham; ^d*P* < 0.01 vs ischemia-reperfusion. I/R: Ischemia-reperfusion.

TNF- α , IL-1 β , IL-6 and myeloperoxidase (MPO) levels were affected by administration of rhANGPTL4. Although the cytokines and MPO increased markedly after I/R, rhANGPTL4 dramatically reduced the proinflammatory response (*P* < 0.01, *P* < 0.05; Figure 4A-C) and MPO level (*P* < 0.05; Figure 4D). To investigate whether rhANGPTL4 influences oxidative damage to tissues, we further determined intestinal

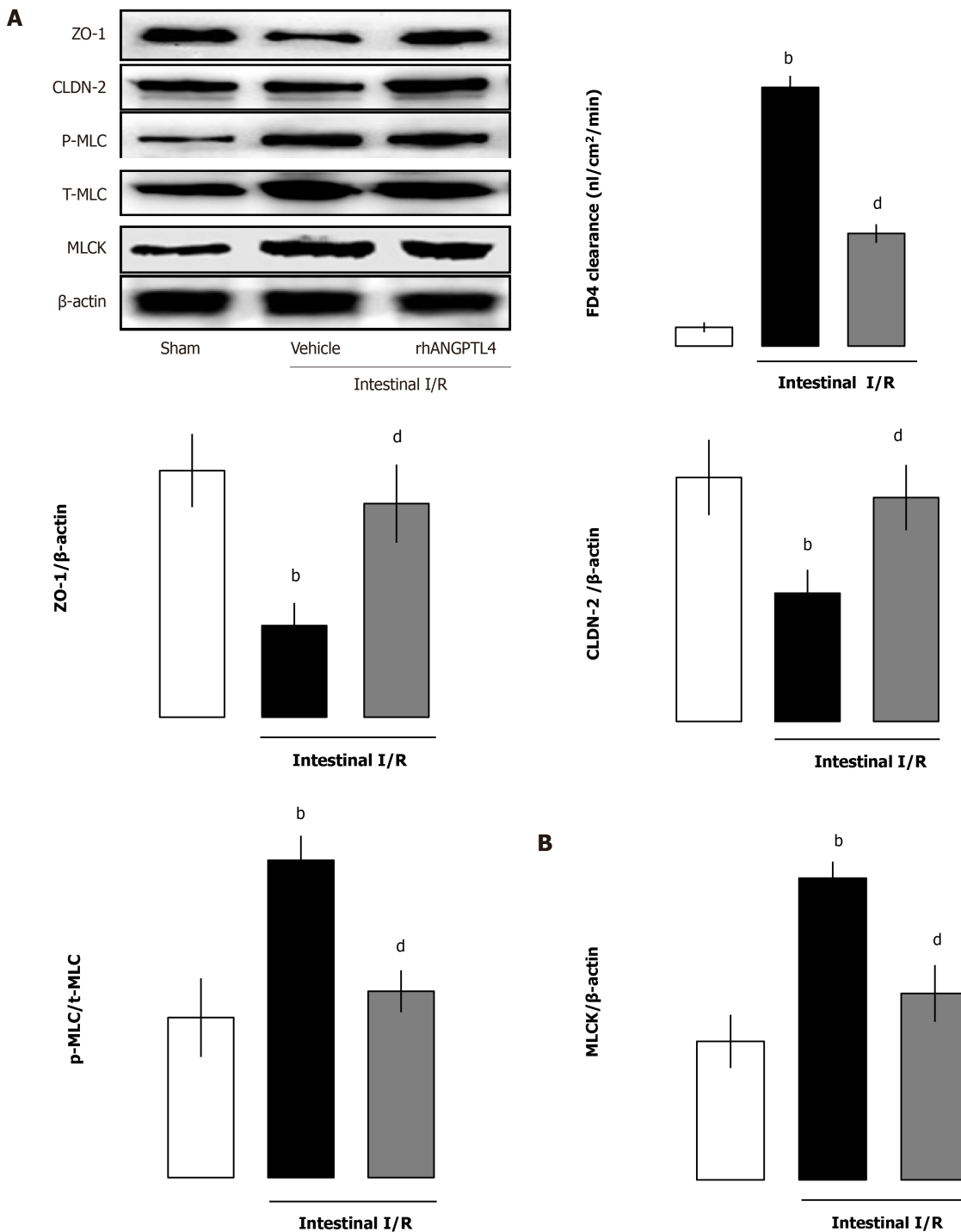


Figure 3 Recombinant human angiopoietin-like protein 4 regulates the intestinal permeability barrier and myosin light chain kinase-tight junction pathway related proteins *in vivo*. Intestinal mucosal tissue myosin light chain kinase (MLCK), phosphorylated-myosin light chain (p-MLC)/myosin light chain, zonula occludens-1 (ZO-1) and claudin-2 (CLDN-2) (A) and intestinal mucosal permeability (B) in different groups (mean \pm SD, $n = 8$). ^b $P < 0.01$ vs sham; ^d $P < 0.01$ vs ischemia-reperfusion (I/R). ANGPTL4: Angiopoietin-like protein 4; t-MLC: Total-myosin light chain.

malondialdehyde (MDA). Intestinal MDA levels reduced significantly after rhANGPTL4 treatment ($P < 0.05$; **Figure 4E**). Changes of these indicators were associated with intestinal barrier dysfunction. This suggests that inflammatory cytokines and the oxidative stress cascade are contributing factors in destructed intestinal barrier.

rhANGPTL4 reduces the increase of intestinal autophagy and apoptosis after I/R

Intestinal I/R increased intestinal autophagy-related protein levels (beclin-1, LC3-I and LC3-II) but decreased the substrate p62 protein levels ($P < 0.05$; **Figure 5A**). As a classical apoptotic marker, the cleaved caspase-3 protein expression and numbers of

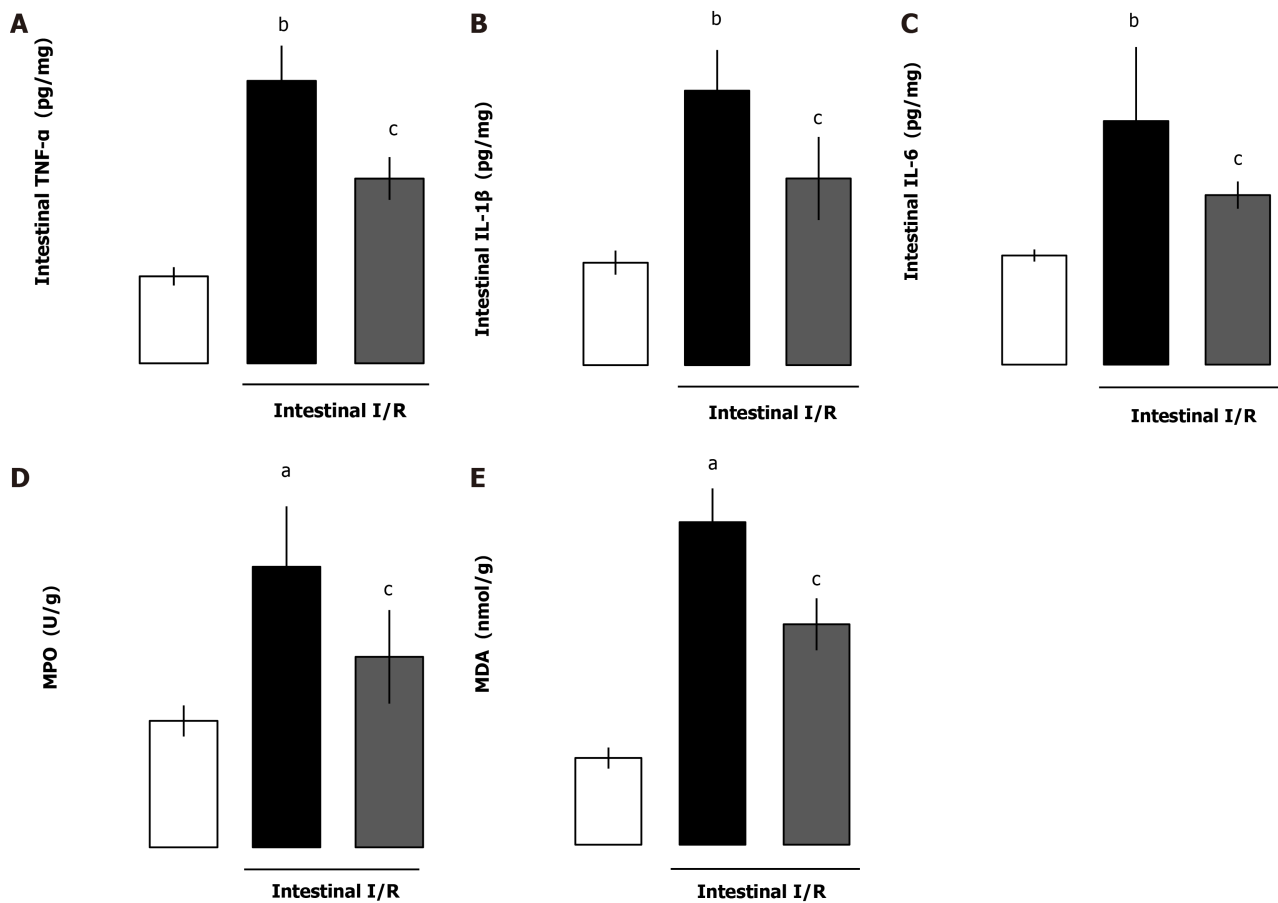


Figure 4 Recombinant human angiopoietin-like protein 4 suppresses the intestinal inflammatory response and oxidation stress after intestinal ischemia-reperfusion. A-E: Intestinal cytokine tumor necrosis factor- α (TNF- α) (A), interleukin (IL)-1 β (B), interleukin-6 (C), intestinal myeloperoxidase (MPO) (D) and malondialdehyde (MDA) (E) levels in different groups (mean \pm SD, $n = 8$). ^a $P < 0.05$, ^b $P < 0.01$ vs sham; ^c $P < 0.05$ vs ischemia-reperfusion (I/R).

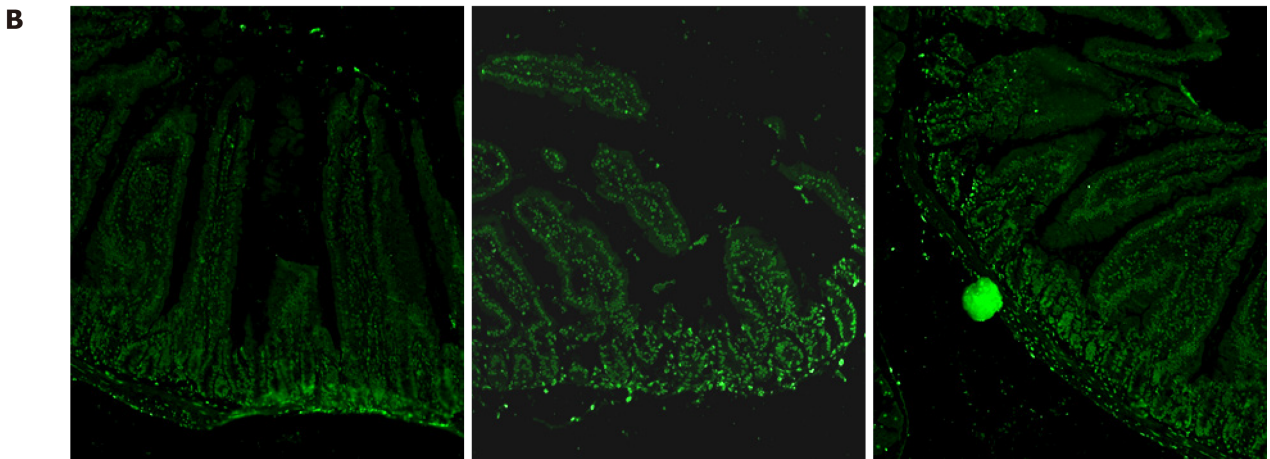
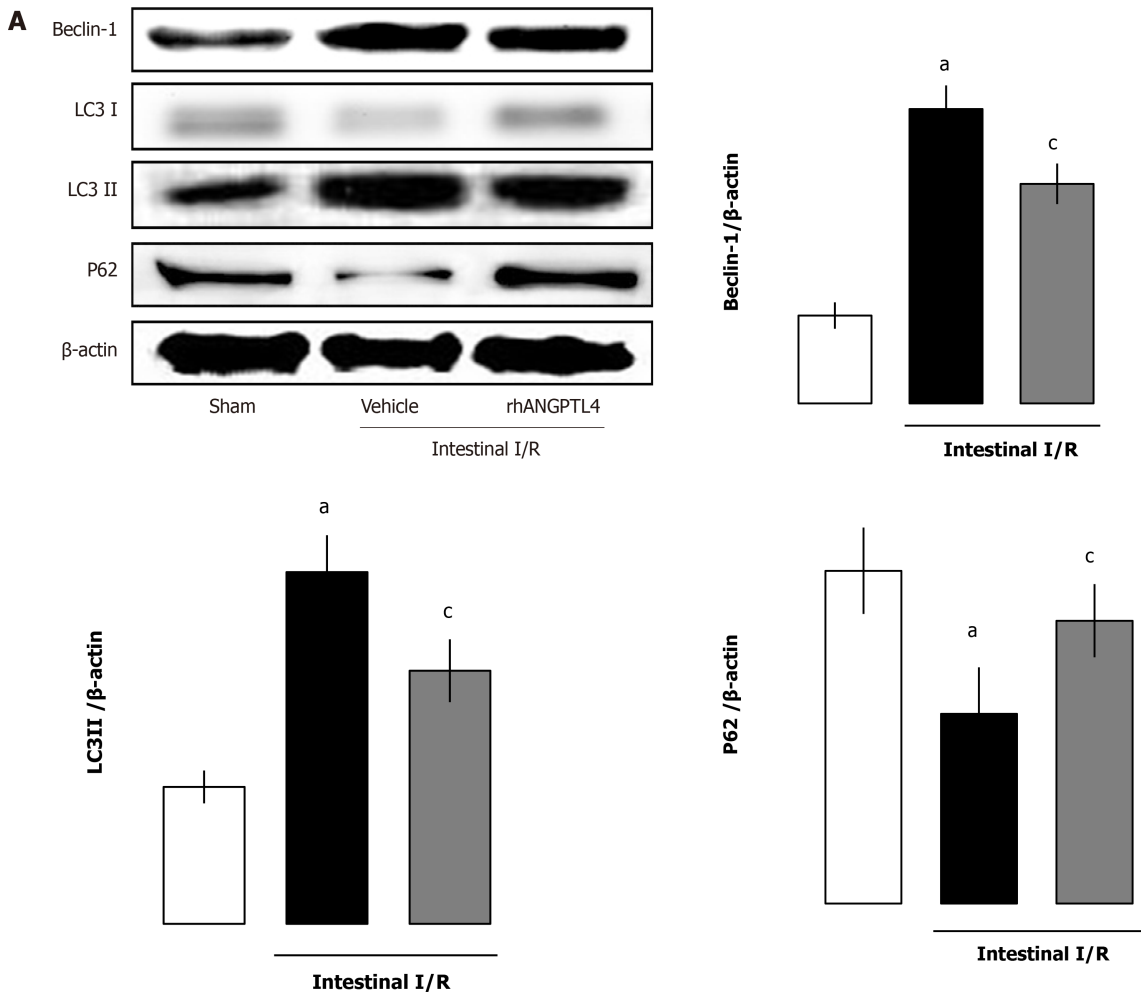
apoptotic cells by TUNEL staining in the intestine was markedly increased after I/R. Treatment with rhANGPTL4 decreased intestinal cleaved caspase-3 levels and apoptotic cell numbers remarkably to those in the sham group ($P < 0.05$; Figure 5B and 5C). At the same time, we found that the autophagy-related proteins (beclin-1, LC3-I, and LC3-II) and the substrate p62 in the intestine also recovered after treatment with rhANGPTL4 to those in sham animals ($P < 0.05$; Figure 5A). This indicates that excessive activated autophagy and apoptosis are crucial in the destruction of intestinal barrier integrity, and rhANGPTL4 is an effective agent to inhibit autophagy and apoptosis in intestinal I/R.

rhANGPTL4 improves animal survival after intestinal I/R

Animals in the vehicle group were sacrificed < 24 h following intestinal I/R injury ($P < 0.05$; Figure 6). However, rhANGPTL4-treated rats exhibited significant longer survival. The 24 h survival rate of rhANGPTL4 group was increased markedly compared to vehicle animals.

ANGPTL4 deficiency aggravates intestinal epithelial cell injury after H/R in vitro

To illustrate the effect of ANGPTL4 in intestinal I/R-induced barrier dysfunction, intestinal epithelial cells were used and siANGPTL4 was challenged by H/R to imitate intestinal I/R. We investigated the inflammatory response, ROS level, autophagy and apoptosis, and intestinal barrier function was measured using the MLCK-tight junction pathway-related protein in the intestinal epithelial cells. Compared with the vehicle group TNF- α and IL-6 levels associated with ROS levels upregulated significantly in both the siANGPTL4 control and siANGPTL4 groups after H/R. The same trends of LC3-II and cleaved caspase-3 but contrary expression of ZO-1 and CLDN-2 were observed correspondingly ($P < 0.01$; Figure 7). These indicate that ANGPTL4 is essential for maintaining the integrity of intestinal epithelial cell barrier function when challenged by H/R.



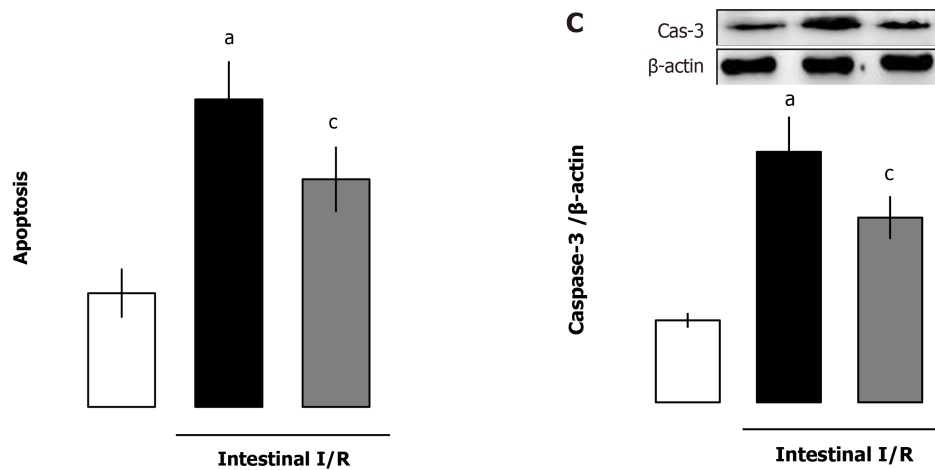


Figure 5 Recombinant human angiopoietin-like protein 4 reduced the increase of intestinal autophagy and apoptosis after ischemia-reperfusion. A: Intestinal autophagy-related protein beclin-1, microtubule-associated light chain 3 (LC3) I/II and p62 in different groups (mean ± SD, $n = 8$). ^a $P < 0.05$ vs sham; ^c $P < 0.05$ vs ischemia-reperfusion (I/R) groups; B and C: Intestinal apoptosis (scale bar = 100 μm) (B) and cleaved caspase-3 (Cas-3) (C) in different groups (mean ± SD, $n = 8$). ^a $P < 0.05$ vs sham; ^c $P < 0.05$ vs I/R. ANGPTL4: Angiopoietin-like protein 4.

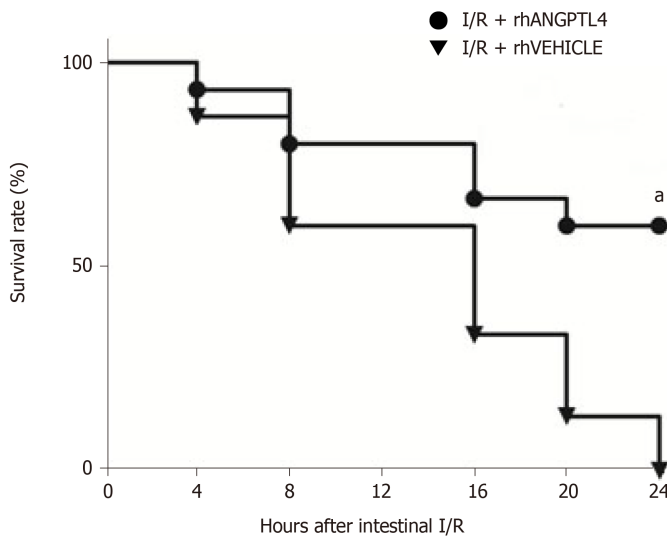


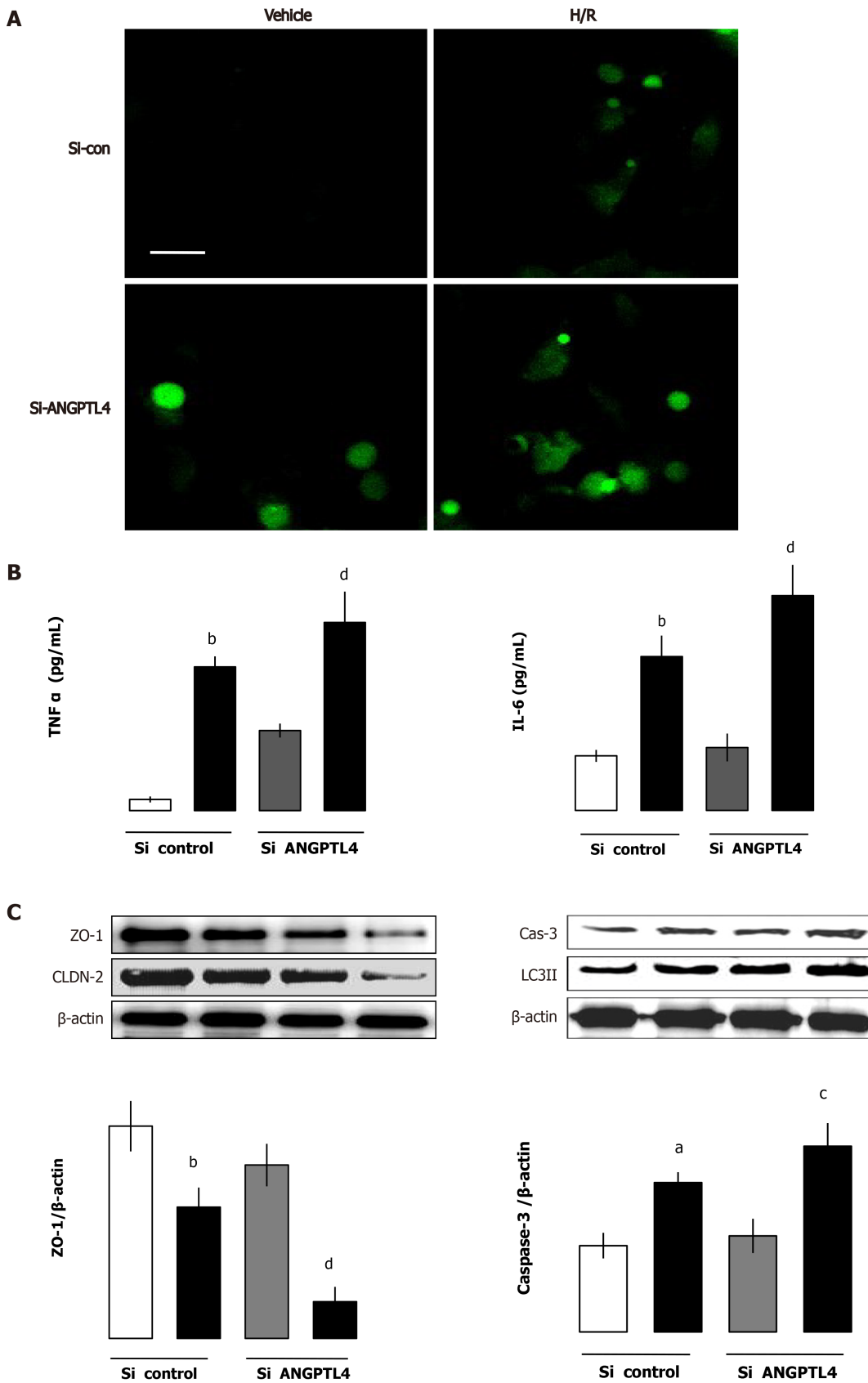
Figure 6 Survival benefit in recombinant human angiopoietin-like protein 4-treated rats after intestinal ischemia-reperfusion injury ($n = 15$, Kaplan Meyer log-rank test). Each point in the figure shows the mean survival rate at each time point. ^a $P < 0.05$ vs vehicle. I/R: Ischemia-reperfusion; rhANGPTL4: Recombinant human angiopoietin-like protein 4.

Administration of rhANGPTL4 protects against intestinal epithelial cell injury after H/R *in vitro*

To assess the effect of rhANGPTL4 on injury induced by H/R in siRNA ANGPTL4 (siANGPTL4) Caco-2 cells, rhANGPTL4 (10 μg/mL) or vehicle was injected before the H/R as previously described. Cell samples were harvested after reoxygenation for 4 h. Proinflammatory cytokines (including TNF-α and IL-6), MDA, cleaved caspase-3 and LC3-II levels and intestinal barrier-regulated protein expression of MLCK, ZO-1 and CLDN-2 were detected. Administration of rhANGPTL4 decreased proinflammatory cytokine (TNF-α and IL-6) levels and oxidative damage (MDA levels), inhibited autophagy (LC3-II levels) and apoptosis (cleaved caspase-3 levels) and reduced MLCK but restored the levels of ZO-1 and CLDN-2 after H/R in siANGPTL4 cells ($P < 0.05$, $P < 0.01$; Figure 8).

Administration of rhANGPTL4 protects against HUVECs injury after H/R *in vitro*

To investigate the role of rhANGPTL4 in vascular leakage induced by H/R in siANGPTL4 HUVECs, VE-cad was used as an indicator that plays a crucial role in the integrity of vascular endothelial function. rhANGPTL4 (10 μg/mL) or vehicle was



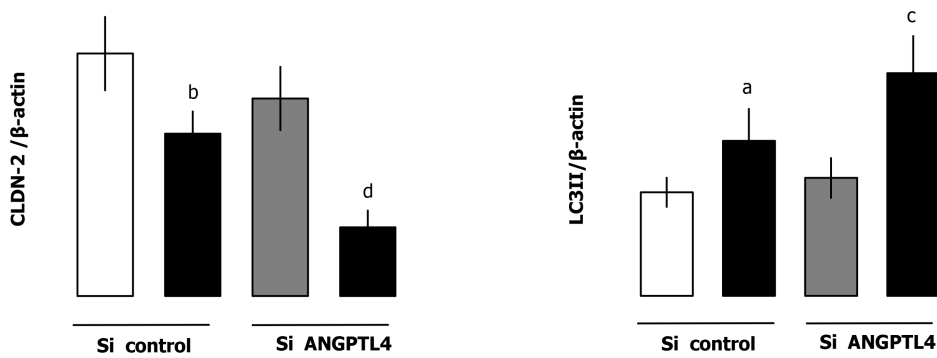


Figure 7 Angiopoietin-like protein 4 deficiency aggravates Caco-2 cells injury challenge by hypoxia/reoxygenation. A and B: Reactive oxygen species (ROS) levels (scale bar = 12.5 μ m) (A) determined by immunofluorescence and tumor necrosis factor- α (TNF- α) and interleukin (IL)-6 levels (B) determined by enzyme-linked immunosorbent assay; C: Tight junction zonula occludens-1 (ZO-1) and claudin-2 (CLDN-2), autophagy marker microtubule-associated protein light chain 3 (LC3) II and apoptosis marker caspase-3 were determined using western blot assays (mean \pm SD, $n = 3$). ^a $P < 0.05$, ^b $P < 0.01$ vs vehicle; ^c $P < 0.05$, ^d $P < 0.01$ vs vehicle ($n = 3$ per group). ANGPTL4: Angiopoietin-like protein 4; H/R: Hypoxia/reoxygenation; si: Small interfering RNA.

injected before H/R. Cell samples were collected at 4 h after reoxygenation. VE-cad protein expression was detected. Administration of rhANGPTL4 restored VE-cad protein expression levels significantly. Both ANGPTL4 vicious and ANGPTL4 control HUVECs exhibited low levels of VE-cad after H/R compared with vehicle cells ($P < 0.01$; Figure 9).

DISCUSSION

In the present study, we provide evidence and a potential mechanism that rhANGPTL4 alleviates intestinal I/R induced injury. *In vivo* rhANGPTL4 was found to (1) ablate intestinal tissue damage after I/R; (2) improve survival rate; (3) relieve the inflammatory response through inhibition of proinflammatory cytokines and restrict MPO, MDA and LDH; (4) lessen the autophagy and apoptosis molecules; and (5) maintain epithelial barrier function by restoration of tight junction (ZO-1 and CLDN2), inhibiting MLCK and phosphorylation of MLC and intestinal barrier permeability (FD-4 clearance rate). *In vitro* studies showed that (1) ANGPTL4 deficiency aggravated the inflammatory and oxidative response, apoptosis and autophagy, associated with the loss of intestinal barrier tight junction; (2) rhANGPTL4 had the ability to inhibit inflammation and oxidation, autophagy and apoptosis and preserve the tighten junctions, and accordingly it maintained the endothelial barrier integrity under ANGPTL4 vicious circumstances; and (3) rhANGPTL4 inhibited vascular leakage *via* limiting the endothelial dysfunction (loss of VE-cad) in HUVECs challenged by H/R.

Intestinal I/R injury is accompanied by enhanced inflammatory cytokines and ROS cascade, augmented apoptosis and autophagy, vascular leakage and aggravated mucosal lesions[1-4,9]. Intestinal barrier breakdown has been implicated as an important turning point in intestinal I/R injury[7]. The intestinal barrier is the largest defender between the intestine and distant organs including lung and liver, which is critical in the development of MODS[13,18]. As a filter with selective permeability, this interface allows absorption of essential nutrients and eliminates the invasion of deteriorating products, including proinflammatory factors, ROS, *etc.* Exacerbating the inflammatory response and oxidative stress can induce intestinal epithelial cell apoptosis and autophagy, consequently destroying the intestinal mucosal barrier. In addition, intestinal mucosal breakdown facilitates the inflammatory mediators and ROS associated with the bacteria-derived products to translocate to extraintestinal organs[1-3,15,20]. Until now, the underlying mechanisms/factors of I/R inducing intestinal barrier breakdown are still unclear. Recent studies reported that MLC phosphorylation mediated by upregulated MLCK is crucial to intestinal barrier breakdown induced by hypoxia or proinflammatory cytokines[7]. Tight junctions ZO-1 and CLDN-2 regulated by the MLCK pathway are the two crucial factors regulating the intestinal barrier in I/R[5].

ANGPTL4 is normally secreted from the intestinal villus epithelium and modulated by the intestinal microbiota. Studies have shown that ANGPTL4 is essential to resist the loss of villus endothelial and lymphocyte populations to radiation-induced apoptosis[21]. As it is reported that ANGPTL4 is crucial in the postnatal lymphatic

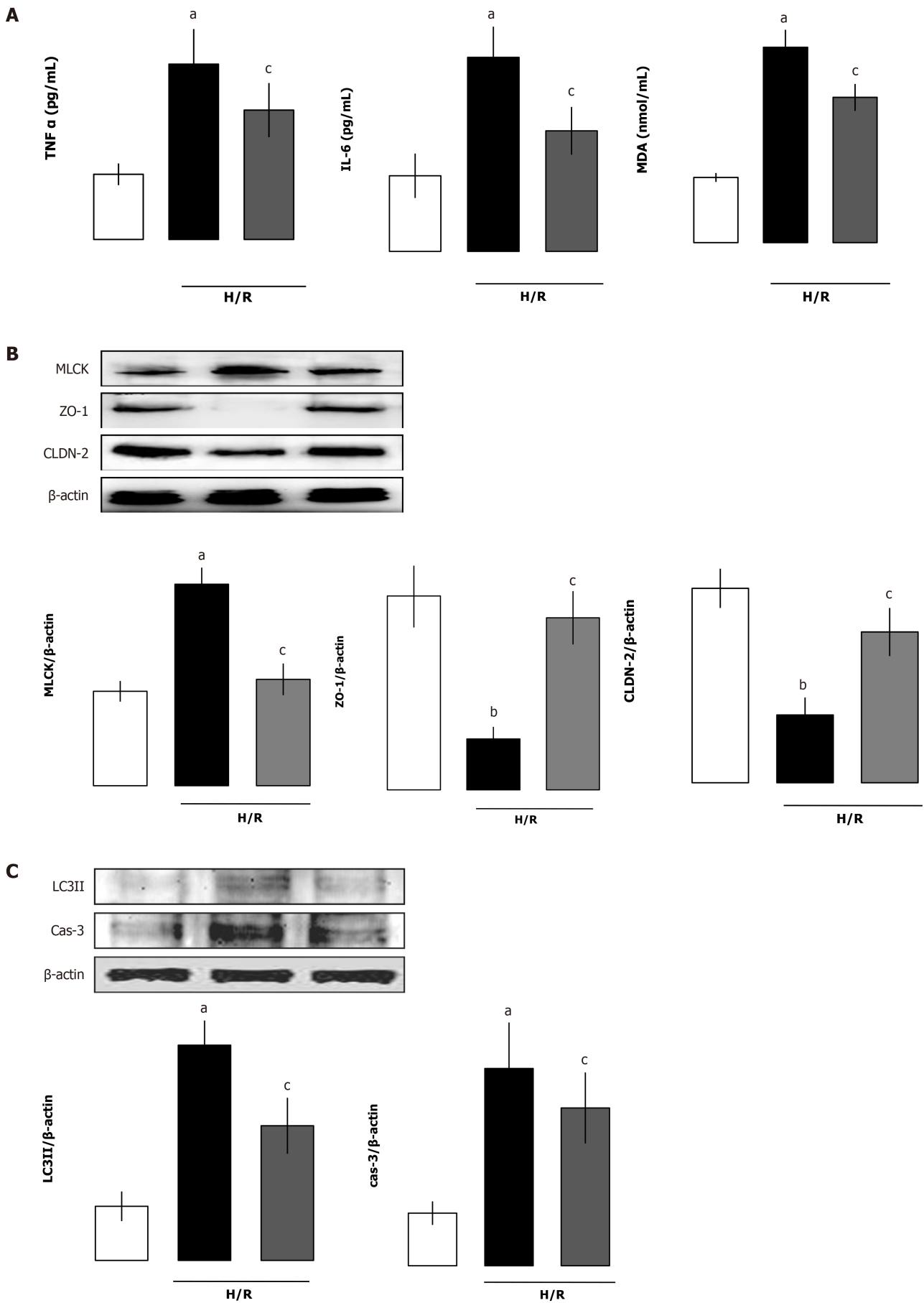


Figure 8 Beneficial effects of recombinant human angiopoietin-like protein 4 on angiopoietin-like protein 4 deficient Caco-2 cells challenged after hypoxia/reoxygenation. A: Cellular levels of tumor necrosis factor-alpha (TNF-α), interleukin (IL)-6 and malondialdehyde (MDA) levels; B:

Myosin light chain kinase (MLCK), zonula occludens-1 (ZO-1) and claudin-2 (CLDN-2) levels; C: Microtubule-associated protein light chain 3II and cleaved caspase-3 levels were measured 4 h after reoxygenation (mean \pm SD, $n = 3$). ^a $P < 0.05$, ^b $P < 0.01$ vs control; ^c $P < 0.05$ vs vehicle. H/R: Hypoxia/reoxygenation.

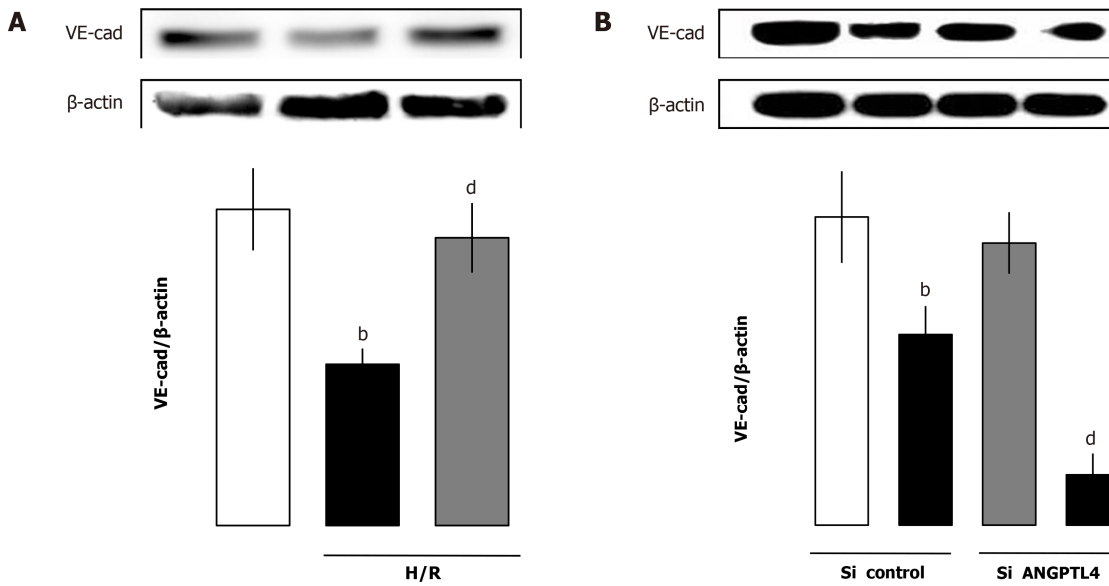


Figure 9 Levels of VE-cadherin after hypoxia/reoxygenation compared with respective vehicle cells. Recombinant human angiopoietin-like protein 4 restored the VE-cadherin (VE-cad) in human umbilical vein endothelial cells (A) after hypoxia/reoxygenation and VE-cadherin levels in small interfering (si) RNA angiopoietin-like protein 4 control and small interfering RNA angiopoietin-like protein 4 (ANGPTL4) human umbilical vein endothelial cells (B) of different groups (mean \pm SD, $n = 3$). ^b $P < 0.01$ vs vehicle; ^d $P < 0.01$ vs vehicle. H/R: Hypoxia/reoxygenation.

partitioning and disease, it is not unexpected that mice missing ANGPTL4 may die during the suckling period with dilated intestinal lymphatic vessels[21,22]. It is noteworthy that injection of rhANGPTL4 *in vivo* blocked VEGF-driven separation of the VEGFR2/VE-cad complexes, reduced myocardial infarct area and the no-reflow degree in animals. ANGPTL4 exhibited a therapeutic vasculoprotection on no-reflow and exerted cardioprotection[23-26].

However, the role of ANGPTL4 in various types of cells has not been evaluated in detail. We investigated the effects of ANGPTL4 and rhANGPTL4 in maintaining the epithelial barrier through various mechanisms under basal and I/R (H/R) conditions. This preliminary analysis indicated an assumed effect of ANGPTL4 in the circumstance of intestinal I/R-associated endothelial and epithelium barrier damage. In this study, we demonstrate that after I/R injury, intestinal barrier breakdown is associated with the up-regulation of both MLCK pathway-related protein expression and permeability of intestinal mucosa. An associated loss of tight junction protein ZO-1 and CLDN-2 as well as increased histological damage of mucosa were observed following I/R. However, treatment with rhANGPTL4 not only blocked the upregulation of MLCK pathway-related protein and intestinal mucosal permeability but also restored the tight junction proteins ZO-1 and CLDN-2 associated with a lower intestinal histological damage of mucosa. Similar results were also observed in ANGPTL4-deficient intestinal epithelial cells when challenged by H/R. However, this was not observed in the intestinal epithelial vehicle cells without H/R. This indicates that the role of ANGPTL4 is silent in normal circumstances but essential in the cellular homeostasis upon H/R stress stimulation.

It is widely accepted that the oxidative stress and inflammation cascade may contribute to the intestinal barrier destruction through various mechanisms. Activated and influxed immune cells including neutrophils and macrophages will release amplified proinflammatory cytokines (including TNF- α , IL-6 and IL-1 β) associated with oxygen free radicals. Higher levels of circulating proinflammatory cytokines and oxygen free radical activation lead to a loss of tight junction, eventually causing intestinal barrier breakdown induced by intestinal I/R[2,16]. Thus, a large number of studies have confirmed that the anti-inflammatory and antioxidative strategies are protective against breakdown of the barrier induced by I/R.

A previous study implicated that ANGPTL4 deficiency can aggravate the severe intestinal inflammation induced by high dietary saturated fat in rats[27]. Further studies showed that rhANGPTL4 protected ischemic stroke and exhibited antioxidative and anti-inflammatory effects[13]. We investigated the effect of ANGPTL4 on oxidative stress and inflammation during intestinal I/R. We found an enhanced expression of ANGPTL4 in rats with intestinal I/R and human intestinal epithelial cells stimulated with H/R, which indicated that ANGPTL4 exerted an effect on modulating the inflammatory milieu following intestinal I/R for triggering the progression of intestinal barrier dysfunction. Our results showed the antioxidative and anti-inflammatory effects of rhANGPTL4 on intestinal barrier dysfunction after I/R, and rhANGPTL4 alleviated the inflammatory and oxidative cascade both *in vivo* and *in vitro*. ANGPTL4-mediated barrier protection is due to, at least partially, the inhibition of the inflammatory and oxidative cascade.

In addition to the inflammatory and oxidative cascade, apoptosis and autophagy are mutual connection pathways, and both have direct disrupting roles in intestinal epithelial cells and the intestinal mucosal barrier in response to I/R[3,4,28]. An essential level of autophagy and apoptosis is important for maintaining intestinal epithelial cellular homeostasis under normal conditions. However, if the stress persists, autophagy will not afford cell surviving anymore. Instead exorbitant autophagy and copious activation of apoptosis will cause dramatic disruption of intestinal mucosa and barrier breakdown[28]. We first explored whether increased autophagy and apoptosis were related with ANGPTL4 in intestinal I/R of a rat model and the inhibition effects of rhANGPTL4 on autophagy and apoptosis both *in vivo* and *in vitro* challenged by I/R (H/R).

Autophagy is a lysosome-mediated degradative pathway of cellular mechanisms for degrading misfolded protein in addition to the ubiquitin-proteasome system of ubiquitinated proteins[29]. The implementation of autophagy involves a series of autophagy-related proteins that are essential for induction of autophagy and recycling of autophagosomes. Microtubule-associated protein LC3 exists in two forms including LC3-I and its proteolytic derivative LC3-II. LC3-I is conjugated with phosphatidylethanolamine to become LC3-II, which can be used as a hallmark of autophagy because its population correlates with the number of autophagosomes. P62/SQSTM1 is selectively incorporated into autophagosomes through binding to LC3 and is affirmed as a specific substrate that degrades *via* the autophagy-lysosomal pathway. Therefore, the p62 contents are oppositely parallel with autophagic activity. Beclin 1 (ATG6) is the first identified mammalian gene to mediate autophagy and is implicated in the nucleation of the autophagic vesicle, which is another marker of autophagy[30].

Recent studies have shown that excessive autophagy that is active in necrotizing enterocolitis and inhibiting autophagy is protective against focal cerebral ischemia in rats[4,31]. Intestinal mucosal barrier disruption is associated with excessive autophagy activation. Our results suggested that ANGPTL4 conferred intestinal mucosal barrier preservation and inhibited the excessive activated autophagy in intestinal I/R. In the present study, intestinal autophagy activated massively in rats with intestinal I/R. Upregulated expression of required autophagy markers (beclin 1 and LC3-II) and the loss of p62 protein are found in intestinal epithelium both *in vivo* and *in vitro* challenged by I/R or H/R. Consequentially activated autophagy caused accumulation of autophagic vacuoles and disrupted the majority of the cytosol and organelles, eventually causing the collapse of vital cell functions and cell death. The attenuated epithelial cell homeostasis makes intestine mucosal injury more vulnerable upon I/R. However, rhANGPTL4 reversed I/R-induced changes of autophagy-related regulators (LC3-II, beclin 1 and p62) both *in vivo* and *in vitro*. This suggested that ANGPTL4 limited intestinal mucosal exorbitant autophagy to maintain the integrity of intestinal barrier.

Apoptosis was demonstrated to be the main type of cell death in intestinal I/R. Apoptosis disrupts the epithelial cell layer directly when the intestine is subjected to I/R[4]. Studies have shown that “anoikis” exerts a crucial effect in inducing apoptosis during intestine I/R. “Anoikis” manifested as contact disrupted cell death occurring between extracellular matrix materials and cells[32]. Ikeda *et al*[3] reported that affected epithelial cells lost their link with the villous mesenchyma, and thus apoptosis induced by I/R could represent “anoikis”. They also revealed that distribution of epithelial cell-matrix interactions (“anoikis”) exhibited a crucial effect on initiating apoptosis in detached enterocytes[4]. It is worth noting that ANGPTL4 has been demonstrated to promote anoikis resistance in cholangiocarcinoma and hepatoma cells grown in a disassociated status. These cells try to shape a synoikis-like multi-cellular assemblage that resists apoptosis occurrence. The inhibition of ANGPTL4 by RNA interference increased detachment-related apoptosis and made tumor cells sensitized

to antitumor drugs[14]. This implicates that intestinal epithelial cells may drive a similar mechanism to resist I/R-related apoptosis in intestinal mucosa. Our current results show that rhANGPTL4 resisted apoptosis and limited the increased levels of cleaved caspase-3 both *in vivo* and *in vitro*. Cells lack of ANGPTL4 showed increased apoptosis and cleaved caspase-3 levels when challenged by H/R. It can be concluded that ANGPTL4 may protect against intestinal mucosal barrier dysfunction due to I/R through anoikis resistance.

Another key factor for the intestinal barrier preservation that cannot be ignored during intestinal I/R is the vascular permeability[9]. Patients exhibited loss of plasma proteins and other macromolecules induced by increased permeability in the colonic microvasculature. During the perpetuation of intestinal I/R, microvascular injury is ubiquitously present. Intestinal microvessels manifested apparently as endothelial dysfunction. Microvascular endothelial cell layer consists of closely arranged ECs that shape a semi-permeable barrier between tissue and blood for the transport of lipids, proteins and electrolytes[33]. Therefore, microvascular barrier dysfunction exerts an important effect in the beginning and progressive phase of I/R injury. Consequently, endothelium reformation induced microvascular permeability changes and exerted a crucial effect on intestinal barrier dysfunction. The bidirectional regulation role of ANGPTL4 in vascular permeability has been extensively studied in various diseases [34-36]. However, the association of ANGPTL4 with vascular leakage induced by I/R remains obscure. In the present study, HUVECs with RNA interference and H/R exhibited a significant loss of the key regulator VE-cad. In addition, rhANGPTL4 inhibited the vascular permeability significantly, manifested as a change of VE-cad in HUVECs challenged by H/R. It is concluded that ANGPTL4 protects the intestinal barrier at least partially *via* inhibiting vascular leakage.

Intestinal I/R could still be an important cause of MODS, and it is of significance to note that besides the reduction of intestinal structure, ANGPTL4 treatment also significantly improved the intestinal barrier function.

CONCLUSION

This study demonstrates that rhANGPTL4 can lessen I/R injury by maintaining intestinal barrier structure and function. ANGPTL4 showed a conspicuous effect on MLCK-related proteins, tight junction and vascular permeability as well as on the inflammatory and oxidative response, autophagy and apoptosis. This implies that ANGPTL4 plays a significant role in modulating intestinal barrier integrity. It is speculated that rhANGPTL4 is important in intestinal barrier function maintenance and may have clinical advantages in I/R-related clinical circumstances. Further studies are needed to investigate the protective role of ANGPTL4 on remote organ dysfunction induced by intestinal I/R and to clarify whether this therapeutic agent targeting protection against the intestinal barrier dysfunction could be applied to patients in intensive care units.

ARTICLE HIGHLIGHTS

Research background

Intestinal barrier breakdown remains frequently complicated in critical care patients of intestinal ischemia-reperfusion (I/R), severe acute pancreatitis and sepsis. Although vigorous experiments are performed in this field, the application of an instant effective agent or therapy in clinical has not yet been discovered. Recombinant human angiopoietin-like protein 4 (rhANGPTL4) is known to be protective to the blood-brain barrier when administered exogenously, and endogenous ANGPTL4 deficiency deteriorates intestinal injury.

Research motivation

We intend to explore and discover a novel and promising agent to confer intestinal barrier protection induced by I/R. Our results indicated recombinant agents that exhibit intestinal barrier protective characteristics. The agents may be safer and facilitated to translate into clinical use.

Research objectives

Understanding and regulating ANGPTL4 as a therapeutic target and recombinant human ANGPTL4 will be an application in clinical use in patients suffering from intestinal barrier dysfunction.

Research methods

This research was executed using Wistar rats treated with intestinal I/R and intestinal epithelial (Caco-2) cells and human umbilical vein endothelial cells stimulated with H/R to intimate the I/R pathogenesis *in vivo*. Further, RNA interference was performed, and recombinant ANGPTL4 has been evaluated.

Research results

A loss of crypt epithelium and myocytes were observed in the muscularis propria. Intraluminal microdialysis were changed, as well as the biochemistry indicators were remarkably enhanced following intestinal I/R. Recombinant human ANGPTL4 treatment significantly reversed indicators above associated with inhibiting the inflammatory and oxidative cascade, excessive activation of cellular autophagy and apoptosis and was associated with an improvement of survival rate. *In vitro* studies showed similar results in Caco-2 and human umbilical vein endothelial cells.

Research conclusions

Recombinant human ANGPTL4 achieved an optimal therapeutic effect for intestinal I/R-induced intestinal barrier injury. Using this model, the intestinal barrier structure and functions indicators were maintained, thus providing a promising therapeutic potential.

Research perspectives

ANGPTL4 may be a valuable predictor, and similar research in patients who suffered critical care conditions could be evaluated.

ACKNOWLEDGEMENTS

The authors wish to thank for Chen DP and Gao J for their excellent technical support and Han CC for gifting antibodies and cells.

REFERENCES

- 1 **Pastores SM**, Katz DP, Kvetan V. Splanchnic ischemia and gut mucosal injury in sepsis and the multiple organ dysfunction syndrome. *Am J Gastroenterol* 1996; **91**: 1697-1710 [PMID: 8792684]
- 2 **Mainous MR**, Ertel W, Chaudry IH, Deitch EA. The gut: a cytokine-generating organ in systemic inflammation? *Shock* 1995; **4**: 193-199 [PMID: 8574754]
- 3 **Ikeda H**, Suzuki Y, Suzuki M, Koike M, Tamura J, Tong J, Nomura M, Itoh G. Apoptosis is a major mode of cell death caused by ischaemia and ischaemia/reperfusion injury to the rat intestinal epithelium. *Gut* 1998; **42**: 530-537 [PMID: 9616316 DOI: 10.1136/gut.42.4.530]
- 4 **Norsa L**, Bonaffini PA, Indriolo A, Valle C, Sonzogni A, Sironi S. Poor Outcome of Intestinal Ischemic Manifestations of COVID-19. *Gastroenterology* 2020; **159**: 1595-1597.e1 [PMID: 32569772 DOI: 10.1053/j.gastro.2020.06.041]
- 5 **Jiang S**, Fan Q, Xu M, Cheng F, Li Z, Ding G, Geng L, Fu T. Hydrogen-rich saline protects intestinal epithelial tight junction barrier in rats with intestinal ischemia-reperfusion injury by inhibiting endoplasmic reticulum stress-induced apoptosis pathway. *J Pediatr Surg* 2020; **55**: 2811-2819 [PMID: 32169342 DOI: 10.1016/j.jpedsurg.2020.01.061]
- 6 **Softeland JM**, Bagge J, Padma AM, Casselbrant A, Zhu C, Wang Y, Hellström M, Olausson M, Oltean M. Luminal polyethylene glycol solution delays the onset of preservation injury in the human intestine. *Am J Transplant* 2021; **21**: 2220-2230 [PMID: 33249756 DOI: 10.1111/ajt.16418]
- 7 **Graham WV**, He W, Marchiando AM, Zha J, Singh G, Li HS, Biswas A, Ong MLDM, Jiang ZH, Choi W, Zuccola H, Wang Y, Griffith J, Wu J, Rosenberg HJ, Snapper SB, Ostrov D, Meredith SC, Miller LW, Turner JR. Intracellular MLCK1 diversion reverses barrier loss to restore mucosal homeostasis. *Nat Med* 2019; **25**: 690-700 [PMID: 30936544 DOI: 10.1038/s41591-019-0393-7]
- 8 **Nalle SC**, Zuo L, Ong MLDM, Singh G, Worthylake AM, Choi W, Manresa MC, Southworth AP, Edelblum KL, Baker GJ, Joseph NE, Savage PA, Turner JR. Graft-versus-host disease propagation depends on increased intestinal epithelial tight junction permeability. *J Clin Invest* 2019; **129**: 902-914 [PMID: 30667372 DOI: 10.1172/JCI98554]
- 9 **Wang X**, Li M, Yang Z, Li H, Wang Y, Tang W, Wu Y, Xiao P, Jiang S, Shi Q, Lu Y. Comparison of

- the Protective Effect of Different Mild Therapeutic Hypothermia Temperatures on Intestinal Injury after Cardiopulmonary Resuscitation in Rats. *Shock* 2021; **56**: 450-460 [PMID: 33555844 DOI: 10.1097/SHK.0000000000001745]
- 10 **Barbaro MR**, Cremon C, Morselli-Labate AM, Di Sabatino A, Giuffrida P, Corazza GR, Di Stefano M, Caio G, Latella G, Ciacci C, Fuschi D, Mastroroberto M, Bellacosa L, Stanghellini V, Volta U, Barbara G. Serum zonulin and its diagnostic performance in non-coeliac gluten sensitivity. *Gut* 2020; **69**: 1966-1974 [PMID: 32060130 DOI: 10.1136/gutjnl-2019-319281]
 - 11 **Babapoor-Farrokhman S**, Jee K, Puchner B, Hassan SJ, Xin X, Rodrigues M, Kashiwabuchi F, Ma T, Hu K, Deshpande M, Daoud Y, Solomon S, Wenick A, Luty GA, Semenza GL, Montaner S, Sodhi A. Angiopoietin-like 4 is a potent angiogenic factor and a novel therapeutic target for patients with proliferative diabetic retinopathy. *Proc Natl Acad Sci U S A* 2015; **112**: E3030-E3039 [PMID: 26039997 DOI: 10.1073/pnas.1423765112]
 - 12 **Wen L**, Zhang Y, Yang B, Han F, Ebadi AG, Toughani M. Knockdown of Angiopoietin-like protein 4 suppresses the development of colorectal cancer. *Cell Mol Biol (Noisy-le-grand)* 2020; **66**: 117-124 [PMID: 33040824 DOI: 10.14715/cmb/2020.66.5.21]
 - 13 **Leth-Espensen KZ**, Kristensen KK, Kumari A, Winther AL, Young SG, Jørgensen TJD, Ploug M. The intrinsic instability of the hydrolase domain of lipoprotein lipase facilitates its inactivation by ANGPTL4-catalyzed unfolding. *Proc Natl Acad Sci USA* 2021; **118** [PMID: 33723082 DOI: 10.1073/pnas.2026650118]
 - 14 **San TT**, Khaenam P, Prachayasittikul V, Sripan B, Kunkeaw N, Chan-On W. Curcumin enhances chemotherapeutic effects and suppresses ANGPTL4 in anoikis-resistant cholangiocarcinoma cells. *Heliyon* 2020; **6**: e03255 [PMID: 32051864 DOI: 10.1016/j.heliyon.2020.e03255]
 - 15 **Fan Z**, Jing H, Yao J, Li Y, Hu X, Shao H, Shen G, Pan J, Luo F, Tian X. The protective effects of curcumin on experimental acute liver lesion induced by intestinal ischemia-reperfusion through inhibiting the pathway of NF- κ B in a rat model. *Oxid Med Cell Longev* 2014; **2014**: 191624 [PMID: 25215173 DOI: 10.1155/2014/191624]
 - 16 **El-Assal ON**, Besner GE. HB-EGF enhances restitution after intestinal ischemia/reperfusion via PI3K/Akt and MEK/ERK1/2 activation. *Gastroenterology* 2005; **129**: 609-625 [PMID: 16083716 DOI: 10.1016/j.gastro.2005.05.054]
 - 17 **Chiu CJ**, McArdle AH, Brown R, Scott HJ, Gurd FN. Intestinal mucosal lesion in low-flow states. I. A morphological, hemodynamic, and metabolic reappraisal. *Arch Surg* 1970; **101**: 478-483 [PMID: 5457245 DOI: 10.1001/archsurg.1970.01340280030009]
 - 18 **Qian J**, Li G, Jin X, Ma C, Cai W, Jiang N, Zheng J. Emodin protects against intestinal and lung injury induced by acute intestinal injury by modulating SP-A and TLR4/NF- κ B pathway. *Biosci Rep* 2020; **40** [PMID: 32915230 DOI: 10.1042/BSR20201605]
 - 19 **Zhai X**, Lin M, Zhang F, Hu Y, Xu X, Li Y, Liu K, Ma X, Tian X, Yao J. Dietary flavonoid genistein induces Nrf2 and phase II detoxification gene expression via ERKs and PKC pathways and protects against oxidative stress in Caco-2 cells. *Mol Nutr Food Res* 2013; **57**: 249-259 [PMID: 23255485 DOI: 10.1002/mnfr.201200536]
 - 20 **Koike Y**, Li B, Ganji N, Zhu H, Miyake H, Chen Y, Lee C, Janssen Lok M, Zozaya C, Lau E, Lee D, Chusilp S, Zhang Z, Yamoto M, Wu RY, Inoue M, Uchida K, Kusunoki M, Delgado-Olguin P, Mertens L, Daneman A, Eaton S, Sherman PM, Pierro A. Remote ischemic conditioning counteracts the intestinal damage of necrotizing enterocolitis by improving intestinal microcirculation. *Nat Commun* 2020; **11**: 4950 [PMID: 33009377 DOI: 10.1038/s41467-020-18750-9]
 - 21 **Crawford PA**, Gordon JI. Microbial regulation of intestinal radiosensitivity. *Proc Natl Acad Sci U S A* 2005; **102**: 13254-13259 [PMID: 16129828 DOI: 10.1073/pnas.0504830102]
 - 22 **Bäckhed F**, Crawford PA, O'Donnell D, Gordon JI. Postnatal lymphatic partitioning from the blood vasculature in the small intestine requires fasting-induced adipose factor. *Proc Natl Acad Sci U S A* 2007; **104**: 606-611 [PMID: 17202268 DOI: 10.1073/pnas.0605957104]
 - 23 **Gur-Cohen S**, Yang H, Baksh SC, Miao Y, Levorse J, Kataru RP, Liu X, de la Cruz-Racelis J, Mehrara BJ, Fuchs E. Stem cell-driven lymphatic remodeling coordinates tissue regeneration. *Science* 2019; **366**: 1218-1225 [PMID: 31672914 DOI: 10.1126/science.aay4509]
 - 24 **Cho DI**, Kang HJ, Jeon JH, Eom GH, Cho HH, Kim MR, Cho M, Jeong HY, Cho HC, Hong MH, Kim YS, Ahn Y. Antiinflammatory activity of ANGPTL4 facilitates macrophage polarization to induce cardiac repair. *JCI Insight* 2019; **4** [PMID: 31434807 DOI: 10.1172/jci.insight.125437]
 - 25 **Huang RL**, Teo Z, Chong HC, Zhu P, Tan MJ, Tan CK, Lam CR, Sng MK, Leong DT, Tan SM, Kersten S, Ding JL, Li HY, Tan NS. ANGPTL4 modulates vascular junction integrity by integrin signaling and disruption of intercellular VE-cadherin and claudin-5 clusters. *Blood* 2011; **118**: 3990-4002 [PMID: 21841165 DOI: 10.1182/blood-2011-01-328716]
 - 26 **Ziegler AL**, Pridgen TA, Blikslager AT. Environmental stressors affect intestinal permeability and repair responses in a pig intestinal ischemia model. *Tissue Barriers* 2020; **8**: 1832421 [PMID: 33100144 DOI: 10.1080/21688370.2020.1832421]
 - 27 **Lichtenstein L**, Mattijssen F, de Wit NJ, Georgiadi A, Hooiveld GJ, van der Meer R, He Y, Qi L, Köster A, Tamsma JT, Tan NS, Müller M, Kersten S. Angptl4 protects against severe proinflammatory effects of saturated fat by inhibiting fatty acid uptake into mesenteric lymph node macrophages. *Cell Metab* 2010; **12**: 580-592 [PMID: 21109191 DOI: 10.1016/j.cmet.2010.11.002]
 - 28 **Chen QS**, Shen A, Dai JW, Li TT, Huang WF, Shi K, Deng Y, Pan L, Wei XF, Wu ZJ. IL37 overexpression inhibits autophagy and apoptosis induced by hepatic ischemia reperfusion injury via modulating AMPK/mTOR/ULK1 signalling pathways. *Life Sci* 2021; **276**: 119424 [PMID:

- 33785334 DOI: [10.1016/j.lfs.2021.119424](https://doi.org/10.1016/j.lfs.2021.119424)]
- 29 **Pandey UB**, Nie Z, Batlevi Y, McCray BA, Ritson GP, Nedelsky NB, Schwartz SL, DiProspero NA, Knight MA, Schuldiner O, Padmanabhan R, Hild M, Berry DL, Garza D, Hubbert CC, Yao TP, Baehrecke EH, Taylor JP. HDAC6 rescues neurodegeneration and provides an essential link between autophagy and the UPS. *Nature* 2007; **447**: 859-863 [PMID: [17568747](https://pubmed.ncbi.nlm.nih.gov/17568747/) DOI: [10.1038/nature05853](https://doi.org/10.1038/nature05853)]
 - 30 **Filali-Mouneef Y**, Hunter C, Roccio F, Zagkou S, Dupont N, Primard C, Proikas-Cezanne T, Reggiori F. The ménage à trois of autophagy, lipid droplets and liver disease. *Autophagy* 2021; 1-24 [PMID: [33794741](https://pubmed.ncbi.nlm.nih.gov/33794741/) DOI: [10.1080/15548627.2021.1895658](https://doi.org/10.1080/15548627.2021.1895658)]
 - 31 **Luo HC**, Yi TZ, Huang FG, Wei Y, Luo XP, Luo QS. Role of long noncoding RNA MEG3/miR-378/GRB2 axis in neuronal autophagy and neurological functional impairment in ischemic stroke. *J Biol Chem* 2020; **295**: 14125-14139 [PMID: [32605923](https://pubmed.ncbi.nlm.nih.gov/32605923/) DOI: [10.1074/jbc.RA119.010946](https://doi.org/10.1074/jbc.RA119.010946)]
 - 32 **Frisch SM**, Francis H. Disruption of epithelial cell-matrix interactions induces apoptosis. *J Cell Biol* 1994; **124**: 619-626 [PMID: [8106557](https://pubmed.ncbi.nlm.nih.gov/8106557/) DOI: [10.1083/jcb.124.4.619](https://doi.org/10.1083/jcb.124.4.619)]
 - 33 **Spain DA**, Wilson MA, Krysztopik RJ, Matheson PJ, Garrison RN. Differential intestinal microvascular dysfunction occurs during bacteremia. *J Surg Res* 1997; **67**: 67-71 [PMID: [9070184](https://pubmed.ncbi.nlm.nih.gov/9070184/) DOI: [10.1006/jsre.1996.4947](https://doi.org/10.1006/jsre.1996.4947)]
 - 34 **Schucht JE**, Matheson PJ, Harbrecht BG, Bond L, Jones S, Alkhateeb KJM, Ashkettle GR, Smith JW. Plasma resuscitation with adjunctive peritoneal resuscitation reduces ischemic intestinal injury following hemorrhagic shock. *J Trauma Acute Care Surg* 2020; **89**: 649-657 [PMID: [32773670](https://pubmed.ncbi.nlm.nih.gov/32773670/) DOI: [10.1097/TA.0000000000002847](https://doi.org/10.1097/TA.0000000000002847)]
 - 35 **Sodhi A**, Ma T, Menon D, Deshpande M, Jee K, Dinabandhu A, Vancel J, Lu D, Montaner S. Angiopoietin-like 4 binds neuropilins and cooperates with VEGF to induce diabetic macular edema. *J Clin Invest* 2019; **129**: 4593-4608 [PMID: [31545295](https://pubmed.ncbi.nlm.nih.gov/31545295/) DOI: [10.1172/JCI120879](https://doi.org/10.1172/JCI120879)]
 - 36 **Fernández-Hernando C**, Suárez Y. ANGPTL4: a multifunctional protein involved in metabolism and vascular homeostasis. *Curr Opin Hematol* 2020; **27**: 206-213 [PMID: [32205586](https://pubmed.ncbi.nlm.nih.gov/32205586/) DOI: [10.1097/MOH.0000000000000580](https://doi.org/10.1097/MOH.0000000000000580)]

Retrospective Study

Prolonged survival in patients with hand-foot skin reaction secondary to cooperative sorafenib treatment

Masanori Ochi, Toshiro Kamoshida, Masahiro Araki, Tadashi Ikegami

ORCID number: Masanori Ochi 0000-0003-0850-6076; Toshiro Kamoshida 0000-0003-4930-1018; Masahiro Araki 0000-0002-8648-9622; Tadashi Ikegami 0000-0002-9216-3186.

Author contributions: Ochi M, Kamoshida T, Araki M, and Ikegami T contributed equally to this work; Ochi M and Kamoshida T collected and analyzed the data; Ochi M and Kamoshida T drafted the manuscript; Ochi M and Kamoshida T designed and supervised the study; Araki M and Ikegami T offered technical or material support; all authors have read and approved the final version to be published.

Institutional review board

statement: The study protocol was approved by the ethics committee of each hospital and was performed according to the ethical standards of the 1975 Declaration of Helsinki.

Informed consent statement:

Informed consent was obtained using an opt-out option on each facility's website (see Institution website uniform resource locators).

Conflict-of-interest statement:

None of the authors have any conflicts of interest related to the manuscript.

Masanori Ochi, Toshiro Kamoshida, Department of Gastroenterology, Hitachi General Hospital, Ibaraki 317-0077, Japan

Masahiro Araki, Department of Gastroenterology and Hepatology, Ibaraki Prefectural Central Hospital, Ibaraki Cancer Center, Ibaraki 309-1793, Japan

Tadashi Ikegami, Division of Gastroenterology and Hepatology, Tokyo Medical University Ibaraki Medical Center, Ibaraki 309-1793, Japan

Corresponding author: Masanori Ochi, MD, Doctor, Department of Gastroenterology, Hitachi General Hospital, Chome-1-1 Jonancho, Ibaraki 317-0077, Japan. maochi-tei@umin.ac.jp

Abstract**BACKGROUND**

Sorafenib is an oral drug that prolongs overall survival (OS) in patients with hepatocellular carcinoma. Adverse events, including hand-foot skin reaction (HFSR), lead to permanent sorafenib discontinuation.

AIM

To clarify the association between interventions for adverse events and patient prognosis.

METHODS

We performed a retrospective, multicenter study of patients treated with sorafenib monotherapy between May 2009 and March 2018. We developed a mutual cooperation system that was initiated at the start of sorafenib treatment to effectively manage adverse events. The mutual cooperation system entailed patients receiving consultations during which pharmacists provided accurate information about sorafenib to alleviate the fear and anxiety related to adverse events. We stratified the patients into three groups: Group A, patients without HFSR but with pharmacist intervention; Group B, patients with HFSR and pharmacist interventions unreported to oncologists (nonmutual cooperation system); and Group C, patients with HFSR and pharmacist interventions known to oncologists (mutual cooperation system). OS and time to treatment failure (TTF) were evaluated using the Kaplan-Meier method.

RESULTS

We enrolled 134 patients (Group A, $n = 41$; Group B, $n = 30$; Group C, $n = 63$). The

Data sharing statement: The original anonymous dataset is available on request from the corresponding author at maochi-tei@umin.ac.jp.

Open-Access: This article is an open-access article that was selected by an in-house editor and fully peer-reviewed by external reviewers. It is distributed in accordance with the Creative Commons Attribution NonCommercial (CC BY-NC 4.0) license, which permits others to distribute, remix, adapt, build upon this work non-commercially, and license their derivative works on different terms, provided the original work is properly cited and the use is non-commercial. See: <http://creativecommons.org/licenses/by-nc/4.0/>

Manuscript source: Unsolicited manuscript

Specialty type: Gastroenterology and hepatology

Country/Territory of origin: Japan

Peer-review report's scientific quality classification

Grade A (Excellent): 0
Grade B (Very good): B
Grade C (Good): 0
Grade D (Fair): 0
Grade E (Poor): 0

Received: April 9, 2021

Peer-review started: April 9, 2021

First decision: May 27, 2021

Revised: June 22, 2021

Accepted: August 10, 2021

Article in press: August 10, 2021

Published online: August 28, 2021

P-Reviewer: Yu F

S-Editor: Ma YJ

L-Editor: A

P-Editor: Yuan YY



median OS was significantly different between Groups A and C (6.2 *vs* 13.9 mo, $P < 0.01$) but not between Groups A and B (6.2 *vs* 7.7 mo, $P = 0.62$). Group A *vs* Group C was an independent OS predictor (HR, 0.41; 95%CI: 0.25-0.66; $P < 0.01$). In Group B alone, TTF was significantly lower and the nonadherence rate was higher ($P < 0.01$). In addition, the Spearman's rank correlation coefficients between OS and TTF in each group were 0.41 (Group A; $P < 0.01$), 0.13 (Group B; $P = 0.51$), and 0.58 (Group C; $P < 0.01$). There was a highly significant correlation between OS and TTF in Group C. However, there was no correlation between OS and TTF in Group B.

CONCLUSION

The mutual cooperation system increased treatment duration and improved prognosis in patients with HFSR. Future prospective studies (*e.g.*, randomized controlled trials) and improved adherence could help prevent OS underestimation.

Key Words: Hepatocellular carcinoma; Sorafenib; Pharmacists; Oncologists; Prognosis; Duration of therapy

©The Author(s) 2021. Published by Baishideng Publishing Group Inc. All rights reserved.

Core Tip: We investigated the effect of cooperation between oncologists and pharmacists (mutual cooperation system) on the prognosis of patients with advanced hepatocellular carcinoma treated with sorafenib and found that cooperation increased medication adherence. Prolonged adherence was correlated with overall survival and time to treatment failure in patients with sorafenib-related hand-foot skin reactions. Our mutual cooperation system could be used to manage patients treated with various multikinase inhibitors and improve overall survival in studies that use sorafenib as the control drug. Future clinical investigations that include measures to improve medication adherence could eliminate the underestimation of medication efficacy that may otherwise occur due to preventable nonadherence.

Citation: Ochi M, Kamoshida T, Araki M, Ikegami T. Prolonged survival in patients with hand-foot skin reaction secondary to cooperative sorafenib treatment. *World J Gastroenterol* 2021; 27(32): 5424-5437

URL: <https://www.wjgnet.com/1007-9327/full/v27/i32/5424.htm>

DOI: <https://dx.doi.org/10.3748/wjg.v27.i32.5424>

INTRODUCTION

Sorafenib is a multikinase inhibitor used to treat advanced hepatocellular carcinoma (HCC)[1,2]. Although sorafenib prolongs overall survival (OS) in patients with HCC, it is associated with various adverse events (AEs) that may lead to permanent discontinuation[3].

Previous studies found that hand-foot skin reaction (HFSR) was a prognostic marker of longer survival[4-6]. While HFSR is an important predictor of survival outcomes in clinical practice and clinical sorafenib trials, AE management could influence the efficacy of HFSR as a prognostic factor. A recent study showed that increased clinician experience with AEs reduced the potential for discontinuing sorafenib therapy, resulting in a longer OS in patients with HCC[7]. Nevertheless, it takes a long time for clinicians to develop the necessary experience for the management of AEs, and even with experience, it takes a substantial amount of time to provide a system of adequate follow-up after sorafenib initiation.

As sorafenib is administered orally, its successful use for HCC treatment relies on patient medication adherence. However, many studies indicate that patients with cancer are sometimes nonadherent when prescribed oral drugs[8,9], and AEs are the main cause of poor adherence[10]. Poor adherence can lead to poor outcomes, and clinicians may wrongly conclude that a drug is ineffective because the response to treatment is insufficient[11].

It is important for patients to actively participate in making treatment decisions and then receive treatment according to their decisions to improve adherence[12]. We introduced behavior change techniques (patient education, medication regimen management, pharmacist-led interventions)[13,14] in our facilities as interventions to promote adherence. Using a preliminary simulation, we estimated that collecting patient information takes at least 20 min. From this, we concluded that it is difficult for oncologists to manage drugs that cause various AEs (*e.g.*, sorafenib) without assistance due to their obligations to many patients. Thus, we developed a mutual cooperation system involving collaboration between oncologists and pharmacists to ensure effective AE management. This mutual cooperation system consisted of the initial intervention by a pharmacist followed by a medical examination by an oncologist. However, this system was affected by the patient's behavior because patients were not obliged to follow the system. Some patients received intervention from a pharmacist after a medical examination by an oncologist.

Effective AE management that improves medication adherence has a considerable impact on survival outcomes. Previous single-center studies suggest that healthcare provider interventions improve adherence, and the onset of HFSR was a favorable prognostic factor of OS in patients with HCC[15,16]. However, little is known about the association between prognosis and medication adherence in patients with HCC, and multicenter studies on this relationship are lacking. Therefore, we aimed to compare the impact of different AE interventions on patient prognosis.

MATERIALS AND METHODS

Study design

We retrospectively evaluated patients with advanced HCC treated with sorafenib monotherapy and no subsequent chemotherapeutic agent between May 2009 and March 2018 using the medical records of the following core hospitals in Japan: Hitachi General Hospital, Ibaraki Prefectural Central Hospital, Ibaraki Cancer Center, and Tokyo Medical University Ibaraki Medical Center. These hospitals are core hospitals that were designated by the government to provide specialized cancer medical care. The patients were separated into three groups: Group A, patients without HFSR but with pharmacist intervention (this intervention was performed by pharmacists who did not share interview information with the oncologist; it is called nonmutual cooperation system); Group B, patients with HFSR and nonmutual cooperation system; and Group C, patients with HFSR and intervention by pharmacists who shared interview information with the oncologist (mutual cooperation system).

Patient selection

We included patients with stage B or C HCC according to the Barcelona Clinic Liver Cancer (BCLC) staging system. The indication criteria for sorafenib administration were as follows: Child-Pugh grade A or B; Eastern Cooperative Oncology Group (ECOG) performance status 0 or 1; alanine aminotransferase < 5-fold the upper limit of the normal range; total bilirubin level < 2.0 mg/dL; neutrophil count > 1500/ μ L; hemoglobin level \geq 8.5 g/dL; platelet count > 75000/ μ L; and no dialysis requirement. The study exclusion criteria were as follows: Patients with a history of thrombosis or ischemic heart disease, pregnant women and those who could become pregnant, and patients with brain metastases. Our study protocol was approved by the ethics committee of each hospital and was performed according to the ethical guidelines of the 1975 Declaration of Helsinki. We obtained informed consent using an opt-out option on each facility's website (see Institution website uniform resource locators). This study was registered with the University Hospital Medical Information Network (UMIN) (ID: UMIN000038701).

Data collection

We collected patient data from the start of sorafenib, including age, sex, etiology of underlying liver disease, Child-Pugh score, history of present illness, medical history, tumor marker level [alpha-fetoprotein (AFP)], ECOG performance status, and relevant laboratory tests, including total bilirubin, albumin, and international normalized ratio (INR). Laboratory tests and tumor marker levels were obtained every 8–10 wk until permanent sorafenib discontinuation.

Computed tomography evaluations

Sorafenib response evaluations on computed tomography (CT) were scheduled for 8 wk after the first treatment, and subsequent evaluations were planned every 8 wk. Thoracic, abdominal, and pelvic CT scans were performed with intravenous iodinated contrast media. CT evaluations were conducted based on the modified Response Evaluation Criteria in Solid Tumors (mRECIST)[17] by an oncologist.

Intervention

Pharmacists with special expertise provided medical care at the pharmacist's outpatient clinic before or after a patient was medically examined by an oncologist. Every 8 wk at each visit, an AE evaluation, a residual drug count, self-management advice, and patient education, including descriptions of successful cases of AE management, pharmacist support, and advice for relieving patient anxiety and misunderstanding, were conducted. AEs were evaluated according to the National Cancer Institute Common Toxicity Criteria for Adverse Events (NCI-CTCAE) version 5.0. Pharmacists recommended that all patients use heparinoids before sorafenib treatment to prevent AEs. Additionally, the prophylactic use of urea cream to prevent dermatologic AEs was recommended after beginning sorafenib treatment. Pharmacist intervention began at the start of sorafenib treatment and continued until treatment ended.

Mutual cooperation system

We developed a mutual cooperation system that was initiated at the start of sorafenib treatment to manage AEs effectively. Although patients in Groups B and C received medical advice from oncologists and pharmacists, the systems differed. Group C received 20- to 30-min consultations during which pharmacists provided accurate information about sorafenib to alleviate fear and anxiety related to AEs. After each visit, the pharmacist summarized the consultation results in a report and discussed their findings with an oncologist. Group B patients received a 5- to 10-min session during which pharmacists provided the same information about sorafenib that Group C had received. These pharmacist consultations were brief because a thorough medical examination by an oncologist had already been completed. Furthermore, the pharmacist did not record the consultation content in the medical chart because the visit involved verbal intervention only, and a detailed report was unnecessary.

Sorafenib therapy and AE management

Sorafenib was administered at a dose of 400 or 800 mg/d. The initial dose of sorafenib was determined by an oncologist. At the start of sorafenib treatment, all patients received information about AEs from a pharmacist and an oncologist. Patients who developed an AE could confer with their consulting pharmacist or prescribing oncologist. Pharmacists collected and recorded patient data, including the AE grade (according to NCI-CTCAE version 5.0), AE time of onset, and emotional response of the patient to the AE. Oncologists performed dose modifications throughout treatment, including reductions, interruptions, and reintroductions, according to the drug manufacturer's package insert for sorafenib.

Criteria for permanent sorafenib discontinuation

Sorafenib was permanently discontinued when any of the following events occurred: (1) Tumor progression, defined as either radiologic (by the mRECIST criteria) or clinically progressive disease (*e.g.*, ECOG performance status decline or onset of severe symptoms with no connection to liver failure); (2) Unacceptable AEs, defined as moderate to severe AEs (*e.g.*, grades 2-4) that persisted after dose reduction or temporary treatment interruption; or (3) Liver decompensation, defined as gastrointestinal bleeding, ascites, jaundice, or encephalopathy[3]. All patients were managed by an oncologist and received excellent supportive care after sorafenib was permanently discontinued. Time to treatment failure (TTF) was defined as the duration from the start of sorafenib treatment to permanent discontinuation. The proportion of days covered (PDC) was defined as the TTF divided by the time to radiologic progressive disease after sorafenib[18]. Nonadherence was defined as a PDC of $\leq 80\%$ [19].

Statistical analysis

Categorical variables were assessed using the chi-square test and are presented as frequencies or percentages. Continuous variables were analyzed using the Mann-Whitney *U* test and are expressed as the mean \pm SD. OS and TTF were evaluated using the Kaplan-Meier method. A landmark analysis[20] was performed to consider HFSR cases that might have occurred if a patient with HCC had not died as a guarantee-time

bias. The analysis was performed using the time when the highest-grade HFSR occurred in 50% or more of the patients as a landmark (here, 30 d). The log-rank test was used to estimate differences in survival curves. Additionally, we used Cox regression analyses to evaluate the relationship between the time to the occurrence of an event and explanatory variables. Logistic regression analyses were used to evaluate the relationship between nonadherence and explanatory variables.

We included the following baseline characteristics as variables in our univariate analysis: age, sex, etiology of liver disease, bilirubin level, albumin level, INR, BCLC stage, ECOG performance status, macrovascular invasion, extrahepatic spread, serum AFP level, and number of previous transarterial chemoembolization (TACE) procedures for liver cancer. Variables identified as significant in the univariate analysis were included in the multivariate analysis. The correlations between OS and TTF were assessed by Spearman's rank correlation coefficient. A *p*-value less than 0.05 was considered statistically significant. We used the Bonferroni correction for multiple comparisons to adjust the familywise error rate when comparing differences between the three groups. The statistical methods of this study were reviewed by Kamoshida T from the Department of Gastroenterology, Hitachi General Hospital, Japan. All statistical analyses were performed using SPSS software, version 22 (IBM Corp., Armonk, NY, United States).

RESULTS

Patients

We included 134 patients [median age, 69 years (range, 41–89 years); male, *n* = 99; female, *n* = 35] with advanced HCC who received sorafenib monotherapy without posttreatment (Group A, *n* = 41; Group B, *n* = 30; Group C, *n* = 63). The main etiological factor was hepatitis C virus (HCV) (77/134 patients, 57.5%), followed by hepatitis B virus (HBV) (30/134 patients, 22.4%).

Baseline characteristics

All patients had cirrhosis [Child-Pugh A, *n* = 117 (87.3%); Child-Pugh B, *n* = 17 (12.7%)]. HCC was BCLC stage B in 55 patients (41.0%) and BCLC stage C in 79 patients (59.0%). None of the patients had a second primary cancer. Portal vein thrombosis was present in 35 patients (26.1%), and extrahepatic metastases were found in 67 patients (50.0%) (Table 1).

AEs

An AE of at least grade 1 was observed in all patients after sorafenib administration. However, none of the patients experienced any grade 4 AEs. The main AEs in all groups were fatigue (30.6%), diarrhea (39.6%), hypertension (31.3%), anorexia (29.9%), and thrombocytopenia (38.8%) (Table 2). Many patients required temporary sorafenib interruption because of AEs (Group A, 19.5%; Group B, 6.7%; Group C, 41.3%). Of patients who temporarily stopped taking sorafenib, the rate of those who resumed treatment at a reduced dose was the highest in Group C (Group A *vs* Group B, *P* = 0.70; Group A *vs* Group C, *P* = 0.11; Group B *vs* Group C, *P* < 0.01) (Table 3).

Radiological response evaluations

CT examinations performed every 2 mo showed that the disease control rate (DCR) gradually decreased in all groups. The response rate (RR) and DCR 8 mo after the start of sorafenib treatment were the highest in Group C (RR, 9.5%; DCR, 65.1%) (Table 4).

Permanent sorafenib discontinuation

The main causes of permanent drug discontinuation were HCC progression and sorafenib-related AE intolerance. Permanent discontinuation due to AE intolerance occurred most frequently in Group B (Group A (17.1%) *vs* Group B (60.0%), *P* < 0.01; Group A (17.1%) *vs* Group C (20.6%), *P* = 1.00; Group B (60.0%) *vs* Group C (20.6%), *P* < 0.05) (Table 5).

OS after sorafenib therapy

The median OS was 6.2 mo in Group A, 7.7 mo in Group B, and 13.9 mo in Group C. The difference in the median OS was significant between Groups A and C (*P* < 0.01). In multivariate analysis, Group A *vs* Group C (HR, 0.41; 95%CI: 0.25–0.66; *P* < 0.01) and BCLC-B (HR, 0.60, 95%CI: 0.41–0.89; *P* = 0.01) were independent predictors of survival

Table 1 Baseline characteristics of patients in Groups A, B, and C

| | Group A (n = 41) | Group B (n = 30) | Group C (n = 63) | P value |
|--------------------------------------|------------------|------------------|------------------|---------|
| Age (yr) | 70 (43–89) | 67 (41–87) | 69 (48–87) | 0.233 |
| Sex | | | | |
| Male, n (%) | 33 (80.5) | 22 (73.3) | 44 (69.8) | 0.481 |
| Child-Pugh class, n (%) | | | | 0.288 |
| A | 33 (80.5) | 27 (90.0) | 57 (90.5) | |
| B | 8 (19.5) | 3 (10.0) | 6 (9.5) | |
| Etiology, n (%) | | | | |
| HCV | 22 (53.7) | 11 (36.7) | 44 (69.8) | 0.235 |
| HBV | 9 (21.9) | 10 (33.3) | 11 (17.5) | 0.417 |
| Other | 10 (24.4) | 9 (30.0) | 8 (12.7) | 0.109 |
| Portal vein thrombosis | 14 (34.1) | 10 (33.3) | 11 (17.5) | 0.099 |
| Extrahepatic spread, n (%) | 20 (48.8) | 19 (63.3) | 28 (44.4) | 0.230 |
| AFP (ng/mL), n (%) | | | | |
| > 400 | 17 (41.5) | 17 (56.7) | 29 (46.0) | 0.437 |
| BCLC staging, n (%) | | | | 0.333 |
| Stage B | 15 (36.6) | 10 (33.3) | 30 (47.6) | |
| Stage C | 26 (63.4) | 20 (66.7%) | 33 (52.4) | |
| ECOG performance status, n (%) | | | | 0.955 |
| 0 | 30 (75.6) | 22 (73.3) | 46 (73.0) | |
| 1 | 10 (24.4) | 8 (26.7) | 17 (27.0) | |
| Total bilirubin (mg/dL) | 0.99 ± 0.36 | 0.91 ± 0.37 | 0.83 ± 0.33 | 0.052 |
| Albumin (g/L) | 3.61 ± 0.50 | 3.73 ± 0.54 | 3.82 ± 0.49 | 0.301 |
| INR | 1.14 ± 0.11 | 1.15 ± 0.16 | 1.14 ± 0.19 | 0.481 |
| Pre-sorafenib TACE procedures, n (%) | | | | 0.531 |
| 0 | 13 (31.7) | 9 (30.0) | 20 (31.8) | |
| 1 | 3 (7.3) | 6 (20.0) | 13 (20.6) | |
| 2 | 6 (14.6) | 1 (3.3) | 4 (6.4) | |
| 3 | 4 (9.8) | 2 (6.7) | 8 (12.7) | |
| 4 | 5 (12.2) | 3 (10.0) | 12 (19.0) | |
| > 5 | 10 (24.4) | 9 (30.0) | 6 (9.5) | |

AFP: Alpha-fetoprotein; BCLC: Barcelona Clinic Liver Cancer; HCV: Hepatitis C virus; HBV: Hepatitis B virus; INR: International normalized ratio; TACE: Transcatheter arterial chemoembolization; ECOG: Eastern Cooperative Oncology Group.

(Figures 1 and 2, Table 6).

Mutual cooperation system evaluation

The median TTF in Group C was 5.0 mo (95%CI: 3.8–6.5), which was the highest of all the groups [Group C (5.0 mo) *vs* Group A (2.1 mo), $P < 0.01$; Group C (5.0 mo) *vs* Group B (0.5 mo), $P < 0.01$]. In multivariable Cox regression analysis, Group A *vs* Group B (HR, 1.69, 95%CI, 1.04–2.75; $P = 0.03$) and Group A *vs* Group C (HR, 0.53; 95%CI: 0.35–0.81; $P < 0.01$) were significant predictors of TTF (Table 7). The proportions of patients with a PDC of < 0.8 were 29.3% in Group A, 73.3% in Group B, and 23.8% in Group C. Group B had a significantly higher sorafenib PDC than Groups A ($P < 0.01$) and C ($P < 0.01$). Adjusted logistic regression analysis showed that nonadherence (PDC ≤ 0.8) was associated with Group B *vs* Group A (OR, 0.11; 95%CI:

Table 2 Prevalence of adverse events after beginning sorafenib, according to CTCAE version 5.0, *n* (%)

| | Group A (<i>n</i> = 41) | | | | Group B (<i>n</i> = 30) | | | | Group C (<i>n</i> = 63) | | | |
|-------------------------|--------------------------|-----------|-----------|----------|--------------------------|-----------|-----------|-----------|--------------------------|-----------|-----------|-----------|
| | All grades | Grade 1 | Grade 2 | Grade 3 | All grades | Grade 1 | Grade 2 | Grade 3 | All grades | Grade 1 | Grade 2 | Grade 3 |
| Any adverse event | 37 (90.2) | 30 (73.2) | 18 (43.9) | 5 (12.2) | 30 (100) | 28 (93.3) | 24 (80.0) | 14 (46.6) | 63 (100) | 58 (92.1) | 36 (57.1) | 14 (22.2) |
| Hand-foot skin reaction | 0 (0) | 0 (0) | 0 (0) | 0 (0) | 30 (100) | 15 (50.0) | 10 (33.3) | 5 (16.7) | 63 (100) | 39 (61.9) | 19 (30.2) | 5 (7.9) |
| Anemia | 17 (41.5) | 8 (19.5) | 8 (19.5) | 1 (2.4) | 20 (66.6) | 13 (43.3) | 4 (13.3) | 3 (10.0) | 23 (36.5) | 14 (22.2) | 7 (11.1) | 2 (3.2) |
| Diarrhea | 15 (36.6) | 12 (29.3) | 3 (7.3) | 0 (0) | 11 (36.6) | 9 (30.0) | 1 (3.3) | 1 (3.3) | 27 (42.8) | 21 (33.3) | 2 (3.2) | 4 (6.3) |
| Fatigue | 14 (34.1) | 10 (26.8) | 3 (7.3) | 0 (0) | 11 (36.6) | 7 (23.3) | 4 (13.3) | 0 (0) | 16 (25.4) | 10 (15.9) | 6 (9.5) | 0 (0) |
| Anorexia | 14 (34.1) | 10 (24.4) | 3 (7.3) | 1 (2.4) | 7 (23.3) | 5 (16.7) | 1 (3.3) | 1 (3.3) | 19 (30.1) | 15 (23.8) | 4 (6.3) | 0 (0) |
| Hypertension | 12 (29.3) | 10 (24.4) | 2 (4.9) | 0 (0) | 7 (23.3) | 2 (6.6) | 5 (16.7) | 0 (0) | 23 (36.5) | 16 (25.4) | 4 (6.3) | 3 (4.8) |
| Thrombocytopenia | 9 (22.0) | 2 (4.9) | 4 (9.7) | 3 (7.3) | 23 (76.7) | 10 (33.3) | 8 (26.7) | 5 (16.7) | 20 (31.7) | 10 (15.9) | 5 (7.9) | 5 (7.9) |
| Alopecia | 6 (14.6) | 4 (9.7) | 2 (4.9) | 0 (0) | 2 (6.6) | 2 (6.6) | 0 (0) | 0 (0) | 20 (31.7) | 19 (30.2) | 1 (1.6) | 0 (0) |
| Hepatic encephalopathy | 1 (2.4) | 0 (0) | 1 (2.4) | 0 (0) | 0 (0) | 0 (0) | 0 (0) | 0 (0) | 0 (0) | 0 (0) | 0 (0) | 0 (0) |

Table 3 Dose modification related to adverse events

| | Group A (<i>n</i> = 41) | Group B (<i>n</i> = 30) | Group C (<i>n</i> = 63) | Group A vs Group B, <i>P</i> value | Group A vs Group C, <i>P</i> value | Group B vs Group C, <i>P</i> value |
|---|--------------------------|--------------------------|--------------------------|------------------------------------|------------------------------------|------------------------------------|
| Dose reduction to initial dose of sorafenib | 8/41 (19.5%) | 2/30 (6.7%) | 26/63 (41.3%) | 0.700 | 0.108 | 0.005 |
| Re-escalation to initial dose of sorafenib | 2/8 (25.0%) | 2/2 (100.0%) | 2/26 (7.7%) | NA | NA | NA |

NA: Not available.

Table 4 Radiological response according to the modified response evaluation criteria in solid tumors

| | Group A (<i>n</i> = 41) | Group B (<i>n</i> = 30) | Group C (<i>n</i> = 63) |
|----------------------|--------------------------|--------------------------|--------------------------|
| Complete response | 0 | 1 | 1 |
| Partial response | 1 | 1 | 5 |
| Stable disease | 10 | 11 | 35 |
| Progressive disease | 30 | 17 | 22 |
| Response rate | 2.4% | 6.7% | 9.5% |
| Disease control rate | 26.8% | 43.3% | 65.1% |

0.04–0.36; *P* < 0.01) and Group B vs Group C (OR, 0.09; 95%CI: 0.03–0.27; *P* < 0.01) (Figure 3, Table 8).

Correlation between OS and TTF

The Spearman’s rank correlation coefficients between OS and TTF in each group were 0.41 (Group A; *P* < 0.01), 0.13 (Group B; *P* = 0.51), and 0.58 (Group C; *P* < 0.01). There was a highly significant correlation between OS and TTF in Group C. However, there was no correlation between OS and TTF in Group B.

Table 5 Reasons for permanent sorafenib discontinuation, *n* (%)

| | Group A (<i>n</i> = 41) | Group B (<i>n</i> = 30) | Group C (<i>n</i> = 63) | Group A vs Group B, <i>P</i> value | Group A vs Group C, <i>P</i> value | Group B vs Group C, <i>P</i> value |
|---------------|--------------------------|--------------------------|--------------------------|------------------------------------|------------------------------------|------------------------------------|
| Progression | 26 (63.4) | 7 (23.3) | 33 (52.4) | 0.006 | 1.000 | 0.046 |
| Intolerance | 7 (17.1) | 18 (60.0) | 13 (20.6) | 0.002 | 1.000 | 0.001 |
| Liver failure | 6 (14.6) | 3 (10.0) | 8 (12.7) | 1.000 | 1.000 | 1.000 |
| Other | 2 (4.9) | 2 (6.7) | 9 (14.3) | 1.000 | 0.690 | 1.000 |

Table 6 Prognostic factors of overall survival by multivariable Cox regression analysis

| | Univariate analysis | | | Multivariate analysis | | |
|---|---------------------|-------------|----------------|-----------------------|-------------|----------------|
| | HR | 95%CI | <i>P</i> value | HR | 95%CI | <i>P</i> value |
| Age (within 70 yr) | 0.867 | 0.603–1.246 | 0.440 | - | - | - |
| Male | 1.216 | 0.802–1.842 | 0.357 | - | - | - |
| Etiology (HBV) | 1.313 | 0.809–2.133 | 0.271 | - | - | - |
| BCLC stage B | 0.667 | 0.459–0.969 | 0.033 | 0.601 | 0.405–0.891 | 0.011 |
| Portal vein thrombosis | 1.677 | 1.092–2.575 | 0.018 | 1.133 | 0.674–1.903 | 0.638 |
| Extrahepatic spread | 0.740 | 0.509–1.074 | 0.113 | 0.671 | 0.419–1.076 | 0.098 |
| AFP (> 400 ng/mL) | 1.282 | 0.893–1.839 | 0.178 | 1.370 | 0.936–2.006 | 0.105 |
| ECOG Performance status 1 | 0.752 | 0.488–1.158 | 0.196 | 1.042 | 0.636–1.708 | 0.869 |
| Group A vs Group B | 0.703 | 0.431–1.147 | 0.159 | 0.658 | 0.398–1.088 | 0.103 |
| Group A vs Group C | 0.431 | 0.281–0.663 | < 0.001 | 0.407 | 0.253–0.654 | < 0.001 |
| Sorafenib administration period (second half vs first half) | 1.205 | 0.840–1.728 | 0.311 | - | - | - |

AFP: Alpha-fetoprotein; BCLC: Barcelona Clinic Liver Cancer; HBV: Hepatitis B virus; ECOG: Eastern Cooperative Oncology Group.

DISCUSSION

We investigated the effect of cooperation between oncologists and pharmacists on the prognosis of patients with advanced HCC treated with sorafenib monotherapy. In the present study, the occurrence of HFSR was associated with improved patient prognosis, and this improvement was significantly enhanced by appropriate medication adherence. Close cooperation between oncologists and pharmacists increased adherence, and a strong correlation was observed between OS and TTF.

Several studies have indicated that the emergence of HFSR is associated with prolonged survival in patients with advanced HCC treated with sorafenib[5,6,21]. However, these studies did not evaluate the correlation between medication adherence and survival after the appearance of an AE, including HFSR. Targeted therapies, including sorafenib, can result in unexpected AEs that do not occur after the administration of earlier chemotherapy drugs[22]. Oncologists must recognize these novel AEs at an early stage and provide appropriate treatment to the extent possible. However, previous studies revealed that optimal AE management requires considerable experience and time[7,23]. Management of sorafenib-related AEs includes data collection for AE grading, patient education, and determination of the appropriate sorafenib dose by an oncologist[15].

The use of sorafenib is associated with various AEs, including gastrointestinal, constitutional, or dermatologic events[1,2], and their management may require dose reduction or temporary discontinuation to avoid sorafenib treatment cessation. For example, an appropriate sorafenib dose reduction yielded a decreased rate of permanent discontinuation due to AEs[7]. However, in many patients, these dose changes do not mitigate intolerable or severe AEs, and permanent sorafenib discontinuation is required[24].

Table 7 Prognostic factors of time-to-treatment failure by multivariable Cox regression analysis

| | Univariate analysis | | | Multivariate analysis | | |
|---|---------------------|-------------|---------|-----------------------|-------------|---------|
| | HR | 95%CI | P value | HR | 95%CI | P value |
| Age (within 70 yr) | 1.059 | 0.747–1.501 | 0.747 | - | - | - |
| Male | 0.926 | 0.625–1.372 | 0.703 | - | - | - |
| Etiology (HBV) | 1.208 | 0.768–1.901 | 0.413 | - | - | - |
| BCLC stage C | 1.311 | 0.921–1.866 | 0.132 | - | - | - |
| Portal vein thrombosis | 1.379 | 0.925–2.056 | 0.115 | 1.011 | 0.662–1.545 | 0.958 |
| Diarrhea | 0.675 | 0.473–0.965 | 0.031 | 0.654 | 0.449–0.952 | 0.027 |
| Hypertension | 1.070 | 0.735–1.556 | 0.725 | - | - | - |
| ECOG Performance status 1 | 0.687 | 0.446–1.058 | 0.089 | 0.725 | 0.463–1.135 | 0.159 |
| Group B vs Group A | 1.670 | 1.034–2.698 | 0.036 | 1.694 | 1.044–2.748 | 0.033 |
| Group C vs Group A | 0.495 | 0.328–0.747 | < 0.001 | 0.529 | 0.346–0.811 | 0.003 |
| Sorafenib administration period (second half vs first half) | 0.980 | 0.694–1.384 | 0.908 | - | - | - |

AFP: Alpha-fetoprotein; BCLC: Barcelona Clinic Liver Cancer; HBV: Hepatitis B virus; ECOG: Eastern Cooperative Oncology Group.

Table 8 Prognostic factors of proportion of days covered by logistic regression analyses

| | Adjusted analyses | | |
|--------------------|-------------------|--------------|---------|
| | OR | 95%CI | P value |
| Male | 0.352 | 0.141–0.877 | 0.025 |
| Child-Pugh stage B | 3.830 | 1.180–12.400 | 0.025 |
| Diarrhea | 0.472 | 0.198–1.120 | 0.089 |
| Group B vs Group A | 0.113 | 0.036–0.356 | < 0.001 |
| Group B vs Group C | 0.091 | 0.031–0.266 | < 0.001 |

In our study, only the mutual cooperation system promoted dose reduction after an AE and extended the TTF. In the mutual cooperation system, pharmacists were responsible for collecting data on AE grades, educating patients, and managing any leftover medicine. Furthermore, they documented their findings in a report for the oncologist. On the other hand, in the nonmutual cooperation system, an oncologist examined the patient before pharmacists were involved in patient management. Oncologists were required to evaluate AE grading data, educate patients, and determine the appropriate sorafenib dose. Only after the medical examination did a pharmacist provide additional patient management, and their findings were not reported to the oncologist. In the nonmutual cooperation system, the oncologist had to obtain a substantial amount of information to maintain or revise the sorafenib treatment regimen within 5 to 10 min.

Given these differences between the systems, our results suggest that the mutual cooperation system led to appropriate dose reductions, as reflected by the extended TTF. However, we do not recommend starting sorafenib at half the standard dose (800 mg/d). Dose reductions were guided by the results obtained by the mutual cooperation system. Additionally, we demonstrated that the best outcomes occur when optimal dosing and good medication adherence are achieved early in the course of sorafenib treatment. In our study, only the mutual cooperation system ensured good adherence in patients who experienced HFSR secondary to sorafenib treatment and prevented unnecessary permanent medication discontinuation.

A previous study showed that despite dramatic improvements in adjuvant hormonal therapy for breast cancer, nonadherence, early discontinuation, and effective cancer treatment are affected by treatment-related toxicity, and appropriate interventions are needed to improve breast cancer survival[25]. Another cohort study indicated that long-term tamoxifen therapy for breast cancer reduced the risk of death,

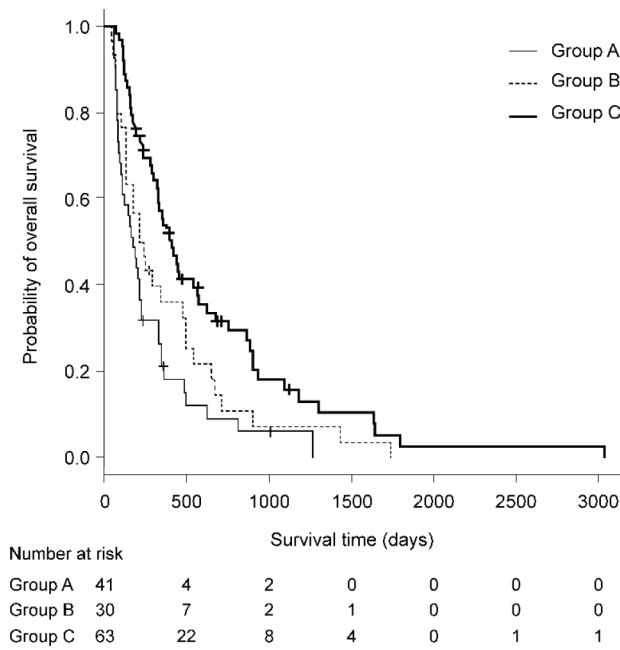


Figure 1 Kaplan-Meier estimates and prognostic factors of overall survival (comparison between each group). Group A, patients without hand-foot skin reaction (HFSR) but with pharmacist intervention; Group B, patients with HFSR and the nonmutual cooperation system; Group C, patients with HFSR and intervention by pharmacists who shared interview information with the oncologist (mutual cooperation system).

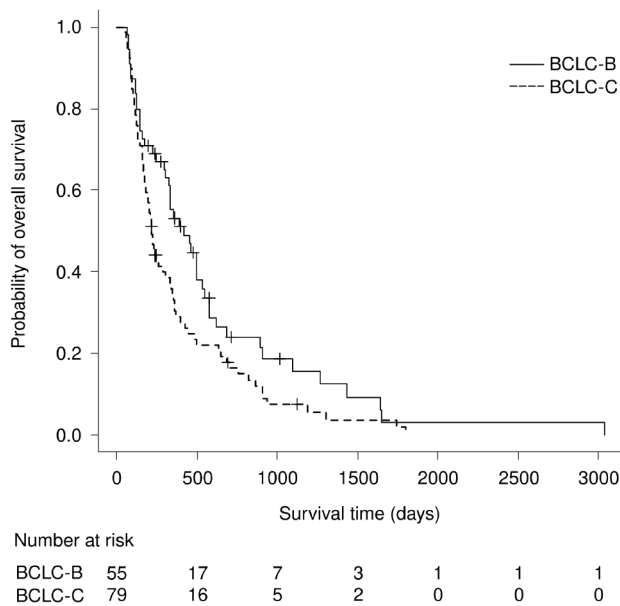


Figure 2 Kaplan-Meier estimates and prognostic factors of overall survival (Barcelona Clinic Liver Cancer B vs Barcelona Clinic Liver Cancer C). BCLC: Barcelona Clinic Liver Cancer.

while the risk of death increased with a low adherence rate[26]. In our study, the medical team continued sharing patient information after the patient started taking sorafenib; therefore, the mutual cooperation system enabled the medical team to prevent HFSR or promptly provide patient management, as appropriate. In contrast, the nonmutual cooperation system did not allow patient information to be shared at an early stage; thus, the medical team was not able to take measures to prevent HFSR or plan palliation care in a timely manner. The differences in the effectiveness of HFSR prevention and palliation between the two systems highlight the importance of the various hurdles that can affect medication adherence.

Hurdles to medication adherence are complex and include patient-, clinician-, and healthcare system-related factors. Patient-related factors, such as limited involvement in the treatment decision-making process, poor health literacy, doubts about

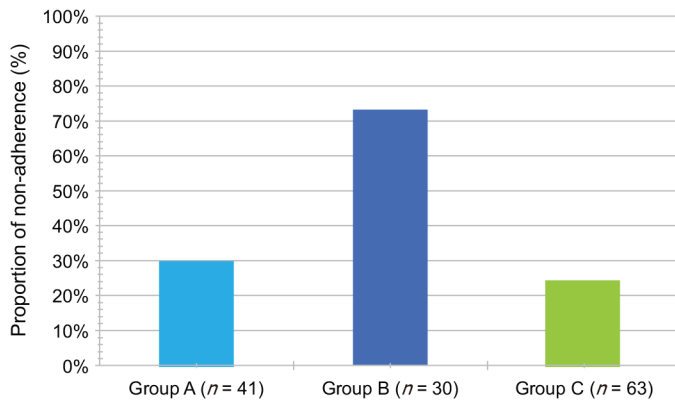


Figure 3 Proportion and prognostic factors of nonadherence. Group A, patients without hand-foot skin reaction (HFSR) but with pharmacist intervention; Group B, patients with HFSR and the nonmutual cooperation system; Group C, patients with HFSR and intervention by pharmacists who shared interview information with the oncologist (mutual cooperation system).

medication effectiveness, and previous adverse effects, influence adherence. Clinician-related factors include failure to recognize nonadherence, poor patient communication, and inadequate multidisciplinary communication between oncologists and pharmacists. Healthcare system-related factors include relationships with clinicians and clinicians' satisfaction with patient care[27,28]. Thus, multiple factors may become hurdles to improving adherence. The mutual cooperation system coordinates interactions among patients, clinicians, and the health system, thereby minimizing barriers to adherence.

Surprisingly, this study revealed that the prognostic value of HFSR was enhanced by appropriate medication adherence. On the other hand, BCLC-B HCC was an independent predictor of improved OS[29]. BCLC stage did not affect the difference in OS between Groups A and C, as there was no significant between-group difference in the baseline stage distribution.

We have reasonable evidence to confirm the validity of our results. First, variables such as age, sex, etiology, ECOG performance status, liver function, comorbidities, and TACE procedure count were not significantly different between the groups. Second, we verified that all patients had received sorafenib monotherapy and no subsequent chemotherapy; therefore, neither our patients' prognoses nor the prolonged OS we observed was affected by other chemotherapeutic agents.

Nevertheless, our study has a few limitations. First, our study design was based on the mutual cooperation system. After a patient was first checked by a specialized pharmacist, the oncologist determined whether to prescribe sorafenib based on the pharmacist's report. However, patients were not required to participate in the mutual cooperation system, and involvement was subject to the patient's wish. After the patients underwent a medical examination by an oncologist, a specialized pharmacist could also provide patient guidance about sorafenib. While patients who were unwilling to participate in the mutual cooperation system may have been included in Group A or B, it is unknown whether this enrollment could have affected the adherence rate. Second, OS and TTF were higher in the mutual cooperation system group (Group C) than in Group A and Group B. It is difficult to determine whether these results were caused by improved adherence or the mechanism underlying the prognostic efficacy of HFSR.

CONCLUSION

The mutual cooperation system increased treatment duration and improved prognosis in patients with HFSR secondary to sorafenib treatment. Additionally, the mutual cooperation system allowed us to promptly initiate sorafenib treatment. Our study clearly demonstrates the clinical and research benefits of this system. The mutual cooperation system for sorafenib treatment management described in this study could be applied to the management of patients treated with other multikinase inhibitors to extend OS. The increased OS resulting from the mutual cooperation system could have a substantial impact on the design of clinical studies in which sorafenib is used as the control drug. Additionally, nonadherence may have adversely affected OS in previous studies, leading researchers to underestimate drug efficacy. We propose that future

clinical investigations designed to improve medication adherence could eliminate OS underestimation.

ARTICLE HIGHLIGHTS

Research background

Although sorafenib prolongs overall survival (OS) in patients with hepatocellular carcinoma (HCC), the drug is associated with various adverse events (AEs) that may lead to permanent discontinuation.

Research motivation

The authors postulated that mutual cooperative intervention for AEs could improve OS in patients with HCC.

Research objectives

The aim of this study is to clarify the association between AE interventions and patient prognosis.

Research methods

The authors developed a mutual cooperation system that was initiated at the start of sorafenib treatment to manage AEs effectively. The system entailed pharmacist consultations during which patients were provided accurate information about sorafenib to alleviate fear and anxiety related to AEs. We stratified patients into three groups: Group A, patients without hand-foot skin reaction (HFSR) but with pharmacist intervention; Group B, patients with HFSR and pharmacist interventions unreported to oncologists (nonmutual cooperation system); and Group C, patients with HFSR and pharmacist interventions known to oncologists (mutual cooperation system).

Research results

The authors enrolled 134 patients (Group A, $n = 41$; Group B, $n = 30$; Group C, $n = 63$). The median OS significantly differed between Groups A and C (6.2 vs 13.9 mo, $P < 0.01$) but not between Groups A and B (6.2 vs 7.7 mo, $P = 0.62$). Group A vs Group C was an independent OS predictor (HR, 0.41; 95%CI: 0.25–0.66; $P < 0.01$). In Group B alone, the time to treatment failure (TTF) was significantly shorter, while the non-adherence rate was higher ($P < 0.01$). Additionally, Spearman's rank correlation coefficients between OS and TTF in each group were 0.41 (Group A; $P < 0.01$), 0.13 (Group B; $P = 0.51$), and 0.58 (Group C; $P < 0.01$). There was a highly significant correlation between OS and TTF in Group C. However, there was no correlation between OS and TTF in Group B.

Research conclusions

The mutual cooperation system increased the treatment duration and improved the prognosis of patients with HFSR.

Research perspectives

Future prospective studies (*e.g.*, randomized controlled trials) and improved adherence could help avoid OS underestimation.

REFERENCES

- 1 Llovet JM, Ricci S, Mazzaferro V, Hilgard P, Gane E, Blanc JF, de Oliveira AC, Santoro A, Raoul JL, Forner A, Schwartz M, Porta C, Zeuzem S, Bolondi L, Greten TF, Galle PR, Seitz JF, Borbath I, Häussinger D, Giannaris T, Shan M, Moscovici M, Voliotis D, Bruix J; SHARP Investigators Study Group. Sorafenib in advanced hepatocellular carcinoma. *N Engl J Med* 2008; **359**: 378-390 [PMID: 18650514 DOI: 10.1056/NEJMoa0708857]
- 2 Cheng AL, Kang YK, Chen Z, Tsao CJ, Qin S, Kim JS, Luo R, Feng J, Ye S, Yang TS, Xu J, Sun Y, Liang H, Liu J, Wang J, Tak WY, Pan H, Burock K, Zou J, Voliotis D, Guan Z. Efficacy and safety of sorafenib in patients in the Asia-Pacific region with advanced hepatocellular carcinoma: a phase III randomised, double-blind, placebo-controlled trial. *Lancet Oncol* 2009; **10**: 25-34 [PMID: 19095497 DOI: 10.1016/S1470-2045(08)70285-7]
- 3 Iavarone M, Cabibbo G, Biolato M, Della Corte C, Maida M, Barbara M, Basso M, Vavassori S,

- Craxi A, Grieco A, Cammà C, Colombo M. Predictors of survival in patients with advanced hepatocellular carcinoma who permanently discontinued sorafenib. *Hepatology* 2015; **62**: 784-791 [PMID: 25645399 DOI: 10.1002/hep.27729]
- 4 **Vincenzi B**, Santini D, Russo A, Addeo R, Giuliani F, Montella L, Rizzo S, Venditti O, Frezza AM, Caraglia M, Colucci G, Del Prete S, Tonini G. Early skin toxicity as a predictive factor for tumor control in hepatocellular carcinoma patients treated with sorafenib. *Oncologist* 2010; **15**: 85-92 [PMID: 20051477 DOI: 10.1634/theoncologist.2009-0143]
 - 5 **Reig M**, Torres F, Rodriguez-Lope C, Forner A, LLarch N, Rimola J, Darnell A, Ríos J, Ayuso C, Bruix J. Early dermatologic adverse events predict better outcome in HCC patients treated with sorafenib. *J Hepatol* 2014; **61**: 318-324 [PMID: 24703956 DOI: 10.1016/j.jhep.2014.03.030]
 - 6 **Díaz-González Á**, Sanduzzi-Zamparelli M, Sapena V, Torres F, LLarch N, Iserte G, Forner A, da Fonseca L, Ríos J, Bruix J, Reig M. Systematic review with meta-analysis: the critical role of dermatological events in patients with hepatocellular carcinoma treated with sorafenib. *Aliment Pharmacol Ther* 2019; **49**: 482-491 [PMID: 30695819 DOI: 10.1111/apt.15088]
 - 7 **Tovoli F**, Ielasi L, Casadei-Gardini A, Granito A, Foschi FG, Rovesti G, Negrini G, Orsi G, Renzulli M, Piscaglia F. Management of adverse events with tailored sorafenib dosing prolongs survival of hepatocellular carcinoma patients. *J Hepatol* 2019; **71**: 1175-1183 [PMID: 31449860 DOI: 10.1016/j.jhep.2019.08.015]
 - 8 **Marin D**, Bazeos A, Mahon FX, Eliasson L, Milojkovic D, Bua M, Apperley JF, Szydlo R, Desai R, Kozlowski K, Paliompeis C, Latham V, Foroni L, Molimard M, Reid A, Rezvani K, de Lavallade H, Guallar C, Goldman J, Khorashad JS. Adherence is the critical factor for achieving molecular responses in patients with chronic myeloid leukemia who achieve complete cytogenetic responses on imatinib. *J Clin Oncol* 2010; **28**: 2381-2388 [PMID: 20385986 DOI: 10.1200/JCO.2009.26.3087]
 - 9 **Partridge AH**, Archer L, Kornblith AB, Gralow J, Grenier D, Perez E, Wolff AC, Wang X, Kastrissios H, Berry D, Hudis C, Winer E, Muss H. Adherence and persistence with oral adjuvant chemotherapy in older women with early-stage breast cancer in CALGB 49907: adherence companion study 60104. *J Clin Oncol* 2010; **28**: 2418-2422 [PMID: 20368559 DOI: 10.1200/JCO.2009.26.4671]
 - 10 **Greer JA**, Amoyal N, Nisotel L, Fishbein JN, MacDonald J, Stagl J, Lennes I, Temel JS, Safren SA, Pirl WF. A Systematic Review of Adherence to Oral Antineoplastic Therapies. *Oncologist* 2016; **21**: 354-376 [PMID: 26921292 DOI: 10.1634/theoncologist.2015-0405]
 - 11 **Ibrahim AR**, Eliasson L, Apperley JF, Milojkovic D, Bua M, Szydlo R, Mahon FX, Kozlowski K, Paliompeis C, Foroni L, Khorashad JS, Bazeos A, Molimard M, Reid A, Rezvani K, Gerrard G, Goldman J, Marin D. Poor adherence is the main reason for loss of CCyR and imatinib failure for chronic myeloid leukemia patients on long-term therapy. *Blood* 2011; **117**: 3733-3736 [PMID: 21346253 DOI: 10.1182/blood-2010-10-309807]
 - 12 **De Geest S**, Sabaté E. Adherence to long-term therapies: evidence for action. *Eur J Cardiovasc Nurs* 2003; **2**: 323 [PMID: 14667488 DOI: 10.1016/S1474-5151(03)00091-4]
 - 13 **Abraham C**, Michie S. A taxonomy of behavior change techniques used in interventions. *Health Psychol* 2008; **27**: 379-387 [PMID: 18624603 DOI: 10.1037/0278-6133.27.3.379]
 - 14 **Viswanathan M**, Golin CE, Jones CD, Ashok M, Blalock SJ, Wines RC, Coker-Schwimmer EJ, Rosen DL, Sista P, Lohr KN. Interventions to improve adherence to self-administered medications for chronic diseases in the United States: a systematic review. *Ann Intern Med* 2012; **157**: 785-795 [PMID: 22964778 DOI: 10.7326/0003-4819-157-11-201212040-00538]
 - 15 **Ochi M**, Kamoshida T, Ohkawara A, Ohkawara H, Kakinoki N, Hirai S, Yanaka A. Multikinase inhibitor-associated hand-foot skin reaction as a predictor of outcomes in patients with hepatocellular carcinoma treated with sorafenib. *World J Gastroenterol* 2018; **24**: 3155-3162 [PMID: 30065561 DOI: 10.3748/wjg.v24.i28.3155]
 - 16 **Shomura M**, Kagawa T, Shiraishi K, Hirose S, Arase Y, Koizumi J, Mine T. Skin toxicity predicts efficacy to sorafenib in patients with advanced hepatocellular carcinoma. *World J Hepatol* 2014; **6**: 670-676 [PMID: 25276283 DOI: 10.4254/wjh.v6.i9.670]
 - 17 **Lencioni R**, Llovet JM. Modified RECIST (mRECIST) assessment for hepatocellular carcinoma. *Semin Liver Dis* 2010; **30**: 52-60 [PMID: 20175033 DOI: 10.1055/s-0030-1247132]
 - 18 **Benner JS**, Glynn RJ, Mogun H, Neumann PJ, Weinstein MC, Avorn J. Long-term persistence in use of statin therapy in elderly patients. *JAMA* 2002; **288**: 455-461 [PMID: 12132975 DOI: 10.1001/jama.288.4.455]
 - 19 **Partridge AH**, Wang PS, Winer EP, Avorn J. Nonadherence to adjuvant tamoxifen therapy in women with primary breast cancer. *J Clin Oncol* 2003; **21**: 602-606 [PMID: 12586795 DOI: 10.1200/JCO.2003.07.071]
 - 20 **Anderson JR**, Cain KC, Gelber RD. Analysis of survival by tumor response. *J Clin Oncol* 1983; **1**: 710-719 [PMID: 6668489 DOI: 10.1200/JCO.1983.1.11.710]
 - 21 **Howell J**, Pinato DJ, Ramaswami R, Bettinger D, Arizumi T, Ferrari C, Yen C, Gibbin A, Burlone ME, Guaschino G, Sellers L, Black J, Pirisi M, Kudo M, Thimme R, Park JW, Sharma R. On-target sorafenib toxicity predicts improved survival in hepatocellular carcinoma: a multi-centre, prospective study. *Aliment Pharmacol Ther* 2017; **45**: 1146-1155 [PMID: 28252185 DOI: 10.1111/apt.13977]
 - 22 **Gangadhar TC**, Vonderheide RH. Mitigating the toxic effects of anticancer immunotherapy. *Nat Rev Clin Oncol* 2014; **11**: 91-99 [PMID: 24445516 DOI: 10.1038/nrclinonc.2013.245]
 - 23 **Raoul JL**, Adhoute X, Penaranda G, Perrier H, Castellani P, Oules V, Bourlière M. Sorafenib: Experience and Better Management of Side Effects Improve Overall Survival in Hepatocellular Carcinoma Patients: A Real-Life Retrospective Analysis. *Liver Cancer* 2019; **8**: 457-467 [PMID:

- 31799203 DOI: 10.1159/000497161]
- 24 **Forner A**, Da Fonseca LG, Díaz-González Á, Sanduzzi-Zamparelli M, Reig M, Bruix J. Controversies in the management of hepatocellular carcinoma. *JHEP Rep* 2019; **1**: 17-29 [PMID: 32039350 DOI: 10.1016/j.jhepr.2019.02.003]
 - 25 **Hershman DL**. Sticking to It: Improving Outcomes by Increasing Adherence. *J Clin Oncol* 2016; **34**: 2440-2442 [PMID: 27217447 DOI: 10.1200/JCO.2016.67.7336]
 - 26 **McCowan C**, Shearer J, Donnan PT, Dewar JA, Crilly M, Thompson AM, Fahey TP. Cohort study examining tamoxifen adherence and its relationship to mortality in women with breast cancer. *Br J Cancer* 2008; **99**: 1763-1768 [PMID: 18985046 DOI: 10.1038/sj.bjc.6604758]
 - 27 **Kini V**, Ho PM. Interventions to Improve Medication Adherence: A Review. *JAMA* 2018; **320**: 2461-2473 [PMID: 30561486 DOI: 10.1001/jama.2018.19271]
 - 28 **Ruddy K**, Mayer E, Partridge A. Patient adherence and persistence with oral anticancer treatment. *CA Cancer J Clin* 2009; **59**: 56-66 [PMID: 19147869 DOI: 10.3322/caac.20004]
 - 29 **Bruix J**, Cheng AL, Meinhardt G, Nakajima K, De Sanctis Y, Llovet J. Prognostic factors and predictors of sorafenib benefit in patients with hepatocellular carcinoma: Analysis of two phase III studies. *J Hepatol* 2017; **67**: 999-1008 [PMID: 28687477 DOI: 10.1016/j.jhep.2017.06.026]

Retrospective Study

Contrast-enhanced ultrasound imaging for intestinal lymphoma

Ning-Yi Cui, Xuan-Tong Gong, Yan-Tao Tian, Yong Wang, Rui Zhang, Meng-Jia Liu, Jie Han, Bo Wang, Di Yang

ORCID number: Ning-Yi Cui 0000-0001-5805-5133; Xuan-Tong Gong 0000-0001-8984-5461; Yan-Tao Tian 0000-0001-6479-7547; Yong Wang 0000-0001-7682-0433; Rui Zhang 0000-0003-1597-3529; Meng-Jia Liu 0000-0002-5898-7114; Jie Han 0000-0001-9863-800X; Bo Wang 0000-0002-6581-7316; Di Yang 0000-0003-0318-1428.

Author contributions: Cui NY and Gong XT contributed equally to this work; Wang Y, Tian YT, Cui NY and Gong XT designed the research study; Zhang R, Liu MJ, Han J, Wang B and Yang D contributed analytic tools; Cui NY and Gong XT analyzed the data and wrote the manuscript; All authors have read and approve the final manuscript.

Supported by National Natural Science Foundation of China, No. 81974268; Medical and Health Science and Technology Innovation Project of Chinese Academy of Medical Sciences, No. 2017-I2M-1-006; and Beijing Hope Run Special Fund of Cancer Foundation of China, No. LC2017B19 and No. LC2016A04.

Institutional review board

statement: Approval of all ethical and experimental procedures and protocols was granted by the Independent Ethics Committee of National Cancer Center/Cancer

Ning-Yi Cui, Xuan-Tong Gong, Yong Wang, Rui Zhang, Meng-Jia Liu, Jie Han, Bo Wang, Di Yang, Department of Ultrasound, National Cancer Center/National Clinical Research Center for Cancer/Cancer Hospital, Chinese Academy of Medical Sciences and Peking Union Medical College, Beijing 100021, China

Xuan-Tong Gong, Department of Ultrasound, Fatou Community Health Service Center Chaoyang District Beijing, Beijing 100023, China

Yan-Tao Tian, Pancreatic and Gastric Surgery, National Cancer Center/National Clinical Research Center for Cancer/Cancer Hospital, Chinese Academy of Medical Sciences and Peking Union Medical College, Beijing 100021, China

Corresponding author: Yong Wang, MD, PhD, Professor, Department of Ultrasound, National Cancer Center/National Clinical Research Center for Cancer/Cancer Hospital, Chinese Academy of Medical Sciences and Peking Union Medical College, No. 17 Panjiayuan Nanli, Chaoyang District, Beijing 100021, China. wangyong@cicams.ac.cn

Abstract**BACKGROUND**

Intestinal lymphoma is a rare tumor. Contrast-enhanced ultrasound (CEUS) findings of intestinal lymphoma have not been reported previously, and the relationship between CEUS and clinicopathological features and prognostic factors is still unknown.

AIM

To describe the B-mode US and CEUS features of intestinal lymphoma and investigate the correlation of CEUS and histopathological features.

METHODS

This was a single-center retrospective study. Eighteen patients with histologically confirmed intestinal lymphoma underwent B-mode US and CEUS examinations between October 2016 and November 2019. We summarized the features of B-mode US and CUES imaging of intestinal lymphoma and compared the frequency of tumor necrosis in intestinal lymphomas with reference to different pathological subtypes (aggressive or indolent) and clinical stage (early or advanced). The time-intensity curve parameters of CEUS were also compared between patients with normal and elevated serum lactate dehydrogenase.

RESULTS

Hospital, Chinese Academy of Medical Sciences and Peking Union Medical College under Application, No. NCC2016YZ-15.

Informed consent statement:

Patients were not required to give informed consent to the study because the analysis used anonymous clinical data that were obtained after each patient agreed to do the examination by written consent.

Conflict-of-interest statement:

There are no conflicts of interest to declare.

Data sharing statement:

No additional data are available.

Open-Access: This article is an open-access article that was selected by an in-house editor and fully peer-reviewed by external reviewers. It is distributed in accordance with the Creative Commons Attribution NonCommercial (CC BY-NC 4.0) license, which permits others to distribute, remix, adapt, build upon this work non-commercially, and license their derivative works on different terms, provided the original work is properly cited and the use is non-commercial. See: <http://creativecommons.org/licenses/by-nc/4.0/>

Manuscript source: Unsolicited manuscript

Specialty type: Gastroenterology and hepatology

Country/Territory of origin: China

Peer-review report's scientific quality classification

Grade A (Excellent): A
Grade B (Very good): B
Grade C (Good): C
Grade D (Fair): 0
Grade E (Poor): 0

Received: April 21, 2021

Peer-review started: April 21, 2021

First decision: June 30, 2021

Revised: July 12, 2021

Accepted: July 20, 2021

Article in press: July 20, 2021

Published online: August 28, 2021

In B-mode imaging, four patterns were observed in intestinal lymphoma: Mass type (12/18, 66.7%), infiltration type (1/18, 5.6%), mesentery type (4/18, 22.2%) and mixed type (1/18, 5.6%). All cases were hypoechoic and no cystic areas were detected. On CEUS, most cases (17/18, 94.4%) showed arterial hyperechoic enhancement. All cases showed arterial enhancement followed by venous wash out. A relatively high rate of tumor necrosis (11/18, 61.1%) was observed in this study. Tumor necrosis on CEUS was more frequent in aggressive subtypes (10/13, 76.9%) than in indolent subtypes (1/5, 20.0%) ($P = 0.047$). There were no correlations between tumor necrosis and lesion size and Ann Arbor stage. There was no significant difference in time-intensity curve parameters between normal and elevated lactate dehydrogenase groups.

CONCLUSION

B-mode US and CEUS findings of intestinal lymphoma are characteristic. We observed a high rate of tumor necrosis, which appeared more frequently in aggressive pathological subtypes of intestinal lymphoma.

Key Words: Intestinal lymphoma; Contrast enhanced ultrasound; B-mode ultrasound; Histopathological features; Lactate dehydrogenase; Quantitative diagnosis

©The Author(s) 2021. Published by Baishideng Publishing Group Inc. All rights reserved.

Core Tip: This is a small pilot study that described the appearance and pattern of intestinal lymphoma on B-mode ultrasound (US) and contrast-enhanced US. We revealed an unexpected contrast-enhanced US enhancement pattern with a high rate of tumor necrosis, which was found more frequently in aggressive than in indolent subtypes. This might provide additional information for clinical diagnosis and treatment of intestinal lymphoma.

Citation: Cui NY, Gong XT, Tian YT, Wang Y, Zhang R, Liu MJ, Han J, Wang B, Yang D. Contrast-enhanced ultrasound imaging for intestinal lymphoma. *World J Gastroenterol* 2021; 27(32): 5438-5447

URL: <https://www.wjnet.com/1007-9327/full/v27/i32/5438.htm>

DOI: <https://dx.doi.org/10.3748/wjg.v27.i32.5438>

INTRODUCTION

Gastrointestinal tract is the most common site for extranodal lymphomas[1,2]. Approximately 20%–25% of primary extranodal lymphomas occur in the gastrointestinal tract [3,4]. Around 50%–70% of the gastrointestinal lymphomas arise in the stomach, 20%–30% in the small bowel and 5%–20% in the large bowel[5]. Primary intestinal lymphomas are less common than gastric lymphomas and differ in clinical features, pathology, treatment and prognosis[6-10]. There are few studies on the ultrasound (US) diagnosis of intestinal lymphoma, most of which are case reports. Intestinal tumors are usually studied through endoscopic or radiological imaging techniques, which may explain the lack of studies on US in intestinal lymphomas[11]. However, previous studies have already shown that US is an effective method for detecting gastrointestinal lesions, especially in experienced hands[12]. US-guided biopsy can also establish a definite pathological diagnosis, avoiding unnecessary surgery.

Contrast-enhanced US (CEUS) has emerged as a new imaging technique that can evaluate tumor vascularity[13]. CEUS is now widely accepted and recommended in inflammatory bowel disease in the European Federation of Societies for Ultrasound in Medicine and Biology (EFSUMB) guidelines. CEUS is suggested for assessment of the vascularity of the gastrointestinal wall and gastrointestinal tumors[14]. To the best of our knowledge, CEUS features of intestinal lymphoma have not previously been described. The aim of this study was to illustrate CEUS patterns of intestinal lymphoma for the first time and to investigate the relationship between CEUS and clinicopathological features and prognostic factors.

P-Reviewer: Angeramo CA,
Mannelli L, Okada M
S-Editor: Fan JR
L-Editor: Filipodia
P-Editor: Yuan YY



MATERIALS AND METHODS

Patients

This is a single-center retrospective study based on a search of our imaging system from October 2016 to November 2019. Patients were excluded if they had a history of any other cancer or if they had previously received treatment. Written informed consent was obtained from each patient before the CEUS examinations.

Eighteen patients with histologically confirmed intestinal lymphoma were included, 10 men and 8 women, with age range 34–85 years. Definitive diagnosis for all the lesions was obtained by US-guided biopsy in 15 (83.3%) cases or by surgical resection in 3 (16.7%) cases. The diagnosis of intestinal lymphoma was based on the World Health Organization classification[15]. According to the Ann Arbor staging system, patients were classified into early stage (I/II) and advanced stage (III/IV). Pathological types were classified into aggressive and indolent lymphoma based on the World Health Organization classification. Primary intestinal lymphoma was defined as predominant intestinal lesion without previous peripheral lymphadenopathy or any lymphoma whose clinical presentation was related to intestinal involvement[16].

US examinations

All patients underwent B-mode US and CEUS with a 3.0–5.0 -MHz C5-1 probe for the iU22 sonography system (Philips Healthcare Ultrasound, Bothell, WA, United States) prior to surgery or biopsy. All patients were fasted for 8–12 h. CEUS was performed on all tumors under same protocols with the following parameters: Mechanical index 0.08–0.11, contrast gain 50%–60% and dynamic range 40 dB and focal zone was set at maximal depth. SonoVue (4.8 mL; Bracco, Milan, Italy) was administrated through a forearm vein in bolus within 1–2 s, followed by flush of 5 mL 0.9% saline. Images were acquired immediately after contrast agent was injected and lasted for 3 min and were recorded and stored as raw data on personal hard disks.

Image analysis

US and CEUS images were reviewed by two experienced radiologists, who were blinded to all clinical and pathological information. If there was disagreement between them, the final determination was made after discussion. The tumor size, internal echogenicity and presence of bowel wall thickening were recorded. Bowel wall thickening was defined as > 3 mm for small bowel and > 5 mm for large bowel. The enhancement pattern, enhancement distribution, tumor necrosis and presence of irregular and enlarged vessels (diameter > 5 mm) were recorded. The enhancement pattern was classified as homogeneous or heterogeneous. The enhancement distribution was clarified as diffuse, centripetal or centrifugal. Tumor necrosis was considered present if a nonenhanced area could be seen within the tumor during the arterial and venous phases.

According to the EFSUMB guidelines[14], the arterial phase is defined as the first 30 s after the contrast agent is injected, and the venous phase as the period between 30 and 120 s. By using Q lab software version 5 (Philips Medical Systems) on the workstation, we selected a region of interest (ROI) in the most enhanced area of the lesion, and the ROI area was set to 25 mm². The time–intensity curve (TIC) was automatically created for each ROI and then TIC parameters including rise time, time to peak, mean transit time, time from peak to one half, peak intensity, wash in slope and area under the curve were automatically obtained.

Statistical analysis

The Fisher's exact test was used to compare rate of tumor necrosis on CEUS between patients with Ann Arbor stage I/II and III/IV intestinal lymphomas and between patients with indolent and aggressive subtypes of intestinal lymphoma. Student's *t* test was used to compare the TIC parameters between normal and elevated serum lactate dehydrogenase (LDH) groups. Statistical significance was determined at $P < 0.05$ (two sided). Statistical analyses were performed using SPSS version 13.0 (SPSS Chicago, IL, United States).

RESULTS

Clinical and histological findings

This patient group comprised 18 patients with non-Hodgkin's lymphoma (NHL) of

various subtypes. Seventeen intestinal lymphomas were of B-cell origin; among which 11 were diffuse large B-cell lymphoma (DLBCL), 3 were follicular lymphoma, 2 were mucosa-associated lymphoid tissue lymphoma and 1 was mantle cell lymphoma. Only one case was of T-cell origin (enteropathy-associated T-cell lymphoma). No instances of intestinal Hodgkin's lymphoma were encountered. Primary intestinal lymphoma was diagnosed in 16 cases, whereas secondary lymphoma infiltration of the bowel was observed in 2 cases. Eight cases were classified as stage II, 4 as stage III and 6 as stage IV. The clinical presentations included abdominal pain ($n = 7$), palpable abdominal mass ($n = 5$), gastrointestinal bleeding ($n = 2$), constipation ($n = 2$), weight loss ($n = 1$) and fever ($n = 1$).

B-mode US

Four sonographic patterns of intestinal lymphoma were observed on B-mode imaging. The mass type ($n = 12$) presented as circumferential, marked bowel wall thickening forming masses, with loss of stratification, and hyperechoic lumen inside the mass (Figure 1A and B)[17,18]. The size of the masses ranged from 7.1 cm to 11.9 cm (mean 9.9 cm). The infiltration type presented as segmental bowel wall thickening without apparent mass formation ($n = 1$), with intestinal wall thickness of 2.6 cm (Figure 2A and B). The mesenteric type ($n = 4$) was characterized by multiple exophytic mesenteric masses with or without involvement of adjacent intestinal wall (Figure 3A and B) [19]. The lesion sometimes encapsulated mesenteric vessels without narrowing of the vascular lumen. The mixed type ($n = 1$) showed a combination of two patterns. Nine (50%) patients presented with bulky lesions (> 10 cm). Dilatation of the bowel was observed in 3 cases. Intestinal lymphomas were located in the small intestine in 5 cases, mesentery in 5, rectum in 1, ascending colon in 1, and 6 cases could not be clearly localized by US. Regional lymphadenopathy was found in 12 patients (66.7%), which manifested as aggregated nodules or masses in the mesentery or retroperitoneum.

CEUS

Rapid arterial enhancement followed by gradual washout in the venous phase was observed in all 18 patients (Figures 1C, 2C, and 3C). The peak enhancement was reached in the arterial phase or early venous phase. Seventeen cases presented with hyperechoic arterial enhancement, and only 1 case revealed hypoechoic arterial enhancement. Enhancement during the arterial phase was homogeneous ($n = 7$) or inhomogeneous ($n = 11$). Fifteen cases presented with diffuse enhancement, whereas three presented with centripetal enhancement. The visualization of irregular vessels was observed in 8 cases (44.4%). Tumor necrosis on CEUS was identified in 11 (61.1%) patients (Figure 1C), in which 1 case revealed extensive necrosis. Detailed information about B-mode US and CEUS findings of the 18 cases are shown in Table 1.

The mean diameter of the lesions with and without necrosis was 8.36 cm and 9.58 cm, respectively ($P = 0.6$). We compared the frequency of tumor necrosis in intestinal lymphomas with reference to different pathological subtypes or clinical stages. Tumor necrosis on CEUS was detected in 20.0% (1/5) of indolent intestinal lymphomas and in 76.9% (10/13) of aggressive subtypes ($P = 0.047$). Tumor necrosis was detected in 80% (8/10) of patients in III/IV stage and in 37.5% (3/8) patients in I/II stage ($P = 0.145$) (Table 2). Quantitative results of TIC parameters are shown in Table 3. The serum LDH value ranged from 130 to 968 U/L, with 10 patients' values exceeding the upper limit of normal (248 U/L). There was no significant difference in TIC parameters between normal and elevated LDH groups (Table 4).

DISCUSSION

In this study, we reported 18 cases of intestinal lymphoma. The mean age of our patients was 58.94 ± 15.89 years with most cases between 50 and 70 years. There was a male predominance with a male to female ratio of 1.25: 1. Lymphomas were predominantly located in the small bowel, and the most common symptoms included palpable abdominal mass and abdominal pain, which is in agreement with the literature[20]. All the intestinal lymphomas were NHL. B-cell lymphomas were more frequent than T-cell lymphomas (17: 1), and the most common pathological subtype was DLBCL (11/18, 61.1%). These results correlated well with previous studies[3,21].

We confirmed some of the sonographic features reported earlier and provided new information regarding the CEUS findings in intestinal NHL. Our data showed that mass type was the most frequent form of intestinal NHL on B-mode imaging (12/18,

Table 1 B-mode ultrasound and contrast-enhanced ultrasound patterns and clinicopathological characteristics of intestinal lymphoma in 18 patients

| No. | Age (yr) | Sex | Location | Pathological subtype | B-mode US pattern | CEUS enhancement pattern | Necrosis |
|-----|----------|-----|----------------------------|----------------------|-------------------|--|----------|
| 1 | 78 | M | Ileocecal region | DLBCL | Mass type | Diffuse, inhomogeneous, arterial hyperechoic uptake. gradually venous wash-out | Yes |
| 2 | 34 | M | Rectum | MATL | Mass type | Diffuse, inhomogeneous, arterial hyperechoic uptake. gradually venous wash-out | Yes |
| 3 | 43 | M | Mesentery | DLBCL | Mesenteric type | Diffuse, inhomogeneous, hyperechoic arterial uptake. gradually venous wash-out | Yes |
| 4 | 46 | M | Small intestine | FL | Mass type | Diffuse, homogeneous, hypoechoic, arterial uptake. gradually venous wash-out | No |
| 5 | 75 | F | Ascending colon | DLBCL | Infiltration type | Diffuse, homogeneous, hyperechoic arterial uptake. gradually venous wash-out | No |
| 6 | 78 | F | Jejunum, ileum | EATL | Mass type | Diffuse, inhomogeneous, hyperechoic arterial uptake. gradually venous wash-out | Yes |
| 7 | 52 | F | Jejunum | DLBCL | Mass type | Diffuse, inhomogeneous, hyperechoic arterial uptake. gradually venous wash-out | Yes |
| 8 | 74 | M | Small intestine | DLBCL | Mass type | Diffuse, inhomogeneous, hyperechoic arterial uptake. gradually venous wash-out | Yes |
| 9 | 52 | M | Jejunum, ileum | MATL | Mass type | Diffuse, homogeneous, hyperechoic arterial uptake. gradually venous wash-out | No |
| 10 | 61 | M | Mesentery | DLBCL | Mesenteric type | Diffuse, inhomogeneous, hyperechoic arterial uptake. gradually venous wash-out | Yes |
| 11 | 41 | F | Mesentery | DLBCL | Mesenteric type | Diffuse, inhomogeneous, hyperechoic arterial uptake. gradually venous wash-out | No |
| 12 | 46 | F | Small intestine | DLBCL | Mass type | Diffuse, inhomogeneous, hyperechoic arterial uptake. gradually venous wash-out | Yes |
| 13 | 64 | M | Ileocecum, ascending colon | DLBCL | Mass type | Diffuse, inhomogeneous, hyperechoic arterial uptake. gradually venous wash-out | Yes |
| 14 | 68 | F | Small intestine | DLBCL | Mixed type | Diffuse, inhomogeneous, hyperechoic arterial uptake. gradually venous wash-out | Yes |
| 15 | 61 | F | Small intestine | FL | Mass type | Diffuse, homogeneous, hyperechoic arterial uptake. gradually venous wash-out | No |
| 16 | 85 | M | Small intestine | MCL | Mass type | Diffuse, homogeneous, hyperechoic arterial uptake. gradually venous wash-out | No |
| 17 | 35 | M | Mesentery | FL | Mesenteric type | Diffuse, homogeneous, hyperechoic arterial uptake. gradually venous wash-out | No |
| 18 | 68 | F | Small intestine | DLBCL | Mass type | Diffuse, homogeneous, hyperechoic arterial uptake. gradually venous wash-out | Yes |

CEUS: Contrast-enhanced ultrasound; DLBCL: Diffuse large B-cell lymphoma; FL: Follicular lymphoma; MCL: Medial collateral ligament; MATL: Melanoma-associated T-lymphocytes; EATL: Enteropathy associated T-cell lymphoma.

66.7%), which was in agreement with previous studies[22]. However, this finding was not specific because various intestinal abnormalities also can lead to bowel wall thickening. Nevertheless, bowel wall thickening in lymphoma is often significant (> 2 cm) compared to other malignancies and often located in the ileocecal region, with coexistence of perivisceral multiple lymph nodes. Diffuse or segmental bowel wall thickening is characteristic of intestinal lymphoma, especially when associated with bowel lumen dilation, but this US pattern only comprised 5.6% in our study.

In our study, rapid arterial enhancement followed by elimination of the contrast media in the venous phase was observed in all cases, which is similar with other malignancies. This finding is believed to be correlated with the presence of arteriovenous shunts and a well-represented circulatory bed. Thirteen cases exhibited diffuse enhancement, in accordance with previous studies[23]. Most (17/18, 94.4%) intestinal lymphomas displayed hyperechoic arterial enhancement, which is different from isoechoic or hypoechoic arterial enhancement observed in lymphoma infiltration

Table 2 Tumor necrosis and tumor size, clinical stage and pathological subtypes

| Characteristic | With necrosis | Without necrosis |
|----------------------|---------------|------------------|
| Tumor size (cm) | 8.36 | 9.58 |
| Stage | | |
| Early stage | 3 | 5 |
| Advanced stage | 8 | 2 |
| Subtype ^a | | |
| Indolent subtype | 1 | 4 |
| Aggressive subtype | 10 | 3 |

^a*P* = 0.047.**Table 3 Time–intensity curve parameters of contrast-enhanced ultrasound**

| TIC parameters | Range | mean ± SD |
|--------------------------------|----------------|------------------|
| Rise time (s) | 2.90-27.62 | 13.74 ± 6.11 |
| Time to peak (s) | 7.64-36.00 | 24.41 ± 6.61 |
| Mean transit time (s) | 29.94-77.75 | 49.94 ± 13.98 |
| Time from peak to one half (s) | 36.38-127.85 | 77.88 ± 24.12 |
| Peak intensity (dB) | 7.8-29.28 | 17.57 ± 5.98 |
| WIS (dB/s) | 0.53-29.28 | 1.35 ± 1.09 |
| AUC | 590.99-3616.03 | 1772.05 ± 824.89 |

AUC: Area under curve; WIS: Wash in slope; TIC: Time–intensity curve.

Table 4 Time–intensity curve parameters and serum lactate dehydrogenase level

| TIC parameters | Normal LDH | Elevated LDH | <i>P</i> value |
|--------------------------------|------------|--------------|----------------|
| Rise time (s) | 14.34 | 12.78 | 0.693 |
| Time to peak (s) | 27.17 | 27.07 | 0.982 |
| Mean transit time (s) | 53.39 | 46.21 | 0.382 |
| Time from peak to one half (s) | 82.70 | 72.49 | 0.442 |
| Peak intensity (dB) | 16.50 | 16.68 | 0.955 |
| Wash in slope (dB/s) | 1.38 | 1.26 | 0.824 |
| Area under the curve (dBs) | 1699.47 | 1712.42 | 0.979 |

TIC: Time–intensity curve; LDH: Lactate dehydrogenase.

of the spleen, lungs and kidneys[24-26]. The reason for this discrepancy is unclear and needs to be confirmed in larger populations.

It is notable that there was a high rate of necrosis (11/18, 61.1%) on CEUS, which is inconsistent with previous studies. Despite necrosis being prone to occur in large tumors, we found no correlation between the presence of tumor necrosis on CEUS and tumor size. Necrosis was not detected in 4 of the 9 cases with bulky lesions. Necrosis may indicate aggressive tumor growth, and thus be associated with poor prognosis. Some researchers have explored the prognostic implications of tumor necrosis at computed tomography (CT) or positron emission tomography in lymphoma. Saito *et al* [27] did not find an association between disease-free survival and presence of necrosis in lymph nodes in 60 patients with different NHL subtypes[27]. However, Adams *et al*

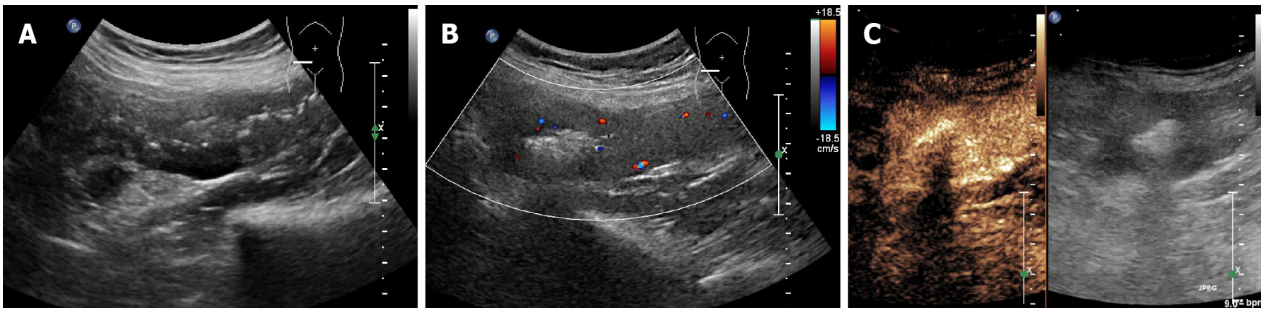


Figure 1 A 78-year-old female patient (case No. 6) with primary enteropathy-associated T-cell lymphoma in small intestine. A: B-mode imaging shows polypoidal lesions presenting “pseudo renal sign”; B: Color Doppler flow imaging shows abundant blood flow in bowel wall; C: Contrast-enhanced ultrasound showing inhomogeneous intense arterial enhancement with small non enhanced area.

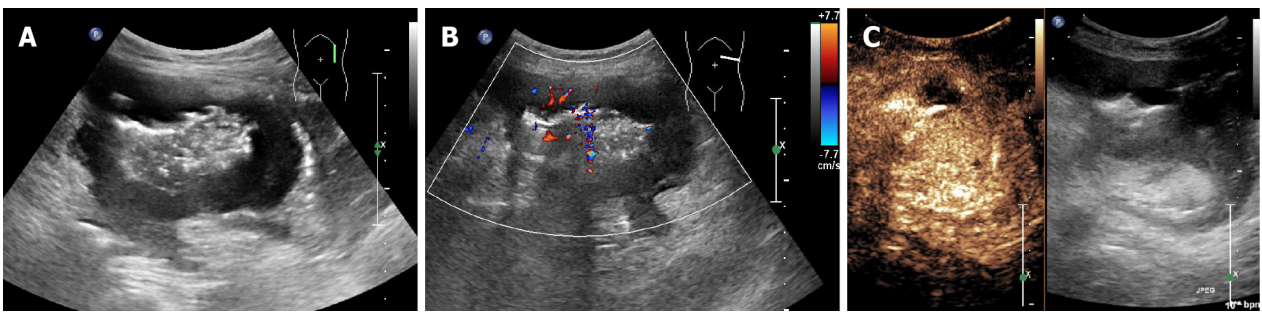


Figure 2 A 75-year-old female patient (case No. 5) with primary diffuse large B-cell lymphoma in the terminal ileum and ascending colon. A: B-mode imaging show circumferential bowel wall thickening with dilation of the bowel; B: Color Doppler flow imaging shows abundant blood flow in bowel wall; C: Contrast-enhanced ultrasound showing homogeneous intense arterial enhancement.

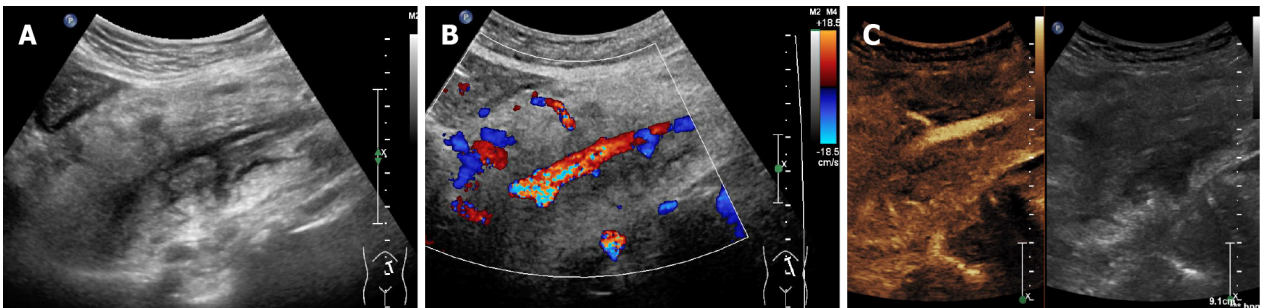


Figure 3 A 68-year-old female patient (case No. 14) with secondary diffuse large B-cell lymphoma intestinal lymphoma in mesentery. A: B-mode imaging shows large mesenteric mass encapsulating mesenteric vessels with ill-defined echoic region; B: Color Doppler flow imaging shows the abdominal aorta and its branches; C: Contrast-enhanced ultrasound showing inhomogeneous moderate arterial enhancement.

[28] showed that patients with newly diagnosed DLBCL with tumor necrosis at CT had significantly worse progression-free survival and overall survival than patients without tumor necrosis at CT. The National Comprehensive Cancer Network International Prognostic Index score did not differ significantly between the two groups. Our study showed that the frequency of necrosis on CEUS was different between indolent and aggressive lymphoma subtypes, but it was not related to clinical stage. Since it as a retrospective study, patients were not followed up to assess prognosis.

Evaluation of prognosis by imaging is desirable but often not possible. It is known that tumor growth is accompanied by neoangiogenesis. The assessment of the bowel vasculature can provide functional information about tumor perfusion, particularly with the advent of the second generation of contrast agents for CEUS. The generation of TICs allows for objective measurement of blood flow parameters[29]. In our previous study, we demonstrated that enhanced intensity is associated with microvascular density in rectal cancer[30]. In the present study, we investigated the relationship between TIC parameters and serum LDH level. LDH can reflect tumor load and is an independent prognostic factor of lymphoma[31]. However, we found no significant

difference in TIC parameters between normal and elevated serum LDH groups.

US is not the method of choice for the diagnosis of intestinal lymphoma, because it may not detect small or deep lesions that can be obscured by bowel gas; it is often used as targeted US for evaluation of suspected region but has difficulty in thorough assessment and staging for advanced lymphoma. Intestinal lymphoma is conventionally diagnosed by CT, magnetic resonance imaging and positron emission tomography/CT. However, CEUS used with second-generation contrast agent, offered a reasonable alternative imaging solution for those who are not suitable for nephrotoxic iodine-based contrast medium injection. Moreover, in our experience, CEUS guided biopsy allows targeting viable regions of the tumor; it has significantly improved our ability to obtain sufficient tissue for immunohistochemistry and molecular testing, which is particularly important in diagnosis and evaluation of lymphoma.

This study had some limitations. Intestinal lymphoma is a rare entity and the sample size was small. Furthermore, the patients included in this study who underwent CEUS examinations were usually referred for US-guided biopsy, which may have led to selection bias. As it was a retrospective study, some clinical data were missing and prognostic information was not included.

CONCLUSION

In this study, our findings on intestinal lymphoma contribute to knowledge of CEUS imaging. In this small group, intestinal lymphomas showed a characteristic enhancement pattern with rapid wash followed by early wash out of the contrast media. A high rate of tumor necrosis was detected, with a tendency to be more likely in aggressive subtypes, which needs to be confirmed in a larger population. Although US is not the primary imaging modality in diagnosis of intestinal lymphoma, it can play an important role in guidance of biopsy and provide more information.

ARTICLE HIGHLIGHTS

Research background

Contrast-enhanced ultrasound (CEUS) is a new imaging technique that can evaluate tumor vascularity, and it has been proved to have value in the diagnosis and assessment of inflammatory bowel disease. However, the CEUS features of intestinal lymphoma remain unclear.

Research motivation

There have been few studies on CEUS findings of intestinal lymphoma and their potential correlation with histopathological features.

Research objectives

Our present study aimed to describe the B-mode US and CEUS features of intestinal lymphoma and investigate the correlation of CEUS and histopathological features.

Research methods

We summarized the features of B-mode US and CUES imaging of intestinal lymphoma of 18 patients and compared the frequency of tumor necrosis in intestinal lymphomas with reference to different pathological subtypes (aggressive or indolent) and clinical stage (early or advanced). Besides, the time-intensity curve parameters of CEUS were also compared between patients with normal and elevated serum lactate dehydrogenase (LDH).

Research results

In B-mode imaging, four patterns were observed in intestinal lymphoma: Mass type (12/18, 66.7%), infiltration type (1/18, 5.6%), mesentery type (4/18, 22.2%) and mixed type (1/18, 5.6%). All cases were hypoechoic and no cystic areas were detected. On CEUS, most cases (17/18, 94.4%) showed arterial hyperechoic enhancement. All cases showed arterial enhancement followed by venous wash out. A relatively high rate of tumor necrosis (11/18, 61.1%) was observed in this study. Tumor necrosis on CEUS was more frequent in aggressive subtypes (10/13, 76.9%) than in indolent subtypes (1/5, 20.0%) ($P = 0.047$). There were no correlations between tumor necrosis and lesion

size and Ann Arbor stage. There was no significant difference in time–intensity curve parameters between normal and elevated LDH groups.

Research conclusions

B-mode US and CEUS findings of intestinal lymphoma are characteristic. We observed a high rate of tumor necrosis, which appeared more frequently in aggressive pathological subtypes of intestinal lymphoma.

Research perspectives

Based on the present results, we will expand the number of enrolled patients and explore the advantages of US compared with other imaging techniques in diagnosing intestinal lymphoma.

ACKNOWLEDGEMENTS

The authors like to thank Professor Hong-Da Chen, biostatistician at Office of Cancer Screening, National Cancer Center/National Clinical Research Center for Cancer/Cancer Hospital, Chinese Academy of Medical Sciences and Peking Union Medical College, Beijing, China.

REFERENCES

- 1 **Freeman C**, Berg JW, Cutler SJ. Occurrence and prognosis of extranodal lymphomas. *Cancer* 1972; **29**: 252-260 [PMID: 5007387 DOI: [10.1002/1097-0142\(197201\)29:1<252::AID-CNCR2820290138>3.0.CO;2-#](https://doi.org/10.1002/1097-0142(197201)29:1<252::AID-CNCR2820290138>3.0.CO;2-#)]
- 2 **Levine MS**, Rubesin SE, Pantongrag-Brown L, Buck JL, Herlinger H. Non-Hodgkin's lymphoma of the gastrointestinal tract: radiographic findings. *AJR Am J Roentgenol* 1997; **168**: 165-172 [PMID: 8976941 DOI: [10.2214/ajr.168.1.8976941](https://doi.org/10.2214/ajr.168.1.8976941)]
- 3 **Foukas PG**, de Leval L. Recent advances in intestinal lymphomas. *Histopathology* 2015; **66**: 112-136 [PMID: 25639480 DOI: [10.1111/his.12596](https://doi.org/10.1111/his.12596)]
- 4 **Ghimire P**, Wu GY, Zhu L. Primary gastrointestinal lymphoma. *World J Gastroenterol* 2011; **17**: 697-707 [PMID: 21390139 DOI: [10.3748/wjg.v17.i6.697](https://doi.org/10.3748/wjg.v17.i6.697)]
- 5 **Nakamura S**, Matsumoto T. Gastrointestinal lymphoma: recent advances in diagnosis and treatment. *Digestion* 2013; **87**: 182-188 [PMID: 23635497 DOI: [10.1159/000350051](https://doi.org/10.1159/000350051)]
- 6 **Dragosics B**, Bauer P, Radaszkiewicz T. Primary gastrointestinal non-Hodgkin's lymphomas. A retrospective clinicopathologic study of 150 cases. *Cancer* 1985; **55**: 1060-1073 [PMID: 3881161 DOI: [10.1002/1097-0142\(19850301\)55:5<1060::aid-cnrcr2820550523>3.0.co;2-8](https://doi.org/10.1002/1097-0142(19850301)55:5<1060::aid-cnrcr2820550523>3.0.co;2-8)]
- 7 **Koch P**, del Valle F, Berdel WE, Willich NA, Reers B, Hiddemann W, Grothaus-Pinke B, Reinartz G, Brockmann J, Temmesfeld A, Schmitz R, Rube C, Probst A, Jaenke G, Bodenstein H, Junker A, Pott C, Schultze J, Heinecke A, Parwaresch R, Tiemann M; German Multicenter Study Group. Primary gastrointestinal non-Hodgkin's lymphoma: I. Anatomic and histologic distribution, clinical features, and survival data of 371 patients registered in the German Multicenter Study GIT NHL 01/92. *J Clin Oncol* 2001; **19**: 3861-3873 [PMID: 11559724 DOI: [10.1200/JCO.2001.19.18.3861](https://doi.org/10.1200/JCO.2001.19.18.3861)]
- 8 **Ruskoné-Fourmestraux A**, Aegerter P, Delmer A, Brousse N, Galian A, Rambaud JC. Primary digestive tract lymphoma: a prospective multicentric study of 91 patients. Groupe d'Etude des Lymphomes Digestifs. *Gastroenterology* 1993; **105**: 1662-1671 [PMID: 8253342 DOI: [10.1016/0016-5085\(93\)91061-I](https://doi.org/10.1016/0016-5085(93)91061-I)]
- 9 **Fischbach W**, Dragosics B, Kolve-Goebeler ME, Ohmann C, Greiner A, Yang Q, Böhm S, Verreet P, Horstmann O, Busch M, Dühmke E, Müller-Hermelink HK, Wilms K, Allinger S, Bauer P, Bauer S, Bender A, Brandstätter G, Chott A, Dittrich C, Erhart K, Eysselt D, Ellersdorfer H, Ferlitsch A, Fridrik MA, Gartner A, Hausmaninger M, Hinterberger W, Hügel K, Ilsinger P, Jonaus K, Judmaier G, Karner J, Kerstan E, Knoflach P, Lenz K, Kandutsch A, Lobmeyer M, Michlmeier H, Mach H, Marosi C, Ohlinger W, Oprean H, Pointer H, Pont J, Salabon H, Samec HJ, Ulsperger A, Wimmer A, Wewalka F. Primary gastric B-cell lymphoma: results of a prospective multicenter study. The German-Austrian Gastrointestinal Lymphoma Study Group. *Gastroenterology* 2000; **119**: 1191-1202 [PMID: 11054376 DOI: [10.1053/gast.2000.19579](https://doi.org/10.1053/gast.2000.19579)]
- 10 **Nakamura S**, Matsumoto T, Iida M, Yao T, Tsuneyoshi M. Primary gastrointestinal lymphoma in Japan: a clinicopathologic analysis of 455 patients with special reference to its time trends. *Cancer* 2003; **97**: 2462-2473 [PMID: 12733145 DOI: [10.1002/cncr.11415](https://doi.org/10.1002/cncr.11415)]
- 11 **Akahoshi K**, Oya M, Koga T, Shiratsuchi Y. Current clinical management of gastrointestinal stromal tumor. *World J Gastroenterol* 2018; **24**: 2806-2817 [PMID: 30018476 DOI: [10.3748/wjg.v24.i26.2806](https://doi.org/10.3748/wjg.v24.i26.2806)]
- 12 **Fukumoto A**, Tanaka S, Imagawa H, Shishido T, Oka S, Yoshida S, Yamada H, Chayama K. Usefulness and limitations of transabdominal ultrasonography for detecting small-bowel tumors.

- Scand J Gastroenterol* 2009; **44**: 332-338 [PMID: 18985540 DOI: 10.1080/00365520802495578]
- 13 **Malone CD**, Fetzter DT, Monsky WL, Itani M, Mellnick VM, Velez PA, Middleton WD, Averkiou MA, Ramaswamy RS. Contrast-enhanced US for the Interventional Radiologist: Current and Emerging Applications. *Radiographics* 2020; **40**: 562-588 [PMID: 32125955 DOI: 10.1148/rg.2020190183]
 - 14 **Piscaglia F**, Nolsøe C, Dietrich CF, Cosgrove DO, Gilja OH, Bachmann Nielsen M, Albrecht T, Barozzi L, Bertolotto M, Catalano O, Claudon M, Clevert DA, Correas JM, D'Onofrio M, Drudi FM, Eyding J, Giovannini M, Hocke M, Ignee A, Jung EM, Klausner AS, Lassau N, Leen E, Mathis G, Saftoiu A, Seidel G, Sidhu PS, ter Haar G, Timmerman D, Weskott HP. The EFSUMB Guidelines and Recommendations on the Clinical Practice of Contrast Enhanced Ultrasound (CEUS): update 2011 on non-hepatic applications. *Ultraschall Med* 2012; **33**: 33-59 [PMID: 21874631 DOI: 10.1055/s-0031-1281676]
 - 15 **Swerdlow SH**, Resea IAF. WHO classification of tumours of haematopoietic and lymphoid tissues. International Agency for Research on Cancer, 2008
 - 16 **Lewin KJ**, Ranchod M, Dorfman RF. Lymphomas of the gastrointestinal tract: a study of 117 cases presenting with gastrointestinal disease. *Cancer* 1978; **42**: 693-707 [PMID: 354774 DOI: 10.1002/1097-0142(197808)42:2<693::aid-cnrcr2820420241>3.0.co;2-j]
 - 17 **Fakhry JR**, Berk RN. The "target" pattern: characteristic sonographic feature of stomach and bowel abnormalities. *AJR Am J Roentgenol* 1981; **137**: 969-972 [PMID: 6975024 DOI: 10.2214/ajr.137.5.969]
 - 18 **Goerg C**, Schwerk WB, Goerg K. Gastrointestinal lymphoma: sonographic findings in 54 patients. *AJR Am J Roentgenol* 1990; **155**: 795-798 [PMID: 2119110 DOI: 10.2214/ajr.155.4.2119110]
 - 19 **Lo Re G**, Federica V, Midiri F, Picone D, La Tona G, Galia M, Lo Casto A, Lagalla R, Midiri M. Radiological Features of Gastrointestinal Lymphoma. *Gastroenterol Res Pract* 2016; **2016**: 2498143 [PMID: 26819598 DOI: 10.1155/2016/2498143]
 - 20 **Smith C**, Kubicka RA, Thomas CR Jr. Non-Hodgkin lymphoma of the gastrointestinal tract. *Radiographics* 1992; **12**: 887-899 [PMID: 1529131 DOI: 10.1148/radiographics.12.5.1529131]
 - 21 **Weindorf SC**, Smith LB, Owens SR. Update on Gastrointestinal Lymphomas. *Arch Pathol Lab Med* 2018; **142**: 1347-1351 [PMID: 30407861 DOI: 10.5858/arpa.2018-0275-RA]
 - 22 **Sener RN**, Alper H, Demirci A, Diren HB. A different sonographic "pseudokidney" appearance detected with intestinal lymphoma: "hydronephrotic-pseudokidney". *J Clin Ultrasound* 1989; **17**: 209-212 [PMID: 2494234 DOI: 10.1002/jcu.1870170310]
 - 23 **Rubaltelli L**, Khadivi Y, Tregnaghi A, Stramare R, Ferro F, Borsato S, Fiocco U, Adami F, Rossi CR. Evaluation of lymph node perfusion using continuous mode harmonic ultrasonography with a second-generation contrast agent. *J Ultrasound Med* 2004; **23**: 829-836 [PMID: 15244307 DOI: 10.7863/jum.2004.23.6.829]
 - 24 **Trenker C**, Neesse A, Görg C. Sonographic patterns of renal lymphoma in B-mode imaging and in contrast-enhanced ultrasound (CEUS)--a retrospective evaluation. *Eur J Radiol* 2015; **84**: 807-810 [PMID: 25650333 DOI: 10.1016/j.ejrad.2014.12.027]
 - 25 **Sutherland T**, Temple F, Galvin A, Hennessy O. Contrast-enhanced ultrasound of the spleen: an introduction and pictorial essay. *Insights Imaging* 2011; **2**: 515-524 [PMID: 22347971 DOI: 10.1007/s13244-011-0106-3]
 - 26 **Görg C**. Transcutaneous contrast-enhanced sonography of pleural-based pulmonary lesions. *Eur J Radiol* 2007; **64**: 213-221 [PMID: 17904322 DOI: 10.1016/j.ejrad.2007.06.037]
 - 27 **Saito A**, Takashima S, Takayama F, Kawakami S, Momose M, Matsushita T. Spontaneous extensive necrosis in non-Hodgkin lymphoma: prevalence and clinical significance. *J Comput Assist Tomogr* 2001; **25**: 482-486 [PMID: 11351202 DOI: 10.1097/00004728-200105000-00024]
 - 28 **Adams HJA**, de Klerk JMH, Fijnheer R, Dubois SV, Nievelstein RAJ, Kwee TC. Prognostic value of tumor necrosis at CT in diffuse large B-cell lymphoma. *Eur J Radiol* 2015; **84**: 372-377 [PMID: 25559168 DOI: 10.1016/j.ejrad.2014.12.009]
 - 29 **Greis C**. Quantitative evaluation of microvascular blood flow by contrast-enhanced ultrasound (CEUS). *Clin Hemorheol Microcirc* 2011; **49**: 137-149 [PMID: 22214685 DOI: 10.3233/CH-2011-1464]
 - 30 **Wang Y**, Li L, Wang YX, Cui NY, Zou SM, Zhou CW, Jiang YX. Time-intensity curve parameters in rectal cancer measured using endorectal ultrasonography with sterile coupling gels filling the rectum: correlations with tumor angiogenesis and clinicopathological features. *Biomed Res Int* 2014; **2014**: 587806 [PMID: 24900973 DOI: 10.1155/2014/587806]
 - 31 **Kim SJ**, Hong JS, Chang MH, Kim JA, Kwak JY, Kim JS, Yoon DH, Lee WS, Do YR, Kang HJ, Eom HS, Park Y, Won JH, Mun YC, Kim HJ, Kwon JH, Kong JH, Oh SY, Lee S, Bae SH, Yang DH, Jun HJ, Kim YS, Yun HJ, Lee SI, Kim MK, Park EK, Kim WS, Suh C. Highly elevated serum lactate dehydrogenase is associated with central nervous system relapse in patients with diffuse large B-cell lymphoma: Results of a multicenter prospective cohort study. *Oncotarget* 2016; **7**: 72033-72043 [PMID: 27713132 DOI: 10.18632/oncotarget.12459]

Observational Study

Intestinal ischemic manifestations of SARS-CoV-2: Results from the ABDOCOVID multicentre study

Lorenzo Norsa, Pietro Andrea Bonaffini, Maja Caldato, Cristiana Bonifacio, Aurelio Sonzogni, Amedeo Indriolo, Clarissa Valle, Federica Furfaro, Alice Bonanomi, Paolo Niccolò Franco, Mauro Gori, Veronica Smania, Lucia Scaramella, Laura Forzenigo, Maurizio Vecchi, Monica Solbiati, Giorgio Costantino, Silvio Danese, Lorenzo D'Antiga, Sandro Sironi, Luca Elli

ORCID number: Lorenzo Norsa 0000-0003-3322-2921; Pietro Andrea Bonaffini 0000-0001-5335-9429; Maja Caldato 0000-0002-6203-7170; Cristiana Bonifacio 0000-0002-8551-6801; Aurelio Sonzogni 0000-0001-5001-9533; Amedeo Indriolo 0000-0002-4815-8937; Clarissa Valle 0000-0003-2478-8878; Federica Furfaro 0000-0002-4308-7295; Alice Bonanomi 0000-0002-7898-7760; Paolo Niccolò Franco 0000-0001-8280-3787; Mauro Gori 0000-0001-5509-8867; Veronica Smania 0000-0002-0201-4313; Lucia Scaramella 0000-0002-9460-3296; Laura Forzenigo 0000-0001-6314-3605; Maurizio Vecchi 0000-0003-1558-8604; Monica Solbiati 0000-0003-1964-3770; Giorgio Costantino 0000-0002-6391-3849; Silvio Danese 0000-0001-7341-1351; Lorenzo D'Antiga 0000-0001-7150-3148; Sandro Sironi 0000-0002-4469-5073; Luca Elli 0000-0002-0873-0759.

Author contributions: Caldato M, Bonifacio C, Valle C, Furfaro F, Gori M, Smania V and Scaramella L did data acquisition; Norsa L, Bonaffini PA, Sonzogni A and Indriolo A drafted the manuscript; Norsa L, Bonanomi A and Franco PN did the figures selection and production; Forzenigo L, Vecchi M, Solbiati M, Costantino G, Danese S,

Lorenzo Norsa, Lorenzo D'Antiga, Department of Pediatric Gastroenterology Hepatology and Transplantation, ASST Papa Giovanni XXIII, Bergamo 24127, Italy

Pietro Andrea Bonaffini, Clarissa Valle, Sandro Sironi, Department of Radiology Papa Giovanni XXIII Bergamo, University of Milano-Bicocca, Milan 20126, Italy

Maja Caldato, Fondazione IRCCS Ca' Granda, Department of Emergency Medicine, Ospedale Maggiore Policlinico, Milano 20122, Italy

Cristiana Bonifacio, Department of Radiology, Humanitas Clinical and Research Center, IRCCS, Rozzano 20089, Italy

Aurelio Sonzogni, Department of Pathology, ASST Papa Giovanni XXIII, Bergamo 24127, Italy

Amedeo Indriolo, Department of Gastroenterology and Endoscopy, ASST Papa Giovanni XXIII, Bergamo 24127, Italy

Federica Furfaro, Silvio Danese, IBD Center, Humanitas Clinical and Research Center IRCCS, Humanitas University, Rozzano 20089, Italy

Alice Bonanomi, Paolo Niccolò Franco, Sandro Sironi, Post-Graduate School of Diagnostic Radiology, University of Milano-Bicocca, Milano 20126, Italy

Mauro Gori, Cardiovascular Department, ASST Papa Giovanni XXIII, Bergamo 24127, Italy

Veronica Smania, Lucia Scaramella, Maurizio Vecchi, Luca Elli, Department of Gastroenterology and Endoscopy, Fondazione IRCCS Ca' Granda Ospedale Maggiore Policlinico, Milano 20122, Italy

Veronica Smania, Lucia Scaramella, Maurizio Vecchi, Luca Elli, Department of Pathophysiology and Transplantation, University of Milan, Milano 20122, Italy

Laura Forzenigo, Department of Radiology, Fondazione IRCCS Ca' Granda Ospedale Maggiore Policlinico, Milano 20122, Italy

Monica Solbiati, Giorgio Costantino, Fondazione IRCCS Ca' Granda, Department of Emergency Medicine, Ospedale Maggiore Policlinico, Department of Clinical Sciences and Community

D'Antiga L, Sironi S and Elli L critically reviewed the paper.

Institutional review board

statement: The study was reviewed and approved by the ASST Papa Giovanni XXIII Institutional Review Board, No. 2020-0096.

Informed consent statement:

Informed consent from patients was waived because of the retrospective nature of the study.

Conflict-of-interest statement:

The authors declare no conflict of interest and no financial support for this study.

Data sharing statement:

Technical appendix, statistical code, and dataset available from the corresponding author at lnorsa@asst-pg23.it.

STROBE statement:

The authors have read the STROBE Statement—checklist of items, and the manuscript was prepared and revised according to the STROBE Statement—checklist of items.

Open-Access:

This article is an open-access article that was selected by an in-house editor and fully peer-reviewed by external reviewers. It is distributed in accordance with the Creative Commons Attribution NonCommercial (CC BY-NC 4.0) license, which permits others to distribute, remix, adapt, build upon this work non-commercially, and license their derivative works on different terms, provided the original work is properly cited and the use is non-commercial. See: <http://creativecommons.org/licenses/by-nc/4.0/>

Manuscript source: Invited manuscript

Specialty type: Gastroenterology and hepatology

Country/Territory of origin: Italy

Peer-review report's scientific quality classification

Grade A (Excellent): 0

Grade B (Very good): B

Health, University of Milan, Milano 20122, Italy

Corresponding author: Lorenzo Norsa, PhD, Doctor, Department of Pediatric Gastroenterology Hepatology and Transplantation, ASST Papa Giovanni XXIII, Piazza OMS 1, Bergamo 24127, Italy. lnorsa@asst-pg23.it

Abstract

BACKGROUND

Intestinal ischemia has been described in case reports of patients with severe acute respiratory syndrome coronavirus 2 (SARS-CoV-2) disease (coronavirus disease 19, COVID-19).

AIM

To define the clinical and histological characteristics, as well as the outcome of ischemic gastrointestinal manifestations of SARS-CoV-2 infection.

METHODS

A structured retrospective collection was promoted among three tertiary referral centres during the first wave of the pandemic in northern Italy. Clinical, radiological, endoscopic and histological data of patients hospitalized for COVID-19 between March 1st and May 30th were reviewed. The diagnosis was established by consecutive analysis of all abdominal computed tomography (CT) scans performed.

RESULTS

Among 2929 patients, 21 (0.7%) showed gastrointestinal ischemic manifestations either as presenting symptom or during hospitalization. Abdominal CT showed bowel distention in 6 patients while signs of colitis/enteritis in 12. Three patients presented thrombosis of main abdominal veins. Endoscopy, when feasible, confirmed the diagnosis (6 patients). Surgical resection was necessary in 4/21 patients. Histological tissue examination showed distinctive features of endothelial inflammation in the small bowel and colon. Median hospital stay was 9 d with a mortality rate of 39%.

CONCLUSION

Gastrointestinal ischemia represents a rare manifestation of COVID-19. A high index of suspicion should lead to investigate this complication by CT scan, in the attempt to reduce its high mortality rate. Histology shows atypical feature of ischemia with important endotheliitis, probably linked to thrombotic microangiopathies.

Key Words: Coronavirus; COVID-19; Ischemic colitis; Small bowel ischemia; Endothelial inflammation

©The Author(s) 2021. Published by Baishideng Publishing Group Inc. All rights reserved.

Core Tip: Ischemic manifestations have been described as possible presenting symptoms of severe acute respiratory syndrome coronavirus 2 (SARS-CoV-2) infection. These manifestations are frequent in the respiratory tract and bear a high fatality rate. Our retrospective observational trial aims to describe the prevalence, the characteristics and the evolution of patients presenting with intestinal ischemic manifestations of SARS-CoV-2 infection.

Citation: Norsa L, Bonaffini PA, Caldato M, Bonifacio C, Sonzogni A, Indriolo A, Valle C, Furfaro F, Bonanomi A, Franco PN, Gori M, Smania V, Scaramella L, Forzenigo L, Vecchi M, Solbiati M, Costantino G, Danese S, D'Antiga L, Sironi S, Elli L. Intestinal ischemic manifestations of SARS-CoV-2: Results from the ABDOCOVID multicentre study. *World J Gastroenterol* 2021; 27(32): 5448-5459

URL: <https://www.wjgnet.com/1007-9327/full/v27/i32/5448.htm>

Grade C (Good): 0
 Grade D (Fair): 0
 Grade E (Poor): 0

Received: March 26, 2021

Peer-review started: March 26, 2021

First decision: April 29, 2021

Revised: April 30, 2021

Accepted: July 23, 2021

Article in press: July 23, 2021

Published online: August 28, 2021

P-Reviewer: Sivanand N

S-Editor: Wu YXJ

L-Editor: Filipodia

P-Editor: Li JH



DOI: <https://dx.doi.org/10.3748/wjg.v27.i32.5448>

INTRODUCTION

The end of December 2019 marked the recent world history for the advent of a new zoonosis caused by severe acute respiratory syndrome coronavirus 2 (SARS-CoV-2). SARS-CoV-2 rapidly spread around the world causing a pandemic responsible for a dramatic number of deaths due to a disease referred to as “coronavirus disease 19 (COVID-19)” (<https://www.healthmap.org/covid-19/>).

The Lombardy region (Italy) was the second epicentre of the pandemic[1]. A recent report of the Italian National Institute of Statistics revealed that in March 2020, there was an overall increase in the general population mortality rate of + 185% (+ 568% in the Bergamo province) compared to the same period of the previous 4 years (2015-2019) (https://www.istat.it/it/files//2020/05/Rapporto_Istat_ISS.pdf).

The most frequent clinical manifestation of COVID-19 is an atypical pneumonia, presenting with respiratory symptoms such as fever, cough, shortness of breath and hypoxia[2]. However, several cohort studies worldwide showed that in a minority of cases COVID-19 can present with isolated gastrointestinal symptoms (GI), including abdominal pain, nausea, vomiting and diarrhoea[3-6]. A metaanalysis demonstrated a poorer prognosis of COVID-19 patients presenting with gastrointestinal symptoms, compared to other COVID-19 patterns of presentation[7]. This may be due to the severe intestinal ischemic lesions found in 3 of the first 12 autopsies performed in COVID-19 patients in Germany[8]. Furthermore, a preliminary report highlighted that, during the first wave of SARS-CoV-2 pandemic, there was a higher prevalence of gastrointestinal ischemic events compared with the same timeframe before the virus advent[9].

During the first wave of the pandemic the medical community was unaware of the multifaceted manifestations of this new infectious agent. Now that the world has faced the second wave of this pandemic, it is crucial to identify retrospectively all the possible life-threatening manifestations of SARS-CoV-2 for which appropriate management may influence the final outcome.

The aim of the present multicentre study, named ABDOCOVID, is to analyse retrospectively the main clinical, endoscopic, pathological and imaging findings in patients with intestinal ischemic manifestations of SARS-CoV-2, in three tertiary referral centres of the highly hit region of Lombardy.

MATERIALS AND METHODS

Patients and methods

All patients admitted from March 1st to May 30th to the emergency department (ED) of one of the three enrolling Hospitals (Papa Giovanni XXIII, Bergamo; Humanitas Clinical and Research Center, IRCCS, Rozzano, Milano; Fondazione IRCCS Ca' Granda Ospedale Maggiore Policlinico, Milan) and with confirmed SARS-CoV-2 infection, were reviewed and analysed. All confirmed COVID-19 patients who underwent abdominal computed tomography (CT) scan or endoscopy were evaluated, and data on the diagnostic workup were retrospectively collected.

In order to calculate the prevalence of intestinal ischemic manifestations, aggregate data on all patients admitted for COVID-19 in the three enrolling Hospital were pooled.

The local Ethical Committee approved the study protocol (protocol 96/20). All patients' data were anonymized and treated in accordance with the declaration of Helsinki.

Clinical data collection

The medical notes of enrolled patients were examined to gather information on their past medical history, symptoms at presentation to the ED, concomitant pulmonary findings and their evolution. In addition, clotting parameters of the patients, such as prothrombin time, partial thromboplastin time, platelet count and D-dimer level were collected.

Imaging acquisition protocol and analysis

All abdominal CT scans performed at Papa Giovanni XXIII Hospital (Bergamo) were acquired with the patient in supine position, on a 64-detector scanner (Revolution EVO; GE Medical), in the ED. All CTs included at least a portal venous phase, acquired 80-90 s following the injection of a non-ionic contrast medium (iomeprol 350 mg/mL, Bracco Imaging, Italy), in an antecubital vein. The mean contrast dose was 1.3-1.5 mL per patient's kg, with a flow rate of 3/3.5 mL/s. A rapid saline solution flush (about 30/40 mL, flow rate at least 3 mL/s) was injected thereafter. In specific cases (suspected bowel ischemia or bleeding), an unenhanced scan and an arterial phase were additionally performed. The CT scanning protocol and contrast medium characteristics were similar for Humanitas (64-detector scanner, Philips Brilliance) and Policlinico (Flash 64 and SOMATON 256, Siemens) cohorts of patients.

Image analysis was performed by expert radiologists: Papa Giovanni XXIII: 2 board-certified radiologists in consensus (Bonaffini PA, and Valle C, 12 and 6 years of experience in abdominal imaging, respectively); Humanitas: 1 radiologist (Bonifacio C, 17 years of experience in abdominal imaging); Ospedale Maggiore Policlinico: 1 radiologist (Forzenigo L, 20 years of experience in abdominal imaging).

On CT scans of enrolled patients we evaluated the following parameters: (1) Small bowel distension, with corresponding maximum calibre (mm) and extension (ileal, jejunal, both); (2) Large bowel distension, with corresponding maximum calibre (mm) and extension (cecum, ascending, transverse, descending, sigmoid colon, rectum, all); (3) Thrombosis in the inferior vena cava (IVC), superior mesenteric vein (SMV) and portal vein (PV) and/or in the superior mesenteric artery (main trunk and branches); (4) Intraluminal air in SMV and/or PV; (5) Bowel wall characteristics (preserved/absent enhancement, layered enhancement, thickening, parietal pneumatosis); (6) Pneumoperitoneum and/or ascites; and (7) Other ischemic sites in the abdomen (either vessels or organs). At the same time, the concomitant presence of pulmonary embolism (PE) with binary score (yes/no) and lung disease stages at chest CT were also recorded, if present. Lung involvement was classified as early, progressive, peak or absorption, as previously reported by Pan *et al*[10].

Endoscopic screening and findings

Endoscopic procedures were performed only in patients with COVID-19 GI symptoms and concomitant clinical history or radiological findings compatible with suspected colitis. All procedures were performed by expert endoscopists for each centre (Indriolo A, Elli L, Furfaro F, experienced endoscopists for more than 10 years). All endoscopic procedures on COVID-19 positive patients were organized in a COVID-19 dedicated operating room or in intensive care unit, depending on patients' clinical conditions. Appropriate protection equipment was worn to perform the endoscopic procedures, and the ventilators used to assist the patients were sanitized according to internal antiseptic protocols.

At GI endoscopy we recorded data on the aspects of ischemic colitis such as haemorrhagic purple nodules, indicating submucosal bleeding. Other common endoscopic findings in cases of ischemic colitis could be petechiae, oedema, easily friable mucosa, and development of pseudo membranes[11-13].

Pathology findings

When available, histological specimens from intestinal biopsies, surgical resection, autoptic samples were analysed. All biopsies were reviewed by the same pathologist with over 20 years of experience in intestinal biopsy interpretation. In addition to routine staining and fixation, CD34 immunostaining for endothelial cells identification was performed systematically on all specimens.

Statistical analysis

Statistical analysis was performed using IBM SPSS Statistics 21. Categorical variables were compared using Chi Square. Correlations were analysed by Pearson or Spearman test depending on parametric or non-parametric variables. Proportions are reported with 95% exact binomial confidence intervals (CI). To compare mortality rate between COVID-19 patients with and without intestinal ischemia we used risk ratios as an effect measure with 95%CI calculated by the Fisher's exact test.

RESULTS

Clinical characteristics upon admission

During the study period, 2929 patients with COVID-19 were admitted to the three enrolling centres. GI presenting symptoms were found in 16% (95% CI: 0.14-0.17) of patients. We identified 21 patients (66% male, median age 69 years, range 62-79), who met the aforementioned inclusion criteria. The prevalence of intestinal ischemia in COVID-19 hospitalized patients was 0.7% (95% CI: 0.04-0.10). Baseline characteristics of the patients are presented in [Table 1](#).

All but one patient presented with positive SARS-CoV-2 nasopharyngeal swab. SARS-CoV-2 diagnosis in one patient was made through SARS-CoV-2 RNA detection in the intestinal mucosa[14]. All patients were admitted to the Hospital after an ED access. In 11/21 (52%) cases, the clinical picture was characterized by gastrointestinal symptoms, being abdominal pain the most represented (5/11, 45%). Two patients did not present any comorbidity, while the most prevalent in the remainders was hypertension (in 10/21, 48%).

Eight of 21 patients (38%) were under anticoagulants or antiplatelets therapies at the time of ED admission. D-dimer was elevated in 17/21 (81%) of patients, while the rest of coagulation parameters were compatible with their treatment.

Radiological findings

Bowel distension was evident in 45% of cases. In 6/20 (30%) patients there was small bowel distension (mean maximum diameter 41.2 mm; range 30-56), generally involving the ileum (4/6 cases) and diffuse in 1 case. Large bowel was distended (mean diameter 94 mm; range 91-97) in 3/20 (15%) patients (2 with associated ileal involvement): In 2 cases the dilatation extended from transverse to cecum, while in 1 it involved the whole colon ([Figure 1](#)).

Six patients (30%) had CT scan evidence of small or large bowel ischemia, with reduced wall thickness and enhancement. In four of these cases there was parietal pneumatosis with associated loop over distension (3 small, 2 large bowel). One patient had pneumoperitoneum. In four cases (3 with bowel ischemia) there were associated splenic (3) or renal (1) parenchymal infarcts.

Twelve patients (60%) had CT evidence of colitis/enteritis, with layered enhancement (mucosal enhancing, submucosal oedema) and wall thickening, (mean thickness 10.9 mm; range 7-17). The most commonly involved sites were left/sigmoid colon and/or terminal ileum; one patient had pancolitis. One patient demonstrated the same features in the oesophagus.

In the majority of cases (13/20, 65%) there was no evidence of venous or arterial acute thrombosis, including almost all patients with CT scan signs of bowel ischemia or colitis/enteritis. Thrombosis of a main abdominal vein was present only in three patients: IVC with SMV (one case with SB ischemia), PV with SMV (1) and PV alone (1). Three patients had iliac-femoral veins thrombosis, without involvement of any other vessel. In one case, we observed an acute splenic artery thrombosis, with associated parenchymal infarcts. None of these patients had evidence of intraluminal arterial or venous air, hematomas or signs of bleeding in the abdomen. In eight cases ascites was present.

Five patients had simultaneous evidence of PE but in 15/21 cases the assessment of pulmonary artery was not feasible. Pulmonary stage evaluation from chest CT was feasible in 11/21 (52%) patients: The most common one was early (5/11), followed by progressive (3/11), peak (2/11) and absorption (1/11).

Endoscopic findings

Endoscopy was performed in 8/21 (38 %) patients. Five (63%) demonstrated typical features of ischemic colitis with active bleeding from an oedematous mucosa, with petechiae in three of them and mucosal oedema and ischemic ulceration in the remaining 2 ([Figure 2](#)). Neither patchy lesions nor stenotic complication of ischemia were found in any of the performed endoscopies.

Histopathology findings

In three colic biopsies collected from four patients' mucosal lamina propria oedema, blood congestion, coagulative epithelial necrosis and ulcerations, intramucosal haemorrhagic foci were observed and interpreted as suggestive of acute ischemic injury. One biopsy showed normal histology; however, endoscopy was performed 2 mo after admission. One specimen from small bowel resection and one from autopsy were analysed. Both showed extensive haemorrhagic necrosis of mucosal layer,

Table 1 Patients clinical characteristics upon admission

| Patients | Age | Sex | Comorbidities | Ongoing ACT/APT | Entry symptoms | D-dimer |
|----------|-----|-----|----------------------------------|-----------------|---|----------|
| 1 | 85 | M | HT, CVD | Yes | Low GI bleeding | Not done |
| 2 | 71 | F | HT | Yes | Loss of appetite, vomiting, low GI bleeding | 10 N |
| 3 | 69 | M | DM, liver cirrhosis | No | Diarrhoea, fever and dyspnea | 8 N |
| 4 | 79 | F | HT, CVD, HCV | Yes | Abdominal pain | 8 N |
| 5 | 63 | M | No | No | Lower limb pain | > 70 N |
| 6 | 62 | M | Obesity, DM, HT, liver cirrhosis | No | Abdominal pain and vomiting | > 70 N |
| 7 | 83 | F | HT | Yes | Abdominal pain and dyspnoea | 4 N |
| 8 | 65 | M | No | No | Abdominal pain | Not done |
| 9 | 88 | M | CVD | Yes | Abdominal pain | N |
| 10 | 79 | M | CVD | No | Cardiac failure | N |
| 11 | 56 | M | HCV, liver cirrhosis | No | Ascites | 5 N |
| 12 | 61 | M | DM, HT | No | Dyspnoea | 3 N |
| 13 | 78 | F | HT | Yes | Lower limb oedema | 8 N |
| 14 | 41 | M | No | No | Fever and mental slowdown | 6 N |
| 15 | 64 | F | HT | Yes | Fever and caught | 2 N |
| 16 | 89 | F | Alzheimer disease | Yes | Caught and diarrhoea | N |
| 17 | 59 | M | Obesity, HT | No | Shortness of breathing | 2 N |
| 18 | 74 | M | CVD, pharynx carcinoma | No | Loss of conscious | 4 N |
| 19 | 63 | M | DM, HT | No | Fever, caught and dyspnoea | 2 N |
| 20 | 62 | F | HCV, COPD | No | Melena and anaemia | Not done |
| 21 | 72 | M | Parkinson disease and dementia | No | Fever and dysuria | > 70 N |

N: Normal value; ACT: Anticoagulant therapy; APT: Antiplatelets therapy; HT: Hypertension; CVD: Cardiovascular disorders; HCV: Hepatitis C virus; DM: Diabetes mellitus; COPD: Chronic obstructive pulmonary disease; GI: Gastrointestinal.

extended to the underlying wall. Necrosis was invariably accompanied by severe acute inflammation with diffuse micro-abscesses.

Findings of microvascular damage (endothelial shrinkage, leucocytes adhesion, vascular wall partial destruction) were reported in colonic (n. 3) and small bowel (n. 2) specimens. These features were studied in depth with CD34 staining for endothelial cells, and considered highly suggestive of SARS-CoV-2 infection related disease (Figure 3).

Outcomes

Surgery was necessary in four (19%) patients. Three had small bowel perforations repaired, and one small bowel resection. None of the surgeries was performed on the colon.

Median hospital stay was 9 d (interquartile range: 6-25). Mortality rate was 38% (95% CI: 0.18-0.62) as specified in Figure 4. No significant difference was found in univariate analysis when comparing patients stratified by outcome (Table 2).

Mortality among all the COVID-19 admitted patients was 23% (95% CI: 0.21-0.25). Mortality in COVID-19 patients with ischemic GI involvement had a relative risk for of 1.47 (95% CI: 0.007-0.031; $P = 0.31$), if compared to all COVID-19 hospitalized patients.

DISCUSSION

After the publication of several case reports or series of patients with COVID-19

Table 2 No significant difference was found in univariate analysis when comparing patients stratified by outcome

| Variables | Recovered, n = 13 | Dead, n = 9 | P value |
|---|-------------------|----------------|---------|
| Age in yr ¹ | 65 (61-78) | 71 (62-82) | 0.63 |
| Sex (F) ² | 6 (46%) | 1 (11%) | 0.17 |
| ACT/APT ² | 5 (38%) | 3 (33%) | 0.99 |
| D-dimer ¹ | 5 N (2 N-9 N) | 5 N (3 N-54 N) | 0.92 |
| PT (INR) ¹ | 1 (0.9-1.3) | 1.1 (1-1.5) | 0.48 |
| aPTT (INR) ¹ | 0.9 (0.8-1.1) | 1 (0.9-1.3) | 0.4 |
| Platelets (× 10 ⁹ /L) ¹ | 271 (226-325) | 232 (68-278) | 0.11 |

¹Express in median (Interquartile range).

²Express in number of subjects (percentage).

F: Female; ACT: Anticoagulant therapy; APT: Antiplatelets therapy; PT: Prothrombin time; INR: International normalized ratio; aPPT: Activated partial thromboplastin time; N: Normal value.

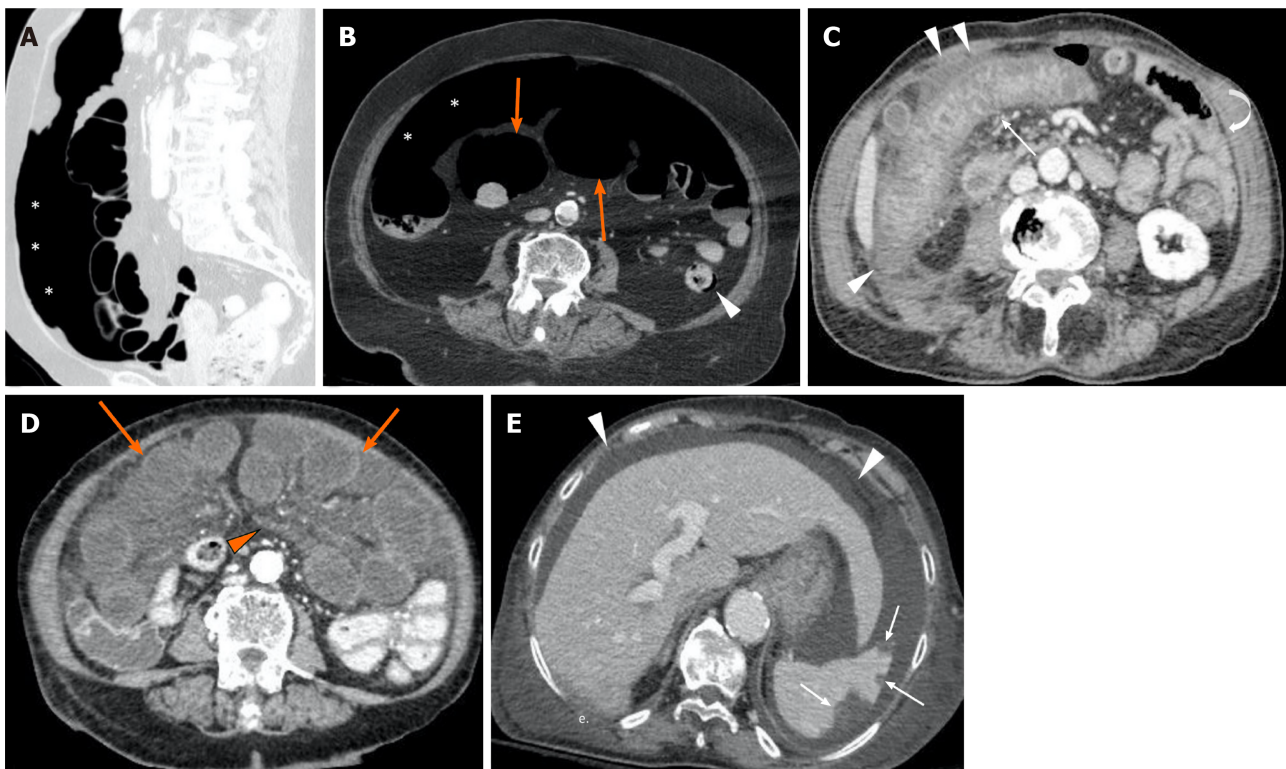


Figure 1 Computed tomography images from positive coronavirus disease 19 patients with abdominal signs and symptoms. A and B: The computed tomography (CT) scan revealed pneumoperitoneum (asterisks, A and B), dilated bowel loops with thin non-enhancing walls (orange arrows, B) and focal areas of pneumatosis in the descending colon (arrowhead, B), in keeping with intestinal ischemia. The main mesenteric vessels were patent (not shown); C: CT evidence of ischemic colitis involving the transverse and right portions of the colon: Markedly thickened and layered walls (thin arrow), compared to other normal appearing small and large bowel loops (curved arrow), with associated free fluid and oedematous stranding of the adjacent fat tissue (arrowheads); D and E: Axial CT scan shows multiple small bowel loops moderately dilated, with reduced thickness and poorly enhancing walls (orange arrows, D); concomitant diffuse oedema of the mesentery (orange arrowhead, D). In the same patient there were associated multiple peripheral splenic infarcts (with the arrows, E) with areas of mottled increased attenuation; the main splenic vessels were patent (not shown). Diffuse ascites (white arrowheads, E) is noted.

gastrointestinal ischemia[15-18], this multicentre retrospective study demonstrated that intestinal ischemic manifestations of SARS-CoV-2 were diagnosed in 0.7% of patients hospitalized with COVID-19 during the first pandemic wave. Ischemic signs must be suspected in all patients presenting to the ED with important abdominal symptoms and a positive SARS-CoV-2 swab, but they may also appear later as complications of SARS-CoV-2 pneumonia. Previous anticoagulant treatment does not seem to protect from the development of this complication. Contrast enhanced CT scan appears to be the best tool to promptly diagnose these manifestations and their

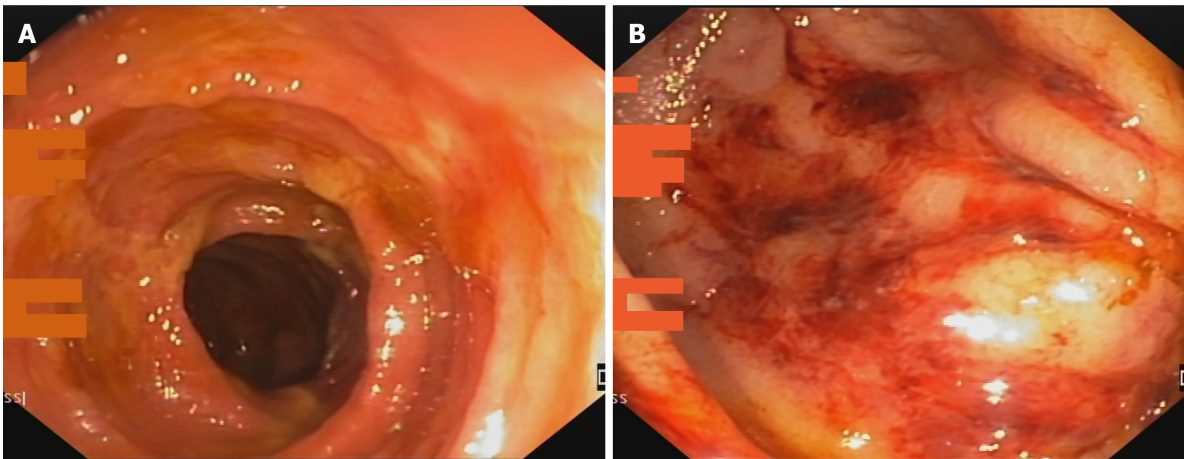


Figure 2 Endoscopic image of ischemic colitis. A: Oedematous mucosa with ischemic ulcerations; B: Presence of petechiae in an oedematous colic mucosa.

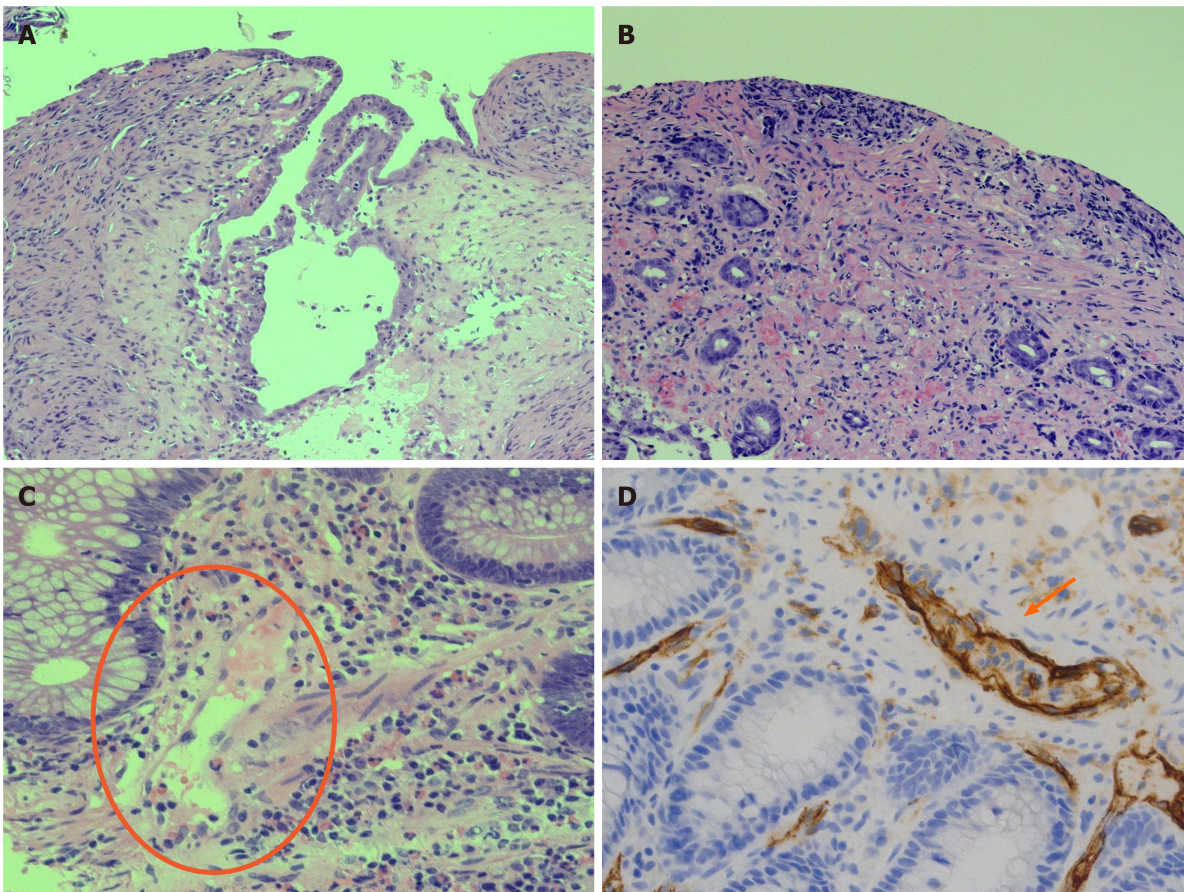


Figure 3 Histological features of ischemic damage of small and large bowel characterized by mucosal ulceration and fibrosis and vascular congestion of lamina propria associated with moderate mixed inflammatory infiltrate. A: Histological features of ischemic damage of small bowel; B: Histological features of ischemic damage of large bowel; C: Distinctive severe acute respiratory syndrome coronavirus 2 blood vessels inflammatory pattern with endothelial shrinkage and layering of granulocytes and lymphocytes on damaged vascular wall; D: Endothelial injury is emphasized by CD34 immunostaining of endothelial cells showing marked infiltration of inflammatory cells.

associated complications. Endoscopy is useful in case of suspected ischemic colitis. Atypical features on GI histology could guide the diagnosis even in patients with a SARS-CoV-2 negative nasopharyngeal swab. Nonetheless, a high index of suspicion must be kept, since mortality in these cases is as high as one in three patients.

Northern Italy and especially the Lombardy region were the most SARS-CoV-2 affected regions worldwide, with a seroprevalence after the first wave ranging from

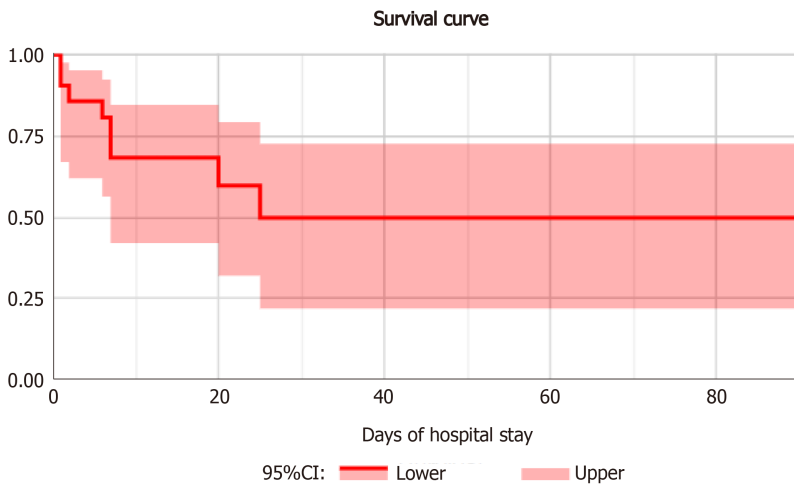


Figure 4 Survival curve of patients with intestinal ischemia.

24% to 38.5% [19-21], and an hospitalisation rate < 1%; thus, intestinal ischemic manifestations seem to be a very rare complication of SARS-Cov-2 infection.

Although the median hospital stay of the studied patients is similar to that of other larger cohorts of COVID-19 patients [22,23], the mortality is confirmed to be higher [22, 23]. Furthermore, if we consider the latest results from Imperial College on Infection Fatality Rate (2.3% in SARS-CoV-2 infected patients in Italy) [24], intestinal ischemic manifestations impact with an over 15 times higher lethality.

As already highlighted by Bhayana and colleagues, the radiologists play a central role in the diagnosis of these complications, with intestinal wall abnormalities described in nearly a third of abdominal CT scans performed in COVID-19 patients admitted to the intensive care unit (ICU) [25]. The main relevant finding in our cohort of patients is that in almost all patients with CT signs of bowel ischemia or colitis/enteritis there was no evidence of acute venous or arterial vessels thrombosis. Only one of six patients with bowel ischemia showed concomitant acute IVC and SMV thrombosis. This is in line with the report from Bhayana [25]. Interestingly, in 4/20 patients CT scan showed splenic (3) or renal (1) parenchymal infarcts, but only in one case we identified splenic artery thrombosis. The rate of complications related to bowel involvement was relatively low, accounting for CT scan evidence of perforation in one case and loops over distension in 6/20 patients. Bowel over distension, with no evidence of obstructing aetiologies, was therefore most likely functional.

Endoscopy may help confirming the diagnosis of patients with ischemic colitis, as outlined by the early published reports [26,27], although caution is mandatory when performing endoscopy in unstable patients admitted to ICU [28]. This is in agreement with a multicentre study on endoscopic findings of SARS-CoV-2 positive patients during the first wave in northern Italy, which showed histologically confirmed colon ischemia as one of the most prevalent findings [29].

In our series the histological analysis of colon biopsies together with small bowel resected segments showed very distinctive aspects of endothelium inflammation and endotheliitis, which were firstly described in the pulmonary, renal and gastrointestinal tract of SARS-CoV-2 infected patients [30]. These findings may give an explanation to the previously mentioned radiological evidence of ischemic damage without main venous or arterial thrombosis. Furthermore, in our cohort they may explain the absence of topographical segmental and patchy distribution of endoscopic ischemic lesions, which are usually expression of occluded vasculature [13].

The strong tropism of SARS-CoV-2 for the gastrointestinal tract is probably mediated by the abundance of Angiotensin Converting Enzyme 2 receptors in the intestinal mucosa [31]. A possible explanation for the virus induced endothelial damage in the gastrointestinal tract could lie in the lectin pathway, which is supposed to be responsible for SARS-CoV-2 mediated thrombotic microangiopathy in lung tissues [32]. The central role of Lectin and mannan-binding lectin-associated serine protease-2 in the gastrointestinal ischemic reperfusion damage has already been described in murine models in the pre-COVID-19 era [33,34]. These findings, if confirmed, could open new interesting therapeutic fields of research on SARS-CoV-2 ischemic manifestations.

CONCLUSION

Despite several limitations, mainly due the retrospective design on an infrequent and previously unknown manifestation of SARS-CoV-2, this multicentre study was able to confirm early isolated observations of gastrointestinal ischemia. Furthermore, new findings on epidemiology, clinical presentation, distinctive diagnostics features and outcomes were illustrated and discussed. This preliminary results in a small series of patients might raise the awareness on an infrequent but potentially lethal manifestation of COVID-19, aiding clinicians in proper management and prognostic stratification of complicated cases.

ARTICLE HIGHLIGHTS

Research background

Clinical manifestations of severe acute respiratory syndrome coronavirus 2 (SARS-CoV-2) virus are heterogenous and can affect different organs, including the gastrointestinal tract. Angiotensin converting enzyme 2 receptor, which mediates SARS-CoV-2 infection, is abundantly present in the intestinal mucosa.

Research motivation

Since the cytokine storm mediated by SARS-CoV-2 in coronavirus disease 19 (COVID-19) seems to determine a vascular damage which could explain hypercoagulability and pulmonary embolism, intestinal ischemic events in SARS-CoV-2 positive patients may be linked to the same pathogenic mechanism.

Research objectives

The aim of the present study is to collect and analyse the intestinal ischemic events in SARS-CoV-2 positive patients in order to calculate the incidence and determine the prognosis of affected subjects.

Research methods

The study was designed as a retrospective observational multicentre collection involving three among the largest COVID hospitals in Lombardy.

Research results

Intestinal ischemia is a rare but fatal manifestation of SARS-CoV-2 infection. The condition should be suspected in case of severe abdominal pain. In order to define localization and extent of intestinal ischemia, abdominal computed tomography scan and possibly endoscopy should be carried out. Intestinal biopsies main finding is endotheilitis.

Research conclusions

Severe endotheilitis in the intestinal mucosa could mediate intestinal ischemic manifestations in the gastrointestinal tract. Such manifestations are rare but frequently fatal, thus they should be ruled out in SARS-CoV-2 positive patients with gastrointestinal symptoms.

Research perspectives

One of the possible mechanisms of ischemic intestinal manifestations of SARS-CoV-2 could be mediated by mannan-binding lectin-associated serine protease-2 which is also a possible target for future therapy of COVID-19.

REFERENCES

- 1 **Alicandro G**, Remuzzi G, La Vecchia C. COVID-19 pandemic and total mortality in the first six months of 2020 in Italy. *Med Lav* 2020; **111**: 351-353 [PMID: [33124605](https://pubmed.ncbi.nlm.nih.gov/33124605/) DOI: [10.23749/mdl.v111i5.10786](https://doi.org/10.23749/mdl.v111i5.10786)]
- 2 **Huang C**, Wang Y, Li X, Ren L, Zhao J, Hu Y, Zhang L, Fan G, Xu J, Gu X, Cheng Z, Yu T, Xia J, Wei Y, Wu W, Xie X, Yin W, Li H, Liu M, Xiao Y, Gao H, Guo L, Xie J, Wang G, Jiang R, Gao Z, Jin Q, Wang J, Cao B. Clinical features of patients infected with 2019 novel coronavirus in Wuhan, China. *Lancet* 2020; **395**: 497-506 [PMID: [31986264](https://pubmed.ncbi.nlm.nih.gov/31986264/) DOI: [10.1016/S0140-6736\(20\)30183-5](https://doi.org/10.1016/S0140-6736(20)30183-5)]

- 3 **Jin X**, Lian JS, Hu JH, Gao J, Zheng L, Zhang YM, Hao SR, Jia HY, Cai H, Zhang XL, Yu GD, Xu KJ, Wang XY, Gu JQ, Zhang SY, Ye CY, Jin CL, Lu YF, Yu X, Yu XP, Huang JR, Xu KL, Ni Q, Yu CB, Zhu B, Li YT, Liu J, Zhao H, Zhang X, Yu L, Guo YZ, Su JW, Tao JJ, Lang GJ, Wu XX, Wu WR, Qv TT, Xiang DR, Yi P, Shi D, Chen Y, Ren Y, Qiu YQ, Li LJ, Sheng J, Yang Y. Epidemiological, clinical and virological characteristics of 74 cases of coronavirus-infected disease 2019 (COVID-19) with gastrointestinal symptoms. *Gut* 2020; **69**: 1002-1009 [PMID: [32213556](#) DOI: [10.1136/gutjnl-2020-320926](#)]
- 4 **Cheung KS**, Hung IFN, Chan PPY, Lung KC, Tso E, Liu R, Ng YY, Chu MY, Chung TWH, Tam AR, Yip CCY, Leung KH, Fung AY, Zhang RR, Lin Y, Cheng HM, Zhang AJX, To KKW, Chan KH, Yuen KY, Leung WK. Gastrointestinal Manifestations of SARS-CoV-2 Infection and Virus Load in Fecal Samples From a Hong Kong Cohort: Systematic Review and Meta-analysis. *Gastroenterology* 2020; **159**: 81-95 [PMID: [32251668](#) DOI: [10.1053/j.gastro.2020.03.065](#)]
- 5 **Nobel YR**, Phipps M, Zucker J, Lebwohl B, Wang TC, Sobieszczyk ME, Freedberg DE. Gastrointestinal Symptoms and Coronavirus Disease 2019: A Case-Control Study From the United States. *Gastroenterology* 2020; **159**: 373-375.e2 [PMID: [32294477](#) DOI: [10.1053/j.gastro.2020.04.017](#)]
- 6 **Pan L**, Mu M, Yang P, Sun Y, Wang R, Yan J, Li P, Hu B, Wang J, Hu C, Jin Y, Niu X, Ping R, Du Y, Li T, Xu G, Hu Q, Tu L. Clinical Characteristics of COVID-19 Patients With Digestive Symptoms in Hubei, China: A Descriptive, Cross-Sectional, Multicenter Study. *Am J Gastroenterol* 2020; **115**: 766-773 [PMID: [32287140](#) DOI: [10.14309/ajg.0000000000000620](#)]
- 7 **Mao R**, Qiu Y, He J-S, Tan J-Y, Li X-H, Liang J, Shen J, Zhu L-R, Chen Y, Iacucci M, Ng SC, Ghosh S, Chen M-H. Manifestations and prognosis of gastrointestinal and liver involvement in patients with COVID-19: a systematic review and meta-analysis. *Lancet Gastroenterol Hepatol* 2020 [DOI: [10.1016/S2468-1253\(20\)30126-6](#)]
- 8 **Wichmann D**, Sperhake JP, Lütgehetmann M, Steurer S, Edler C, Heinemann A, Heinrich F, Mushumba H, Kniep I, Schröder AS, Burdelski C, de Heer G, Nierhaus A, Frings D, Pfefferle S, Becker H, Brederke-Wiedling H, de Weerth A, Paschen HR, Sheikhzadeh-Eggers S, Stang A, Schmiedel S, Bokemeyer C, Addo MM, Aepfelbacher M, Püschel K, Kluge S. Autopsy Findings and Venous Thromboembolism in Patients With COVID-19: A Prospective Cohort Study. *Ann Intern Med* 2020; **173**: 268-277 [PMID: [32374815](#) DOI: [10.7326/M20-2003](#)]
- 9 **Norsa L**, Bonaffini PA, Indriolo A, Valle C, Sonzogni A, Sironi S. Poor Outcome of Intestinal Ischemic Manifestations of COVID-19. *Gastroenterology* 2020; **159**: 1595-1597.e1 [PMID: [32569772](#) DOI: [10.1053/j.gastro.2020.06.041](#)]
- 10 **Pan F**, Ye T, Sun P, Gui S, Liang B, Li L, Zheng D, Wang J, Hesketh RL, Yang L, Zheng C. Time Course of Lung Changes at Chest CT during Recovery from Coronavirus Disease 2019 (COVID-19). *Radiology* 2020; **295**: 715-721 [PMID: [32053470](#) DOI: [10.1148/radiol.2020200370](#)]
- 11 **Moszkowicz D**, Mariani A, Trésallet C, Menegaux F. Ischemic colitis: the ABCs of diagnosis and surgical management. *J Visc Surg* 2013; **150**: 19-28 [PMID: [23433833](#) DOI: [10.1016/j.jvisc Surg.2013.01.002](#)]
- 12 **Theodoropoulou A**, Koutroubakis IE. Ischemic colitis: clinical practice in diagnosis and treatment. *World J Gastroenterol* 2008; **14**: 7302-7308 [PMID: [19109863](#) DOI: [10.3748/wjg.14.7302](#)]
- 13 **Brandt LJ**, Feuerstadt P, Longstreth GF, Boley SJ; American College of Gastroenterology. ACG clinical guideline: epidemiology, risk factors, patterns of presentation, diagnosis, and management of colon ischemia (CI). *Am J Gastroenterol* 2015; **110**: 18-44; quiz 45 [PMID: [25559486](#) DOI: [10.1038/ajg.2014.395](#)]
- 14 **Norsa L**, Valle C, Morotti D, Bonaffini PA, Indriolo A, Sonzogni A. Intestinal ischemia in the COVID-19 era. *Dig Liver Dis* 2020; **52**: 1090-1091 [PMID: [32532607](#) DOI: [10.1016/j.dld.2020.05.030](#)]
- 15 **Bianco F**, Ranieri AJ, Paterniti G, Pata F, Gallo G. Acute intestinal ischemia in a patient with COVID-19. *Tech Coloproctol* 2020; **24**: 1217-1218 [PMID: [32506344](#) DOI: [10.1007/s10151-020-02255-0](#)]
- 16 **Hassan W**, Ramadan HK. COVID-19 and pneumatosis intestinalis: An early sign of intestinal ischemia. *Dig Liver Dis* 2021; **53**: 289-290 [PMID: [33187918](#) DOI: [10.1016/j.dld.2020.10.036](#)]
- 17 **Singh B**, Mechineni A, Kaur P, Ajdir N, Maroules M, Shamooun F, Bikkina M. Acute Intestinal Ischemia in a Patient with COVID-19 Infection. *Korean J Gastroenterol* 2020; **76**: 164-166 [PMID: [32969365](#) DOI: [10.4166/kjg.2020.76.3.164](#)]
- 18 **Cheung S**, Quiwa JC, Pillai A, Onwu C, Tharayil ZJ, Gupta R. Superior Mesenteric Artery Thrombosis and Acute Intestinal Ischemia as a Consequence of COVID-19 Infection. *Am J Case Rep* 2020; **21**: e925753 [PMID: [32724028](#) DOI: [10.12659/AJCR.925753](#)]
- 19 **Pagani G**, Conti F, Giacomelli A, Bernacchia D, Rondanin R, Prina A, Scolari V, Gandolfi CE, Castaldi S, Marano G, Ottomano C, Boracchi P, Biganzoli E, Galli M. Seroprevalence of SARS-CoV-2 significantly varies with age: Preliminary results from a mass population screening. *J Infect* 2020; **81**: e10-e12 [PMID: [32961253](#) DOI: [10.1016/j.jinf.2020.09.021](#)]
- 20 **Perico L**, Tomasoni S, Peracchi T, Perna A, Pezzotta A, Remuzzi G, Benigni A. COVID-19 and lombardy: TESTING the impact of the first wave of the pandemic. *EBioMedicine* 2020; **61**: 103069 [PMID: [33130396](#) DOI: [10.1016/j.ebiom.2020.103069](#)]
- 21 **Norsa L**, Cosimo P, Indriolo A, Sansotta N, D'Antiga L, Callegaro A. Asymptomatic Severe Acute Respiratory Syndrome Coronavirus 2 Infection in Patients With Inflammatory Bowel Disease Under Biologic Treatment. *Gastroenterology* 2020; **159**: 2229-2231.e2 [PMID: [32860790](#) DOI: [10.1053/j.gastro.2020.07.030](#)]

- 10.1053/j.gastro.2020.08.046]
- 22 **Docherty AB**, Harrison EM, Green CA, Hardwick HE, Pius R, Norman L, Holden KA, Read JM, Dondelinger F, Carson G, Merson L, Lee J, Plotkin D, Sigfrid L, Halpin S, Jackson C, Gamble C, Horby PW, Nguyen-Van-Tam JS, Ho A, Russell CD, Dunning J, Openshaw PJ, Baillie JK, Semple MG; ISARIC4C investigators. Features of 20 133 UK patients in hospital with covid-19 using the ISARIC WHO Clinical Characterisation Protocol: prospective observational cohort study. *BMJ* 2020; **369**: m1985 [PMID: 32444460 DOI: 10.1136/bmj.m1985]
 - 23 **Karagiannidis C**, Mostert C, Hentschker C, Voshaar T, Malzahn J, Schillinger G, Klauber J, Janssens U, Marx G, Weber-Carstens S, Kluge S, Pfeifer M, Grabenhenrich L, Welte T, Busse R. Case characteristics, resource use, and outcomes of 10 021 patients with COVID-19 admitted to 920 German hospitals: an observational study. *Lancet Respir Med* 2020; **8**: 853-862 [PMID: 32735842 DOI: 10.1016/S2213-2600(20)30316-7]
 - 24 **Imperial College London**. Report 34 - COVID-19 Infection Fatality Ratio Estimates from Seroprevalence. 29 October 2020. [cited 26 March 2021]. Available from: <http://www.imperial.ac.uk/medicine/departments/school-public-health/infectious-disease-epidemiology/mrc-global-infectious-disease-analysis/covid-19/report-34-ifr/>
 - 25 **Bhayana R**, Som A, Li MD, Carey DE, Anderson MA, Blake MA, Catalano O, Gee MS, Hahn PF, Harisinghani M, Kilcoyne A, Lee SI, Mojtabah A, Pandharipande PV, Pierce TT, Rosman DA, Saini S, Samir AE, Simeone JF, Gervais DA, Velmahos G, Misdrabi J, Kambadakone A. Abdominal Imaging Findings in COVID-19: Preliminary Observations. *Radiology* 2020; **297**: E207-E215 [PMID: 32391742 DOI: 10.1148/radiol.2020201908]
 - 26 **Almeida Vargas A**, Valentí V, Sánchez Justicia C, Martínez Regueira F, Martí Cruchaga P, Luján Colás J, Aliseda Jover D, Esteban Gordillo S, Cienfuegos JA, Rotellar Sastre F. Severe colon ischemia in patients with severe coronavirus-19 (COVID-19). *Rev Esp Enferm Dig* 2020; **112**: 784-787 [PMID: 32954769 DOI: 10.17235/reed.2020.7329/2020]
 - 27 **Paul T**, Joy AR, Alsoub HARS, Parambil JV. Case Report: Ischemic Colitis in Severe COVID-19 Pneumonia: An Unforeseen Gastrointestinal Complication. *Am J Trop Med Hyg* 2021; **104**: 63-65 [PMID: 33146121 DOI: 10.4269/ajtmh.20-1262]
 - 28 **Chan KH**, Lim SL, Damati A, Maruboyina SP, Bondili L, Abu Hanoud A, Slim J. Coronavirus disease 2019 (COVID-19) and ischemic colitis: An under-recognized complication. *Am J Emerg Med* 2020; **38**: 2758.e1-2758.e4 [PMID: 32499176 DOI: 10.1016/j.ajem.2020.05.072]
 - 29 **Massironi S**, Viganò C, Dioscoridi L, Filippi E, Pagliarulo M, Manfredi G, Conti CB, Signorelli C, Redaelli AE, Bonato G, Iiritano E, Frego R, Zucchini N, Ungari M, Pedaci M, Bono F, Di Bella C, Buscarini E, Mutignani M, Penagini R, Dinelli ME, Invernizzi P. Endoscopic Findings in Patients Infected With 2019 Novel Coronavirus in Lombardy, Italy. *Clin Gastroenterol Hepatol* 2020; **18**: 2375-2377 [PMID: 32480008 DOI: 10.1016/j.cgh.2020.05.045]
 - 30 **Varga Z**, Flammer AJ, Steiger P, Haberecker M, Andermatt R, Zinkernagel AS, Mehra MR, Schuepbach RA, Ruschitzka F, Moch H. Endothelial cell infection and endotheliitis in COVID-19. *Lancet* 2020; **395**: 1417-1418 [PMID: 32325026 DOI: 10.1016/S0140-6736(20)30937-5]
 - 31 **Xiao F**, Tang M, Zheng X, Liu Y, Li X, Shan H. Evidence for Gastrointestinal Infection of SARS-CoV-2. *Gastroenterology* 2020; **158**: 1831-1833.e3 [PMID: 32142773 DOI: 10.1053/j.gastro.2020.02.055]
 - 32 **Rambaldi A**, Gritti G, Micò MC, Frigeni M, Borleri G, Salvi A, Landi F, Pavoni C, Sonzogni A, Gianatti A, Binda F, Fagioli S, Di Marco F, Lorini L, Remuzzi G, Whitaker S, Demopulos G. Endothelial injury and thrombotic microangiopathy in COVID-19: Treatment with the lectin-pathway inhibitor narsoplimab. *Immunobiology* 2020; **225**: 152001 [PMID: 32943233 DOI: 10.1016/j.imbio.2020.152001]
 - 33 **Schwaible WJ**, Lynch NJ, Clark JE, Marber M, Samani NJ, Ali YM, Dudler T, Parent B, Lhotta K, Wallis R, Farrar CA, Sacks S, Lee H, Zhang M, Iwaki D, Takahashi M, Fujita T, Tedford CE, Stover CM. Targeting of mannan-binding lectin-associated serine protease-2 confers protection from myocardial and gastrointestinal ischemia/reperfusion injury. *Proc Natl Acad Sci U S A* 2011; **108**: 7523-7528 [PMID: 21502512 DOI: 10.1073/pnas.1101748108]
 - 34 **Vincenti M**, Behrends M, Dang K, Park YH, Hirose R, Blasi-Ibanez A, Liu T, Serkova NJ, Niemann CU. Induction of intestinal ischemia reperfusion injury by portal vein outflow occlusion in rats. *J Gastroenterol* 2010; **45**: 1103-1110 [PMID: 20549254 DOI: 10.1007/s00535-010-0262-0]



Published by **Baishideng Publishing Group Inc**
7041 Koll Center Parkway, Suite 160, Pleasanton, CA 94566, USA
Telephone: +1-925-3991568
E-mail: bpgoffice@wjgnet.com
Help Desk: <https://www.f6publishing.com/helpdesk>
<https://www.wjgnet.com>

